

# **Fifth generation district energy systems for low carbon cities**

**Thèse N° 7332**

Présentée le 29 novembre 2019

à la Faculté des sciences et techniques de l'ingénieur

Groupe SCI STI FM

Programme doctoral en énergie

pour l'obtention du grade de Docteur ès Sciences

par

**Raluca-Ancuta SUCIU**

Acceptée sur proposition du jury

Dr P. Ott, président du jury

Prof. F. Maréchal, directeur de thèse

Prof. A. Bardow, rapporteur

Dr K. Orehounig, rapporteuse

Prof. D. Favrat, rapporteur

2019



*To my family (especially my sweet niece)*

*“Nothing in life is to be feared, it is only to be understood. Now is the time to understand more, so that  
we may fear less.”*

Marie Curie





# Acknowledgments

First of all, I would like to thank my thesis supervisor, François Maréchal for taking a leap of faith by not hiring a chemical engineer, or even a mechanical or electrical engineer - just a physicist. Thank you for offering me an interesting project, in which you took great interest and consequently never lacked ideas on directions to move forward.

I would also like to thank my jury members, Dr. Orehounig, Prof. Bardow, Prof. Favrat and the jury president Dr. Ott for accepting to be part of it and for all the fruitful discussions and useful comments.

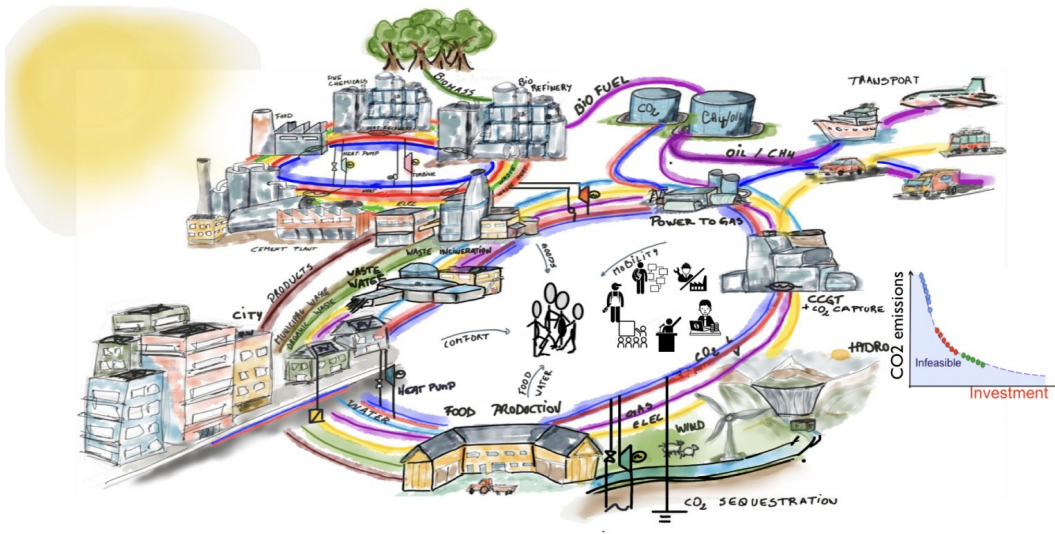
Next in line are of course my post-docs. Araz, thank you for being the first one to "adopt" me, for always being serene, knowing how to break down François's requests into achievable goals, and never doubting that I would make it. Luc, thank you for joining the "5G network team" (it wouldn't be my thesis if I wouldn't write this at least once in the acknowledgements) and for doing your best to publish our 5G paper, although 3 years later we still haven't done it. Last but of course not least, Ivan, thank you for taking me under your wing, although I was not really one of the "industrial energy efficiency" people. Thank you for all the fruitful conversations, for taking the time to review my papers and my thesis, for never lacking ideas (as the true scientist and future professor that you are and will be) and for always being there for me!

I would also like to thank all the current, past and floating members of the IPESE group. As François's new year photo shows (see below) and as someone beautifully put it during the ski weekend, I was "everywhere" on the photo, collaborating to a smaller or greater extent with each and every one of you.

The acknowledgements section is not long enough to thank each of you individually, but I will do my best. I would like to thank Samuel, for creating the foundation of this thesis; Hür, for teaching me basic engineering concepts, reviewing all my papers and the thesis, spending ten fold more time on "unit conversion" in Osmose due to my models and helping me integrate all the other features that I needed; Paul, for being the first one to introduce me to Osmose (although you never used it for your work), for having the patience to co-write n+1 conference/journal articles and to hear "this doesn't make sense" more times than others in a life-time; Dilan, for receiving me so warmly in the IPESE community, for being a true friend and always ready to help; Sophia, for all the data on solar models (models that you actually had and those you didn't even know you "had") and of

## Acknowledgments

---



course for being you. I would also like to thank everyone for the great times we had in conferences together (Elfie, Ligang, Victor, Shivom, Sophia and Dilan for the first conference in Slovenia; Daniel and Hür for the first conference in San Diego, Theodoros and Hür for the conference in Graz and the second conference in San Diego and Francesca and Francesco for the conference in Prague), the great times we had on trips (Dilan, Maziar and Katie for our time in Lyon and Dilan, Hür, Maziar and Katie for our trip to Napoli) and all my other predecessors: Nils for hosting me in my first month at EPFL and together with Sebastien for making parallel coordinates the state of the art of the lab, Maziar for your help with Osmose (especially reducing my computation time), Jean-Loup for all the Geneva data, Stefano for your help with geothermal wells, Stéphane for your help with Vali and for bringing light into the management consulting world and Alberto for organizing our amazing ski weekends together with Victor. Of course I would also want to thank the "future" of our lab: Alessio and Francesca, for our great moments teaching and evaluating students together; Luise, for being the future of the urban system group; Julia, for making the french classes less miserable and Rafael, for all the help with the ski weekend, for the summer body encouragement and for a promising optimism-based future in the lab. I would of course also like to thank the GEM people, Guillaume, Giorgio and naturally Manuel and Priscilla for all the delicious Italian meals, our great couple vacation in Provence and all the other events where we had the pleasure to spend time with you.

Next, I would like to thank my friends: Ivona, for all the shopping sessions in Freiburg, for visiting me in Basel, for all your kind words and for being the shoulder I could always turn to; Yulia, for always remaining my most dear girl-friend and for my sweet godson Leo; Ioana for our long, precious friendship born out of love for physics, Stefana and Maria, for staying among my closest high school friends and for keeping me in your lives and hearts despite the long distance and Dănă (Alexandra), for always understanding how I feel, for never changing, and for all our lovely meetings in Zürich.

## Acknowledgments

---

I would also like to thank my family, my mom and dad, for making it possible for me to be here, for believing and supporting every day of my life; Oana and Sorin, for giving me one of the most beautiful gifts during this PhD: my long-awaited, smart, beautiful niece Tanya; Rares, the first person I ever met (although the doctors didn't respect my wish of coming to this world together - i.e. had my arm wrapped around your neck - you respected it and have always been there for me) and his beautiful wife Greta.

Lastly, I would like to come back to thanking Hür and his family. You made either the biggest mistake or the best thing in your life by turning my table next to yours a couple of weeks after I joined the lab and never left my side since, thank you, canim!

*Sion, 24.09.2019*



# Abstract

The focus and challenge for energy engineering in the context of rapid climate change is summarised by the Europe 20-20-20 targets, committing to a reduction in energy consumption of 20%. The most logical approach to achieve these goals is to target the most energy intensive sectors, namely residential and industrial. In the residential sector, centralised district energy networks are favoured as the best means of heat distribution. They have been constantly evolving, from high temperature steam generated by fossil fuel resources, to water-based solutions supplying heat at the required temperature using renewable electricity. In the industrial sector, process integration must be performed on site, to ensure optimal resource utilisation and recovery is achieved. Extending these concepts, heat and mass integration must also be performed between different industries, and between industry and other sectors, such as residential. This enables systems thinking to revolutionise the current production system toward more efficient and sustainable solutions, leveraging connectivity to maximise the usage of energy and material resources.

In this context, this thesis addresses a series of open questions and offers methods and solutions for improvement. Chapter 1 addresses the lack of demand data in the residential sector. In view of this, it presents a geographically parameterized residential sector profile based on heating signature models for heating and cooling demands, on real consumption profiles for domestic hot water and on Swiss society of engineers and architects norms for electricity and refrigeration. Additional demands such as mobility and waste treatment are also provided.

The following chapter makes use of the sector profile introduced in Chapter 1 to integrate the latest refrigerant-based district energy network in four climate zones in Europe. Additional to the state of the art CO<sub>2</sub> network, this chapter examines many possibilities of natural resource valorization, such as fresh water thermal sources (e.g. lakes), geothermal sources (geothermal wells), municipal waste and solar energy. The contributions of each additional urban resource is highlighted and the variations across the climate zones in Europe are underlined.

Chapter 3 takes the parameterized sector profile one step further, extending the boundaries to include consumption of major products and their associated production requirements. The urban profile is thus extended to include industrial production from 10 different industries, namely oil refining, cement, brewing, aluminum, steel, waste incineration, sugar, pulp and paper, plastics, and dairy production. The temperature-enthalpy profiles of the different industries were taken from previously-developed industrial blueprints, while the production data was considered according to

European reference documents. The updated parameterized sector profile is utilised in this chapter to study industrial waste heat recovery potential for three typical European city scales (those of Zurich, Munich and London) and a real city (Rotterdam,NL) with its 4 main oil refineries and cement plants and the city brewery.

Chapter 4 bridges the gap between building- and urban-scale analysis, therefore adding a more precise spatial scale to the optimisation problems, and proposes a method to integrate renewable energy and low-carbon resources in cities.

This thesis contributes to the field of future urban energy system planning by developing models and methods for generating optimal solutions to efficient urban energy provision. Results from each chapter show large improvement potentials in energy requirements and associated environmental impacts which could lead to zero- or negative-emission, autonomous cities.

### **Keywords**

residential sector profile, district heating and cooling, power to gas, low-carbon resources, long term energy storage, industrial heat recovery, process integration, CO<sub>2</sub> network, multi-energy networks, energy autonomy, optimal cities, parametric optimisation

# Résumé

L'objectif et le défi de l'ingénierie énergétique dans le contexte du changement climatique rapide sont résumés par les objectifs « 20-20-20 » de l'Europe qui visent à accroître l'efficacité énergétique de 20% d'ici à 2020. L'approche la plus logique pour atteindre ces objectifs est de cibler les secteurs les plus énergivores, à savoir les secteurs résidentiel et industriel. Dans le secteur résidentiel, les réseaux énergétiques centralisés urbains sont considérés comme le meilleur moyen de distribution de chaleur. Ils ont constamment évolué, passant de la vapeur à haute température générée par des ressources en combustibles fossiles à des solutions à base d'eau fournissant de la chaleur à la température requise en utilisant de l'électricité renouvelable. Dans le secteur industriel, l'intégration des procédés doit se faire sur place, afin de garantir une utilisation et une récupération optimales des ressources. En élargissant ces concepts, l'intégration de la chaleur et de la masse doit également être réalisée entre les différentes industries et entre l'industrie et d'autres secteurs, comme le résidentiel. Cela permet à la pensée systémique de révolutionner le système de production actuel vers des solutions plus efficaces et durables, en tirant parti de la connectivité pour maximiser l'utilisation de l'énergie et des ressources matérielles.

Dans ce contexte, cette thèse aborde une série de questions ouvertes et propose des méthodes et des solutions d'amélioration. Le chapitre 1 traite du manque de données sur la demande dans le secteur résidentiel. Dans cette optique, il présente un profil géographiquement paramétré du secteur résidentiel basé sur des modèles de signature énergétique pour les besoins de chauffage et de refroidissement, sur des profils de consommation réelle pour l'eau chaude sanitaire et sur les normes de la Société suisse des ingénieurs et architectes dans les domaines de l'électricité et de la réfrigération. Des données pour d'autres demandes telles que la mobilité et le traitement des déchets sont également apportées.

Le chapitre suivant s'appuie sur le profil sectoriel présenté dans le premier chapitre pour intégrer le dernier réseau énergétique urbain à base de fluide frigorigène dans quatre zones climatiques en Europe. Outre le réseau de pointe basé sur l'utilisation de CO<sub>2</sub>, ce chapitre examine de nombreuses possibilités de valorisation des ressources naturelles, telles que les sources thermiques d'eau douce (p. ex. lacs), les sources géothermiques (puits géothermiques), les déchets ménagers et l'énergie solaire. Les contributions de chaque ressource urbaine supplémentaire sont mises en évidence et les variations entre les zones climatiques en Europe sont soulignées.

Le chapitre 3 va plus loin avec le profil sectoriel paramétré en élargissant les limites pour inclure la consommation des principaux produits et leurs besoins de production associés. Le profil urbain est

ainsi étendu pour inclure la production industrielle de 10 industries différentes : raffinage du pétrole, ciment, brasserie, aluminium, acier, incinération des déchets, sucre, pâtes et papiers, plastiques et production laitière. Les profils température-enthalpie des différentes industries ont été établis à partir de résultats d'études de la signature énergétique précédemment élaborées, tandis que les données de production ont été prises en compte selon les documents de référence européens. Le profil sectoriel paramétré actualisé est utilisé dans ce chapitre pour étudier le potentiel de récupération de la chaleur résiduelle industrielle à trois échelles urbaines européennes typiques (Zurich, Munich et Londres) et dans une ville réelle (Rotterdam, NL) avec ses 4 principales raffineries de pétrole et cimenteries ainsi que la brasserie de la ville.

Le chapitre 4 comble le fossé entre l'analyse à l'échelle du bâtiment et à l'échelle urbaine, ajoutant ainsi une échelle spatiale plus précise aux problèmes d'optimisation, et propose une méthode pour intégrer les énergies renouvelables et les ressources à faible émission de carbone dans les villes.

Cette thèse contribue au domaine de la planification des futurs systèmes énergétiques urbains en développant des modèles et des méthodes pour générer des solutions optimales pour un approvisionnement énergétique urbain efficace. Les résultats de chaque chapitre montrent d'importantes possibilités de diminution des besoins en énergie et des impacts environnementaux associés qui pourraient conduire à des villes autonomes à émissions nulles ou négatives.

### **Mots-clés**

profil du secteur résidentiel, chauffage et refroidissement urbains, conversion d'électricité en gaz, ressources à faible émission de carbone, stockage d'énergie à long terme, récupération de chaleur industrielle, intégration des procédés, réseau CO<sub>2</sub>, réseaux multi-énergies, autonomie énergétique, villes optimales, optimisation paramétrique



# Contents

<b>Acknowledgments</b>	<b>i</b>
<b>Abstract (English/French)</b>	<b>v</b>
<b>Table of content</b>	<b>ix</b>
<b>List of figures</b>	<b>xiii</b>
<b>List of tables</b>	<b>xvii</b>
<b>Acronyms and abbreviations</b>	<b>xxi</b>
<b>List of symbols</b>	<b>xxii</b>
<b>Introduction</b>	<b>1</b>
Evolution of district energy networks . . . . .	1
Heat pumping technologies . . . . .	4
Contributions and novelty . . . . .	4
Chapter 1: Estimating urban energy demand . . . . .	5
Chapter 2: Valorizing natural resources and human waste . . . . .	5
Chapter 3: Valorizing excess industrial heat . . . . .	6
Chapter 4: Systematic integration of energy- optimal buildings with district networks	6
Mathematical formulation . . . . .	6
Definition of sets . . . . .	7
Objective function and constraints . . . . .	7
<b>1 Estimating urban energy demand</b>	<b>11</b>
1.1 Introduction . . . . .	11
1.2 State of the art . . . . .	12
1.3 Materials and methods . . . . .	15
1.3.1 Service energy demand . . . . .	15
1.3.2 Sector profile validation . . . . .	22
1.3.3 MILP formulation . . . . .	22

## Contents

---

1.3.4	City service optimization scenarios . . . . .	23
1.4	Results and discussion . . . . .	26
1.4.1	Single-objective optimization of city service provision . . . . .	26
1.4.2	Optimal solutions for multiple objectives . . . . .	27
1.5	Conclusion . . . . .	30
<b>2</b>	<b>Valorizing natural resources and human waste</b>	<b>31</b>
2.1	Introduction . . . . .	32
2.2	State of the art . . . . .	33
2.3	Materials and methods . . . . .	35
2.3.1	Scenario 1: base case 5G DEN . . . . .	35
2.3.2	Scenario 2: 5G DEN coupled to geothermal wells . . . . .	35
2.3.3	Scenario 3: 5G DEN coupled to GWs and municipal waste plant . . . . .	36
2.3.4	Scenario 4: 5G DEN coupled to GWs, MWP and solar energy . . . . .	36
2.3.5	Investment and operating cost . . . . .	37
2.3.6	Process integration . . . . .	38
2.3.7	Urban morphology and energy demand . . . . .	40
2.4	Results and discussion . . . . .	42
2.4.1	Energy demand and energy consumption . . . . .	42
2.4.2	Scenario 1: base case 5G DEN . . . . .	42
2.4.3	Scenario 2: 5G DEN coupled to geothermal wells . . . . .	44
2.4.4	Scenario 3: 5G DEN coupled to GWs and municipal waste plant . . . . .	44
2.4.5	Scenario 4: 5G DEN coupled to GWs, MWP and solar energy . . . . .	46
2.5	Conclusion . . . . .	49
<b>3</b>	<b>Valorizing excess industrial heat</b>	<b>51</b>
3.1	Introduction . . . . .	51
3.2	State of the art . . . . .	53
3.3	Materials and methods . . . . .	54
3.3.1	Typical European city . . . . .	54
3.3.2	Heat distribution losses . . . . .	62
3.4	Results and discussion . . . . .	64
3.4.1	Typical European city . . . . .	64
3.4.2	Real city: Rotterdam, NL . . . . .	71
3.5	Conclusion . . . . .	77
<b>4</b>	<b>Systematic integration of energy- optimal buildings with district networks</b>	<b>79</b>
4.1	Introduction . . . . .	80
4.2	State of the art . . . . .	81
4.3	Materials and methods . . . . .	85

## Contents

---

4.3.1	Mathematical Formulation . . . . .	87
4.3.2	Case Study . . . . .	92
4.3.3	Time Resolutions: Typical Days Algorithm . . . . .	95
4.3.4	Measure of Energy Autonomy . . . . .	97
4.4	Results and discussion . . . . .	98
4.4.1	Monthly vs. Typical Day Time Resolution . . . . .	98
4.4.2	5G DEN Penetration with Population Density . . . . .	100
4.4.3	Detailed Results of Solution with Lowest Operating Cost and Emissions . . . . .	100
4.5	Conclusion . . . . .	104
<b>Conclusions</b>		<b>107</b>
Main results and contributions . . . . .		107
Chapter 1: Estimating urban energy demand . . . . .		107
Chapter 2: Valorizing natural resources and human waste . . . . .		108
Chapter 3: Valorizing industrial waste heat . . . . .		108
Chapter 4: Systematic integration of energy- optimal buildings with district networks . . . . .		109
Future perspectives . . . . .		110
<b>Appendix</b>		<b>113</b>
<b>A (Chapter 1)</b>		<b>115</b>
A.1	Unit models . . . . .	115
A.1.1	Scenario 1 . . . . .	115
A.1.2	Scenario 2 (additional utilities) . . . . .	117
<b>B (Chapter 2)</b>		<b>123</b>
B.1	Unit models: Decentralized energy conversion technologies . . . . .	123
B.2	Unit models: centralized energy conversion technologies . . . . .	125
B.2.1	PV panels . . . . .	125
B.2.2	SOEC-SOFC co-generation and methanation . . . . .	126
B.2.3	CO <sub>2</sub> and CH <sub>4</sub> storage . . . . .	128
B.2.4	Municipal waste plant and steam network . . . . .	129
B.2.5	Central plant HP and geothermal wells . . . . .	130
B.3	Investment cost of energy conversion technologies . . . . .	132
<b>C (Chapter 3)</b>		<b>135</b>
C.1	Heat transfer results . . . . .	135
C.1.1	Steam network . . . . .	137
C.1.2	Hot water loop . . . . .	137
C.2	Industrial symbiosis heat flows . . . . .	137

## Contents

---

<b>D (Chapter 4)</b>	<b>139</b>
D.1 Unit Models at Building Level . . . . .	139
D.1.1 Building . . . . .	139
D.1.2 Boiler . . . . .	139
D.1.3 Electrical heater . . . . .	140
D.1.4 Heat Pumps . . . . .	140
D.1.5 Storage Units . . . . .	141
D.2 Unit Models at City Level . . . . .	143
D.2.1 PV Panels . . . . .	143
D.2.2 SOEC-SOFC Co-Generation and Methanation . . . . .	144
D.2.3 Steam Network . . . . .	145
D.2.4 CO <sub>2</sub> and CH <sub>4</sub> Storage . . . . .	146
D.2.5 Central Plants . . . . .	146
D.2.6 Investment Cost of Energy Conversion Technologies . . . . .	147
D.3 Heat Distribution Cost . . . . .	147
D.4 RegBL Database Parameter Names . . . . .	149
D.5 Energy Service Demand of Different Building Categories . . . . .	150
D.6 Results from Parallel Coordinates . . . . .	156
<b>Curriculum Vitae</b>	<b>183</b>

# List of figures

1	5G DHC concept. . . . .	3
1.1	Residential sector energy consumption by country. . . . .	12
1.2	Top-down and bottom-up approaches (adapted from [1]). . . . .	13
1.3	European climate zones. . . . .	17
1.4	Building distribution of a typical urban center. . . . .	18
1.5	Heating signatures for different building types and ages. . . . .	19
1.6	Composite curves (heating and cooling demand) for different European zones, De- cember. . . . .	21
1.7	Composite curves (heating and cooling demand) for different European zones, July. . . . .	22
1.8	Real profile resource consumption in Rotterdam, MWh. . . . .	23
1.9	Sector profile resource consumption in Rotterdam, MWh. . . . .	23
1.10	Schematic description scenario 1. . . . .	24
1.11	Schematic description of additional utilities in scenario 2. . . . .	24
1.12	Schematic description scenario 3. . . . .	25
1.13	Schematic description of additional utilities in scenario 4. . . . .	25
1.14	Schematic description of waste boiler integration. . . . .	26
1.15	Total cost optimization for different scenarios. . . . .	27
1.16	Environmental impact optimization for different scenarios. . . . .	28
1.17	Key performance indicators for CO <sub>2</sub> emission $\epsilon$ -constraints. . . . .	29
1.18	Key performance indicators for investment cost $\epsilon$ -constraints. . . . .	29
1.19	Key performance indicators for operating cost and environmental impact $\epsilon$ -constraints. . . . .	30
2.1	Energy consumption and greenhouse gas emissions in the EU breakdown by sector. . . . .	32
2.2	Schematic description of 5G DENs. . . . .	34
2.3	P2G with electrolysis, methanation and co-generation using a SOFC. . . . .	34
2.4	Schematic description of scenario 2. . . . .	36
2.5	Schematic description of scenario 3. . . . .	36
2.6	Schematic description of scenario 4a. . . . .	37

## List of figures

---

2.7	European climate zones. . . . .	41
2.8	Compact urban block with share of building type/refurbishment stage. . . . .	41
2.9	Energy demand by service for different European areas. . . . .	43
2.10	Energy consumption for heating and cooling for different European areas, scenario 1. . . . .	43
2.11	Energy consumption for heating and cooling for different European areas, scenario 2. . . . .	44
2.12	Electricity import/export breakdown for different European areas, scenario 3. . . . .	45
2.13	Heat import/export breakdown for different European areas, scenario 3. . . . .	45
2.14	Electricity import/export breakdown for different European areas, scenario 4. . . . .	46
2.15	Heat import/export breakdown for different European areas, scenario 4. . . . .	47
2.16	PV panel and GW area required for autonomy for different European areas. . . . .	47
2.17	Payback time for different European zones. . . . .	48
3.1	Yearly EIH potential worldwide. . . . .	52
3.2	CCs (left) and GCC (right) of the average European cement production process, scaled for the consumption of a population of 1 million inhabitants. . . . .	57
3.3	CCs (left) and GCC (right) of the average European oil refinery process, scaled for the consumption of a population of 1 million inhabitants. . . . .	57
3.4	CCs (left) and GCC (right) of the average European brewery process, scaled for the consumption of a population of 1 million inhabitants. . . . .	58
3.5	CCs (left) and GCC (right) of the average European pulp and paper process, scaled for the consumption of a population of 1 million inhabitants. . . . .	58
3.6	CCs (left) and GCC (right) of the average European dairy process, scaled for the consumption of a population of 1 million inhabitants. . . . .	58
3.7	CCs (left) and GCC (right) of the average European secondary aluminum process, scaled for the consumption of a population of 1 million inhabitants. . . . .	59
3.8	CCs (left) and GCC (right) of the average European steel process, scaled for the consumption of a population of 1 million inhabitants. . . . .	59
3.9	CCs (left) and GCC (right) of the average European sugar process, scaled for the consumption of a population of 1 million inhabitants. . . . .	59
3.10	CCs (left) and GCC (right) of the average European plastic process, scaled for the consumption of a population of 1 million inhabitants. . . . .	60
3.11	Integrated composite curve (ICC) of the Shell refinery. . . . .	61
3.12	Integrated composite curves of the brewery (left) and cement (right) plants considered. . . . .	62
3.13	Schematic description of brewery and cement plants interaction with DHC network. . . . .	62
3.14	Industry location coordinates in a small city. . . . .	65
3.15	Heat transfer results, small city. . . . .	66
3.16	Heat transfer to the district, small city. . . . .	66
3.17	Heat transfer between industries, small city. . . . .	67
3.18	Heat transfer results, medium city. . . . .	67

## List of figures

---

3.19 Heat transfer to the district, medium city. . . . .	68
3.20 Heat transfer between industries, medium city. . . . .	68
3.21 Heat transfer results, large city. . . . .	68
3.22 Heat transfer to the district, large city. . . . .	69
3.23 Heat transfer between industries, large city. . . . .	69
3.24 Highlighted solutions, A (a), B (b). . . . .	70
3.25 Hot water loop transfer, solution A (a), solution B (b). . . . .	70
3.26 Steam network transfer to district, solution A (a), solution B (b). . . . .	71
3.27 Steam network transfer between industries , solution A (a), solution B (b). . . . .	71
3.28 Carnot composite curve highlighting heat transfer vs. processes and other utilities for solution A. Note: colors are used to highlight the share of heat transfer from different sources, not the exact temperature level at which the transfer takes place. . . . .	72
3.29 Heat transfer and losses, refinery/cement plant couples considered individually. . . .	73
3.30 Integrated composite curve of the processes considered, refinery/cement plant cou- ples considered individually. . . . .	74
3.31 Operating cost and CO <sub>2</sub> emissions, refinery/cement plant couples considered individ- ually. . . . .	74
3.32 Heat transfer and losses, refinery/cement plant couples considered individually. . . .	75
3.33 Integrated composite curve of the processes considered, refinery/cement plant cou- ples added sequentially. . . . .	76
3.34 Operating cost and CO <sub>2</sub> emissions, refinery/cement plant couples added sequentially. 76	
4.1 5G network schematic representation. . . . .	84
4.2 P2G schematic representation. . . . .	84
4.3 Systematic generation method for each building type (i.e., age and renovation). . . .	85
4.4 Pareto frontier of residential SFH with different utility configurations and renovation stages. . . . .	86
4.5 Methodology overview. . . . .	87
4.6 Population density of communes in the canton of Geneva. . . . .	93
4.7 Refurbishment level building distribution in Geneva city center. . . . .	94
4.8 Hourly specific energy service demand of administrative buildings. . . . .	95
4.9 Performance indicator evolution using the k-medoids algorithm for selecting the number of typical days. . . . .	96
4.10 Typical days algorithm. . . . .	96
4.11 Error load duration curve of typical day attributes. . . . .	97
4.12 Self-sufficiency and self-consumption visual depiction. . . . .	98
4.13 Pareto Geneva city center different time resolutions. . . . .	99
4.14 Geneva city center cost breakdown for different time resolutions. . . . .	99
4.15 5G network cost. . . . .	101

## List of figures

---

4.16	Parallel coordinate representation of the canton solutions. . . . .	101
4.17	Parallel coordinate representation of the communes for the lowest operating cost solution. . . . .	101
4.18	Breakdown of electricity/natural gas import/export by commune and at building/canton level. . . . .	102
4.19	Breakdown of investment and total cost at buildings/canton level. . . . .	103
4.20	Breakdown of electricity/natural gas import/export by month, for Genève Cité. . . . .	103
B.1	COP for heating HPs and REF cycle by month, zone CWest / Schematic flowsheet of a CO <sub>2</sub> DEN. . . . .	125
C.1	Heat transfer/losses integration of refineries considered individually. . . . .	138
C.2	Heat transfer/losses integration of refineries added sequentially. . . . .	138
D.1	1R1C building model. . . . .	140
D.2	Hourly specific energy service demand of residential SFH buildings. . . . .	150
D.3	Hourly specific energy service demand of residential MFH buildings. . . . .	151
D.4	Hourly specific energy service demand of commercial buildings. . . . .	152
D.5	Hourly specific energy service demand of education buildings. . . . .	153
D.6	Hourly specific energy service demand of hospital buildings. . . . .	154
D.7	Hourly specific energy service demand of mixed buildings. . . . .	155



## List of tables

1.1	Advantages and limitations of bottom-up and top-down approaches. . . . .	14
1.2	Heating signature parameters for typical urban center. . . . .	18
1.3	Temperature profile parameters. . . . .	19
1.4	Building parameters for a typical urban center. . . . .	20
1.5	Energy demand per capita for different European zones. . . . .	21
1.6	Parameters for energy consumption, economic and environmental analysis. . . . .	26
2.1	Share of primary energy, efficiency and price by service, for the current H <sub>2</sub> O network. . . . .	38
2.2	Resource flows (-: flow in, +: flow out. . . . .	40
2.3	Typical indicators for a central European urban center. . . . .	42
3.1	Typical European city industrial production by sector. . . . .	60
3.2	Refinery yearly flow and distance from the district. . . . .	61
4.1	Sets used in the mathematical formulation. . . . .	92
4.2	Building types present in the model of the canton of Geneva. . . . .	93
4.3	Yearly specific energy service demand of administrative buildings. . . . .	94
A.1	Boiler streams. . . . .	115
A.2	Central heating streams. . . . .	115
A.3	Electrical heating streams. . . . .	116
A.4	Refrigeration cycle streams. . . . .	116
A.5	Municipal waste plant streams. . . . .	116
A.6	CO <sub>2</sub> vaporization HE streams. . . . .	117
A.7	Direct heating supply HE streams. . . . .	117
A.8	Steam network parameters. . . . .	117
A.9	Combined heat and power plant streams. . . . .	118
A.10	Investment cost parameters. . . . .	118
A.11	Solar thermal panels parameters. . . . .	119
A.12	PV panel parameters. . . . .	119
A.13	PV panel streams. . . . .	120

## List of tables

---

A.14 Heat pump streams. . . . .	120
A.15 Electrolyzer streams. . . . .	121
B.1 Parameters for decentralized energy conversion technologies. . . . .	123
B.2 Streams for space heating HP. . . . .	124
B.3 Streams for domestic hot water HP. . . . .	124
B.4 Streams for refrigeration cycle. . . . .	124
B.5 Streams for air cooling heat exchanger. . . . .	125
B.6 Parameters for PV panels. . . . .	126
B.7 Streams for PV panel. . . . .	126
B.8 Streams for SOEC unit. . . . .	127
B.9 Streams for SOFC-GT unit. . . . .	127
B.10 Streams for methanation unit. . . . .	128
B.11 Streams for municipal waste plant. . . . .	129
B.12 Streams for CO <sub>2</sub> vaporization HE. . . . .	129
B.13 Streams for direct heating supply HE. . . . .	129
B.14 Parameters for steam network. . . . .	130
B.15 Parameters for central plant HP. . . . .	130
B.16 Streams for central plant HP (winter). . . . .	131
B.17 Parameters for geothermal wells. . . . .	131
B.18 Streams for geothermal wells. . . . .	132
B.19 Streams for central plant HE (summer). . . . .	132
B.20 Parameters for IC. . . . .	132
C.1 Heat transfer solutions, Zurich. . . . .	135
C.2 Heat transfer solutions, Munich. . . . .	136
C.3 Heat transfer solutions, London. . . . .	136
C.4 Parameters for steam network. . . . .	137
C.5 Parameters for hot water loop. . . . .	137
D.1 Parameter data. . . . .	140
D.2 Parameter data (ELH). . . . .	140
D.3 Default parameters values for the AHP second-law efficiency and part-load limit, evaluated from [2]. . . . .	141
D.4 Default parameters values for the VAC second-law efficiency and part-load limit, evaluated from [2]. . . . .	141
D.5 Parameter data (BAT). . . . .	142
D.6 Parameter data (HST). . . . .	143
D.7 Parameters for PV panels. . . . .	144
D.8 Streams for PV panel. . . . .	144

## List of tables

---

D.9 Streams for SOEC unit. . . . .	144
D.10 Streams for SOFC-GT unit. . . . .	144
D.11 Streams for methanation unit. . . . .	145
D.12 Parameters for steam network. . . . .	146
D.13 Parameters for central plant HP. . . . .	146
D.14 Streams for central plant HP (winter). . . . .	147
D.15 Streams for central plant HE (summer). . . . .	147
D.16 Parameters for IC. . . . .	148
D.17 Network cost parameters. . . . .	149
D.18 RegBL database corresponding parameter notations. . . . .	149
D.19 Yearly specific energy service demand of residential SFH buildings. . . . .	150
D.20 Yearly specific energy service demand of residential MFH buildings. . . . .	151
D.21 Yearly specific energy service demand of commercial buildings. . . . .	152
D.22 Yearly specific energy service demand of education buildings. . . . .	153
D.23 Yearly specific energy service demand of hospital buildings. . . . .	154
D.24 Yearly specific energy service demand of mixed buildings. . . . .	155
D.25 Heat signature coefficients for all building types and ages. . . . .	156
D.26 Detailed results for Figure 4.16. . . . .	157
D.27 Detailed results for Figure 4.17. . . . .	158



# Acronyms and abbreviations

1G	first generation
2G	second generation
3G	third generation
4G	fourth generation
5G	fifth generation
AC	air cooling
AEEI	Advanced Energy Economy Institute
AHP	air-water heat pump
BAT	battery stack
BOI	boiler
CC	composite curve
CDD	cooling degree days
CEast	central east
CHP	co-generation heat and power
COP	coefficient of performance
CP	central plant
CWest	central west
DB	Davies-Bouldin (index)
DEN	district energy network
DH	district heating
DHC	district heating and cooling
DHN	district heating network
DHW	domestic hot water
ECI	european cooling index
EH	european heating index
EIH	excess industrial heat
EL	electricity
ELDC	error load duration curve
ELH	electrical heater
ERA	energy reference area

## Acronyms and abbreviations

---

EZ	european zone
GI	global horizontal irradiation
GT	gas turbine
GW	geothermal well
HDD	heating degree days
HE	heat exchanger
HHV	higher heating value
HP	heat pump
HST	heat storage tank
IC	total investment cost
ICC	integrated composite curve
IDA ICE	IDA indoor climate energy
IWH	industrial waste heat
MFH	multi-family house
MILP	mixed-integer linear programming
Mob	mobility
MWP	municipal waste plant
P2G	power to gas
PI	process integration
PV	photo-voltaic
RE/SE	residential/service existing
REF	refrigeration
RN/SN	residential/service new
RR/SR	residential/service renovated
SC	self-consumption
SF	self-sufficiency
SFH	single-family house
SH	space heating
SOEC	solid oxyde electrolysis cell
SOFC	solid oxyde fuel cell
ST	solar thermal
VAC	refrigeration cycle
WT	waste treatment

# List of symbols

## Sets

<b>BT</b>	set of building types
<b>BUC<sub>c</sub></b>	set of building units connected to CO <sub>2</sub> network in commune <i>c</i>
<b>BUR<sub>rs</sub></b>	set of building units of renovation stage <i>rs</i>
<b>BUT<sub>bt</sub></b>	set of building units of type <i>bt</i>
<b>C</b>	set of communes
<b>K</b>	set of temperature intervals
<b>L</b>	set of locations
<b>P</b>	set of periods
<b>PA</b>	set of parents
<b>PORD<sub>rd</sub></b>	set of periods of real day <i>rd</i>
<b>POU<sub>u</sub></b>	set of parents of unit <i>u</i>
<b>PU</b>	set of process units
<b>R</b>	set of resources
<b>RD</b>	set of real days
<b>RS</b>	set of renovation stages
<b>RT</b>	set of real times
<b>RTORD<sub>rd</sub></b>	set of real times of real day <i>rd</i>
<b>S</b>	set of streams
<b>SL<sub>l</sub></b>	set of streams in location <i>l</i>
<b>SOP<sub>pa,l</sub></b>	set of streams of parent <i>pa</i> in location <i>l</i>
<b>SU</b>	set of storage units
<b>T</b>	set of operating times
<b>TOP<sub>p</sub></b>	set of times of period <i>p</i>
<b>TOPNC<sub>p</sub></b>	set of times of period <i>p</i> non cumulative
<b>TORD<sub>rd</sub></b>	set of times of real day <i>rd</i>
<b>U</b>	set of units $U = UU \cup PU$
<b>UU</b>	set of utility units

## List of symbols

### Parameters (MILP)

$\rho$	density	[kg/m <sup>3</sup> ]
$\eta$	efficiency	[-]
$\lambda$	thermal conductivity	[W/(m · K)]
$\phi_b^{\text{sun}+0}$	stochastic gains from solar and occupancy sources of building $b$	[kW]
$\sigma$	self-discharge rate	[-]
$A$	area	[m <sup>2</sup> ]
$a_1, a_2$	heat transmission coefficients	[W/(m <sup>2</sup> ·K)/W/(m <sup>2</sup> ·K <sup>2</sup> )]
$c_1, c_2$	network cost parameters	[€/m <sup>2</sup> ], [€]
cap	capita	[-]
$C_b$	capacity of building $b$	[kW/K]
$C^{\text{el}, +}$	cost of electricity export	[€/h]
$C^{\text{el}, -}$	cost of electricity import	[€/h]
$C_u^{\text{inv}, 1}$	fixed investment cost of unit $u$	[€/y]
$C_u^{\text{inv}, 2}$	variable investment cost of unit $u$	[€/y]
$C_u^{\text{op}, 1}$	fixed operating cost of unit $u$	[€/h]
$C_u^{\text{op}, 2}$	variable operating cost of unit $u$	[€/h]
$c_p$	specific heat	[kJ/(kg · K)]
$D_h$	hydraulic diameter	[m]
$D$	diameter	[m]
$d$	distance	[km/(cap year)]
$E$	fuel consumption	[kWh/km]
$E_e$	electricity export	[kW]
$E_g$	electricity generation	[kW]
$EI_u^1$	fixed environmental impact of unit $u$	[kgCO <sub>2</sub> /h]
$EI_u^2$	variable environmental impact of unit $u$	[kgCO <sub>2</sub> /h]
$E_i$	electricity import	[kW]
$f^{\text{an}}$	annualisation factor	[1/y]
ff	friction factor	[-]
$f^{\text{glass}}$	fraction of irradiation passing through PV glass	[-]
$f_u^{\text{max}}$	maximum sizing factor of unit $u$	[-]
$f_u^{\text{min}}$	minimum sizing factor of unit $u$	[-]
$H'/H$	corrected/actual pipe depth	[m]
$h$	convective heat transfer coefficient	[W/(m <sup>2</sup> ·K)]
$i$	interest rate	[-]
$I$	global solar irradiation	[W/m <sup>2</sup> ]
$k_1, k_2$	heat signature parameters	[-]
$L$	length	[m]



## List of symbols

---

$l_t$	lifetime	[y]
$L^v$	latent heat of vaporisation	[kJ/kg]
$\dot{m}_{r,u,t}^-$	reference output flow of resource $r$ of unit $u$ in time step $t$	[kW]
$\dot{m}_{r,u,t}^+$	reference input flow of resource $r$ of unit $u$ in time step $t$	[kW]
$N$	number	[-]
$p_p^{\text{occ}}$	period occurrence of period $p$	[-]
$\Delta P$	pressure drop	[bar]
$q$	specific heat demand	[kWh/m <sup>2</sup> ]
$\dot{q}$	heat loss	[W]
$\dot{q}_{s,t,k}$	reference heat flow from to stream $s$ in temperature interval $k$ in time step $t$	[kW]
$\dot{q}_{u,t,k}$	reference heat flow from to unit $u$ in temperature interval $k$ in time step $t$	[kW]
$r$	ratio	[%]
$R$	thermal resistance	[K/W]
$R_b^{\text{int}}$	internal insulation resistance of building $b$	[K/kW]
$SL_u^{\text{max}}$	maximum storage level of unit $b$	[-]
$SL_u^{\text{min}}$	minimum storage level of unit $b$	[-]
$T$	temperature	[K]
$\Delta T^{\text{min}}$	minimum temperature difference	[°C]
$t_t^{\text{op}}$	operating time in time step $t$	[h]
$U$	thermal transmission coefficient	[W/(m <sup>2</sup> ·K)]
$v$	velocity	[m/s]

### Variables (MILP)

$b_{pa,l,t}$	sizing factor of parent $pa$ in location $l$ and time step $t$	[-]
$\dot{E}l_{u,t}^-$	supply of electricity of unit $u$ in time step $t$	[kW]
$\dot{E}l_{u,t}^+$	demand of electricity of unit $u$ in time step $t$	[kW]
$f_u$	sizing factor of unit $u$	[-]
$f_{u,p,t}''$	sizing factor of unit $u$ in period $p$ and time step $t$	[-]
$f_{u,t}'$	sizing factor of unit $u$ in time step $t$	[-]
$g_{s,t}$	sizing factor of stream $s$ in time step $t$	[-]
$\dot{M}_{r,u,t}^-$	supply of resource $r$ of unit $u$ in time step $t$	[kW]
$\dot{M}_{r,u,t}^+$	demand of resource $r$ of unit $u$ in time step $t$	[kW]
$\dot{R}_{t,k,l}$	residual heat flow in time step $t$ in temperature interval $k$ / in location $l$	[kW]
$\dot{R}_{t,k}$	residual heat flow in time step $t$ in temperature interval $k$	[kW]
$\dot{S}L_t$	storage level in time step $t$	[kW]
$y_u$	integer variable to use unit $u$ or not	[-]
$y_{u,p,t}''$	integer variable to use unit $u$ or not in period $p$ and time step $t$	[-]
$y_{u,t}'$	integer variable to use unit $u$ or not in time step $t$	[-]

**Superscripts**

ad	adiabatic
amb	ambient
b	building type
ch	charging
comp	compressor
cond	condensor
dch	discharging
dd	degree days = HDD/CDD
el	electrical
ERA	energy reference area
evap	evaporator
footpr	footprint
g	ground
geoth	geothermal
h	heating
i	insulating material/insulation
int	internal
liq	liquid
0	dimensioning
p	pipe
r	return
ref	reference
s	supply
th	thermal
v	energy service = SH/AC
vap	vapor
var	variable

**Indexes**

<i>b</i>	building
<i>bt</i>	building type
<i>bu</i>	building unit
<i>c</i>	commune
<i>k</i>	temperature interval
<i>l</i>	location
<i>p</i>	period

## List of symbols

---

<i>pa</i>	parent
<i>pr</i>	period of real day
<i>pu</i>	process utility
<i>r</i>	resource
<i>rd</i>	real day
<i>rs</i>	renovation stage
<i>s</i>	stream
<i>t</i>	time step
<i>u</i>	unit



# Introduction

*"If you can't explain it simply, you don't understand it well enough."*

Albert Einstein

## Overview

- Context and motivation;
- Contributions and novelty;
- Mathematical formulation.

Global quality of human life has increased in the last centuries, leading not only to raised comfort standards, but also to high energy demands for residential services. According to the World Bank [3] over 50% of the global population lives in urban areas today and by 2045 this percentage is expected to increase 1.5 times. Consequently, energy consumption in urban areas and the resulting environmental impact are becoming increasingly challenging. Nevertheless, improving the efficiency of energy distribution and use in buildings is regarded as one of the greatest potentials to reduce greenhouse gas emissions [4]; however, it is crucial to develop highly efficient energy conversion and dispensation technologies to satisfy thermal services in densely-populated areas.

District energy networks (DENs) are networks of pipes that connect buildings with each other, with centralized energy conversion technologies, and other energy-providing units. They allow the valorization of all available energy sources in a given area, such as heat from the environment, industrial excess heat [5], geothermal energy, or solar energy [6]. DENs also play an important role in the increase of energy efficiency in densely-populated areas.

## Evolution of district energy networks

The first generation (1G) district heating network (DHN) used steam as the main energy vector and heat was delivered by steam condensation in radiators [7]. The main reason behind introducing this system was to replace individual boilers in buildings to reduce the risk of boiler explosion [8]. They were first developed in the USA in the 1880s and were the dominant technology in the USA and Europe until the 1930s; they are still used in some places, such as New York and Paris. The first generation district cooling systems, introduced in the end of the 19th century, used centralized

condensers, decentralized evaporators, and refrigerants as fluids [9].

The second generation (2G) of district heating (DH) systems used pressurized water as the main heat carrier. The supply temperature of these networks was generally above 100°C [10, 11]. They entered the market in the 1930s and were used until the 1970s. The motivation behind this technology varied between countries, but generally the driving factors were higher comfort level and reduced fuel consumption (achieved by using co-generation heat and power (CHP) units). The corresponding generation of cooling systems introduced in the 1960s was based on large scale mechanical chillers and used cold water as a fluid.

Third generation (3G) heating systems also used pressurized water as the heat carrier, but with a reduced supply temperature. The technology was developed after concerns related to energy supply due to the two oil crises, which led to an interest in increasing the energy efficiency of CHPs and replacing oil by other fuels such as coal, waste, or biomass [12, 13]. The third generation cooling networks which emerged in the 1990s also used cold water as the heat transfer fluid. However, they had a wider selection of utilities compared to the second generation, among which were absorption chillers, mechanical chillers, and direct cooling with various sources such as lakes, cold streams or cold storage.

Described by Lund et al. [8], the fourth generation (4G) DEN was introduced as a network which should have "lower distribution temperatures, assembly-oriented components, and more flexible pipe materials". The main motivation behind a new generation of DEN is the movement towards a sustainable energy system. This network should be able to supply low temperature heating with low grid losses, recycle heat from low temperature heat sources, integrate renewable energy sources (e.g. geothermal, solar thermal), and integrate with smart energy systems. The equivalent district cooling system has been suggested as a third generation system, better integrated with the electric, heating, and gas grids [8]. Several fourth generation networks are in various project/realization stages, such as GeniLac [14], the anergy network at ETH [15] or the Geneve-Lac-Nation project [16]. To date, 4G networks have not considered the possibility of a combined heating and cooling network, which allows for the entry of 5G (refrigerant-based) networks, which are extensively discussed in this thesis. 5G district energy networks are networks which provide heating and cooling at the same time by distributing the environment. Moreover, they use decentralised heat pumps to upgrade the temperature of the heat to the temperature of demand of each individual user, they are able to harvest heat at the temperature of the environment and can be coupled with advanced technologies for long/term energy storage.

Refrigerant-based district energy networks are still at research stage; they rely on the latent heat of evaporation/condensation of a refrigerants to collect and transfer heat across the network. Weber et al. [17] introduced the concept of distributing CO<sub>2</sub> in the DHN at a temperature below the critical pressure of 74 bar. A more detailed description of the refrigerant based network that uses CO<sub>2</sub> as

the heat transfer fluid is given by [17] and possible energy services and corresponding conversion technologies for refrigerant-based networks have been investigated by [18–20]. Compared to current technologies in place, CO<sub>2</sub> networks have been shown to reduce energy consumption by up to 84% [18]. The purpose of 5G DENs includes distributing heat at the temperature of environment with low temperature lifts and low exergy losses, addressed by the usage of individual decentralised heat pumps; harvesting heat and electricity, achieved by coupling the network to heat harvesting units (harvesting heat from lakes, from the ground, or from other waste heat sources) and to PV panels; and managing and balancing the network, realised by coupling it to a power to gas long-term energy storage system (see Figure 1).

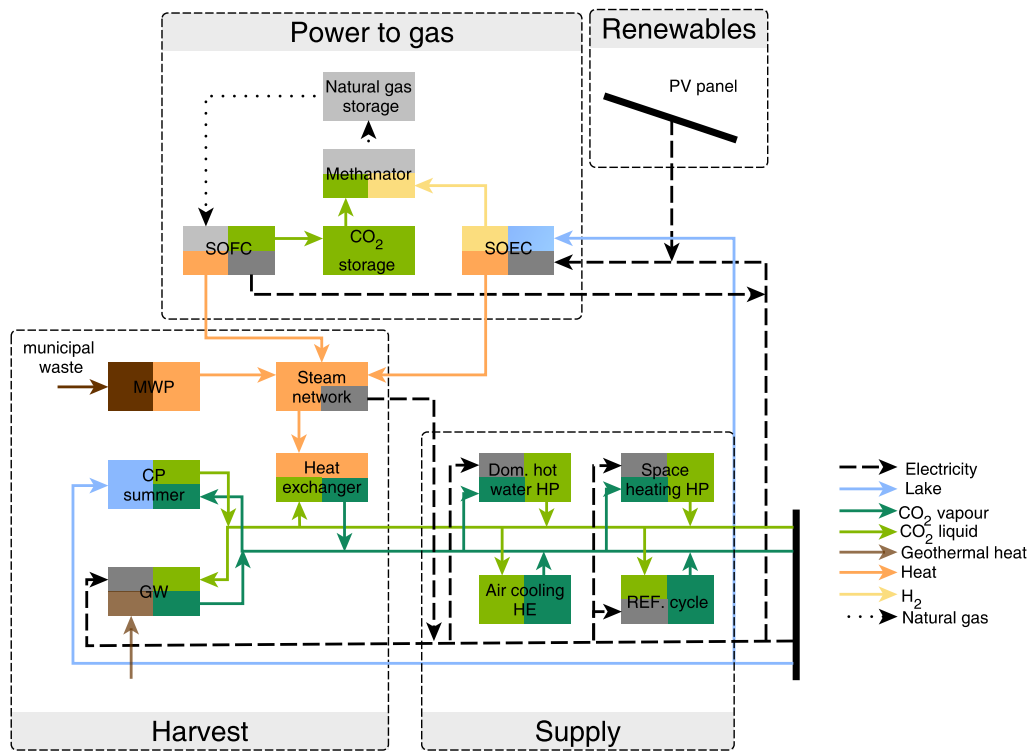


Figure 1 – 5G DHC concept.

The main research gaps for integrating 5G DENs are, 1) a systematic and replicable way to define urban energy demand; 2) a network which combines district heating and cooling while maximising the direct use of electricity, managing the excess electricity production and using waste and valorising resources up to the temperature of environment; 3) an integrated method to recover excess industrial heat for district heating applications, with a detailed implementation (system design, economic and environmental impact); 4) the interaction between the building and urban scale optimization and a good understanding of the self/consumption in integrated systems using 5G DENs. These gaps are addressed in this thesis by 1) providing a parameterized residential and service sector profile for any European city; 2) valorizing lake, ground and waste heat using 5G

DENs and integrating 5G DENs with power to gas for energy management; 3) building on the sector profile proposed in Chapter 1 by adding production data for 10 different industries and studying the economic and environmental impact of recovering EIH while considering the locations of the industrial facilities and the expected heat losses; 4) proposing a method which performs a detailed multi/level energy integration optimization, where the link between the building and the urban scale is the 5G DEN and meta-models are used to embed optimal building solutions into the urban-level optimization

### **Heat pumping technologies integration with district energy networks**

Besides DENs, energy conversion technologies also play an important role in the efficiency of energy systems. According to thermodynamic laws (i.e. Carnot's second law of thermodynamics), if heat has to be provided at 20°C using a source at 0°C, only one unit of electricity is required to supply 10 units of useful heat, while the rest of the energy can be harvested from the environment. Considering this in contrast to current approaches of supplying heat, clear flaws are observed in the concept of purchasing 11 units of energy in the form of natural gas to provide the required 10 units of useful heat, releasing excess heat to the environment and emitting CO<sub>2</sub>. The technological solution to overcome this flaw is to employ heat pumps (HPs), which harvest heat in the environment and deliver it in buildings, at a temperature appropriate to the demand.

Heat pump technologies have been integrated with low-temperature district energy networks and optimized for a dense urban area in Switzerland [18]. The results show that, while the current network in place requires 59.8 GWh/year of heating oil and 10.5 GWh/year of electricity to supply the heating and cooling requirement of the city center of Geneva, a potential low-temperature 5G DEN would require only 11.0 GWh/year of electricity (and no heating oil) to satisfy the same demand.

HPs have also been integrated in smaller systems, at building scale, together with PV panels and energy storage units, in the search for self-sufficient buildings [21]. However, their full potential has not been exploited, i.e. harvesting heat at ambient temperature, employing trans-critical cycles for optimal performance, integration with advanced technologies for energy storage.

This section represents the introduction (context) and motivation of the thesis. The main contributions and novelty of each chapter are presented in the following section, while the general mathematical formulation used is addressed in the final section of the chapter.

### **Contributions and novelty**

The main chapters of the thesis are presented, following four main research questions.



## Chapter 1: Estimating urban energy demand

*"How do we estimate urban energy demand?"*

In scientific literature the potential of low temperature refrigerant-based networks has only been addressed in the context of densely-populated urban areas in Switzerland. This chapter primarily aims at expanding the scope of this study by assessing potentials in cities within different European climate zones; however, estimating urban energy demand is a challenging task, since the demand is influenced by a variety of factors, such as system size, location, weather conditions, architectural design, energy systems used, and occupancy. Consequently, the second aim of the chapter is to provide a geographically parameterized residential energy sector profile, for demands such as space heating (SH), domestic hot water (DHW), air cooling (AC), refrigeration (REF), electricity (EL) for appliances, waste treatment (WT) and mobility (Mob).

The work uses heat signature models and climate data to build the parameterized residential sector profile for different climatic zones in Europe. The profile is also suited to evaluate optimal energy conversion technologies to supply residential requirements, by applying process integration (PI) techniques within a mixed-integer linear programming (MILP) formulation.

## Chapter 2: Valorizing natural resources and human waste

*"How do we valorize urban renewable resources?"*

5G district energy networks have so far been deployed as heat pump-based district heating and cooling (DHC) systems in dense urban areas. One of the most important characteristics of refrigerant-based networks is that leveraging the refrigerants' latent heat reduces the cost of heat distribution, while allowing recovery of waste heat which is typically rejected to the environment. This chapter assesses the best valorization options for renewable resources available in urban areas, using 5G DHC networks. More specifically, it considers:

- valorization of thermal energy stored in water reservoirs: integration of centralized HPs which balance the network and harvest heat in the environment (from fresh water sources, e.g. lakes);
- geothermal energy valorization: integration of geothermal well (GW)/geothermal heat pumps which balance the network and harvest heat from the environment (geothermal heat);
- waste valorization: integration of waste boiler/steam network systems to incinerate inorganic municipal waste and produce electricity and low temperature heat. The low temperature heat is used either for direct heating or to vaporize CO<sub>2</sub>;
- solar energy valorization: integration of PV panels to harvest solar energy and produce electricity. Given that the DEN is fully electrical when heat pumps are installed throughout the

system, this integration also highlights the autonomy potential for the urban areas studied.

### **Chapter 3: Valorizing excess industrial heat (EIH)**

*"How do we valorize excess industrial heat?"*

Extensive research focuses on heat recovery within the industrial sector. Excess heat can either be recovered and reused on site to increase energy efficiency, or converted to cold, electricity, or heat at different temperatures and then used for other applications, such as residential district energy systems. To study the potential of EIH valorization, production data for ten different industries are added to the parameterized sector profile defined in chapter 1. The industries considered are cement, oil refining, aluminum, steel, brewing, pulp and paper, sugar, plastic, waste incineration and dairy products. Previously-developed industrial blueprints are used to build the parameterized industrial sector profile for a typical (average) European city.

This chapter also looks at EIH valorization in a real city — Rotterdam — and the oil refineries, cement plants and breweries present in its industrial port.

### **Chapter 4: Systematic integration of energy- optimal buildings with district networks**

*"How do we bridge the gap between building scale and district scale analysis?"*

The fourth chapter considers a refined temporal and spatial resolution for analysis of urban energy systems. Temporally, the previous chapters consider monthly averages, while this chapter considers a more precise temporal resolution using a typical daily profile; therefore, introducing hourly variation to the problem of system design and operation. Spatially, the previous chapters look at typical cities, while this chapter studies simultaneous optimisation of individual buildings and districts by using a double-optimisation approach with meta-models at the building scale. The optimisation includes interactions between the two scales, renewable energy integration and long-term energy storage solutions.

Additionally, this chapter studies the penetration of 5G DENs with energy distribution (i.e. network) cost, population and building density.

### **Mathematical formulation**

Solving simultaneously the design and operation of complex flowsheets is a challenging task, which can be achieved, in a first approach, by process integration. PI techniques [22, 23] based on pinch analysis methods [24] are a mature technology to evaluate the optimal thermo-economic size and operation of steady-state heat and power systems, without examining in detail the complexity of

the heat exchanger configuration. Since the introduction of mixed-integer linear programming to model heat and material balances, design equations and physical and logical constraints [25], the methodology has been subject to continuous developments [26, 27]. For instance, multi-period problems can be solved as a succession of steady-state operations assuming constant or piece-wise linearized costs and efficiency parameters around the equipment range of operation [28].

### Definition of sets

The optimisation problems solved throughout the thesis are defined using discrete monthly time intervals, e.g.  $t \in \mathbf{T} = \{1, 2, \dots, 12\}$ . The system to be optimized is represented through a number of units, belonging to the set  $\mathbf{U}$ . The units are grouped in two subsets: the set of utility units ( $\mathbf{UU} = \{\text{boilers, refrigeration cycles, electrical heaters, HPs, heat exchanger (HE)s, CHPs, PV panels, ST panels}\}$ ) and the set of process units ( $\mathbf{PU} = \{\text{urban demands: space heating, domestic hot water, air cooling, refrigeration, electricity for utilities, mobility, waste treatment; industrial processes: oil refinery, cement production, beer production}\}$ ). The process units represent production demands and hence have a fixed size, while the utility units are technologies which satisfy these demands, with variable sizes, which are to be optimized. Units supply, demand, or convert resources ( $r \in \mathbf{R}$ ) (electricity and material) and heat (at different temperature intervals  $k \in \mathbf{K}$ ).

### Objective function and constraints

The problems use different objective functions, such as minimization of operating cost (Eq. 1), minimization of investment cost (Eq. 2) or minimization of environmental impact (Eq. 3). Economic calculations account for fixed ( $C_u^{\text{op},1}$ ,  $C_u^{\text{inv},1}$ ,  $\text{EI}_u^1$ ) and variable ( $C_u^{\text{op},2}$ ,  $C_u^{\text{inv},2}$ ,  $\text{EI}_u^2$ ) operating costs, investment costs and environmental impacts. The environmental impact indicator considered in this thesis is overall greenhouse gas emissions. Emissions are based on background databases for the resources which satisfy energy demands of the city and industrial sites (i.e. electricity and fossil fuels). The additional terms involved in the objective functions are the integer ( $y'_{u,t}$ ,  $y_u$ ) variables which dictate the usage of each unit, the continuous variables ( $f'_{u,t}$ ,  $f_u$ ) which determine the size of a unit in each time step  $t$ , and the operating time parameter ( $t_t^{\text{op}}$ ).

$$\min_{y_u, f_u} \sum_{u \in \mathbf{U}} \left( \sum_{t \in \mathbf{T}} \left( C_u^{\text{op},1} \cdot y'_{u,t} + C_u^{\text{op},2} \cdot f'_{u,t} \right) \cdot t_t^{\text{op}} \right) \quad (1)$$

$$\min_{y_u, f_u} \sum_{u \in \mathbf{U}} \left( C_u^{\text{inv},1} \cdot y_u + C_u^{\text{inv},2} \cdot f_u \right) \quad (2)$$

$$\min_{y_u, f_u} \sum_{u \in \mathbf{U}} \left( \sum_{t \in \mathbf{T}} (\text{EI}_u^1 \cdot y'_{u,t} + \text{EI}_u^2 \cdot f'_{u,t}) \cdot t_t^{\text{op}} \right) \quad (3)$$

Parametric optimisation on operating cost (Eq. 4), investment cost (Eq. 5) and environmental impact (Eq. 6) are used to systematically generate multiple solutions to the integration problem. This method defines limits on each objective and a step-size between ( $\epsilon$ ) which therefore generates multiple solutions using secondary and tertiary objectives as implied boundaries. This approach is often referred to as applying  $\epsilon$ -constraints, referring to the step-size for the alternative objectives [29].

$$\sum_{u \in \mathbf{U}} \left( \sum_{t \in \mathbf{T}} (C_u^{\text{op},1} \cdot y'_{u,t} + C_u^{\text{op},2} \cdot f'_{u,t}) \cdot t_t^{\text{op}} \right) \leq \epsilon \quad \epsilon \in [C_{\min}^{\text{op},2}, C_{\max}^{\text{op},2}] \quad (4)$$

$$\sum_{u \in \mathbf{U}} (C_u^{\text{inv},1} \cdot y_u + C_u^{\text{inv},2} \cdot f_u) \leq \epsilon \quad \epsilon \in [C_{\min}^{\text{inv},2}, C_{\max}^{\text{inv},2}] \quad (5)$$

$$\sum_{u \in \mathbf{U}} \left( \sum_{t \in \mathbf{T}} (\text{EI}_u^1 \cdot y'_{u,t} + \text{EI}_u^2 \cdot f'_{u,t}) \cdot t_t^{\text{op}} \right) \leq \epsilon \quad \epsilon \in [\text{EI}_{\min}^2, \text{EI}_{\max}^2] \quad (6)$$

The main constraints of the problem include the energy conversion technology sizing and selection. Equations 7a and 7b set the size of the unit in each time smaller than the purchase size of the equipment. Eq. 7c ensures that the purchase size of the equipment is between the minimum and maximum boundaries set ( $f_u^{\min}, f_u^{\max}$ ), and Eq. 7d and 7e fix the size of the process units ( $pu$ ).

$$y'_{u,t} \leq y_u \quad \forall u \in \mathbf{U}, \forall t \in \mathbf{T} \quad (7a)$$

$$f'_{u,t} \leq f_u \quad \forall u \in \mathbf{U}, \forall t \in \mathbf{T} \quad (7b)$$

$$f_u^{\min} \cdot y'_{u,t} \leq f'_{u,t} \leq f_u^{\max} \cdot y'_{u,t} \quad \forall u \in \mathbf{U}, \forall t \in \mathbf{T} \quad (7c)$$

$$y'_{u,t} = 1 \quad \forall u \in \mathbf{PU}, \forall t \in \mathbf{T} \quad (7d)$$

$$f_u^{\min} = f_u^{\max} = 1 \quad \forall u \in \mathbf{PU} \quad (7e)$$

**Heat cascade** The heat cascade equations ensure that heat is transferred from higher temperature intervals to lower temperature intervals and close the energy balance in each temperature interval  $k$  (Eq. 8a). This is achieved using the residual heat  $\dot{R}_{t,k}$ , which cascades excess heat from higher temperature intervals ( $k$ ) to lower temperature intervals ( $k - 1$ ). The minimum residual heat is zero, where heat cannot be transferred from the corresponding temperature interval to lower ones (Eq. 8b). Similarly, residual heat in the first interval ( $\dot{R}_{t,1}$ ) is zero, as lower temperature intervals do not exist to accept a transfer of heat. Logically, heat cannot be cascaded to the  $k^{\text{th}}$  interval as it is the highest, so  $\dot{R}_{t,k+1}$  is also zero (Eq. 8c).  $\dot{q}_{u,t,k}$  represents the reference heat load of a unit  $u$  in time step  $t$  and temperature interval  $k$ .

$$\sum_{u \in \mathbf{U}} f'_{u,t} \cdot \dot{q}_{u,t,k} + \dot{R}_{t,k+1} - \dot{R}_{t,k} = 0 \quad \forall t \in \mathbf{T}, \forall k \in \mathbf{K} \quad (8a)$$

$$\dot{R}_{t,k} \geq 0 \quad \forall t \in \mathbf{T}, k \in \mathbf{K} \quad (8b)$$

$$\dot{R}_{t,1} = 0 \quad \dot{R}_{t,k+1} = 0 \quad \forall t \in \mathbf{T} \quad (8c)$$

**Mass and resource balance** For each unit  $u$ , the supply  $\dot{M}_{r,u,t}^-$  and the demand  $\dot{M}_{r,u,t}^+$  of a specific resource  $r \in \mathbf{R}$  are computed (Eq. 9a, 9b) and the balance of each resource is closed for each time step  $t$  (Eq. 9c).

$$\dot{M}_{r,u,t}^- = \dot{m}_{r,u,t}^- \cdot f'_{u,t} \quad \forall r \in \mathbf{R}, \forall u \in \mathbf{U}, \forall t \in \mathbf{T} \quad (9a)$$

$$\dot{M}_{r,u,t}^+ = \dot{m}_{r,u,t}^+ \cdot f'_{u,t} \quad \forall r \in \mathbf{R}, \forall u \in \mathbf{U}, \forall t \in \mathbf{T} \quad (9b)$$

$$\sum_{u \in \mathbf{U}} \dot{M}_{r,u,t}^- = \sum_{u \in \mathbf{U}} \dot{M}_{r,u,t}^+ \quad \forall r \in \mathbf{R}, \forall t \in \mathbf{T} \quad (9c)$$



# Estimating urban energy demand

## Overview

- Previous studies focus on urban areas in Switzerland;
- This work takes one step further, by defining a "typical European city".

*This chapter is partially a summary of [30, 31]*

1

The large share of energy consumption in the residential sector has necessitated better understanding and evaluation of its energy needs, with the objective of identifying possible pathways for improvement. This work uses heat signature models and climate data to build a parameterized residential sector profile for different climatic zones in Europe. The sector profile is validated using Rotterdam, NL as a case study and the results show variations from the real energy demand profile of less than 10%, primarily caused by cultural and climatic differences between Rotterdam and the rest of Western Europe. The energy and service profile constructed herein is well-suited for exploring the best technologies for supplying residential requirements, drawing from the domain of process integration. This work demonstrates the usefulness of the residential profile by applying process integration techniques within a mixed-integer linear programming formulation to evaluate optimal energy conversion technologies for different district energy networks. The results show that switching to a fully electric energy providing system can lead to operating cost savings of 48% and CO<sub>2</sub> emission savings up to 100%, depending on the mix of electricity generation.

## 1.1 Introduction

Population growth, improvement of building services and comfort levels, and increased time spent inside buildings have led to a significant rise in building energy consumption. More specifically, energy consumption in the residential sector represents between 16-50% of national totals, varying by country, and averages 30% worldwide [32] (Figure 1.1). Given the large share of energy consumption in the residential sector and energy policies implemented worldwide in the past decades (e.g. Europe 20-20-20 [33]), a better understanding of the defining characteristics of residential energy consumption is clearly required.

Energy systems in buildings are very complex, especially given the variety of energy demands and

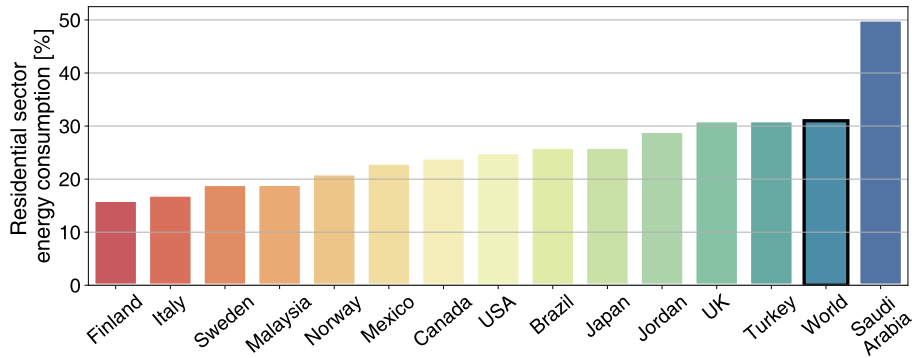


Figure 1.1 – Residential sector energy consumption by country.

1

building types. The energy demands typically considered are heating, cooling, hot water and electricity consumption and the main building types are administrative, residential and industrial [34]. Size and location are also key factors for energy consumption in the residential sector, for example small flats require less energy since they have less heat transfer area and fewer occupants. The amount and type of energy used in this sector are also related to weather conditions, architectural design, energy systems used, economic level and occupants. For instance, energy consumption in OECD countries is much greater than in emerging economies and forecasts show continued growth caused by installation of new appliances, such as air conditioners or computers [35].

Given the complexity of these energy systems, accurately predicting consumption is very difficult. A variety of approaches have been proposed for energy demand forecasting, varying from building sub-systems to regional or national models, which are reviewed in more detail in the following section.

## 1.2 State of the art

Estimates of residential sector energy consumption are typically published by governments, which compile values from energy providers [36]; however, these values may be inaccurate as they do not account for on-site generation. Methods which provide more detailed information are desirable, conducting house surveys [37] for example, but also have limitations such as data collection difficulties and cost. Billing data and surveys have been used to develop the residential sector consumption profiles, but they highly depend on the purpose of the model. The main approaches for residential energy demand models can be classified as top-down and bottom-up [38]. Figure 1.2 displays schematically the idea behind bottom-up and top-down approaches and Table 1.1 describes their advantages and limitations.

Top-down approaches generally aim at fitting data such as national energy consumption or CO<sub>2</sub>



## 1.2. State of the art

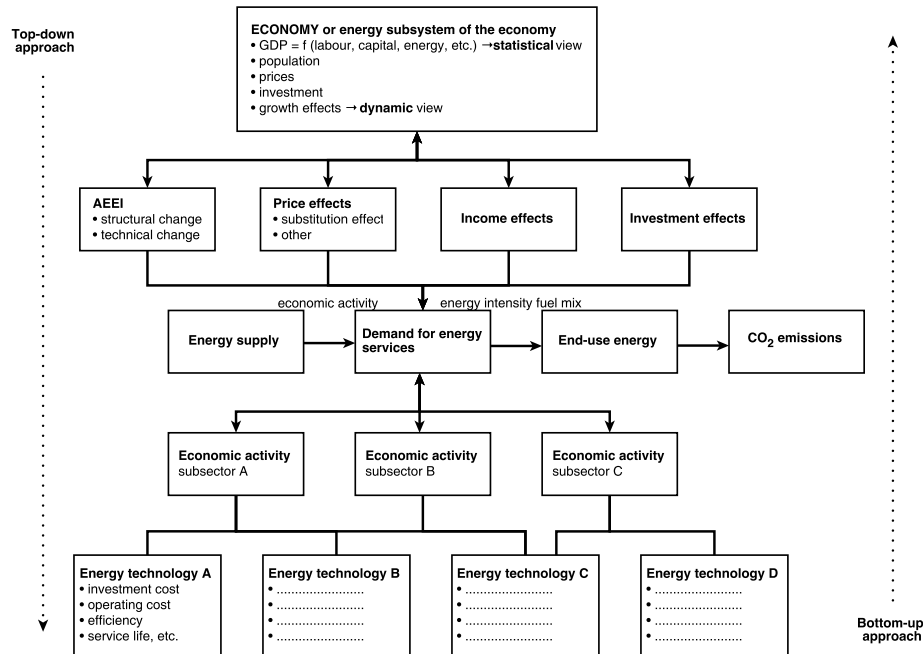


Figure 1.2 – Top-down and bottom-up approaches (adapted from [1]).

emissions. They are typically used to investigate the connection between the energy and economic sectors and can be categorized as econometric or technological [1]. Econometric models evaluate energy consumption using variables such as income, gross domestic product or fuel prices and lack details on existing or future technologies, since their aim is to study macroeconomic trends rather than individual building characteristics [39]. The reliance on past energy consumption data might also cause problems when dealing with climate change scenarios, where social, economic and environmental factors are completely different from those experienced in the past. Technological top-down approaches include other factors which impact energy consumption, such as technological progress or structural changes [40].

An econometric top-down model was used to evaluate annual household energy consumption in the UK based on average temperatures and inflation adjusted energy prices [41]. The aim of the model was to allow the public to determine if energy consumption stayed within the model predicted values, given the inputs considered. Zhang et al. [42] developed a top-down approach to examine residential unit energy consumption in China and compared it with the ones of Japan, Canada and the United States of America (USA). Haas and Schipper [38] created a model to quantify the consumer response to the rise in energy prices and in the energy efficiency of different technologies. To summarize, top-down approaches do not distinguish energy consumption of individual users. The information used in these models typically uses macroeconomic indicators, house construction/demolition rates, or climatic conditions. They use data which are widely available and relatively simple, but lack of detail regarding individual user consumption reduces the ability of the model to identify key

Table 1.1 – Advantages and limitations of bottom-up and top-down approaches.

Characteristic	Top-down	Bottom-up	Characteristic	Top-down	Bottom-up
Advantages	Focus on the interaction between the economic and energy sector	Describe current and prospective technologies	Limitations	Depend on past interaction between the economic and energy sector	Poorly describe market interactions
	Avoid detailed technology descriptions	Determine typical end-use energy consumption		Lack technology details	Do not consider the relationship between energy consumption and macroeconomic indicators
	Model the impact of social-cost benefit and emission policies	Enable policies to efficiently target energy consumption		Are not suitable for evaluating technology policies	Require a large amount of data
	Use aggregated economic data	Estimate the minimum cost utility configuration to meet the demand		Rely on a series of assumptions (e.g. efficient markets)	Require large samples

areas where reductions in energy consumption can be achieved.

Bottom-up models are often seen as ways to identify the most economic options to achieve carbon emission targets given the current technologies and processes [43]. Based on the input data and the structure of the model, they are typically classified in statistical and physics-based models [44]. Statistical models are generally based on regression techniques [44, 45] and an extended review of these models can be found in [44]. One example is the Princeton score-keeping method (PRISM), a linear regression model using a year of monthly billing data to create an index of consumption [46], which has been used by the US government and research organizations to study building refurbishment potentials.

Building physics models require a series of input data, such as efficiency and characteristics of

heating systems, building characteristics (walls, floors, windows, doors and their corresponding heat transfer coefficients), energy consumption of appliances, ventilation rates, occupancy levels, outdoor temperatures, etc. Ghedamsi et al. [47] used such an approach to model and forecast the energy consumption in residential buildings until 2040. Fischer et al. [48] presented a modelling approach based on coupling behavioral and energy balance models with stochastic modelling to generate realistic and consistent load profiles for end user demand and Girardin et al. [49] introduced a linear model to determine the thermal power requirements of buildings based on the outdoor temperature and on the heating and cooling threshold temperatures. Bottom-up approaches are thus summarized as those using data from single users, single houses, or groups of houses and extrapolate the data to reach regional or national energy consumption totals. The usual parameters used in these models include building properties, climate properties, occupancy levels and equipment use. The primary drawback of these approaches is the lack of available data and the large number of input parameters, which makes the models complex, and therefore more difficult to solve.

Due to the trade-off between the difficulties of data collection and model complexity, hybrid methods have emerged. This work uses such a method to build a residential sector profile, which provides an estimate of demand for different energy requirements. The time-dependent formulation of the heating and cooling demands is based on [49], while the domestic hot water profile is modelled from demand data of a city. Electricity, refrigeration, mobility and waste treatment are considered constant throughout the year. Parameterized data are provided for all four climate zones in Europe, allowing the sector profile to be applied to any European city. The resulting profile is intended for use in an optimization framework to determine the best utility mix to satisfy the energy demand of a city.

## 1.3 Materials and methods

The residential sector profile consists of district energy and service demands such as space heating, domestic hot water, refrigeration, air cooling, electricity for utilities, mobility and waste treatment. Some of the demand (e.g. electricity) is assumed to be constant throughout a year while heat-related demand is estimated as a function of outdoor air temperature. The profile is parameterized to require only climate zone, building distribution and population. The usability is demonstrated within an MILP framework to find the optimal utility configuration to satisfy the district demand.

### 1.3.1 Service energy demand

The sector profile can be used in different regions, requiring only:

- the population;

- the climate zone: this work considers four climate zones in Europe;
- the building distribution: share of building types (residential and service) and renovation stages (existing, new and renovated) of a reference city.

Among the service energy demands estimated, heating and cooling are built using heat signature models, while domestic hot water follows the real demand of a reference city and electricity, refrigeration, mobility and waste treatment are considered constant throughout the year.

The climate zones are obtained using a classification for net-zero energy buildings [50] based on the Köppen-Geiger classification and on the European heating and cooling indices (EHI, ECI). The European heating and cooling indices are normalized indices, where 100 represents an average European condition. EHI normalization uses 2600 degree-days, corresponding to an annual average outdoor temperature just above 10°C and the ECI is constructed based on similar principles [51]. This classification states that there are four prevailing climatic zones in Europe:

- Csa (Zone 1 & 2): temperate with dry, hot summer;
- Cfb (Zone 3): temperate without dry season and warm summer;
- Dfb (Zone 4): temperate continental/humid continental without dry season and with warm summer;
- Dfc (Zone 5): cold, without dry season and with cold summer.

In this work, the European zones (EZs) are referred to as South (1&2), Central East (CEast, 3), Central West (CWest, 4), and North (5) (Figure 1.3).

The second input required for the model is building distribution. Urban centers are considered to include residential and service buildings, where the latter includes administrative, commercial, education, healthcare, hostel, industrial and other non-residential uses. Three renovation stages are considered for both types, namely:

- existing (built before 2005 and not renovated);
- new (built after 2005);
- renovated.

A typical urban center building distribution (from the city of Geneva) is used as a reference (Figure 1.4) [52].

A series of service energy demands are included in the current sector profile: space heating, domestic hot water, refrigeration, air cooling, electricity (for utilities), mobility, and waste treatment. A heating signature model of a typical urban center is used to evaluate the specific space heating and air conditioning demands ( $q_{v, EZ}$ ,  $v = SH/AC$  [kWh/m<sup>2</sup>]) [49]. However, these demands do not fully represent the demands of an urban center so domestic hot water, electricity, mobility and waste treatment were added to express a more comprehensive list of demands. The model relies on input

### 1.3. Materials and methods

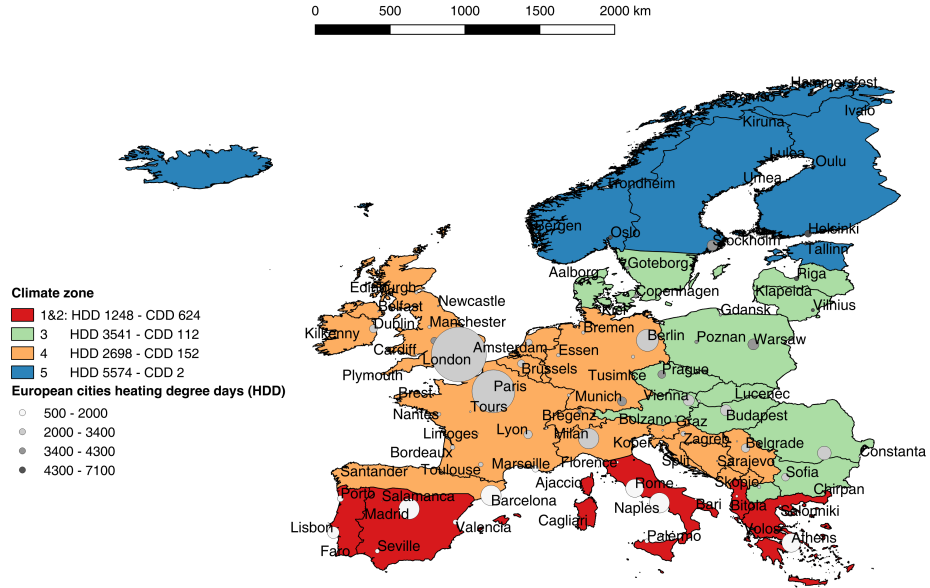


Figure 1.3 – European climate zones.

data for external temperature ( $T^{\text{amb}}$ ) and two linear regression coefficients ( $k_1$  and  $k_2$ ):

$$q_{v, \text{EZ}, b}(t) = k_{1, v, b} \cdot T_{\text{EZ}}^{\text{amb}}(t) + k_{2, v, b} \quad v = \text{SH/AC} \quad (1.1)$$

with

$$k_{1, v, b} = \frac{q_{v, b}^{\text{typical city}}}{\text{dd}^{\text{typical city}}} \quad v = \text{SH/AC, dd} = \begin{cases} \text{HDD,} & \text{if } v = \text{SH} \\ \text{CDD,} & \text{if } v = \text{AC} \end{cases} \quad (1.2)$$

and

$$k_{2, v, b} = -k_{1, v, b} \cdot T_{v, b}^{\text{base}} \quad v = \text{SH/AC} \quad (1.3)$$

where HDD/CDD represent the number of heating/cooling degree days [50] and  $q_{v, b}^{\text{typical city}}$  and  $T_{v, b}^{\text{base}}$  the specific heating and cooling demands [53] and threshold heating/cooling temperatures [49] for the typical urban center and building distribution considered (Geneva, CH) (Figure 1.4). The values of all parameters are given in Table 1.2 and the heating and cooling signatures of the different

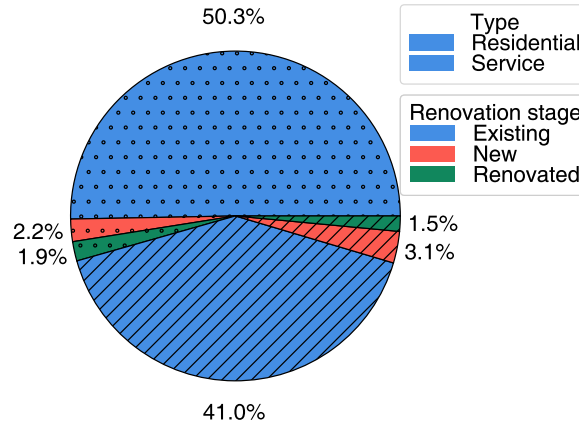


Figure 1.4 – Building distribution of a typical urban center.

Table 1.2 – Heating signature parameters for typical urban center.

Building type (b)	$q_{SH}$ [kWh/m <sup>2</sup> ]	$q_{AC}$ [kWh/m <sup>2</sup> ]	HDD	CDD	$T_{SH}^{base}$ [°C]	$T_{AC}^{base}$ [°C]
Residential Existing (RE)	94.0	0.0	2104	226	15.5	18
Residential New (RN)	42.5	0.0	2104	226	15.5	18
Residential Renovated (RR)	51.4	0.0	2104	226	15.5	18
Service Existing (SE)	78.9	20.1	2104	226	14.2	18
Service New (SN)	35.0	76.9	2104	226	14.2	18
Service Renovated (SR)	41.5	87.9	2104	226	14.2	18

building types and ages are represented in Figure 1.5.

The supply and return temperature calculations for space heating and air cooling are calculated using Eq. 1.4 - 1.7, based on the work of [49]:

$$\alpha_v = \frac{T_v^{s,0} - T^{int}}{T_v^{r,0} - T^{int}} \quad v = SH/AC \quad (1.4)$$

$$(\dot{m}^0 \cdot c_p)_v = \frac{\max(\dot{Q}_v(t))}{T_v^{s,0} - T_v^{r,0}} \quad v = SH/AC \quad (1.5)$$

$$T_{SH}^s(t) = T^{int} - \frac{\dot{Q}_{SH}(t)}{(\dot{m}^0 \cdot c_p)_{SH}} \cdot \frac{\alpha_{SH}}{1 - \alpha_{SH}} \quad (1.6a)$$

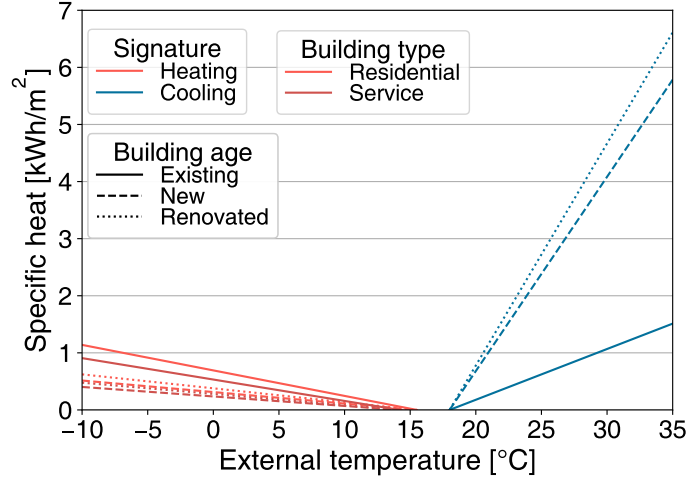


Figure 1.5 – Heating signatures for different building types and ages.

Table 1.3 – Temperature profile parameters.

Parameter	Value [°C]
$T_{SH,0}^s$	65
$T_{SH,0}^r$	50
$T_{AC,0}^s$	12
$T_{SH,0}^s$	17
$T^{int}$	20

$$T_{SH}^r(t) = T_{SH}^{s,0} - \frac{\dot{Q}_{SH}(t)}{(\dot{m}^0 \cdot c_p)_{SH}} \quad (1.6b)$$

$$T_{AC}^r(t) = T^{int} - \frac{\dot{Q}_{AC}(t)}{(\dot{m}^0 \cdot c_p)_{AC}} \cdot \frac{\alpha_{AC}}{1 - \alpha_{AC}} \quad (1.7a)$$

$$T_{AC}^s(t) = T_{AC}^{r,0} - \frac{\dot{Q}_{AC}(t)}{(\dot{m}^0 \cdot c_p)_{AC}} \quad (1.7b)$$

The dimensioning space heating/air cooling supply ( $T_v^{s,0}$ ) and return ( $T_v^{r,0}$ ) temperatures and the indoor comfort temperature ( $T^{int}$ ) are given in table 1.3 [49].

The demand profile for domestic hot water in each time step  $t$  requires the specific demand in each european zone ( $q_{DHW, EZ}$  [kWh/m<sup>2</sup>]) [54]. Real consumption data from a typical urban center

Table 1.4 – Building parameters for a typical urban center.

Building type (b)	$r_b$ [%]	$A_b$ [ $\cdot 10^6$ m <sup>2</sup> ]
Residential Existing	50.3	8.14
Residential New	2.2	0.35
Residential Renovated	1.0	0.31
Service Existing	41.0	6.63
Service New	3.1	0.51
Service Renovated	1.5	0.23

1

$(Q_{DHW}^{typical\ city}(t) \text{ [kW]})$  [55] were used to calibrate Eq. 1.8.

$$q_{DHW, EZ, b}(t) = q_{DHW, EZ, b} \cdot \frac{Q_{DHW}^{typical\ city}(t)}{\sum_{t=1}^N Q_{DHW}^{typical\ city}(t)} \quad (1.8)$$

The supply and return temperature for domestic hot water are assumed constant, at  $T_{DHW}^s = 55^\circ\text{C}$  and  $T_{DHW}^r = 10^\circ\text{C}$  [49]. A constant consumption profile throughout the year is assumed for refrigeration and electricity (Not including the air conditioning load), and the specific demands ( $q_{REF/EL, EZ}$  [kWh/m<sup>2</sup>]) are considered according to [54]. The supply and return temperatures for refrigeration are assumed constant, at  $T_{REF}^s = 1^\circ\text{C}$  and  $T_{REF}^r = 6^\circ\text{C}$  [56]. The demands per capita ( $q_{EZ, b}^{cap}(t)$  [kW/-cap]) are computed using specific demands ( $q_{EZ, b}(t)$  [kWh/m<sup>2</sup>]), total floor area ( $A_b$  [m<sup>2</sup>] [57]), ratio of the different building types ( $r_b$  [%] [57]) and population ( $N^{cap}$  [cap]) of a typical urban center and the number of operating hours ( $N^{hours}(t)$  [h]):

$$q_{EZ, b}^{cap}(t) = \frac{q_{EZ, b}(t) \cdot A_b}{N^{cap} \cdot r_b \cdot N^{hours}(t)} \quad (1.9)$$

The value of the different parameters are given in Table 1.4.

An average distance ( $d_{EZ}$  [km/(cap · y)]) [54] is used to assess the energy requirement for mobility. The waste production ( $m_{WT, EZ}$  [kg/(cap · y)]) [58] is also provided and a constant profile over the year is assumed.

The sector profile, the annual average of the demands per capita for different building types, services, and european zones can be found in Table 1.5 and the composite curves (CCs) for the months of December and July for different european zones are shown in Figures 1.6 and 1.7. The CCs depict the thermal demands provided by the sector profile, such as the variation in the amount and temperature level of thermal energy demands across the climatic zones.



### 1.3. Materials and methods

Table 1.5 – Energy demand per capita for different European zone.

Zone	Building type	SH [kW/cap]	DHW [kW/cap]	AC [kW/cap]	REF [kW/cap]	EL [kW/cap]	Mob [10 <sup>3</sup> km/(cap · y)]	WT [kg/(cap · y)]
South	RE	0.266	0.104	0.000	0.000	0.186	16.5	748
	RN	0.118	0.102	0.000	0.000	0.182	16.5	748
	RR	0.145	0.104	0.000	0.000	0.185	16.5	748
	SE	0.202	0.069	0.235	0.049	0.177	16.5	748
	SN	0.091	0.070	0.918	0.050	0.175	16.5	748
	SN	0.103	0.060	0.993	0.047	0.214	16.5	748
CEast	RE	0.720	0.214	0.000	0.000	0.196	16.5	609
	RN	0.318	0.209	0.000	0.000	0.192	16.5	609
	RR	0.392	0.213	0.000	0.000	0.195	16.5	609
	SE	0.605	0.142	0.084	0.049	0.187	16.5	609
	SN	0.275	0.143	0.330	0.050	0.175	16.5	609
	SN	0.308	0.123	0.357	0.047	0.214	16.5	609
CWest	RE	0.500	0.182	0.000	0.000	0.254	17.9	689
	RN	0.221	0.178	0.000	0.000	0.248	17.9	689
	RR	0.272	0.181	0.000	0.000	0.252	17.9	689
	SE	0.396	0.121	0.072	0.049	0.241	17.9	689
	SN	0.180	0.122	0.281	0.050	0.238	17.9	689
	SN	0.202	0.105	0.304	0.047	0.257	17.9	689
North	RE	1.076	0.288	0.000	0.000	0.264	23.5	861
	RN	0.475	0.281	0.000	0.000	0.258	23.5	861
	RR	0.585	0.286	0.000	0.000	0.262	23.5	861
	SE	0.925	0.191	0.022	0.049	0.251	23.5	861
	SN	0.420	0.193	0.088	0.050	0.247	23.5	861
	SN	0.471	0.166	0.095	0.047	0.267	23.5	861

1

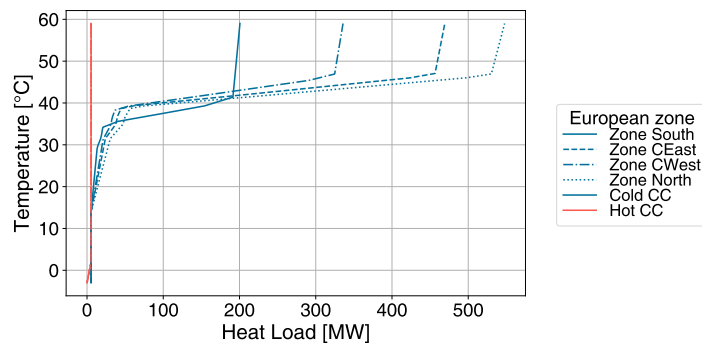


Figure 1.6 – Composite curves (heating and cooling demand) for different European zones, December.

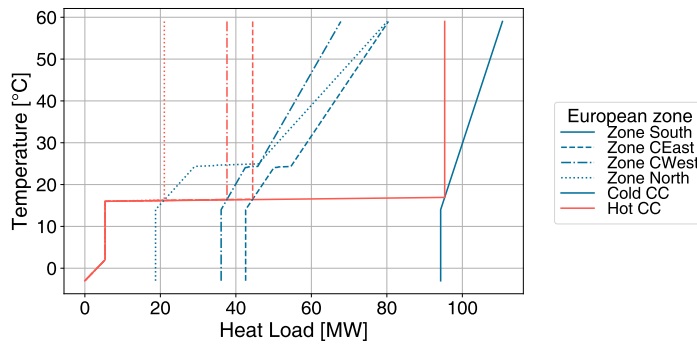


Figure 1.7 – Composite curves (heating and cooling demand) for different European zones, July.

### 1.3.2 Sector profile validation

The residential sector profile presented in Section 1.2 must first be validated before utilization in process integration problems. Validation was previously completed using the city of Geneva, CH [30], but should be performed for other cities as well to ensure broad applicability and replicability. Thus, validation is also completed here for the city of Rotterdam, NL, which is the location of the case study for this work. Such validation requires the real energy demand of Rotterdam from [59] to compare well with the demand obtained using the sector profile. Figure 1.8 displays the quantities of resources consumed for each energy service (e.g. heating, utilities, mobility) based on data gathered from Rotterdam, while figure 1.9 shows the corresponding results obtained using the sector profile. The Sankey diagrams show service demands on the right and the supply for these services on the left; thus, the current demand for heating in Rotterdam is 5077 MWh annually and is supplied by natural gas, oil, central heating and electricity according to the source mix shown in Figure 1.8. Overall, the energy service profile obtained using the proposed sector profile is very similar to the real energy consumption profile of Rotterdam [59]. Deviations for different services vary between 3% for electricity and 8% for mobility. The real consumption profile shows lower energy consumption for mobility since the average distance per inhabitant per year is 16666 km [60] in Rotterdam, compared to the average western European value of approximately 18000 km. The real consumption profile also shows higher energy consumption for heating, which is attributed to the average ambient temperature of Rotterdam being lower than the western European average.

### 1.3.3 MILP formulation

The profile is suited for finding the best energy technologies to supply the required services. This can be achieved using process integration techniques based on a mixed-integer linear programming formulation [61], as explained in detail in the introduction.

### 1.3. Materials and methods

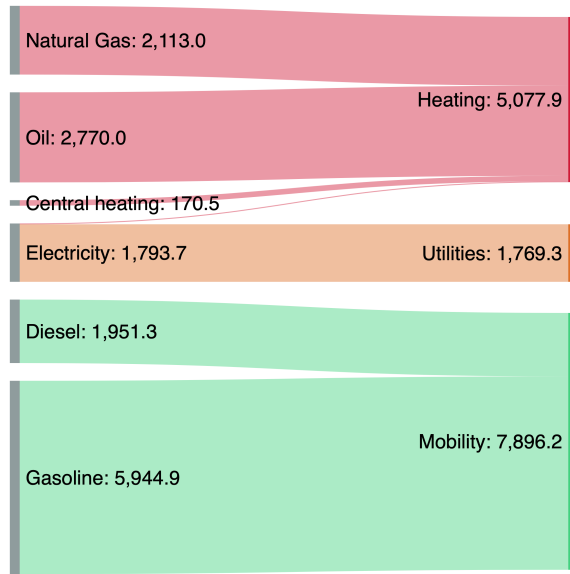


Figure 1.8 – Real profile resource consumption in Rotterdam [MWh].

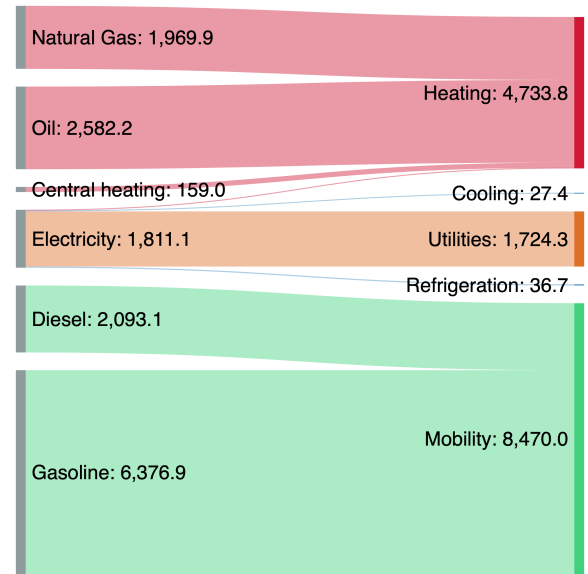


Figure 1.9 – Sector profile resource consumption in Rotterdam [MWh].

#### 1.3.4 City service optimization scenarios

The sector profile is validated using a typical European urban center, namely the city of Rotterdam ( $N_{cap} = 630\,000$ , climate zone: central west), using a monthly resolution. The utilization of the sector profile is exemplified using:

- Scenario 1: the existing water/air-based network;
- Scenario 2: an improved water/air-based network;
- Scenario 3: a potential low-temperature, refrigerant-based DHC network;
- Scenario 4: an improved refrigerant-based network.

The first scenario assesses the current system using water and air as the main heat transfer fluids. In this case, two independent loops are used: a water loop for heating at 90°C and an air loop for cooling at 25°C. This network uses a mix of natural gas boilers, oil boilers, electrical heaters, and centralized district heating to provide heating services, refrigeration cycles to provide cooling services, and a mix of diesel and gasoline for mobility (Figure 1.10).

The second scenario is also based on the current system, using water and air as the main heat transfer fluids. It includes all utilities present in the first scenario, but optional additional technologies such as co-generation heat and power units, heat pumps using lake water as a heat source, solar thermal panels, photo-voltaic panels and electrolyzers which produce hydrogen for mobility. The additional utilities are represented schematically in Figure 1.11.

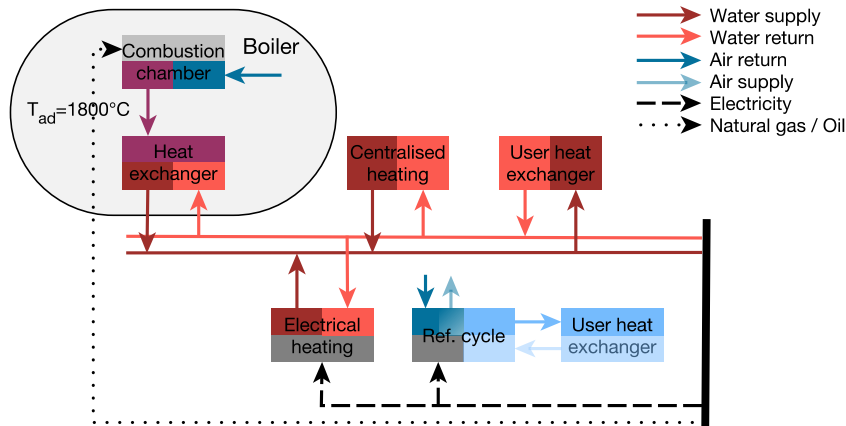


Figure 1.10 – Schematic description scenario 1.

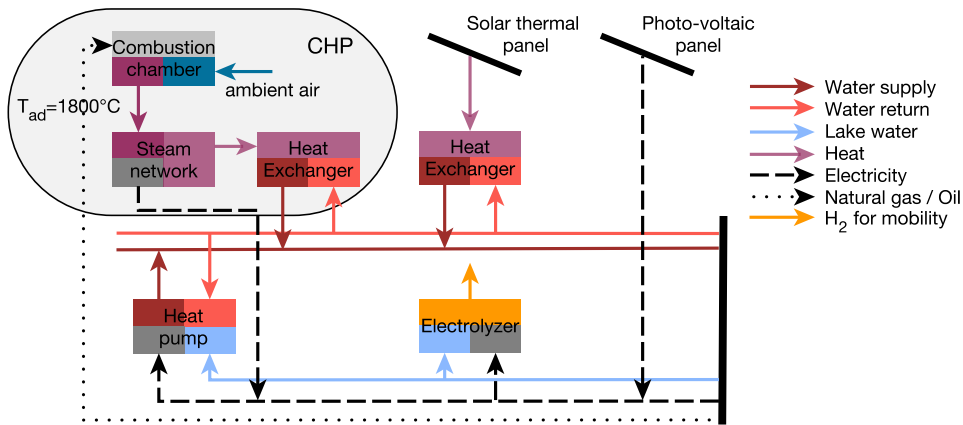


Figure 1.11 – Schematic description of additional utilities in scenario 2.

The third scenario includes a potential future 5G district energy network as the principle heat transfer fluid. This network has a single loop: a vapor line at  $15^{\circ}\text{C}$  and a liquid line at  $13^{\circ}\text{C}$ . Unlike water-based networks, 5G networks use phase change to realize heat transfer, and allow cooling applications to provide heating which cannot be accomplished with independent loops. Weber and Favrat [17] introduced the idea of distributing  $\text{CO}_2$  in DENs at an intermediate temperature, below the critical pressure of 74 bar. A pressure of 50 bar is selected for the system to stay in the saturation temperature range of  $12 - 18^{\circ}\text{C}$ , as the system can take advantage of the small pressure difference between phases to provide cooling services using gas expansion. 5G networks use on-location heat pumps to provide heating services, heat exchangers for cooling, and vapor compression chillers for

### 1.3. Materials and methods

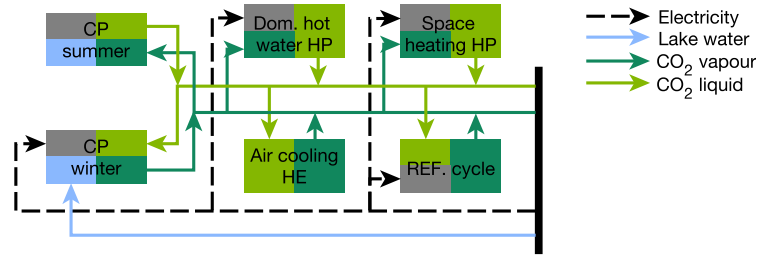


Figure 1.12 – Schematic description scenario 3.

refrigeration (see Figure 1.12).

The fourth scenario is also based on a 5G DEN. It comprises all the utilities present in the third scenario, with the addition of technology options discussed for Scenario 2 (ST panels, PV panels and electrolyzers which produce hydrogen for mobility). This scenario is the most flexible representation of potential future energy systems discussed in this work. The additional utilities are represented schematically in Figure 1.13.

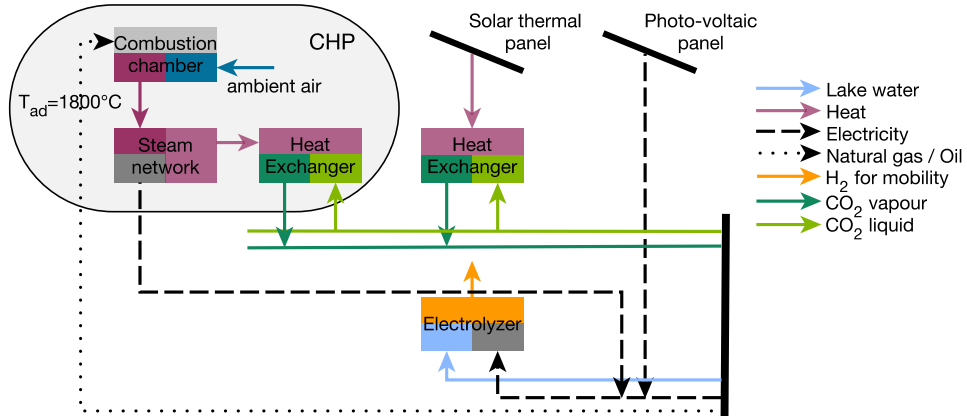


Figure 1.13 – Schematic description of additional utilities in scenario 4.

The main assumptions made for the water network are listed in Table 1.6. Details on the model parameters and efficiencies are given in the section A.1. The price of natural gas and oil are considered according to [62], the price of central heating and electricity according to [63] and the price of diesel and gasoline according to [64]. The CO<sub>2</sub> emissions of the different resources are taken from [65].

The 5G network consumes electricity, with a buying price of 0.15 €/kWh [63] and CO<sub>2</sub> emissions of 362 kg/MWh [65]. For both networks, a waste boiler is used to incinerate municipal solid waste, and a steam network is integrated to recover the heat of the boiler, produce electricity and deliver heat at lower temperatures. This can be used to provide heating services or vaporize CO<sub>2</sub>, which is needed

Table 1.6 – Parameters for energy consumption, economic and environmental analysis.

Service	Resource	Share [%]	Efficiency/COP/ Consumption	Price [€/kWh]	CO <sub>2</sub> emissions [kg/MWh]
Heating	Nat. gas	41.5	96.7	0.05	201.2
	Oil	54.5	96.7	0.08	278.7
	Central heating	3.5	-	0.11	-
	Electricity	0.5	-	0.15	362.0
Cooling	Electricity	0.5	AC:8.65, REF:4.02	0.15	362.0
Utilities	Electricity	0.5	-	0.15	362.0
Mobility	Diesel	26	6.63 L/100 km	1.56	266.8
	Gasoline	74	8.09 L/100 km	1.57	249.5

for heating in the case of the refrigerant-based network (Figure 1.14).

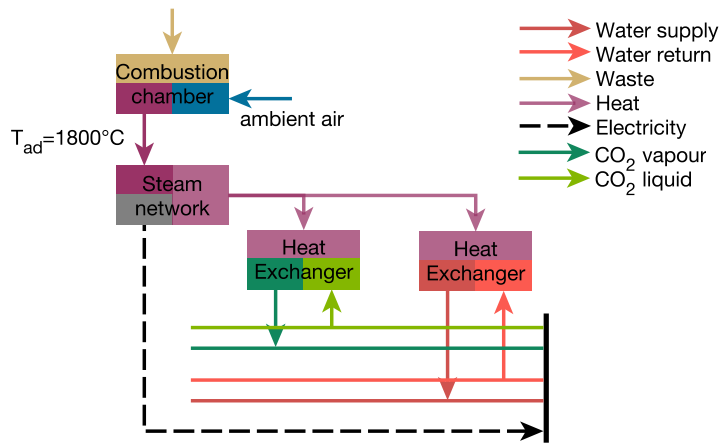


Figure 1.14 – Schematic description of waste boiler integration.

## 1.4 Results and discussion

### 1.4.1 Single-objective optimization of city service provision

With the demand values obtained using the validated sector profile model, utility integration was performed using process integration techniques.

First, total cost optimization is performed in each scenario (Figure 1.15). The second set of utilities causes the system to shift toward electrical consumption, investing partially in air-water heat pumps for heating and electrolyzers for mobility, reducing both CO<sub>2</sub> emissions and operating cost. Investments are not made for PV panels, since the savings in operating cost do not compensate for the investment cost. In the third scenario, the heating/cooling services are provided by the 5G

## 1.4. Results and discussion

DHC network, while the mobility demand is satisfied using diesel and gasoline. The operating cost and environmental impact of this scenario are lower compared to the baseline, but the operating cost is higher than in the second scenario. Finally, in the last scenario, the best system includes investments in CO<sub>2</sub> HPs for heating/cooling and electrolyzers for mobility. This scenario leads to reductions in operating cost and CO<sub>2</sub> emissions of 48% and 29%, respectively, compared to the first scenario and has an internal rate of return [66] of 36% and a net present value [67] of 6625 M€, showing the economic profitability of this scenario.

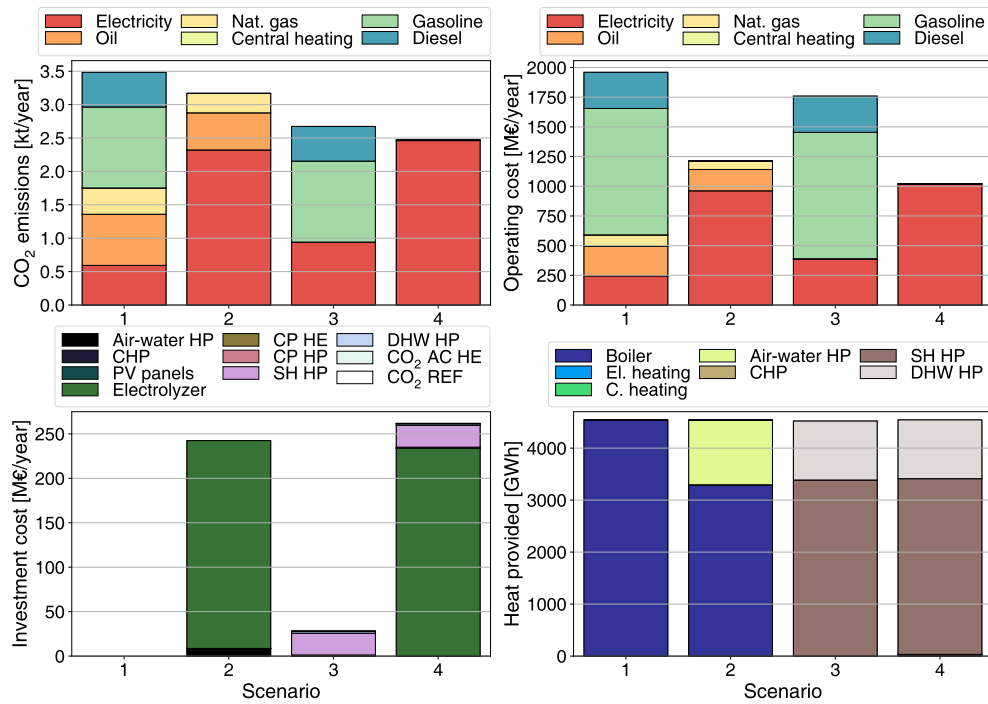


Figure 1.15 – Total cost optimization for different scenarios.

Next, an environmental impact optimization is performed (Figure 1.16). The main distinctions from the previous case are that the system invests in PV panels and that central heating emerges as a preferred way of providing heating services, due to its low environmental impact, since it consists mainly of waste heat available in the district area. The most economic scenario is still scenario 4, with an internal rate of return of 29% and a net present value of 7256 M€.

### 1.4.2 Optimal solutions for multiple objectives

Although single-objective optimization provides a single, best solution for a given problem, this optimal solution might not be practically feasible since mathematical formulations overlook some constraints related to implementation. Hence, parametric optimization with constraints ( $\epsilon$ -constraints) on investment cost and CO<sub>2</sub> emissions is used to systematically create a set of optimal solutions.

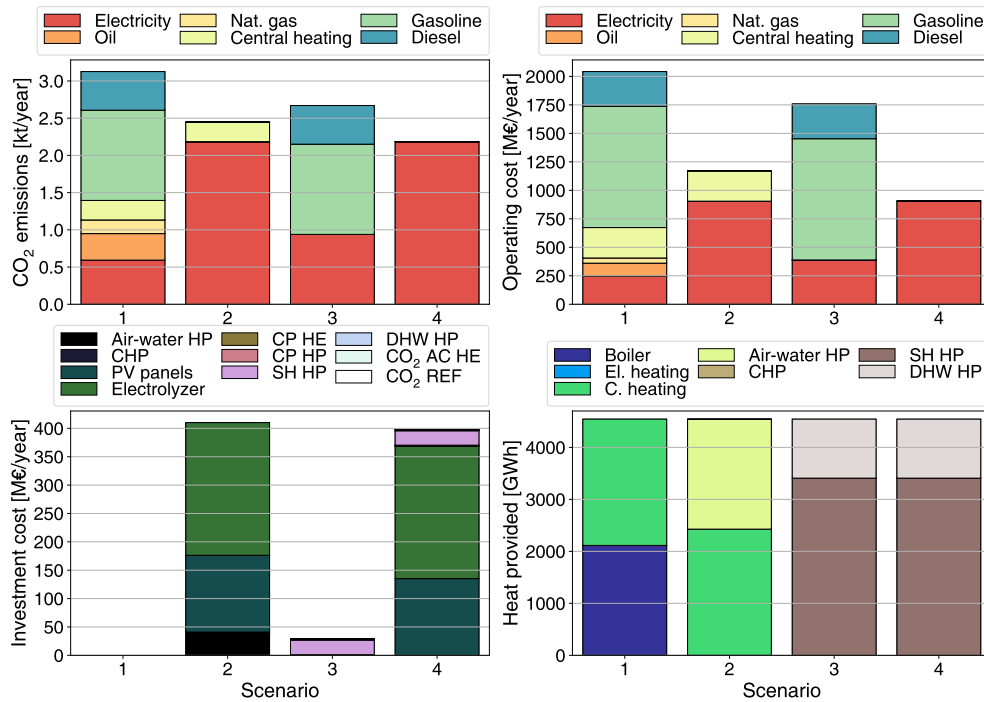


Figure 1.16 – Environmental impact optimization for different scenarios.

The objective function in the case of the environmental impact  $\epsilon$ -constraints is the minimization of the investment cost. In this case, as the CO<sub>2</sub> emissions are allowed to increase, the system gradually shifts from a fully electric 5G network and electrolyzer-based system to diesel and gasoline mobility, central heating and finally natural gas and oil boilers (Figure 1.17).

With investment cost  $\epsilon$ -constraints, the objective function was minimization of operating cost. As observed in Figure 1.18, as the investment cost increases, the best solutions are to invest in CO<sub>2</sub> heat pumps, electrolyzers for hydrogen mobility and PV panels. The switch to full electrical mobility is more gradual than with environmental impact  $\epsilon$ -constraints and central heating is not favored in this case, since it is not advantageous from the operating cost perspective.

Finally, a double  $\epsilon$ -constraint optimization is performed. The constraints are applied on operating cost and environmental impact and the objective function is minimum investment cost. As observed in Figure 1.19, low investment cost and high operating cost solutions lead to a high environmental impact, while high investment cost and low operating cost solutions have a low environmental impact. Additionally, it is observed that with only 25% of the maximum investment, the operating cost and environmental impact can be reduced by more than 15%.



## 1.4. Results and discussion

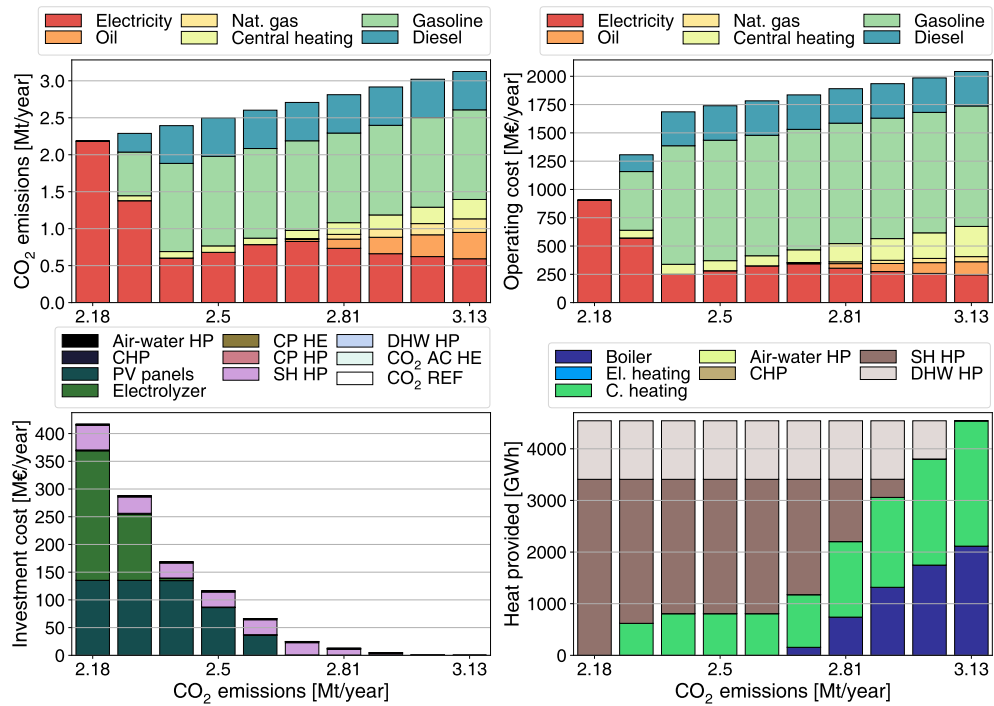


Figure 1.17 – Key performance indicators for CO<sub>2</sub> emission  $\epsilon$ -constraints.

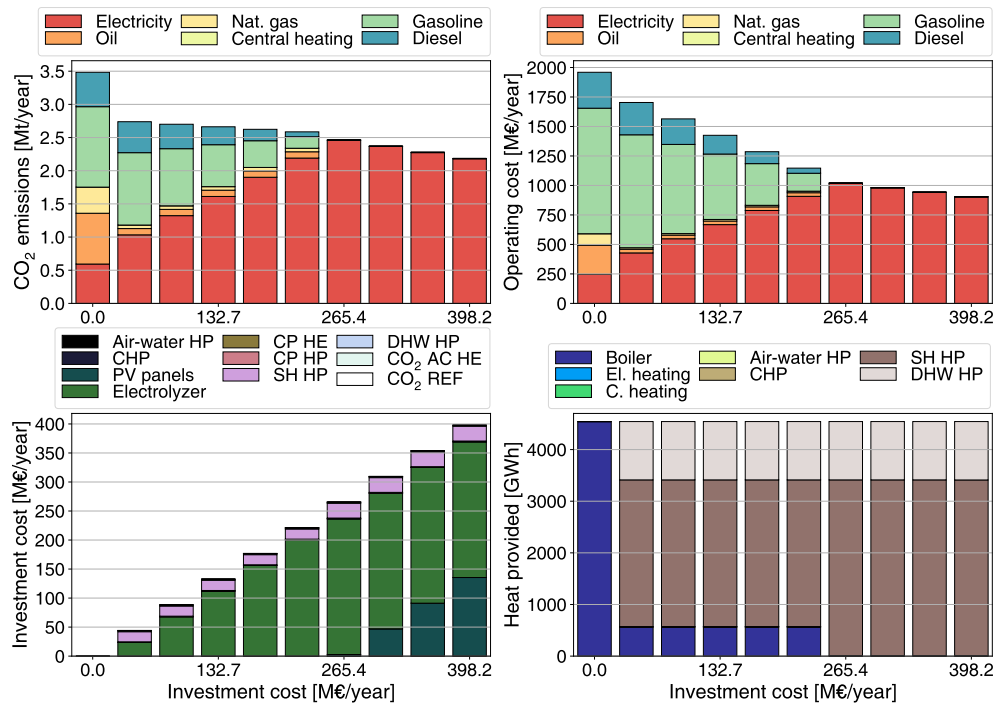


Figure 1.18 – Key performance indicators for investment cost  $\epsilon$ -constraints.

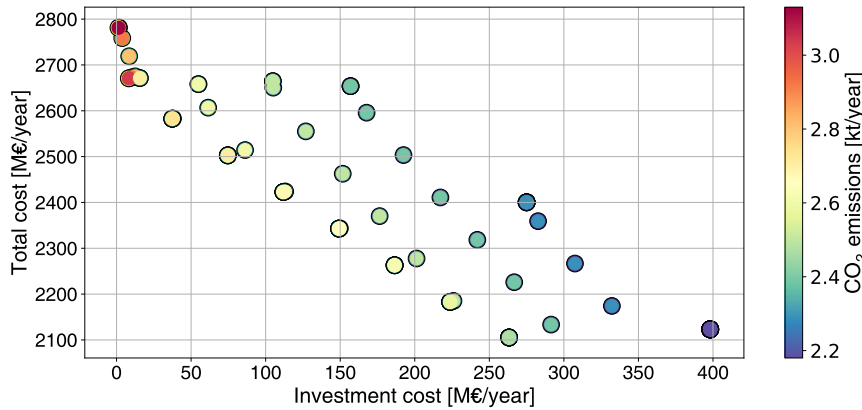


Figure 1.19 – Key performance indicators for operating cost and environmental impact  $c$ -constraints.

## 1.5 Conclusion

This chapter aims at providing a residential energy and service sector profile for any city in Europe, which gives an estimate of demands for heating in the form of space heating and domestic hot water, cooling in the form of air conditioning and refrigeration, mobility, waste treatment, and electricity for utilities. The sector profile is thus purpose-built for analyzing the best set of technologies to provide services required by urban populations.

The profile is validated using a typical European city, the city of Rotterdam. Deviations between the real demand and proposed profile vary between 3 - 8% for the different services, showing the differences between the Dutch energy consumption profile and the western European average. The functionality and effectiveness of the profile is illustrated comparing an existing water/air based district energy network, an advanced water/air-based network, a potential low-temperature 5G DHC network and an advanced low-temperature 5G network. Changing objectives yields different solutions for providing urban services, though consistent results show good performance with a fully electrical system both for heating and for mobility, potentially reaching zero CO<sub>2</sub> emissions, given a renewable electricity mix. The proffered scenario is also the most economically profitable, with an internal rate of return of 36% and a net present value of 6625 M€.

Utilization of the residential sector profile for integrating new technologies and finding the best energy technologies is also exemplified by performing parametric optimization on the system. These results show that significant operating cost and environmental impact reductions of 15% can be achieved with only 25% of the investment required for maximum emission reductions.

# Valorizing natural resources and human waste

## Overview

- The "typical European" urban demand is estimated in chapter 1;
- This chapter looks into valorizing resources available in urban areas:
  - Natural resources: lakes (rivers);
  - Geothermal energy;
  - Renewable resources: sun (wind, hydro);
  - Waste resources: inorganic (& organic).

*This chapter is a summary of [52, 68, 69]*

The concept of urban 5G networks has been developed to deploy heat pump based district heating and cooling systems in dense urban areas. The use of the CO<sub>2</sub> phase change reduces the cost of the heat distribution while allowing to recover waste heat that is typically rejected to the environment. The use of heat pumps to harvest heat from the environment and to supply heat to buildings allows one to propose district systems with COP as high as 6. Heat pumps can use the electricity produced by photo-voltaics already providing up to 60 % of the total consumption. This chapter studies the integration of fuel cell based power to gas for the seasonal storage of the excess electricity produced in the summer by PV panels. The methane stored in liquid form is used in the winter to balance the electrical needs by fuel cell based co-generation, making therefore the city 100% supplied by renewable energy. The present work evaluates the integration of 5G district energy network including power to gas systems on a compact urban block considering heating, cooling, electricity and waste management for different European climatic zones. In order to reach fully autonomous blocks using solar PV and municipal and industrial waste heat, a PV area of 10 to 40 m<sup>2</sup>/cap would be needed. The rooftop area available appears to be sufficient in areas like Southern Europe, while more area or alternative renewable sources such as wind or hydro are needed for other climatic zones. Regarding the economic feasibility of the system, the results show that an investment of 800 to 2500 €/cap would be needed, with a payback time between 15 and 17 years, depending on the different climate zones in Europe.

## 2.1 Introduction

More than 50% of the energy consumption and more than 60% of the greenhouse gas emissions in the EU are due to the residential and industrial sectors [70]. Taking a closer look at the breakdown of electricity and heat in these sectors, around 35% of the total energy consumption and 45% of the total greenhouse gas emissions are due to providing heating services [71, 72] (figure 2.1).

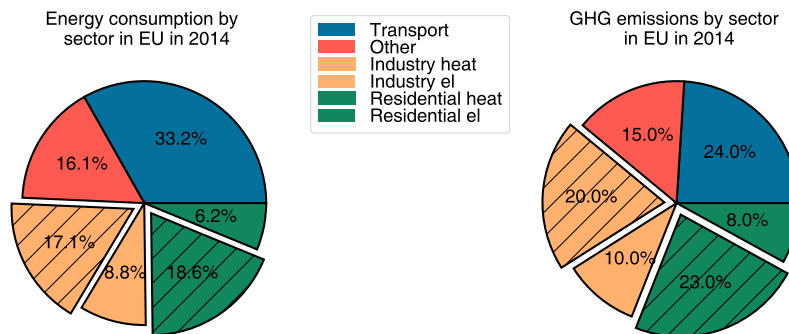


Figure 2.1 – Energy consumption and greenhouse gas emissions in the EU breakdown by sector.

Almost 75% of the European population lives in urban areas [73], so there is a high interest in increasing the energy efficiency of the technologies used to supply energy services in these areas. An improvement of the current state proposed in literature is zero energy cities [74, 75]. Zero energy cities are urban areas whose energy import is equal to the energy export summed up over the year. An improvement of the zero energy cities would be energy autonomous cities, namely cities that live on their own resources completely disconnected from the grid [76]. Nevertheless, there is a major problem when it comes to energy autonomy, since the energy demand of urban areas is high in winter and lower in summer, while the production profile of the main resource (solar energy) is high in summer and lower in winter. Therefore, there is a mismatch between demand and supply, which leads to a need for long term energy storage. One of the possible solutions is to couple 5G district heating networks with a long term chemical energy storage system that stores the excess of the photo-voltaic panel production in the form of methane, that is later on converted back into electricity using co-generation [69, 76].

Carbon dioxide is a natural fluid extensively used in the past for refrigeration technologies. Abandoned after World War II due to the low energy efficiency of the equipment and failure of CO<sub>2</sub> compressor manufacturers to keep up with technological developments, CO<sub>2</sub> is now reconsidered as a working fluid for a wide variety of applications. Among the fluid properties which lead to the re-entry of CO<sub>2</sub> on the refrigerant market are the fact that it is very abundant in the environment, it is non-flammable and non-toxic, inert, compatible with all materials encountered in a REF cycle, and since it is the waste of many technological processes it has an extremely low cost [77, 78].

Weber and Favrat [17] introduced the concept of distributing CO<sub>2</sub> in the district heating network below the critical conditions (74 bars, 31°C), at a temperature that allows to use the fluid as a heat and cold source. An average pressure of 50 bars is chosen, to stay in the saturation temperature range of 12°–18°C. At this temperature, the system takes advantage of the small pressure difference between the pipes (the liquid pressure being just slightly higher than the vapor pressure) by allowing free air cooling services (no pump and no compressor).

5G networks are fully electrical systems, which allow the use of PV panels to produce the electricity required. However, the excess electricity produced in summer needs to be stored to be used in winter, if fully autonomous systems are targeted. The aim of the work is to present the potential of 5G district energy networks, which integrate both 5G district heating networks, the advanced power to gas concept for tri-generation (heating, cooling and electricity) and long-term energy storage. As the performance depends on the profile of the energy demand, the optimal design and operation of 5G DENs is compared for the same urban block transposed in four different climate zones in Europe.

## 2.2 State of the art

Most of the district heating and cooling networks nowadays use water as the heat transfer medium [8]. The current systems use either renovated networks at 60°–90°C or high temperature networks at 90°–120°C [79, 80]. However, in most of the cases, the supply temperature of the water networks is selected according to the consumer with the highest temperature demand, while other users are supplied at a temperature higher than their needs. Another major drawback of water based networks is the fact that they do not allow recovery of any heat discharged in the cooling network (due to the two independent water loops).

Systems using CO<sub>2</sub> as the heat transfer fluid utilize the latent heat of vaporization as the main storage and heat transfer source. The 5G network also allows for recovery of waste heat from cooling in heating, due to the two-pipe system (figure 2.2). A more detailed description of the refrigerant based network that uses CO<sub>2</sub> as the heat transfer fluid is given by Weber and Favrat [17], Henchoz et al. [20] and possible energy services and corresponding conversion technologies for refrigerant based networks have been investigated by Henchoz et al. [18], Henchoz [19].

In order to offset the intermittent character of renewable power, a P2G concept has been proposed by [81, 82] to store power in the form of gas fuel: hydrogen is first produced by water electrolysis in a solid oxide electrolysis cell (SOEC) and then converted with carbon dioxide into methane in a methanator using the Sabatier reaction (figure 2.3).

This P2G system has the potential to reach a round-trip efficiency of more than 60% [83, 84] on a higher heating value (HHV) basis. Al-Musleh et al. [85] introduced the idea of integrating these systems with secondary technologies such as solid oxide fuel cells (SOFCs) to reach a round trip

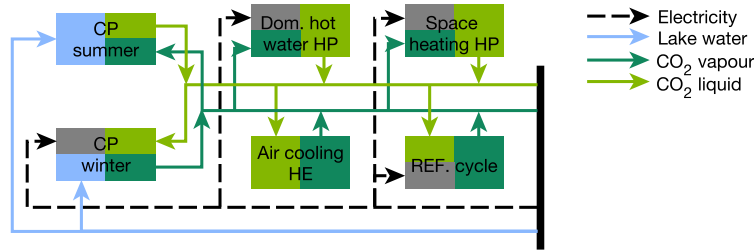


Figure 2.2 – Schematic description of 5G DENs.

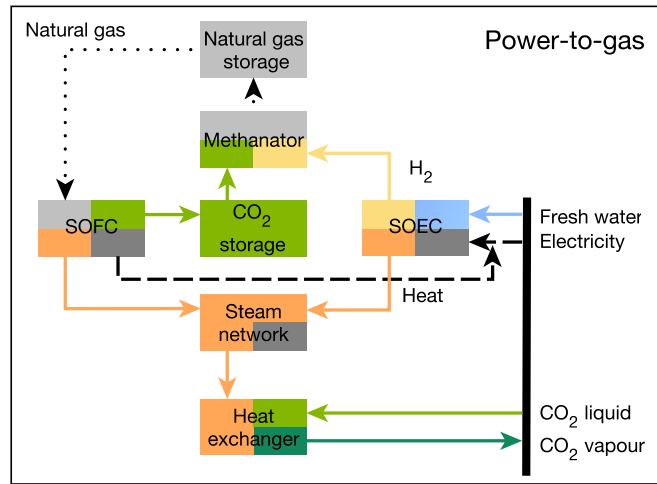


Figure 2.3 – P2G with electrolysis, methanation and co-generation using a SOFC.

efficiency of 55%-58% for electricity storage (figure 2.3).

In order to promote the emergence of autonomous cities, this work further evaluates the integration of P2G, using SOFC and gas turbine (GT) co-generation technologies, with the CO<sub>2</sub> distribution network. The round-trip losses of the proposed system are minimized by recovering the waste heat of the co-generation units (SOFC-GT) in a steam network [86] including Rankine cycles and heat recovery exchangers with the 5G DHN (figure 2.3).

This chapter uses a MILP formulation in order to model an integrated system comprising the urban energy demand (the process) and the available resources (the utilities) interlinked by a low temperature 5G DEN, and to optimize the design and operation of the system on a monthly basis, for four different climate zones in Europe.

## 2.3 Materials and methods

The sector profile described in chapter 1 not only offers an estimate of urban energy demands, but also the opportunity to find the best suited energy conversion technologies which satisfy this demand, while valorizing all the urban resources available:

- fresh water: rivers, lakes;
- geothermal energy;
- municipal solid waste;
- solar energy.

The natural choice for a district heating and cooling network which can recover heat until ambient temperature is the low-temperature (refrigerant-based) 5G network. Four different scenarios are studied, in which the resources available in the urban areas are appended to the system gradually, as described in the following subsections.

### 2.3.1 Scenario 1: base case 5G DEN

The base case scenario is introduced to present the state of the art 5G network technologies. The decentralized energy conversion technologies which supply energy services at the user end are: HPs for space heating and domestic hot water, HE for air cooling and CO<sub>2</sub> vapor compression chillers for refrigeration (Figure 2.2). The HP and REF cycles are optimized taking into account the minimum temperature differences in the HEs [18]. The refrigerants used are R1234yf for the space heating HP and CO<sub>2</sub> for the domestic hot water HP and for the REF cycle.

The network also needs a heat source from the environment, which in this scenario is modelled as a central plant (CP) heat pump (optimized taking into account the minimum temperature differences in the HEs [18]), which uses CO<sub>2</sub> as a refrigerant and harvests heat from a lake, i.e. valorizes the fresh water resource of urban settlements. Details on the unit models are given in Appendix B.1 and B.2.

### 2.3.2 Scenario 2: 5G DEN coupled to geothermal wells

In the second scenario, the heat source from the environment is replaced by geothermal wells, i.e. the network harvests renewable energy from the ground (figure 2.4). Details on the geothermal well model are given in Appendix B.2.

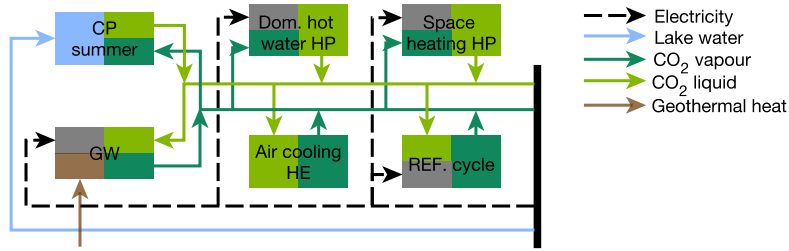


Figure 2.4 – Schematic description of scenario 2.

### 2.3.3 Scenario 3: 5G DEN coupled to GWs and municipal waste plant

In the third scenario, the inorganic part of the municipal solid waste produced in cities is incinerated, and a steam network is integrated to recover the heat and use it to co-generate electricity and low temperature heat, either for direct heating or to vaporize CO<sub>2</sub> (figure 2.5). The vapor CO<sub>2</sub> can be condensed in the central plant in cooling mode or in the decentralized heat pumps in heating mode. Details on the municipal waste plant (MWP) and steam network models are given in Appendix B.2.

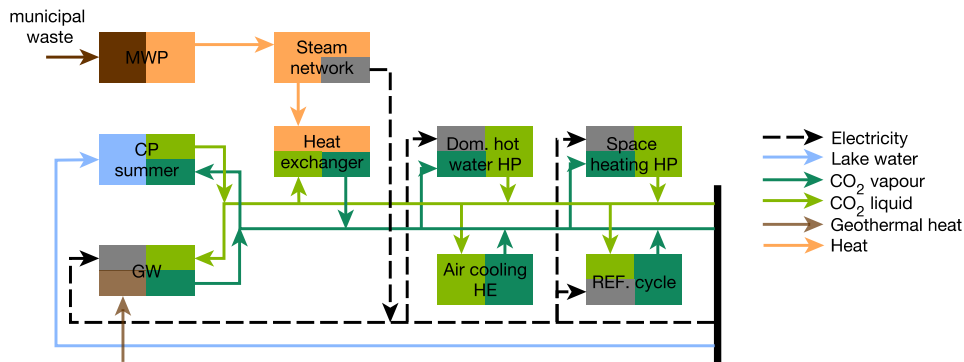


Figure 2.5 – Schematic description of scenario 3.

### 2.3.4 Scenario 4: 5G DEN coupled to GWs, MWP and solar energy

The fourth scenario additionally integrates photo-voltaic panels, which harvest solar energy and produce electricity and a power to gas system to perform long-term energy storage (figure 2.6). The PV panels and CO<sub>2</sub> and CH<sub>4</sub> storage models are described in detail in [76], the co-generation SOFC-GT unit is modelled according to [87] and the co-generation SOEC unit according to [88]. The steam network integrated at the MWP also recovers waste heat from the co-generation units and produces electricity and heat. More details on the unit models are given in Appendix B.2.





Table 2.1 – Share of primary energy, efficiency and price by service, for the current H<sub>2</sub>O network.

Service	Resource	Share of primary energy [%]	Energy conversion efficiency	Price [€/kWh]
Heating	Nat. gas	41.5	0.85 %	0.05
	Oil	54.5	0.95 %	0.09
	District heating	3.5	-	0.11
	Electricity	0.5	-	0.15
Cooling	Electricity	100	COP: 3.05	0.15
Building equipment	Electricity	100	-	0.15
Mobility	Diesel	26	-	0.13
	Gasoline	74	-	0.14

heating oil is considered according to [94], the price of electricity bought from the grid is set to 0.15 €/kWh [18] and the price of district heating is set to 0.11 €/kWh [18] .

For the air cooling and refrigeration services an average coefficient of performance (COP) of 3.05 is assumed [95] and the prices of fuel for mobility are considered according to [62].

### 2.3.6 Process integration

The main differences from the formulation presented in the introduction and some specific explanations are provided in this section.

#### 2.3.6.1 Definition of sets

Given that energy demand is time dependent, the problem is defined using discrete time intervals,  $t \in \mathbf{T} = \{1, 2, \dots, 14\}$  (12 months and two extreme days). The set of utility units for this problem is ( $\mathbf{UU} = \{\text{HPs space heating, HP domestic hot water, REF cycle, HE air cooling, PV panels, SOEC, SOFC-GT, methanator, HP central plant winter, geothermal wells, HE central plant summer, waste boiler, steam network, CO}_2 \text{ storage, CH}_4 \text{ storage}\}$ ) and the set of process units ( $\mathbf{PU} = \{\text{Buildings: space heating, domestic hot water, air cooling, refrigeration, utilities, mobility}\}$ ).

#### 2.3.6.2 Objective function and constraints

The objective function of the problem is the minimization of the operating and maintenance cost (Eq. 2.1). The rest of the formulation is equivalent to the one presented in the introduction, except

for epsilon-constraints, which are not used in this study.

$$\min_{y_u, f_u} \sum_{u \in \mathbf{U}} \left( \sum_{t=1}^T \left( C_u^{\text{op},1} \cdot y_{u,t} + C_u^{\text{op},2} \cdot f_{u,t} + C^{\text{el},-} \cdot \dot{E}l_{grid,t}^- - C^{\text{el},+} \cdot \dot{E}l_{grid,t}^+ \right) \cdot t_t^{\text{op}} \right) \quad (2.1)$$

The operation and maintenance cost is set to 10% of the investment cost:

$$C_u^{\text{op},1} = 10\% \cdot f^{\text{an}} \cdot C_u^{\text{inv},1} \quad (2.2a)$$

$$C_u^{\text{op},2} = 10\% \cdot f^{\text{an}} \cdot C_u^{\text{inv},2} \quad (2.2b)$$

With  $f^{\text{an}}$  the annualization factor:

$$f^{\text{an}} = \frac{i \cdot (i + 1)^{l_t}}{(i + 1)^{l_t} - 1} \quad (2.3)$$

Where  $i$  is the interest rate and  $l_t$  the lifetime of the equipment.

**Mass and resource balance** The electricity balance is explicitly given in Eq. 2.4.

$$\begin{aligned} \dot{E}l_{PV,t}^- + \dot{E}l_{\text{SOFC-GT},t}^- + \dot{E}l_{\text{Steam network},t}^- &= \dot{E}l_{\text{HP space heating},t}^+ + \dot{E}l_{\text{HP dom. hot water},t}^+ \\ &+ \dot{E}l_{\text{HP Central plant},t}^+ + \dot{E}l_{\text{REF cycle},t}^+ + \dot{E}l_{\text{Utilities},t}^+ + \dot{E}l_{\text{Mobility},t}^+ + \dot{E}l_{\text{SOEC},t}^+ \quad \forall t \in \mathbf{T} \end{aligned} \quad (2.4)$$

The main resource flows of the units present in the system are represented in table 2.2.

**Example: SOFC-GT unit** This formulation is generic. For example, the SOFC-GT unit is represented by:

$$\dot{m}_{\text{electricity, SOFC-GT},t}^- = \dot{m}_{\text{CH}_4, \text{SOFC-GT},t}^+ \cdot \text{HHV}^{\text{CH}_4} \cdot \eta^{\text{el, SOFC-GT}} \quad \forall t \in \mathbf{T} \quad (2.5a)$$

$$\sum_{k \in \mathbf{K}} \dot{Q}_{\text{SOFC-GT},t,k} = \dot{m}_{\text{CH}_4, \text{SOFC-GT},t}^+ \cdot \text{HHV}^{\text{CH}_4} \cdot \eta^{\text{th, SOFC-GT}} \quad \forall t \in \mathbf{T} \quad (2.5b)$$

Table 2.2 – Resource flows (-: flow in, +: flow out.)

Units	Resources			
	Electricity	CH <sub>4</sub>	CO <sub>2</sub> <sup>liq</sup>	CO <sub>2</sub> <sup>vap</sup>
HP space heating	-		+	-
HP domestic hot water	-		+	-
HE cooling			-	+
Refrigeration cycle	-		-	+
PV panel	+			
Co-generation SOFC-GT	+	-	+	
Co-generation SOEC	-	+		-
Geothermal wells	-		-	+
Central plant winter	-		-	+
Central plant summer			+	-
Waste boiler + steam network	+		-	+
CO <sub>2</sub> storage			-, +	
CH <sub>4</sub> storage		-, +		

With  $\text{HHV}^{\text{CH}_4}$  the higher heating value of methane and  $\eta^{\text{el, SOFC-GT}}$  and  $\eta^{\text{th, SOFC-GT}}$  the electrical and thermal efficiencies of the SOFC-GT unit.

### 2.3.7 Urban morphology and energy demand

The feasibility of the system is assessed for all four different European climate zones introduced in chapter 1 (figure 2.7).

A typical central European urban center is used for the analysis. Some typical parameters can be found in table 2.3. The network pipe length is computed according to [49].

As explained in the description of the parameterized sector profile, two types of buildings are considered for the urban center, namely residential and service, and 3 categories based on the refurbishment stage: new, existing, and renovated and a typical European center building distribution is used (figure 2.8).

## 2.3. Materials and methods

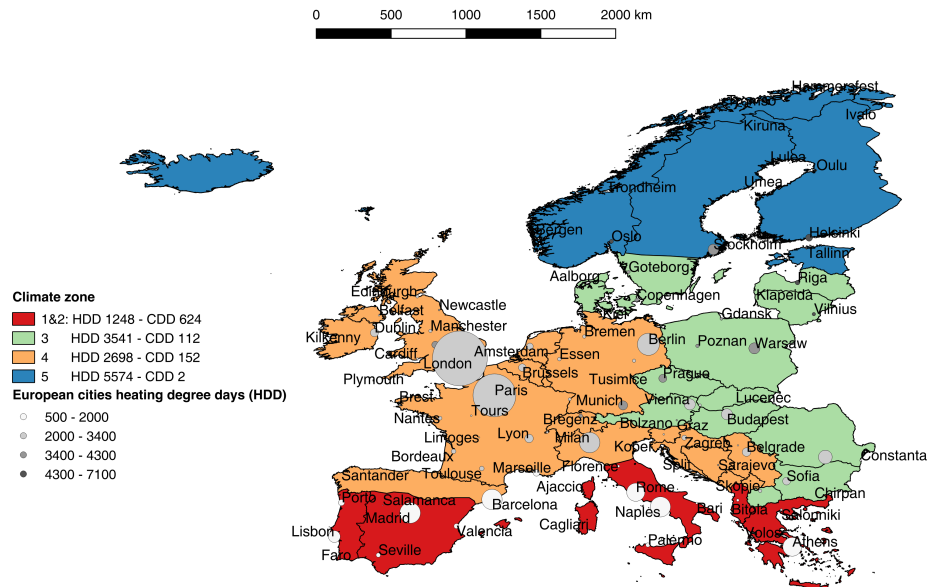


Figure 2.7 – European climate zones.

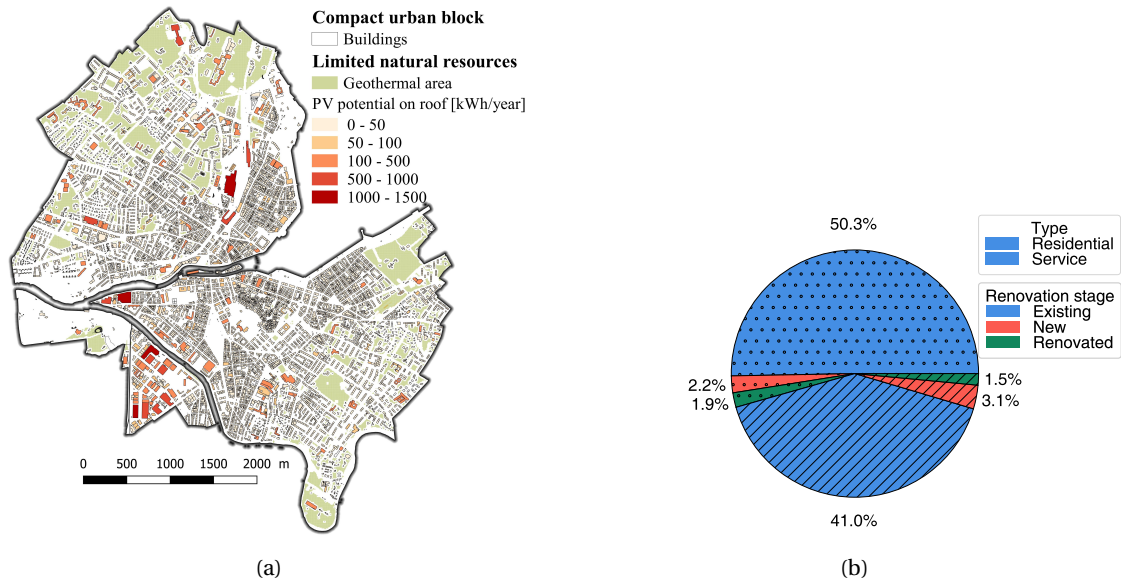


Figure 2.8 – Compact urban block with share of building type/refurbishment stage.

The average monthly demands for space heating, domestic hot water, cooling, electricity, mobility and waste generation for each zone are found using the sector profile described in chapter 1.

Table 2.3 – Typical indicators for a central European urban center.

Urban unit	Parameter	Value	Unit
Buildings	Population density	12'668	$cap/m_{land}^2$
	Surface coverage	0.19	$m_{footpr}^2/m_{land}^2$
	Heated floor area ratio (building density)	0.98	$m_{ERA}^2/m_{land}^2$
	Heated floor area (ERA) per capita	77.2	$m_{ERA}^2/cap$
	Mean height	6.2 (23.2 m)	$floors$
	Network length	12.6	$km/km_{land}^2$
Photo-voltaic	Footprint ratio	0.27	$m_{PV}^2/m_{footpr}^2$
	Area per capita	4.0	$m_{PV}^2/cap$
	Specific annual potential	9.7	$kWh^{el}/m_{ERA}^2$
Geothermal	Available area ratio	0.12	$m_{geoth}^2/m_{land}^2$
	Specific potential of extraction/injection	18.2 / 10.8	$W^{th}/m_{ERA}^2$
Groundwater	Available area ratio	0.35	$m_{groundwater}^2/m_{land}^2$
	Specific potential	0.5	$W/m_{ERA}^2$

## 2.4 Results and discussion

### 2.4.1 Energy demand and energy consumption

Figure 2.9 depicts the energy requirement of the different services. The annual energy requirements for heating and cooling vary between 5.4 MWh/cap and 14.7 MWh/cap for the different zones. Between 72.8% and 97.6% of this demand is required for heating, and between 2.4% and 27.2% for cooling. The heating peak occurs in January and it reaches its minimum in summer, when the only heating demand is the one for domestic hot water. The cooling peak occurs in July.

### 2.4.2 Scenario 1: base case 5G DEN

An analysis of the energy savings of the 5G network compared to the system in place is done for the four European climate zones considered. The assumptions made for the calculation are listed in table 2.1. Compared to the energy consumption for heating and cooling of the current system (which uses REF cycles for cooling and a mix of natural gas boilers, oil boilers, electrical heaters, and centralized district heating for heating), the 5G network leads to reductions in energy consumption of 82.7 to 88%. Taking a closer look at the 5G system (figure 2.10), the heating and cooling network has an annual electricity consumption of 0.3 MWh/cap to 1.3 MWh/cap, depending on the climatic zone. The minimum load occurs in summer when space heating is not required and the CP works in dissipation mode. The end user HPs account for the largest share of energy consumption with, on average, 69.9%, the CP is the second consumer with 28.2%, and refrigeration accounts for 1.9%.

## 2.4. Results and discussion

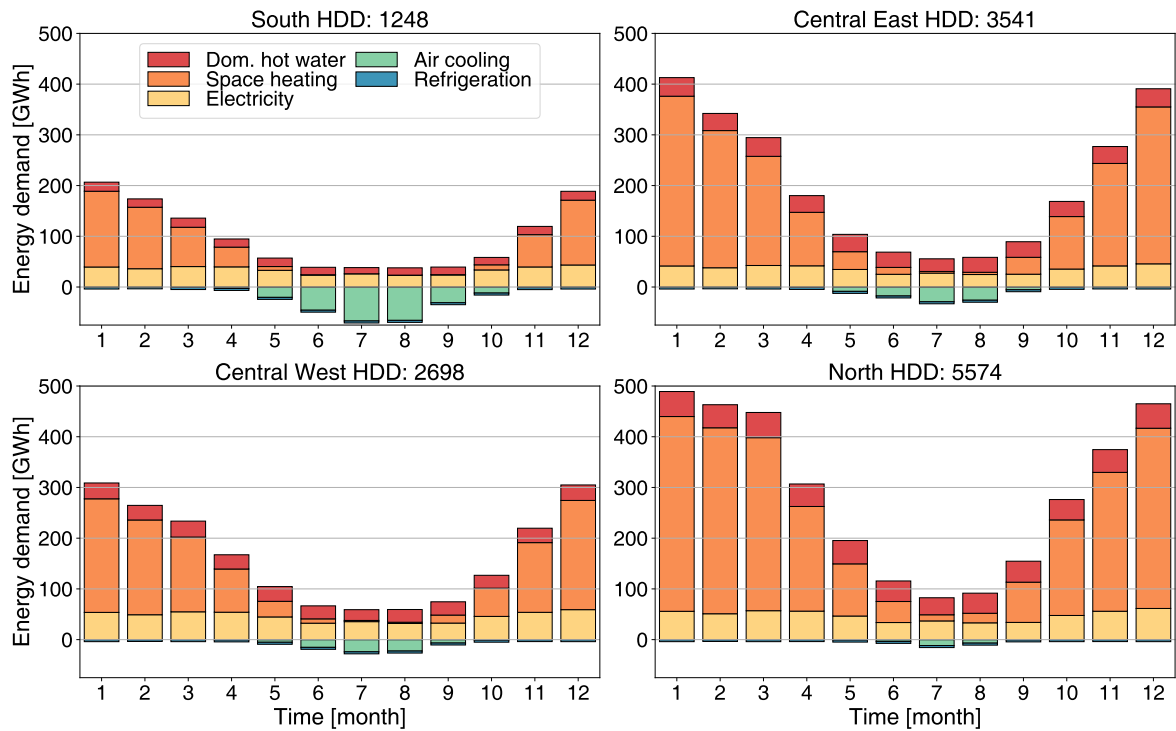


Figure 2.9 – Energy demand by service for different European areas.

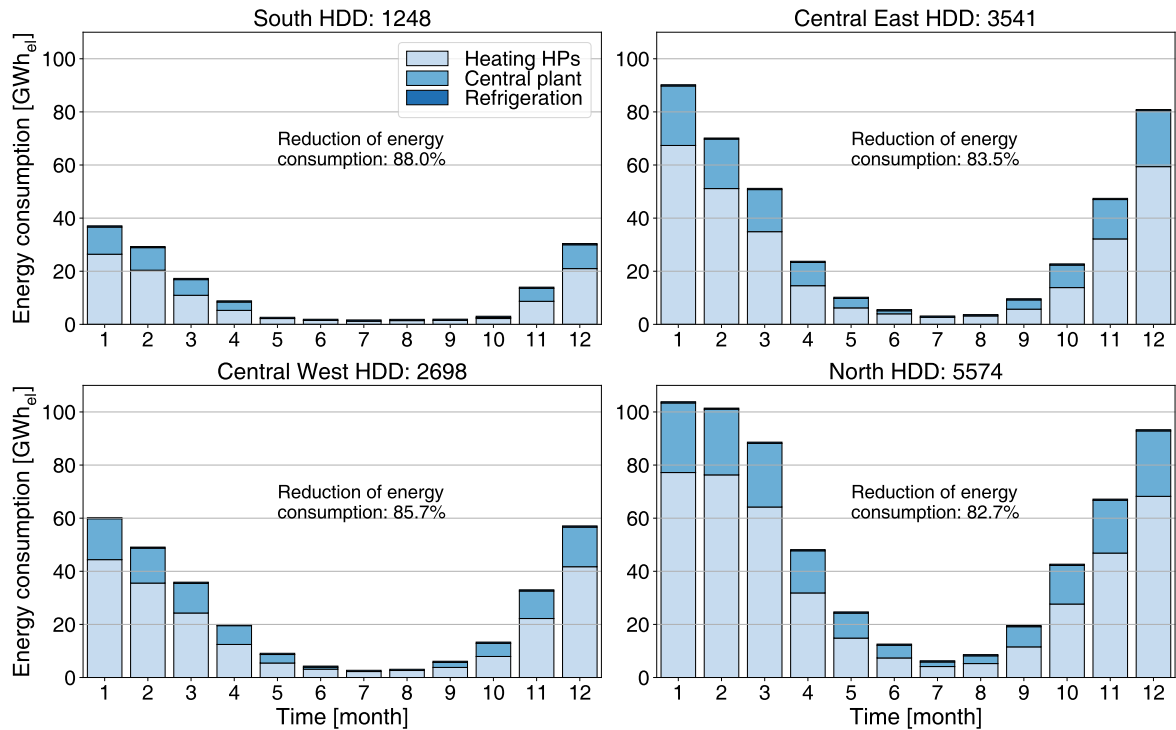


Figure 2.10 – Energy consumption for heating and cooling for different European areas, scenario 1.

### 2.4.3 Scenario 2: 5G DEN coupled to geothermal wells

When the central plant heat pump is replaced by geothermal wells, the electricity consumption in the first stage reduces, as more heat is extracted from the environment for the same demand (figure 2.11). Almost half ( $\approx 43\%$ ) of the electricity required in the first stage, which accounts for almost 30% of the total demand (figure 2.10) is saved.

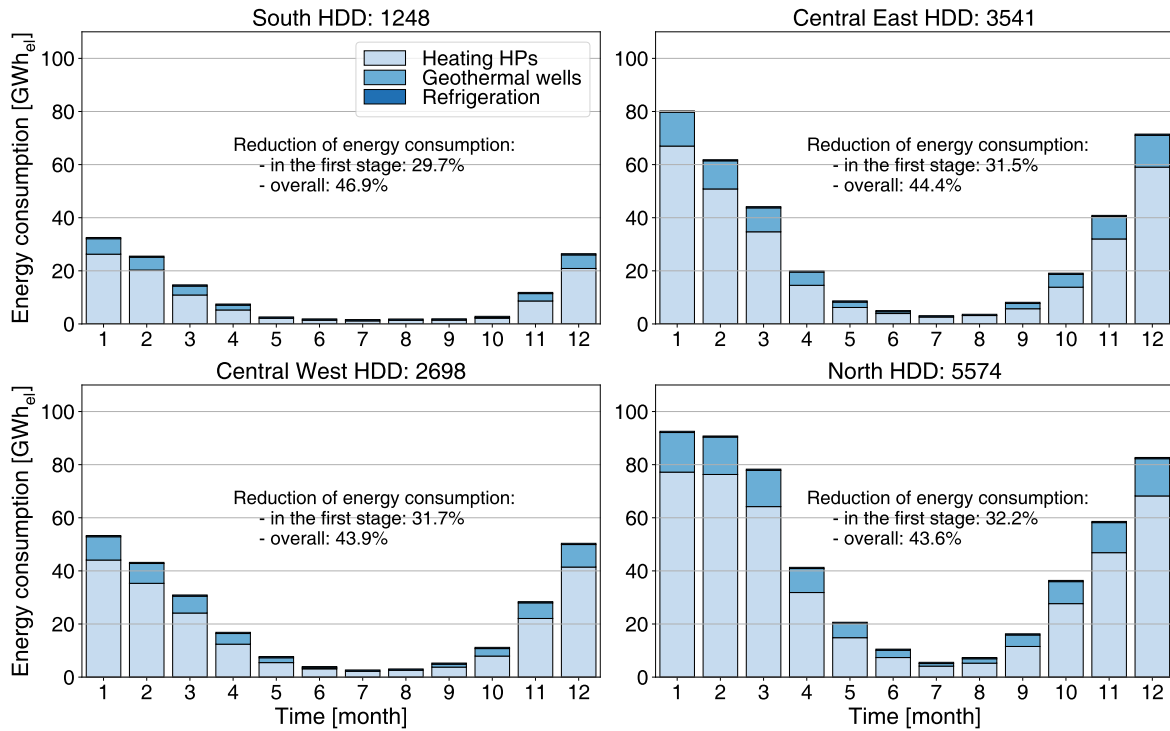


Figure 2.11 – Energy consumption for heating and cooling for different European areas, scenario 2.

### 2.4.4 Scenario 3: 5G DEN coupled to GWs and municipal waste plant

When the municipal waste plant is used to incinerate the inorganic urban waste, 5.4 - 10% of the electricity supplied from the grid is replaced by electricity supplied by the steam network integrated at the municipal waste plant (figure 2.12).

At the same time, 11.3 - 31.2% of the heat is supplied by low temperature heat from the municipal solid waste - steam network installed (figure 2.13). Consequently, as seen by comparing figure 2.12 with figure 2.11, valorizing the municipal solid waste decreases the electricity consumption of the space heating and domestic hot water heat pumps (10.2 - 27.6%) and the one of the geothermal wells (10.1 - 22.9%).



## 2.4. Results and discussion

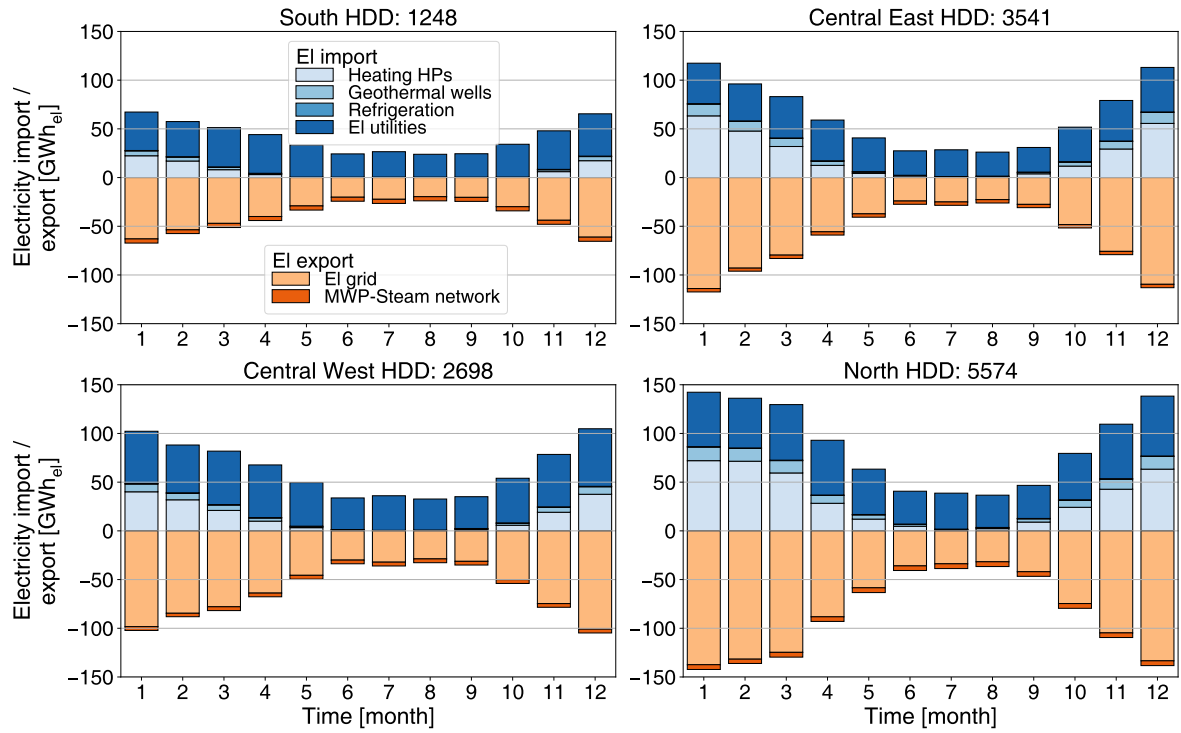


Figure 2.12 – Electricity import/export breakdown for different European areas, scenario 3.

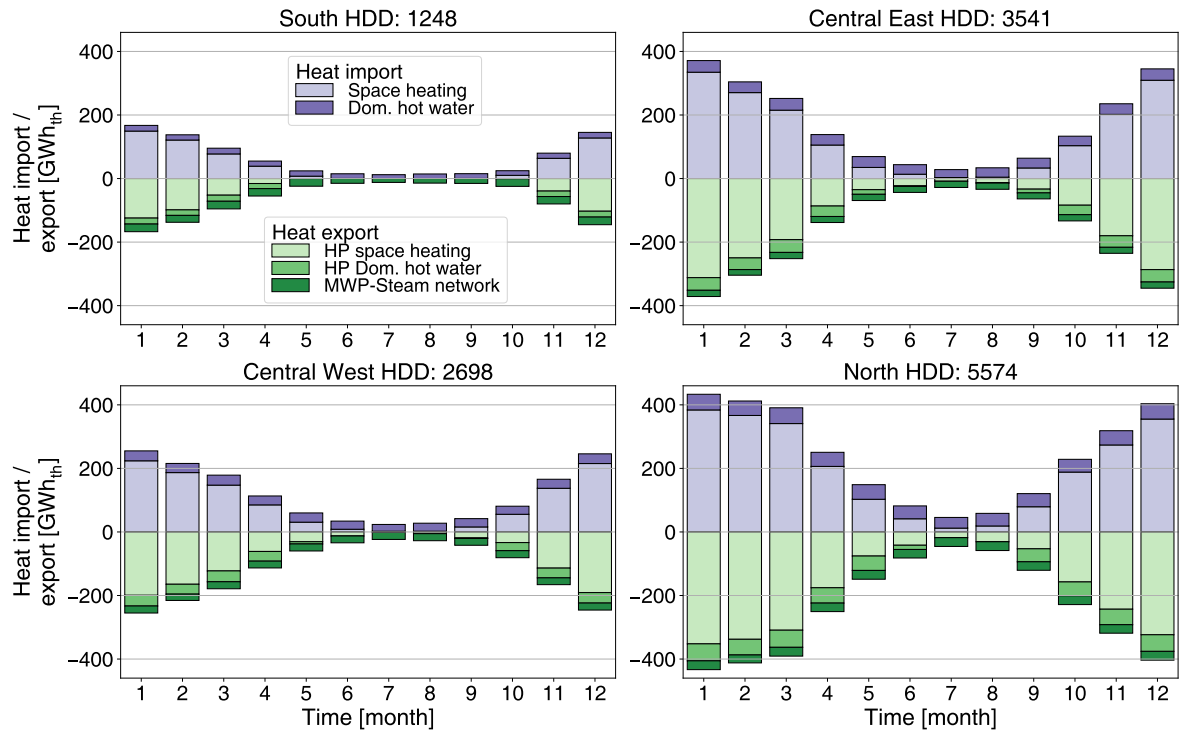


Figure 2.13 – Heat import/export breakdown for different European areas, scenario 3.

### 2.4.5 Scenario 4: 5G DEN coupled to GWs, MWP and solar energy

This scenario outlines results for 5G-P2G autonomous systems. Figure 2.14 displays the breakdown of electricity import and export. As observed, the PV panels account, on average, for about 73.5% of the total electricity export, followed by the SOFC co-generation unit with 21% and the MWP-steam network with 5.5%.

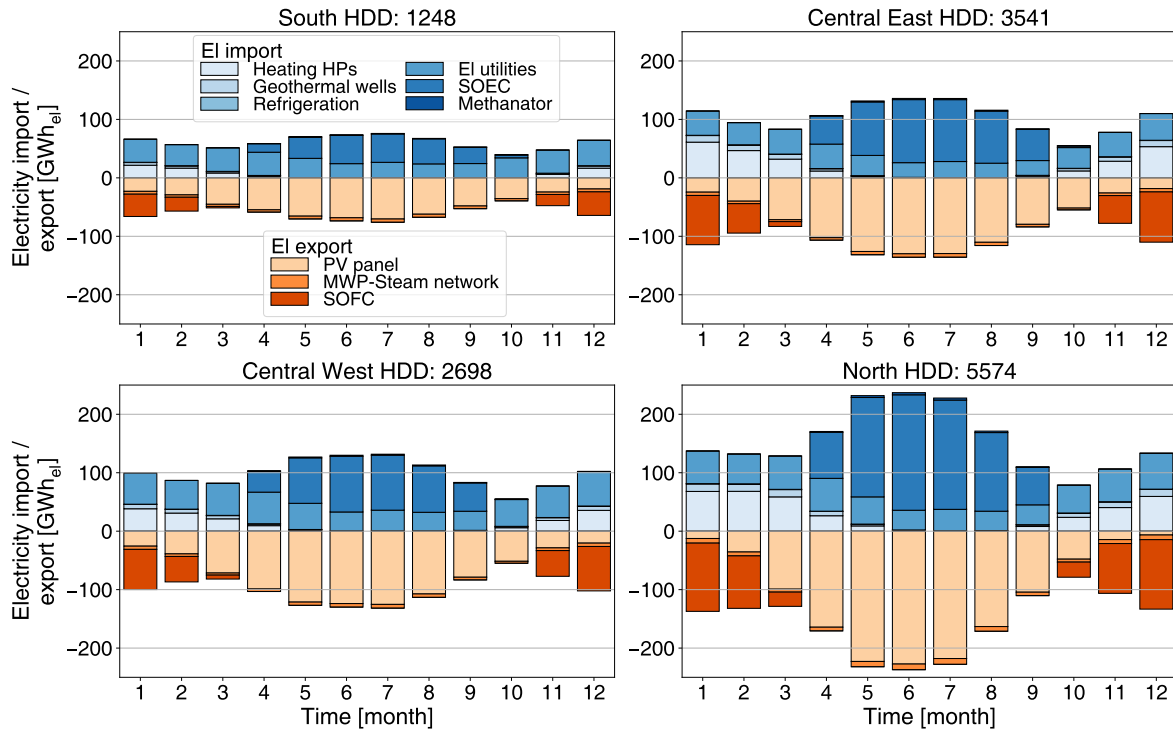


Figure 2.14 – Electricity import/export breakdown for different European areas, scenario 4.

Looking at the breakdown of heat import and export shown in figure 2.15, the amount of heat provided by the MWP increased to 18.3- 33%. This is due to the fact that the steam network also recovers waste heat from the power to gas units, in order to produce electricity and low temperature heat. Consequently, the electricity consumption of the space heating and domestic hot water heat pumps and of the geothermal wells further reduces by, on average, 4.9% and 9%, respectively.

As seen in figure 2.16, for a fully autonomous urban center, PV panel areas of 9.8 - 39.5 m<sup>2</sup>/cap and geothermal potentials of extraction of 6.1 - 18.5 W<sub>th</sub>/m<sup>2</sup><sub>ERA</sub> are required. The real PV potential of the area (11 m<sup>2</sup>/cap, [96]) is not sufficient for all climatic zones. Therefore, alternative energy sources should be considered, such as wind energy, hydro energy or the renewable energy mix. Alternative solutions include using higher efficiency PV panels, or increasing the PV potential by not only considering the available rooftop area, but also the building facades.

The real geothermal well potential of the area (18.2 W<sub>th</sub>/m<sup>2</sup><sub>ERA</sub> (table 2.3)) is also not always sufficient

## 2.4. Results and discussion

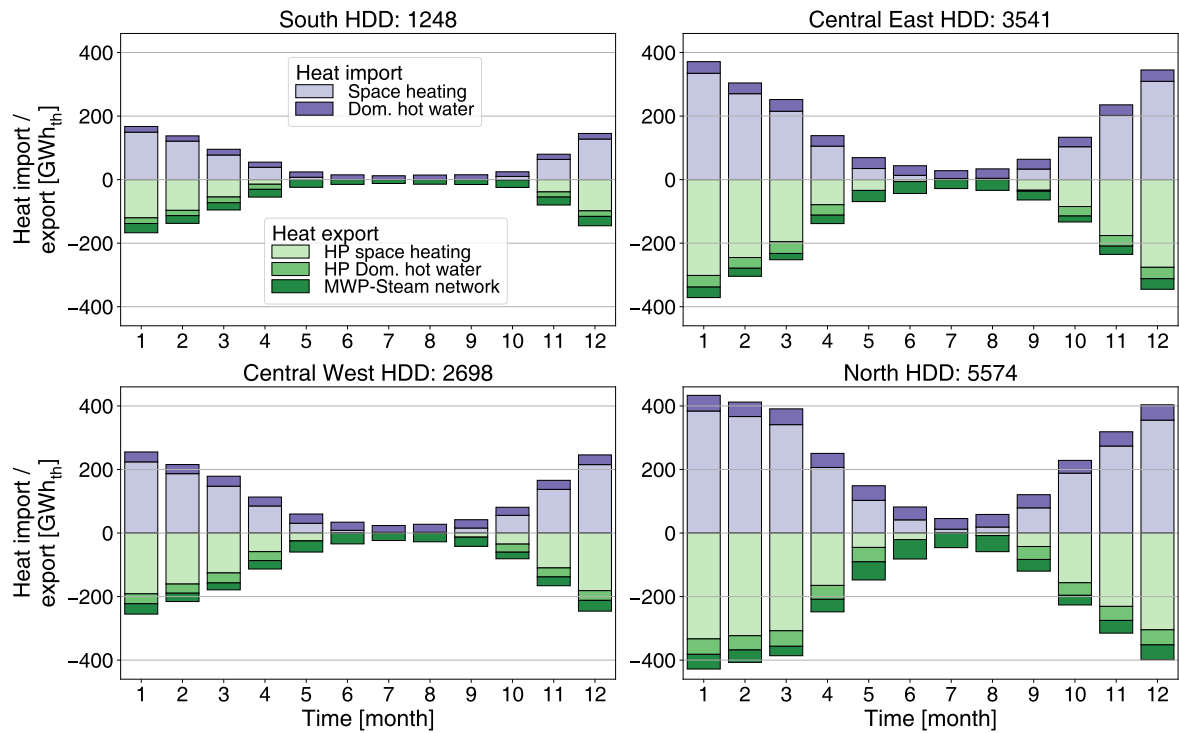


Figure 2.15 – Heat import/export breakdown for different European areas, scenario 4.

for energy autonomy. One of the ways to overcome this, is by using the significant ground water potential of the urban center (table 2.3). Since the temperature of the ground water is higher than the one of the lake, the load of the CP would reduce (i.e. the temperature lift in the HP would decrease, and therefore also its electricity consumption).

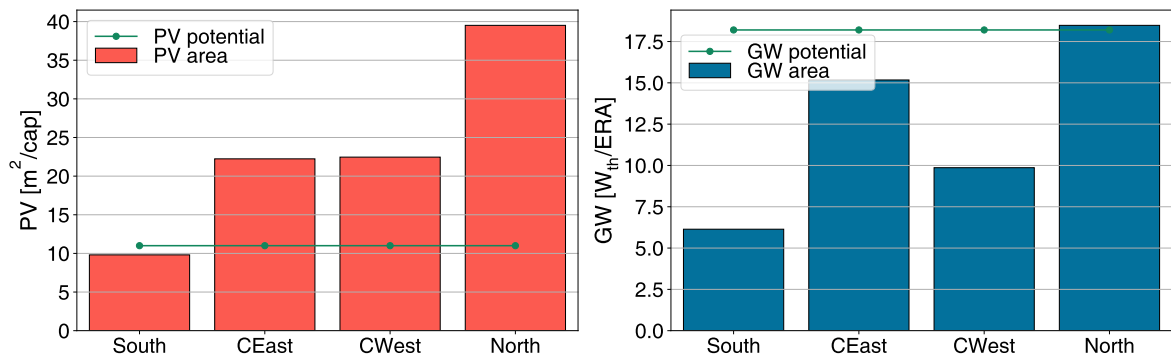


Figure 2.16 – PV panel and GW area required for autonomy for different European areas.

### 2.4.5.1 Economic feasibility

The economic feasibility of the systems proposed is first analyzed by looking at the operating cost of the different scenarios for each climate zone, and at the investment cost breakdown of autonomous cities, i.e. scenario 4 (Figure 2.17).

Compared to the current district energy network (natural gas and oil boilers, central heating, electrical heating, refrigeration cycles), integrating the basic 5G network (Scenario 1) decreases the operating cost in different European zones by approximately 38%, integrating geothermal wells instead of central plant heat pumps (Scenario 2) further decreases it, by about 4% and valorizing the inorganic municipal waste (Scenario 3) leads to an additional reduction, of around 10%. Finally, for scenario 4, in which PV panels and power to gas storage are integrated, the cities are completely autonomous, i.e. their operating cost is zero. The investment cost for the 4<sup>th</sup> scenario (Figure 2.17) varies between approximately 800 €/cap-year for zone south and 2500 €/cap-year for zone north. The main contributors to the investment cost are PV panels ( $\approx 40\%$ ), the SOEC-SOFC co-generation unit ( $\approx 27\%$ ), the network pipes ( $\approx 23\%$ ), and the space heating heat pump ( $\approx 9\%$ ).

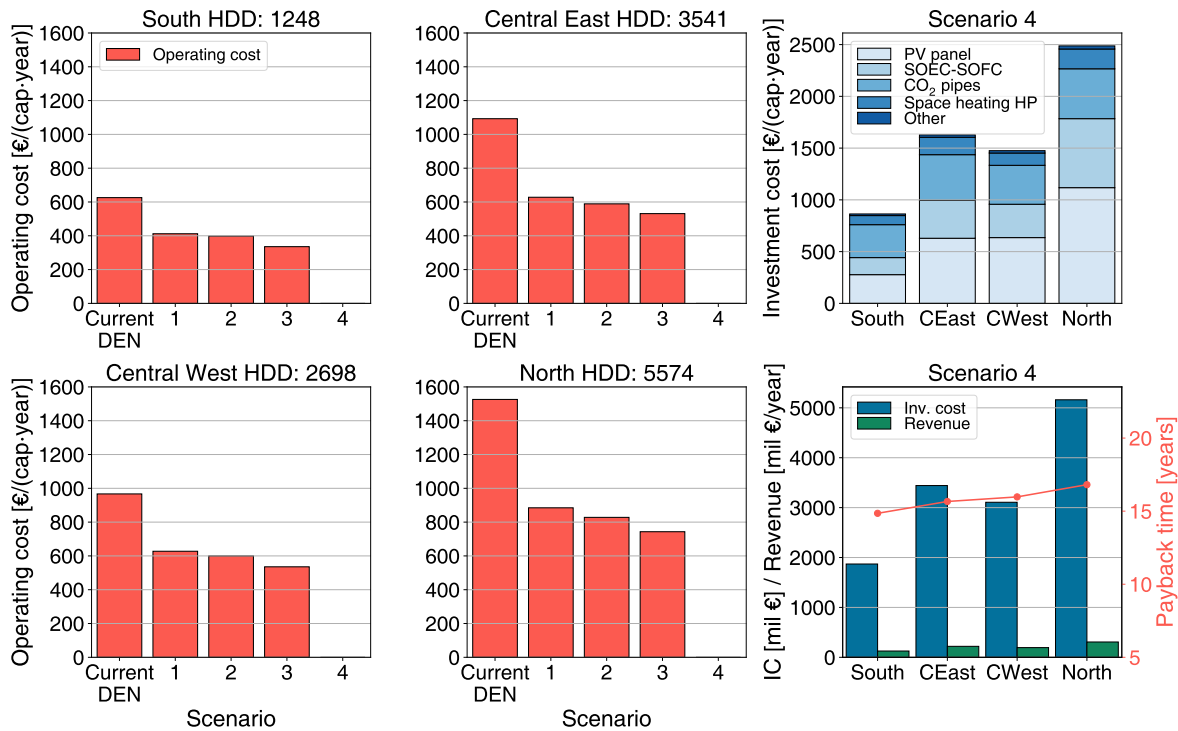


Figure 2.17 – Payback time for different European zones.

A comparative profitability analysis for the 4<sup>th</sup> scenario is also performed. The performance indicator chosen is payback time. Payback time is an indicator that shows the number of years needed to amortize the investment using the gain in revenue (the revenue represents the difference between the previous and the current operating cost). The payback time for the different cases is computed

considering:

- The initial investment;
- The cost of buying electricity from the grid for the current technology;
- The cost of buying natural gas and heating oil for the boilers of the current technology;
- The cost of operation and maintenance.

As described in section 2.3, the interest rate is assumed to be 8% and the lifetime of the equipment 20 years. With these parameters, a company which invests in the network would make a profit of 8% per year if the payback time is shorter than 20 years, at the price at which people are ready to pay for energy services today.

The payback time for fully energy autonomous cities can be observed in figure 2.17 for the four European zones. The number of years needed to amortize the investment varies across the zones, from 14.9 years for zone south, which has the lowest total energy demand, to 16.8 years for zone north, which has the highest energy demand.

2

## 2.5 Conclusion

The energy transition towards carbon and nuclear waste-free urban districts relies on the local renewable energy assets. In constrained urban areas, the potential of renewable heat present in water, underground and solid waste exceeds the energy needs for heating and cooling. However, harvesting, storing, distributing and upgrading environmental heat, as well as producing carbon-free fuel come at the cost of a further generation of intermittent and fluctuating renewable power.

This chapter aims at evaluating the capacity of future energy systems to capitalize on the territorial energy wealth of European urban centers while fulfilling the comfort requirements of the community. The challenge is to select and deploy technologies with a dual performance objective: to minimize the thermal use of electricity with the distribution of heat at the right temperature level and to maximize the capture and valorization of local renewable resources.

The approach is based on a CO<sub>2</sub> "closed-loop" concept, making the best use of local renewable resources for heat and power generation and is applied on a typical city center placed in different climatic zones in Europe. Compared to water based DENs, 5G networks lead to savings in energy consumption of 83 to 88%, depending on the climatic zone. The proposed energy system combines a novel concept of a compact DHC distribution network, using CO<sub>2</sub> as a heat and mass transfer fluid, and a P2G plant driven by a SOFC-GT coupled with a SOEC co-electrolizer.

A series of different scenarios are analyzed, showing the contribution of changing the source of heat from the environment from fresh water to geothermal, heat recovery from municipal solid waste incineration, and valorizing solar energy. Changing the heat source from the environment from a

lake to GWs saves almost half of the electricity required in the first stage, which accounts for almost 30% of the total electricity demand of the network, while including the heat recovery from waste treatment not only reduces the load of the central plant, but also the one of the heating HPs and decreases the operating cost by an additional 10%.

The monthly analysis on the potential for autonomy in the different climate zones shows that full autonomy can be reached in zone south, using just the PV panel area available on the existing rooftops, while approximately 50% of the electricity must be supplied by the grid for the central zones (CEast and CWest) and almost 70% of the electricity for zone north.

With an estimated payback time of less than 17 years and the current cost of technologies, the system is not only economically viable, but technically feasible within the next decade. The technology of 5G networks is already mature and implemented worldwide in the food retail industry and SOFC demonstrators are on the way to commercial readiness.

# Valorizing excess industrial heat

## Overview

- The "typical European" urban demand is estimated in chapter 1;
- The natural and renewable resource valorization is explored in chapter 2;
- This chapter looks into valorizing other resources available in urban areas:
  - Waste heat from industry.

*This chapter is partially a summary of [30, 31]*

## 3.1 Introduction

Energy consumption is an important metric, which not only reflects the influence of a certain sector on the economy of a region, but also its environmental impact. Existing reports from energy statistics agencies show that industrial and residential activities are the most energy consuming sectors worldwide [97–101] and, as a consequence, responsible for large quantities of greenhouse gas emissions. More specifically, the industrial and residential sectors account for 25.3% and 25.4% of the energy consumption in the EU and 28.6% and 14.7% of the energy consumption worldwide, respectively [97, 99]. Given the current and foreseen shortage of fossil fuels and the environmental pressure exerted by international treaties (e.g. Kyoto protocol, Paris agreement, etc.), introducing more sustainable, eco-friendly energy sources is becoming increasingly crucial. Recovering and reusing excess industrial heat is an attractive opportunity to supply a low-carbon, less costly energy resource and reduce the environmental impact and costs [102].

Excess industrial heat sources consist of a variety of hot gaseous exhaust, waste process liquids, cooling media, chemical waste and hot equipment surfaces [103, 104]. Various researchers have focused on heat recovery within the industrial sector [105–107]. Waste heat can be recovered within the process to increase the overall energy efficiency and take advantage of simple improvements such as air preheating [108], water desalination [109], or power generation [110]. However, such solutions are not capable of valorizing all industrial heat sources. Low-grade industrial waste heat, which does not match any internal demands and is uneconomical in co-generation, is generally discharged into the environment via cooling towers [111].

Figure 3.1 (adapted from [112]) shows the yearly industrial waste heat potential for a variety of countries. In the case when more than one value is found per country, the average amounts are considered. The European potential is shown both as an aggregated value and as a breakdown by country; a lack of data is noted for countries in South America, Asia, Australia and Africa. The studies which lead to these results are presented in detail in [112].

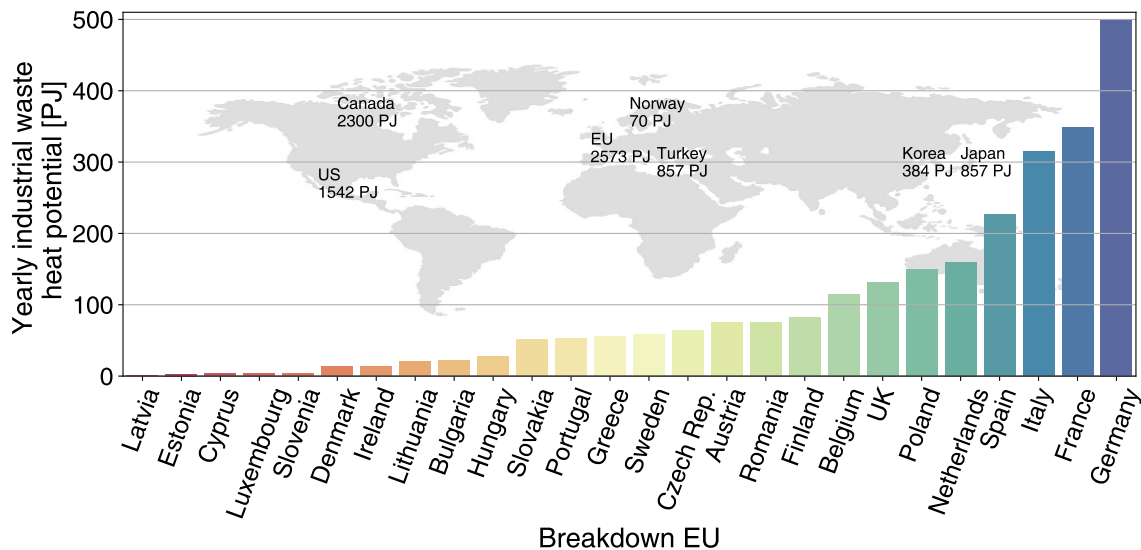


Figure 3.1 – Yearly EIH potential worldwide.

Other studies have also shown that excess industrial heat potential is very large. Johnson et al. found that as much as 20–50% of energy is lost as waste heat in metal and non-metallic mineral manufacturing in United States [113], Sogut et al. found that 51% of the overall heat of the process is wasted in a cement plant in Turkey [114] and McKenna et al. established a model to estimate the industrial heat loads and technical recovery potentials for energy-intensive industries in the UK, and concluded that about 10% of the heat load is technically recoverable [115]. At the same time, in China it is believed that at least 50% of all the energy used in industry is wasted, mostly in the form of low-grade waste heat [116].

Low-temperature heat can potentially be valorized in the residential and service sector, providing possibilities for district heating. The use of industrial excess heat for district heating applications has a great potential, especially in cold climates where heat demand for space heating is high during most of the year. It is particularly attractive if the industrial plant is located close to a large urban area and if investments in the DH infrastructure have already been made (in full or in part) [117].

Excess industrial heat is usually at a low temperature, while the high-temperature part is recovered inside the production process or used for power generation. Consequently, the energy quality of



excess industrial heat cannot always meet the required temperature level of a district heating system. In order to achieve the required supply water temperature of the primary network, other high-temperature heat sources such as boilers should be used for peak demand, or the low-temperature heat sources should be upgraded e.g. by using heat pumps.

This chapter explores excess industrial heat recovery of optimized industries (i.e. maximum on-site heat recovery has already been achieved) in a typical European city, including 10 different industries (oil refinery, cement, aluminum, steel, plastic, municipal waste incineration, dairy, pulp and paper, brewery and sugar) and in a real city — Rotterdam, NL — including four main oil refineries and four theoretical cement plants present in the industrial port, and the brewery of the city. Further industries, not considered in this work, include other food production (e.g. meat), waste water treatment, ceramics, fertilizers, other organic and inorganic chemicals, and textiles. Nevertheless, more than 50% of the total industrial energy consumption is covered in the typical European city demand [101].

## 3.2 State of the art

Studies investigating excess industrial heat recovery for district heating have been conducted mostly in times of economic crisis or environmental concern, i.e. in the 1980s or after 2007. For example, some of the studies conducted in Europe in the 1980s focused on EIH recovery from a steel mill for a district heating network in Germany [118], EIH reuse from a cement plant in a DH network in Switzerland [119], or EIH upgrade by an electrically driven heat pump for a DH in the Netherlands [120].

In later studies, Ajah et al. evaluated the technical, economic and environmental feasibility of pharmaceutical EIH integration with a DH in the Netherlands by upgrading the low temperature heat with chemical and mechanical heat pumps [121, 122], Holmgren assessed the impact of EIH integration with DHNs while focusing on the impact of electricity price on the performance of CHP systems [117], Sogut et al. designed a heat recovery unit which utilizes waste heat from a rotary kiln in a cement plant and concluded that the harvested heat could satisfy the thermal loads of 678 dwellings in the vicinity [114], Chen et al. proposed a condensing boiler - heat pump unit to recover sensible and latent heat from flue gases for DH networks in the UK and EU [123] and Svensson et al. looked at the competition between the external and internal use of waste heat from a kraft pulp mill, and concluded that external use, i.e. for DH, is more effective in reducing CO<sub>2</sub> emissions [124].

Other studies worth mentioning are those of Fang et al. who showed that, if in northern China 38% of the low grade waste heat from energy intensive industrial sectors would be recovered, the future DH demand could be served [125], or Kapil et al. who looked at waste process heat integration with district heating, with respect to the economic impact on the DH networks. They showed that the low

grade heat from the industrial site is not enough to compensate penalties associated with resulting part-load performance of existing energy-generating facilities [126]. Additionally, Morandin et al. studied the DH delivery from excess heat of a petrochemical cluster at the Swedish West Coast and showed the maximum theoretical potentials by identifying the conditions in terms of yearly delivery and installed capacity that could make DH an economically interesting option, namely achieving 10% discounted cash flow rate of return in 15 years [5].

Nevertheless, few of the studies propose an integrated method in which different equipment can be used to recover waste heat at different temperature levels and in an efficient way. Moreover, very few of these studies presented a detailed full-scale implementation, combining system design, economics and environmental impact assessments. This work studies the usefulness of the sector profile proposed in chapter 1 by integrating excess industrial heat recovery to provide district heating services, and studies the economic and environmental impact feasibility by accounting for the location of industrial facilities and the expected heat losses.

### 3

## 3.3 Materials and methods

The sector profile introduced in chapter 1 encourages exploration of integration opportunities for new technologies and between residential services while also introducing interfaces with external providers such as industrial processes to provide district heating. In this chapter excess industrial heat recovery is analyzed for two case studies, namely a 'typical' European city and a real city (Rotterdam, NL). The EIH potential of the typical city is built using average European productions and previously developed blueprints for 10 different industries [127]. In the case of Rotterdam, the industries considered are its four main oil refineries and cement plants, and a brewery which fulfills the consumption of the whole city.

### 3.3.1 Typical European city

First, a typical European city is considered. To represent the residential and industrial needs, the parameterized sector profile introduced in chapter 1 and previously developed industrial blueprints [127] are used. The industries included are oil refineries, breweries, pulp and paper mills, aluminum, steel, cement, dairy, sugar, plastic and municipal waste incineration plants.

**Cement** The main process in cement production is the production of clinker, typically consisting of two parts, namely pre-calcination and pyro-processing. The former implies heating the raw material from 50°C to 850°C, the temperature at which the calcination reaction takes place. The latter consists of further heating the calcined material to 1450°C where a chemical reaction transforms the material into clinker. The thermal requirement of the processes is generally satisfied using external fuels,

such as coal, dry sewage sludge, or by-products coming from municipal or industrial waste. The heat profile of the plant was taken from [127] and the average European cement production is estimated at 267 Mt/year [128].

**Oil refinery** Crude oil refining represents a basic, energy intensive process. Refinery processes require heating to separate components in distillation columns, or to provide reactor heating. In parallel, they require cooling to condense vapor streams from distillation columns and cool reactors and product streams. Most refineries use combined heat and power plants to generate heat and distribute it to the plant through a steam network while co-generating electricity (which is used by other equipment on-site). The thermal profiles of the refinery are considered according to [127] and the European oil refinery production is about 880 Mt/year [129].

**Brewery** Beer production converts a mixture of grains, water and hops (raw materials) into beer (product) through a series of sub-processes, such as cooking, filtering, and fermentation. The sub-processes require heat for cooking and cooling for fermentation and conditioning. The temperature-enthalpy profile of the beer production process [27] (Figure 3.4) shows that breweries can be largely energy self-sufficient and that the utility requirements can be supplied at a relatively low temperature since brewing has a low process pinch temperature. This makes brewing an ideal candidate to receive heat from other industrial plants. The European beer production is estimated at 381 13.4 ML/year [130].

**Pulp and paper** Although pulp production and paper making are two separate steps, they are commonly regarded as one process. In Europe, the two main routes available for pulp production from wood are chemical pulping (67%) and mechanical pulping (33%) [131]. The pulp production process starts by steaming and screening the wood chips, in preparation for cooking. In the chemical route, the wood chips are sent to a high pressure digester, where cellulosic fibers are separated from the chips. This process takes place at medium temperatures (i.e. 160 - 170 °C) and heat is generally provided by direct steam blowing or indirect heating in steam/liquor heat exchangers. In the mechanical route, the cooking stage is replaced by mechanical and thermal processes. After cooking, the pulp is bleached and either sent to the paper mill or dried and sold. Water is also necessary for processes such as washing, bleaching, evaporation, or steam productions; clean, cold water is required for cooling and dilution. Paper manufacturing generally follows a fixed series of processes, namely preparing the pulp, pressing, dyeing, drying and coating. The thermal profile of this step is dominated by the drying process, which takes place at a moderate temperature, making it a good candidate for waste heat recovery from other industries. The average European pulp and paper production is approximately 41 Mt/year, while the old paper de-inking production amounts to 48.6 Mt/year [131]. The heat profile of the plant was taken from [127].

**Dairy** The dairy industry includes all the conversion processes of milk into concentrated milk, pasteurized milk, cream, cheese, yogurt and desserts. Milk is generally first cooled down and stored, then treated by pasteurization, i.e. milk is preheated and the cream is separated by centrifugation. The pasteurized milk is then distributed between concentrated milk, yogurt and dessert production. One of the main energy consumers in the dairy process is the milk evaporation, in which milk is sent to a multi-effect evaporator. The early stage uses steam to evaporate a part of the milk, and the evaporated milk is used to heat up the inlet milk stream and to evaporate the milk in the middle stage. The same principle is used in the late stage of evaporation. The evaporation temperatures of the stages are between 60°C and 70°C. The energy requirements for the yogurt and dessert lines include heating up the milk, homogenisation, and cooling down the product to storage temperature. Auxiliary processes such as cleaning in place, hot water production and cold storage should also be considered. The temperature-enthalpy profile of the process is taken from [127]. The dairy processes considered here are drinking milk and yoghurt; their average European production is estimated at 30.4 Mt/year and 15.1 MT/year, respectively [130].

### 3

**Aluminum** The main processes in secondary aluminum production are aluminum melting, alloy addition, metal treatment, and casting. The most heat intensive process is the melting, which occurs at temperatures of up to 800°C. The temperature-enthalpy profile of the process is taken from [132] and the average European production is estimated at 1.7 Mt/year [133]. Only the secondary aluminum process is considered in this work.

**Steel** The major steel production method in Europe is via the classical blast/basic oxygen furnace route, i.e. producing steel from iron ore, recycled steel, coal and minerals. Steel production begins with the reduction of coal to coke, where coal undergoes a pyrolysis reaction at high temperature to remove non-carbon elements, especially oxygen and hydrogen and with the sinter plant, where iron ore is mixed with other materials and undergoes a combustion process to yield sinter. The sinter and the coke then enter a blast furnace, where iron oxides are reduced by coke and the result is then fed to the basic oxygen furnace, where the final adjustments for steel are performed. The temperature-enthalpy profile of steel production is taken from [127] and the average European production is estimated at 198 Mt/year [134].

**Sugar** Sugar extraction processes from sugar beet and sugar cane are quite similar. For example, in the former case, beets are cut into thin slices, which are then passed through water-based counter-current extraction in a diffuser. Then, they emerge as impure sugar juice and beet pulp. The temperature inside the diffuser is around 68°- 72°C. The crystallization process takes place in vacuum pans, in which the juice is boiled under vacuum. Finally, the sugar crystals are removed by centrifugation. The temperature-enthalpy profile of the process is taken from [132] and the average

### 3.3. Materials and methods

European production is estimated at 13.3 Mt/year [130].

**Plastics** Plastics production requires energy, even in the case of polymerization systems where the process itself is exothermic. The demand for energy generally depends on the situation, i.e. if the polymerization unit is integrated into a larger complex with, for example, the need for low pressure steam. In this work the temperature-enthalpy profile of the plastic production process is considered according to work done in the Enhanced energy and resource Efficiency and Performance in process industry Operations via onsite and cross-sectorial Symbiosis (EPOS) project and the average European production is estimated at 53.0 Mt/year [135].

The composite curves and the grand composite curve of the processes are given in figures 3.2 (cement), 3.3 (oil refinery), 3.4 (brewery), 3.5 (pulp and paper mills), 3.6 (dairy), 3.7 (aluminum), 3.8 (steel), 3.9 (sugar), 3.10 (plastic), scaled for 1 million inhabitants. The typical European productions per inhabitant are also given in table 3.1.

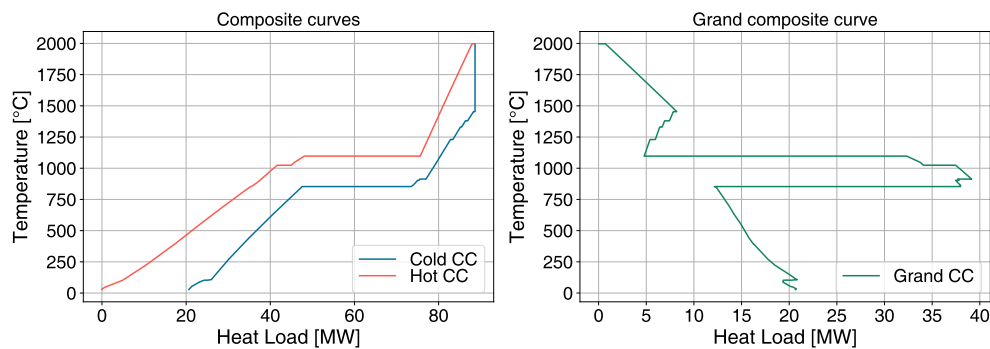


Figure 3.2 – CCs (left) and GCC (right) of the average European cement production process, scaled for the consumption of a population of 1 million inhabitants.

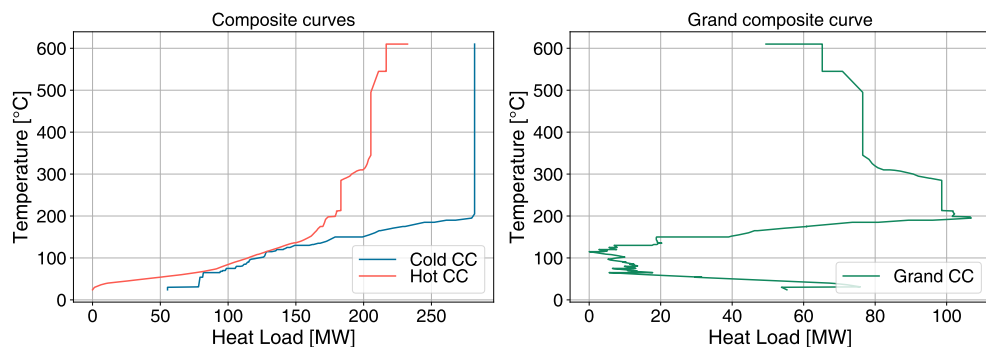


Figure 3.3 – CCs (left) and GCC (right) of the average European oil refinery process, scaled for the consumption of a population of 1 million inhabitants.

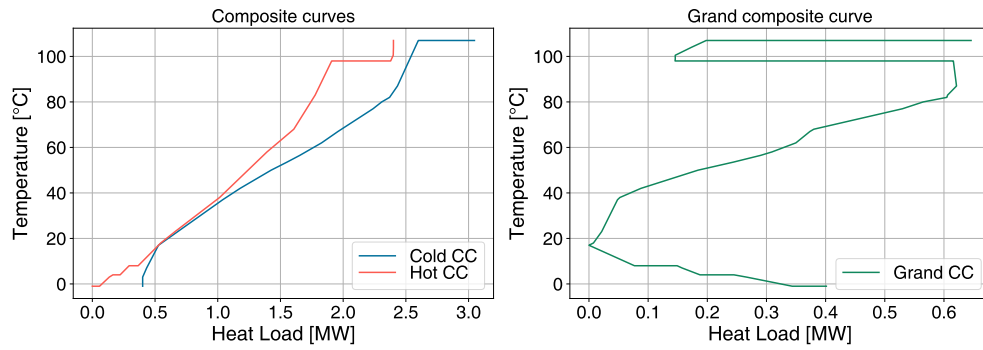


Figure 3.4 – CCs (left) and GCC (right) of the average European brewery process, scaled for the consumption of a population of 1 million inhabitants.

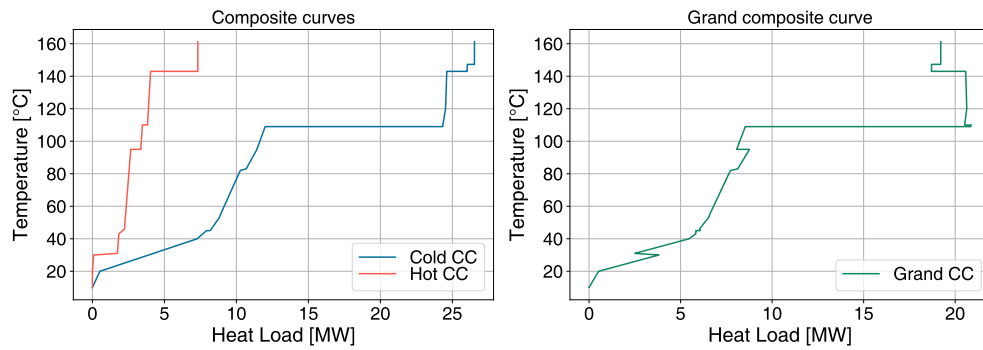


Figure 3.5 – CCs (left) and GCC (right) of the average European pulp and paper process, scaled for the consumption of a population of 1 million inhabitants.

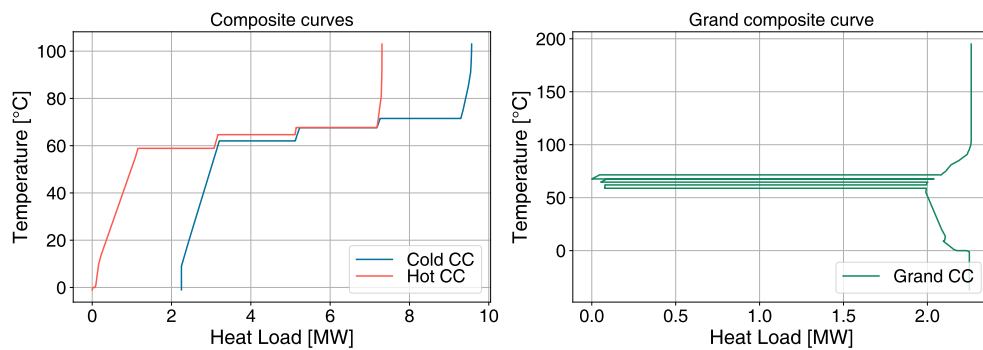


Figure 3.6 – CCs (left) and GCC (right) of the average European dairy process, scaled for the consumption of a population of 1 million inhabitants.

### 3.3. Materials and methods

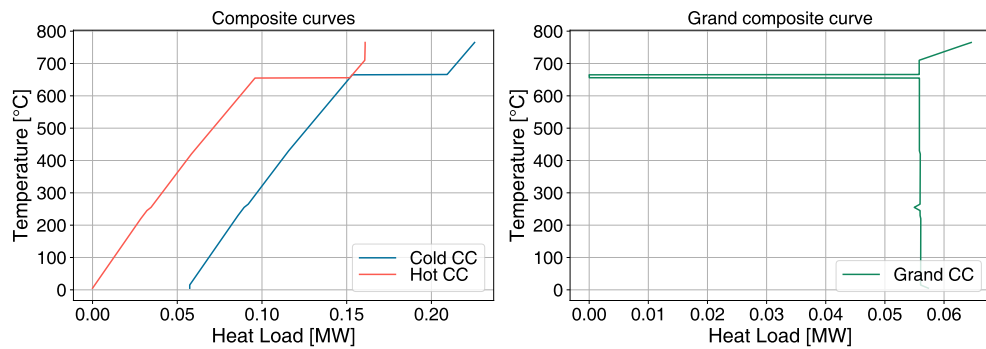


Figure 3.7 – CCs (left) and GCC (right) of the average European secondary aluminum process, scaled for the consumption of a population of 1 million inhabitants.

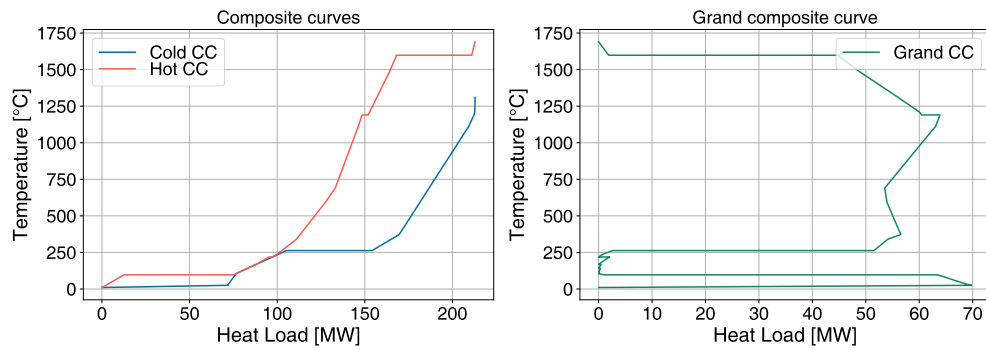


Figure 3.8 – CCs (left) and GCC (right) of the average European steel process, scaled for the consumption of a population of 1 million inhabitants (with utilities on site).

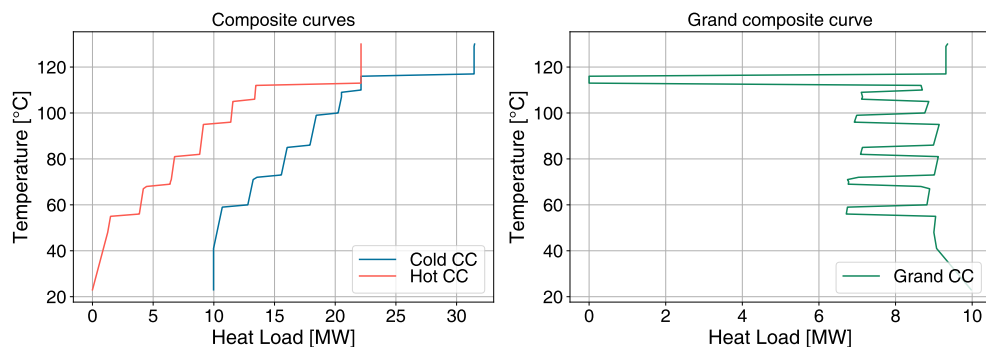


Figure 3.9 – CCs (left) and GCC (right) of the average European sugar process, scaled for the consumption of a population of 1 million inhabitants.

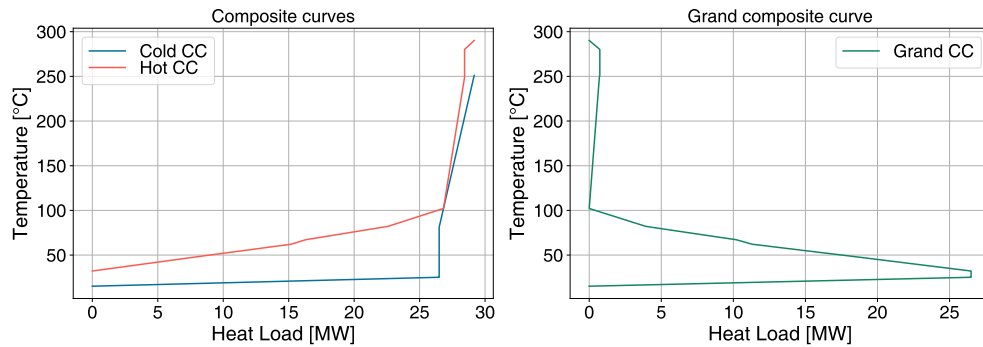


Figure 3.10 – CCs (left) and GCC (right) of the average European plastic process, scaled for the consumption of a population of 1 million inhabitants (with utilities on site).

Table 3.1 – Typical European city industrial production by sector.

Industry	Flow	Unit	Details
Pulp and paper	192.1	kg/(cap · y)	$\left\{ \begin{array}{l} \text{pulp} \left\{ \begin{array}{l} \text{thermocheccmical pulp: } 29.5 \text{ kg}/(\text{cap} \cdot \text{y}) \\ \text{sulphite pulp: } 59.3 \text{ kg}/(\text{cap} \cdot \text{y}) \end{array} \right. \\ \text{old paper: } 103.3 \text{ kg}/(\text{cap} \cdot \text{y}) \end{array} \right.$
Cement	536.6	kg/(cap · y)	
Oil refinery	1768.5	kg/(cap · y)	
Brewery	76.6	L/(cap · y)	
Dairy	91.4	kg/(cap · y)	$\left\{ \begin{array}{l} \text{drinking milk: } 61.1 \text{ kg}/(\text{cap} \cdot \text{y}) \\ \text{yoghurt: } 30.3 \text{ kg}/(\text{cap} \cdot \text{y}) \end{array} \right.$
Aluminum	3.4	kg/(cap · y)	
Steel	397.9	kg/(cap · y)	
Sugar	26.7	kg/(cap · y)	
Plastics	12.2	kg/(cap · y)	

### 3.3.1.1 Real city: Rotterdam

The second case study considered is the city of Rotterdam, Europe's largest port. Its pivotal location in Europe, maritime access, wide range of service providers and excellent connection by inland waterways, rail and road make Rotterdam the port of choice for the world's leading (petro-) chemical and energy companies. Among the industries present in the port, this work considers oil refineries, cement manufacturing and breweries; therefore, studying their integration with the district energy network of the city.

Four refineries from the port of Rotterdam are taken into account, namely Shell, Esso, Gunvor and BP. Their annual flows [136] and Manhattan distance (i.e. the sum of the distances in each dimension) from the district are given in Table 3.2. The thermal profiles of the refineries were considered



### 3.3. Materials and methods

according to [127] and a sample one (the profiles scale with the production rate) is displayed in Figure 3.11.

Table 3.2 – Refinery yearly flow and distance from the district.

Refinery	Flow [kt/year]	Distance [km]
Shell	31200	5
Esso	14800	9
Gunvor	7900	20
BP Raffinaderj	26430	30

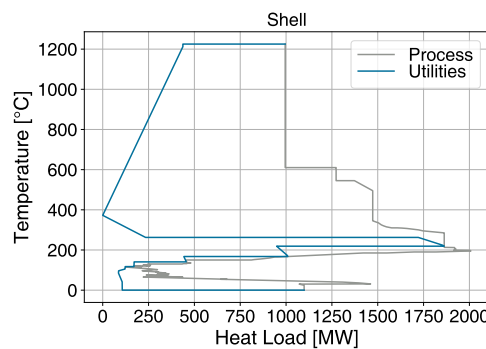


Figure 3.11 – Integrated composite curve (ICC) of the Shell refinery.

Four theoretical cement plants are considered, one at each location where a refinery exists. As seen in Figure 3.12, large quantities of waste heat are available, which provide opportunities for process integration and symbiosis between plants and with the nearby district.

The temperature-enthalpy profile of the beer production process is taken from [27] and represented in Figure 3.12 for a production rate of 70 L/(cap · year) [137]. Since brewing has a low process pinch temperature, it can receive heat from the other industrial plants; therefore, the brewery competes with other low-temperature demands, such as the district, to obtain excess heat from the other industries.

Figure 3.13 schematically represents the location of the industrial plants considered and the interaction between the different industries and the district energy network of the city. The figure also depicts allowable heat transfers, taking one location with a refinery and cement plant as an example. For the scenarios considered here, cement plants may transfer heat to any heat consumer, refineries can transfer heat to the brewery and/or district while the brewery and district cannot transfer heat to any of the other plants. As observed in Figure 3.13, the industrial plants are not always in close proximity to the city, the consequences of which (i.e. resulting heat losses and profitability of heat transfer between locations) are also analyzed in this paper.

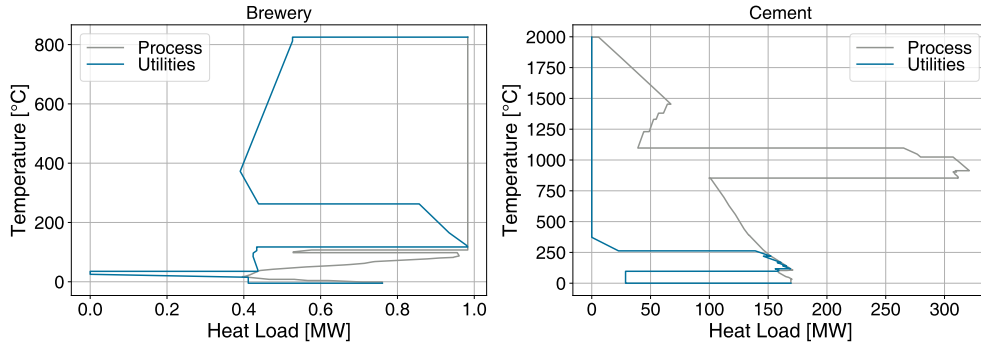


Figure 3.12 – Integrated composite curves of the brewery (left) and cement (right) plants considered.

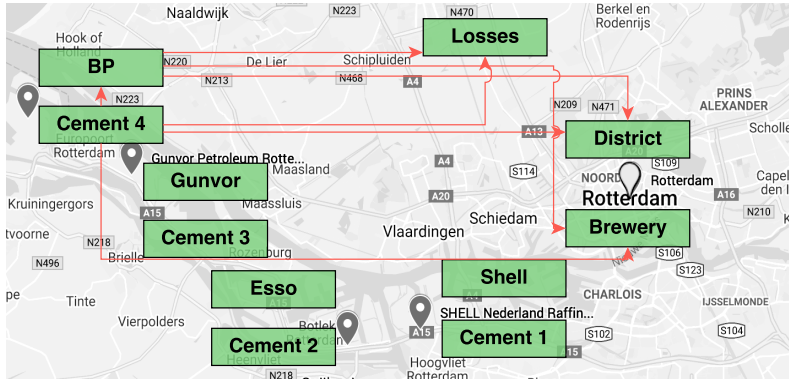


Figure 3.13 – Schematic description of brewery and cement plants interaction with DHC network.

### 3.3.2 Heat distribution losses

When heat exchange between industrial plants and urban district networks is considered, heat losses related to separation distance must be taken into account. The MILP formulation must be altered to reflect this [138] and the modifications from the formulation presented in the introduction are listed below. Primarily, the MILP formulation is modified to account for the location of the heat streams and losses resulting from the distance between them. A series of new sets must therefore be defined; namely, a set of locations ( $L$ ), a set comprising all the streams in a given location ( $SL_l$ ), a set of parents ( $PA$ ) and streams of parents ( $SOP_{pa,l}$ ) describing the streams which can be used in different locations and their corresponding sub-streams in each location, and a set of parents of unit ( $POU_u$ ) containing all the parents belonging to unit  $u$ .

Heat cascade constraints in the classical formulation are indexed over time steps ( $t$ ) and temperature intervals ( $k$ ), this formulation adds an additional location index ( $l$ ), to close the heat cascade in each

location:

$$\sum_{s \in \mathbf{SL}_l} g_{s,t} \cdot \dot{q}_{s,t,k} + \dot{R}_{t,k+1,l} - \dot{R}_{t,k,l} = 0 \quad \forall t \in \mathbf{T}, \forall k \in \mathbf{K}, \forall l \in \mathbf{L} \quad (3.1a)$$

$$\dot{R}_{t,k,l} \geq 0 \quad \forall t \in \mathbf{T}, k \in \mathbf{K}, \forall l \in \mathbf{L} \quad (3.1b)$$

$$\dot{R}_{t,1,l} = 0 \quad \dot{R}_{t,k+1,l} = 0 \quad \forall t \in \mathbf{T}, \forall l \in \mathbf{L} \quad (3.1c)$$

In the classical formulation, the stream sizing factor  $g_{s,t}$  is equal to the sizing factor of their corresponding unit  $f_{u,t}$ . Considering heat losses, each parent stream can be split in several streams of parent across different locations. Therefore, additional constraints must be considered, such as setting the sum of the sizing factors of the streams of a parent equal to the sizing factor of the unit the parent belongs to (Eq 3.2a), and setting the sizing factor of each stream of a parent equal to the sizing factor of the parent (Eq 3.2b):

$$\sum_{l \in \mathbf{L}} b_{pa,l,t} = f_{u,t} \quad \forall pa \in \mathbf{PA}, \forall u \in \mathbf{U}, \forall t \in \mathbf{T}: pa \in \mathbf{POU}_u \quad (3.2a)$$

$$b_{pa,l,t} = g_{s,t} \quad \forall pa \in \mathbf{PA}, \forall l \in \mathbf{L}, \forall s \in \mathbf{SOP}_{p,l}, \forall t \in \mathbf{T} \quad (3.2b)$$

Heat losses due to the transfer of heat between different locations is adapted from a steady-state heat loss formulation for buried pre-insulated district heating pipes [139]. Since the case study considered is an urban area, it is assumed that pipes will be installed underground. The corrected pipe depth (H) is defined as:

$$H = H' + \frac{\lambda^g}{h^{\text{air}}} \quad (3.3)$$

where  $H'$  is the depth at which the pipes are located,  $\lambda^g = 2.7 \text{ W/(m}\cdot\text{K)}$  [140] the thermal conductivity of the ground and  $h^{\text{air}} = 14.6 \text{ W/(m}^2\cdot\text{K)}$ , the convective heat transfer coefficient of air. The thermal resistances of the transfer between the supply and return pipes ( $R^m$ ), of the ground ( $R^g$ ) and of the insulating material ( $R^i$ ) are computed according to:

$$R^m = \frac{1}{4 \cdot \pi \cdot \lambda^g} \cdot \ln \left( 1 + \left( \frac{2 \cdot H}{E} \right)^2 \right), \quad R^g = \frac{1}{2 \cdot \pi \cdot \lambda^g} \cdot \ln \left( \frac{4 \cdot H}{D^i} \right), \quad R^i = \frac{1}{2 \cdot \pi \cdot \lambda^i} \cdot \ln \left( \frac{D^i}{D^p} \right) \quad (3.4)$$

with  $E$  as the distance between the pipes,  $\lambda^i$  the thermal conductivity of the insulating material and  $D^i$  and  $D^p$  the diameter of the pipe with and without insulation, respectively. The heat loss coefficients ( $U_1$ ,  $U_2$ ) and the supply ( $\dot{q}^s$ ) and return ( $\dot{q}^r$ ) heat losses are calculated using:

$$U_1 = \frac{R^g + R^i}{(R^g + R^i)^2 - (R^m)^2}, \quad U_2 = \frac{R^m}{(R^g + R^i)^2 - (R^m)^2} \quad (3.5)$$

$$\dot{q}^s = ((U_1 - U_2) \cdot (T^s - T^g) + U_2 \cdot (T^s - T^r)) \cdot L^p \quad (3.6)$$

$$\dot{q}^r = ((U_1 - U_2) \cdot (T^r - T^g) - U_2 \cdot (T^s - T^r)) \cdot L^p \quad (3.7)$$

with  $L^p$  being the pipe length and  $T^s$ ,  $T^r$  and  $T^g$  the supply, return and ground temperatures, respectively.

3

## 3.4 Results and discussion

### 3.4.1 Typical European city

The typical European city results are shown using three European city sizes as examples: small (e.g. Zurich, radius: 5290 m, population: 403 000), medium (e.g. Munich, radius: 9950 m, population 1 450 000), large (e.g. London, radius: 21390 m, population: 8 139 000). The 10 industries introduced in Section 3.3 were positioned around the city according to a simple set of heuristic rules:

- all industries are located at a distance from the city center (i.e. district) between 100 m and double the radius of the city;
- the low temperature industries (brewery, dairy, pulp and paper, sugar) are located at a distance from the city center between 40% and 100% of the radius of the city, with a minimum distance between each other of 20% of the radius;
- the maximum distance between the low temperature industries is 30% of the radius of the city;
- the aluminum and steel industries are situated at the same location. This assumption is made given that the aluminum size is very small and for simplicity, to reduce the degrees of freedom of industry location permutations;
- the high temperature industries (cement, steel and aluminum, oil refinery, waste incineration and plastic) are located at a distance from the city center between 40% and 200% of the radius of the city, with a minimum distance between each other of 40% of the radius;

- the maximum distance between the high temperature industries is 50% of the radius of the city;

Euclidean distances are considered in this case, since this is an exploratory study and the real locations of the plants are not known. This work assumes that heat recovery is possible from all industrial processes, either by steam network or through a hot water loop. Details on the heat recovery technologies can be found in Appendix C.1.1 and C.1.2. Figure 3.14 depicts the industry location coordinates for a small city scale. The locations for medium and large scales are determined by linearly scaling the distances with the radii of the cities.

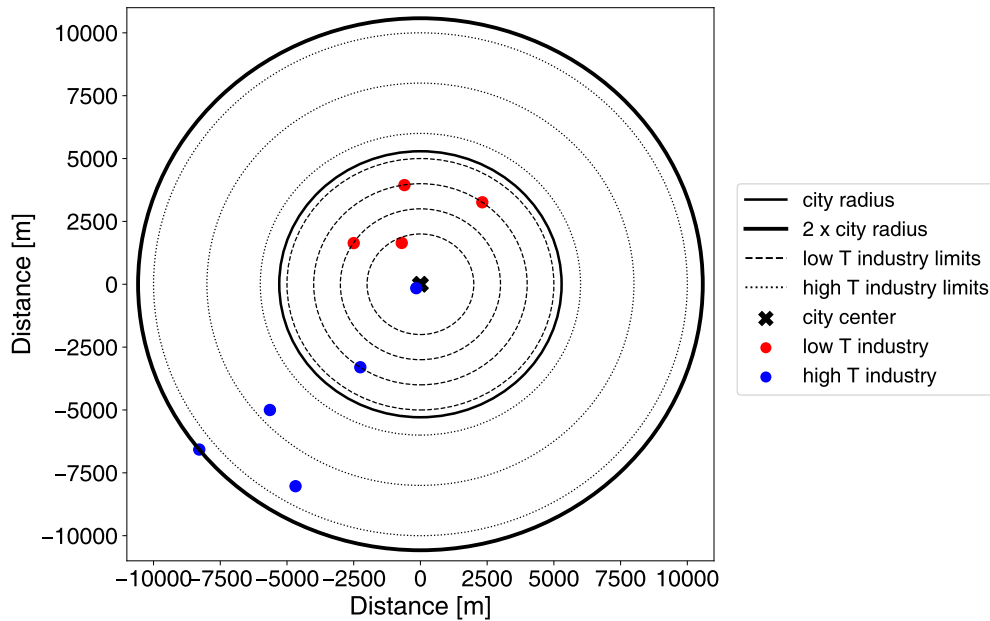


Figure 3.14 – Industry location coordinates in a small city.

Since the district represents the highest energy demand of the city, almost no heat is transferred to any of the other low-temperature industries; therefore, their locations are assumed fixed. However, the high temperature industry locations are permuted to explore effects of industry topology from an energy integration point of view, i.e.  $5! = 120$  solutions are analyzed.

**Small city** Figure 3.15 shows the first set of results for a small city, namely the heat transferred (excluding heat losses), the heat lost through steam network and hot water sharing and the relative difference in energy import, compared to the case when no heat sharing occurs between the different locations (i.e. dark blue curve). 122 results are shown: no heat sharing (dark blue curve) heat sharing with no losses (dark red curve), and 120 location permutations of high-temperature industries.

The results show that 800 - 1400 GWh/year of heat is shared through steam and 400 - 500 GWh/year is shared through hot water loops. Heat losses through steam vary between 9.7 and 32.7%, while

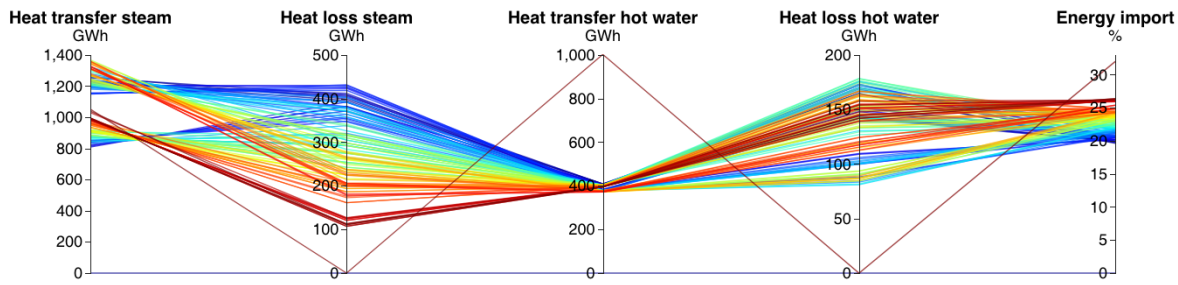


Figure 3.15 – Heat transfer results, small city.

the heat losses through hot water loops vary between 17.7 and 30.9%. Moreover, the maximum theoretical energy import savings amount to 32% (i.e. theoretical maximum by sharing heat using utilities), while with realistic industry locations, the energy import savings vary between 20 - 26%. The corresponding operating cost and environmental impact savings are 11 - 15% and 16 - 23%, respectively (see Appendix C.1).

Moreover, two distinct sets of solutions emerge (800 - 1000 GWh/year and 1200 - 1400 GWh/year transfer through steam), depending mainly on the relative location of the district, and on whether the waste incineration facility transfers heat directly to the district, or it first satisfies the high temperature requirements of the refinery and then the refinery transfers heat to the district at a lower temperature.

Figures 3.16 and 3.17 display the breakdown of hot water (HW) and steam network (SN) transfers to the district and between the different industries; the colors correspond to the solutions shown in Figure 3.15.

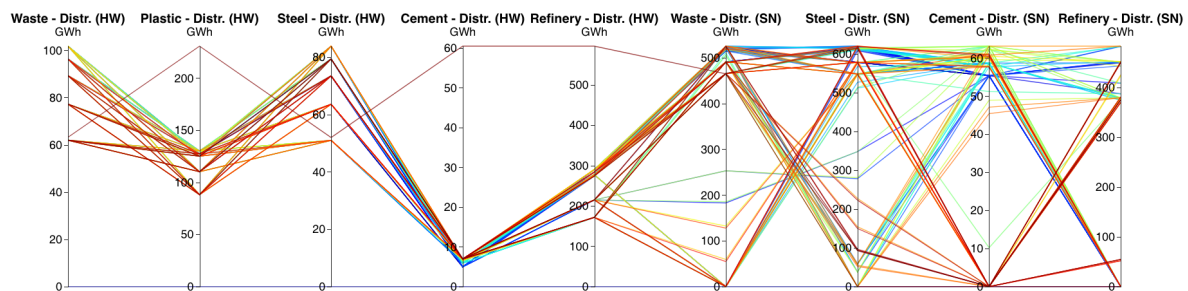


Figure 3.16 – Heat transfer to the district, small city.

The industries transferring the most heat to the district are the waste incineration and the steel plant, the oil refinery passes on heat that it receives at high temperature and first uses on site, while the cement and plastic plants send their own excess heat, though the absolute values of these loads are lower than the other industries. Additionally, as shown in Figure 3.17, the heat demand of the oil refinery is satisfied by waste incineration, steel or cement and the one of plastic by waste incineration, cement or the oil refinery, depending on the proximity of the different industries. More

### 3.4. Results and discussion

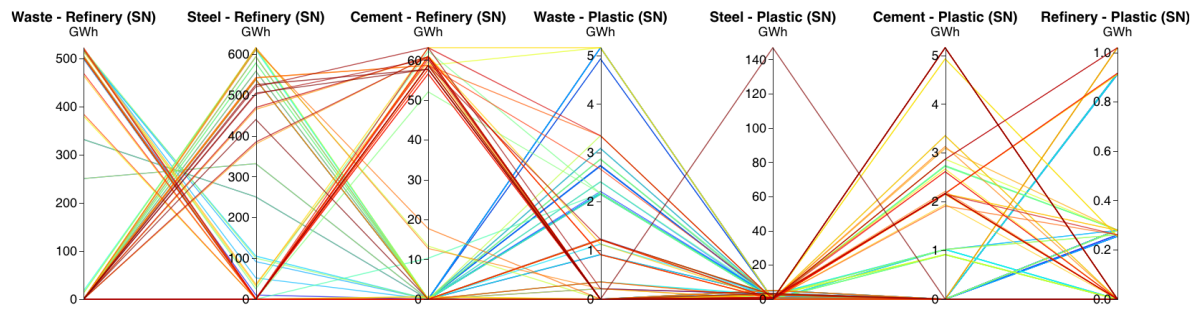


Figure 3.17 – Heat transfer between industries, small city.

detailed results, with exact industry locations and inter-distances are shown in Section 3.4.1.1.

**Medium city** Figures 3.18 - 3.20 show the corresponding results for a medium city. As seen in Figure 3.18, the potential energy import savings decrease compared to the small city to 10 - 16%, since the absolute distances between the heat sharing parties increase, therefore rendering higher heat losses and consequently fewer connections. The corresponding potential decreases in operating cost and environmental impact are 7 - 11% and 8 - 14%, respectively (see Appendix). Moreover, the steam network sharing heat losses decrease to 3 - 27%, while the heat losses in the hot water loop increase to 29 - 39%. Consequently, the solutions with the highest energy savings correspond to high steam network heat sharing at short distances (i.e. low heat losses).

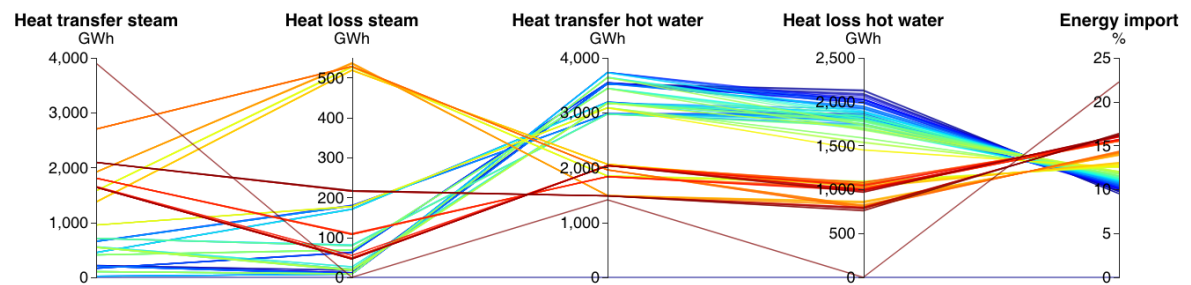


Figure 3.18 – Heat transfer results, medium city.

As observed in Figure 3.19, similarly to the case of a small city, the industries transferring the largest amount of heat to the district are waste incineration, steel and oil refining (which receives heat from other industries, uses it on site and then delivers it to the district at lower temperature).

Also in the case of a medium city, heat transfer to the plastic plant alternates between the waste incineration, steel plant, cement plant and oil refinery, always satisfying its full demand. An additional result introduced with the medium-size city is that no steam network transfer occurs above a distance of 10 km between any two parties (i.e. in the case of transfer to the district, the hot water loop is the only heat transfer medium used above a distance of 10 km).



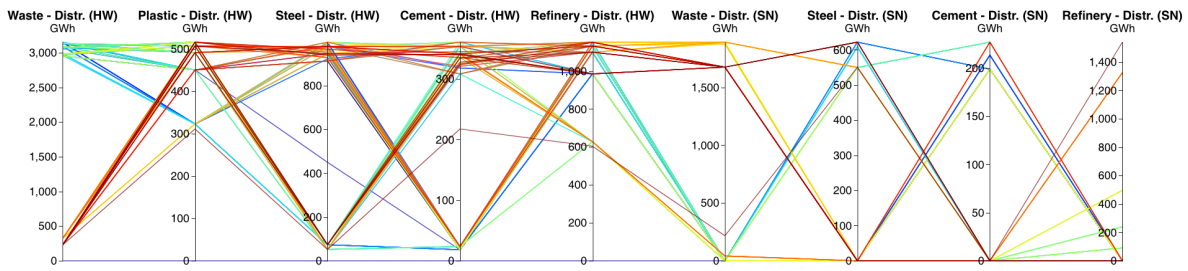


Figure 3.19 – Heat transfer to the district, medium city.

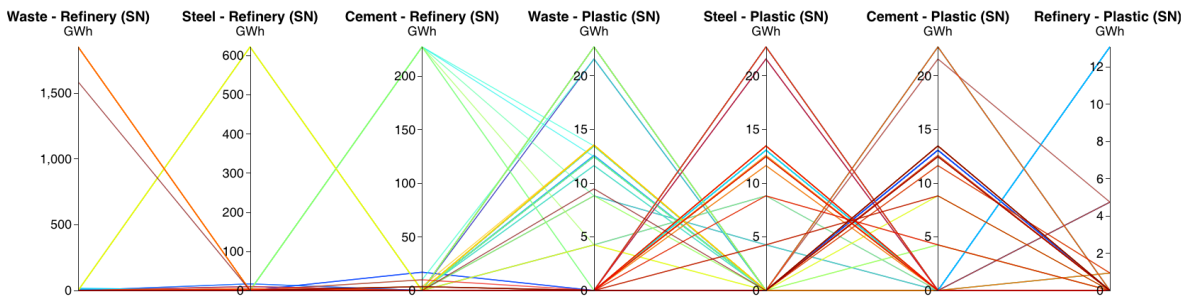


Figure 3.20 – Heat transfer between industries, medium-sized city.

3

**Large city** Figures 3.21 - 3.23 show the results for a large city. In this case, the energy import savings further decrease, to 4 - 14%, as well as the operating cost and environmental impact savings, which drop to 3 - 11% and 4 - 12%, respectively (see Appendix). Similarly to the case of a medium city, this results from an increase in the absolute distances between the industries and district, leading to higher heat losses and therefore fewer connections. Also in the case of large-scale cities, solutions with the highest energy import savings are those in which a large amount of heat is transferred by steam networking, however with low losses, i.e. over short distances. The steam network heat losses in this case vary between 6 and 64%, while the hot water loop heat losses are between 25 and 44%.

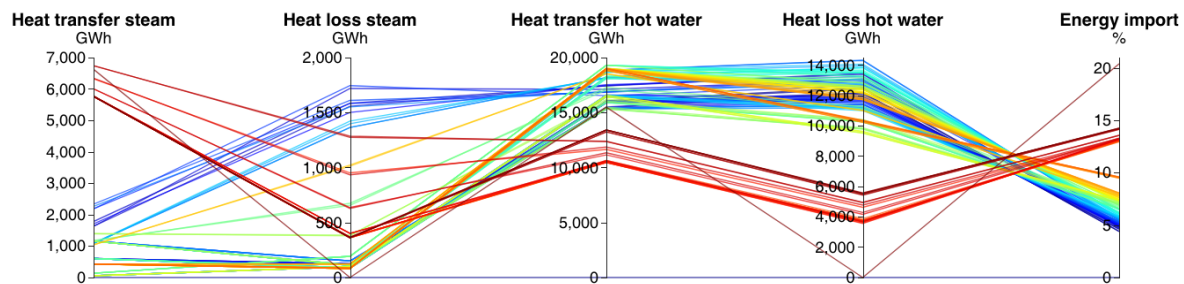


Figure 3.21 – Heat transfer results, large city.

In the case of a large city, the waste incineration plant is by far the industry sharing the most heat with the district (see Figure 3.22). Nevertheless, the other industries also transfer heat to the district, mostly using the hot water loop, since also in this case, no steam network transfer is realized above a distance of 10 km due to high resulting heat losses.



### 3.4. Results and discussion

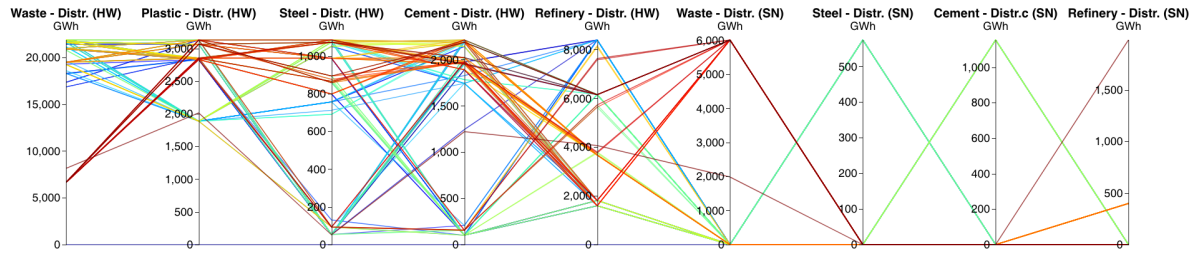


Figure 3.22 – Heat transfer to the district, large city.

Between industries, as for small cities, heat demand from oil refining and plastic production can be satisfied by nearby industries, though exactly which depends on plant locations.

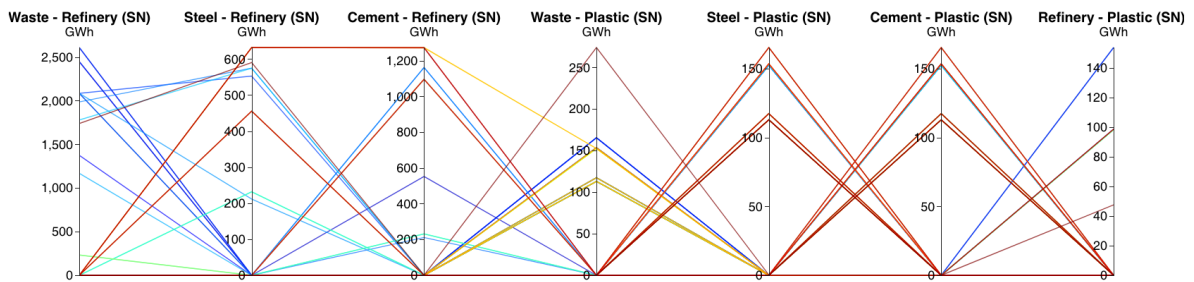


Figure 3.23 – Heat transfer between industries, large city.

#### 3.4.1.1 Detailed scenarios similar objective

This section presents in detail two of the best energy saving scenarios for the small city, as displayed in Figure 3.24. The solution with higher steam network heat sharing will be referred to as solution A and the solution with lower steam network heat sharing as solution B.

Figure 3.25 shows the locations of the high temperature industries (refinery, steel, waste incineration, cement and plastic) corresponding to solutions A and B and the hot water heat transfer from the high temperature industries to the district. The figure also provides a detailed perspective on the transfer from the industry located closest to the district. As observed, for solution A, the plastic, cement and waste incineration plants transfer 3%, 4% and 30% more heat, respectively, while the steel plant and refinery transfer 20% and 26% less heat to the district, respectively.

Furthermore, figures 3.26 and 3.27 show the steam network transfer to the district and between the high temperature industries. As observed in these figures, in the case of solution A, the waste incineration plant is located further from the district, and therefore transfers less heat directly through the steam network to the district, but it rather transfers heat to the refinery first. This heat is then transferred from the refinery to the district at a lower temperature.

The heat demand of the plastic industry is satisfied by other industries for both solutions, either

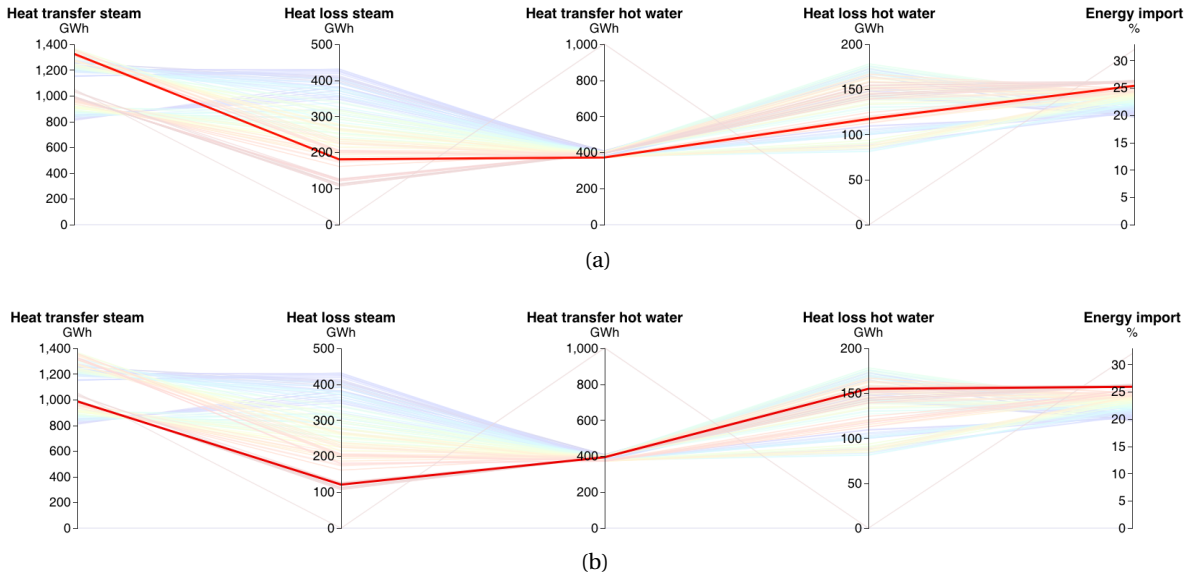


Figure 3.24 – Highlighted solutions, A (a), B (b).

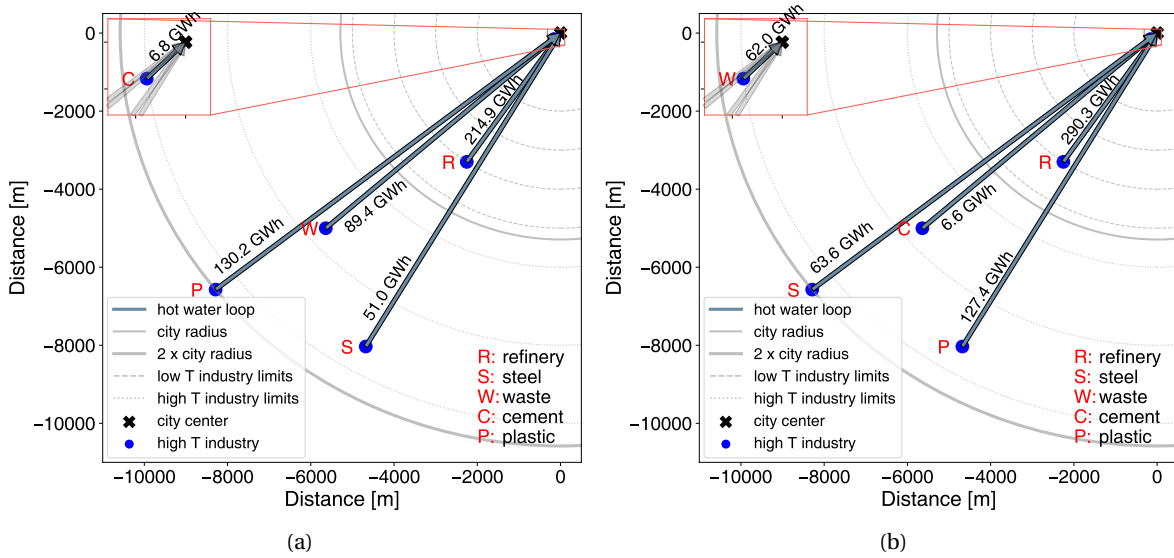


Figure 3.25 – Hot water loop transfer, solution A (a), solution B (b).

by the cement and waste incineration plant (solution A), or by the cement plant and oil refinery (solution B). However, while in solution A the cement plant transfers its excess heat to the refinery, in solution B it transfers excess heat directly to the district.

The Carnot composite curves (Figure 3.28) further details the heat transfer between different parties for solution A, including details on the temperature levels at which the transfers take place and the relative amount of heat compared to the size of the whole energy system studied.

### 3.4. Results and discussion

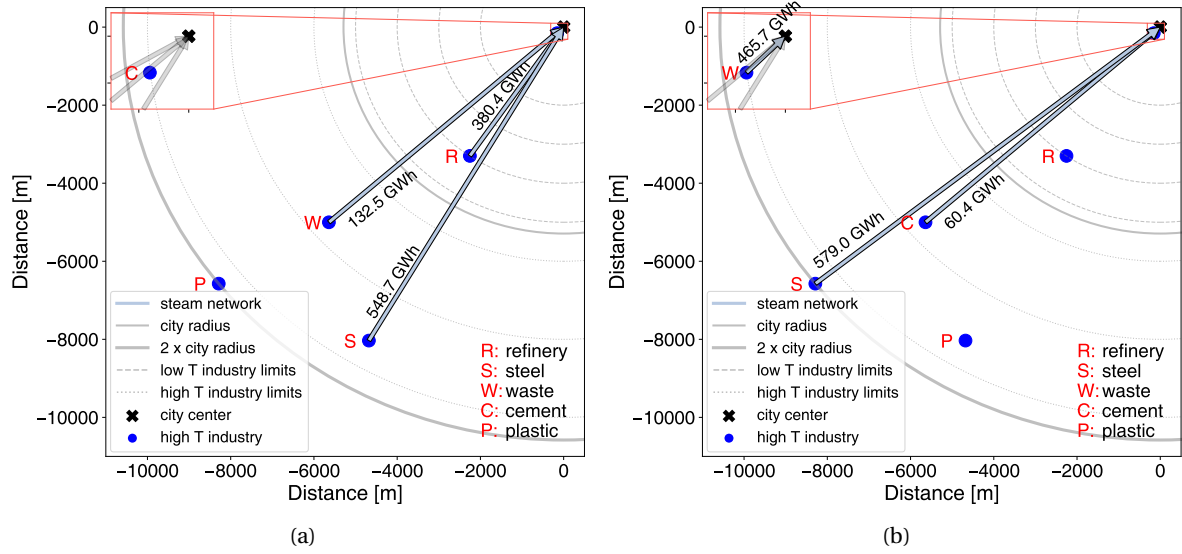


Figure 3.26 – Steam network transfer to district, solution A (a), solution B (b).

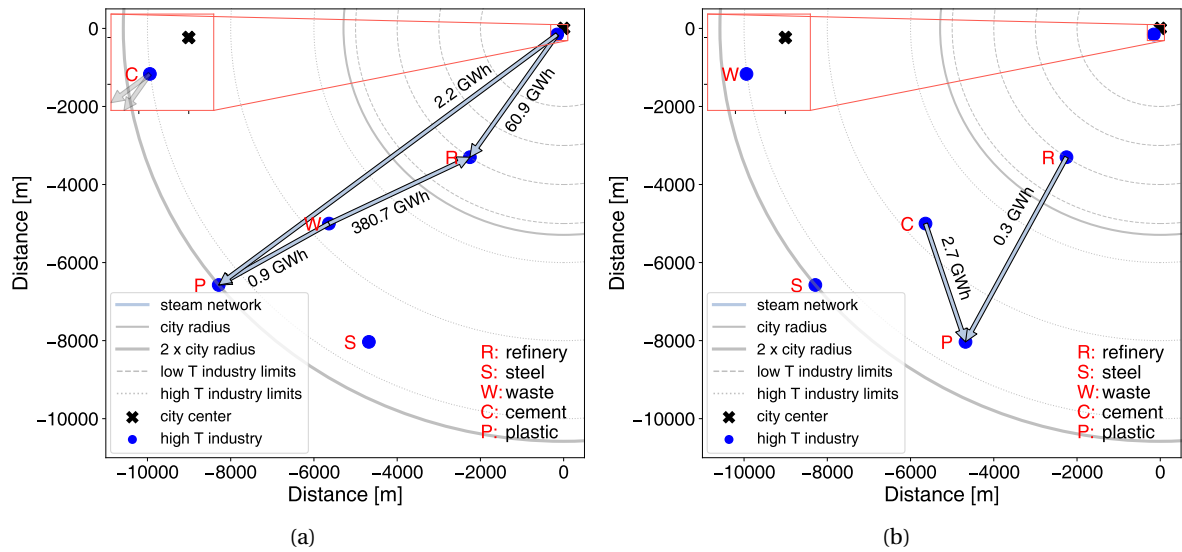


Figure 3.27 – Steam network transfer between industries, solution A (a), solution B (b).

#### 3.4.2 Real city: Rotterdam, NL

This section assesses integration between the district heating and cooling network with various nearby industrial plants, considering only steam network heat sharing. The integration was first studied by individually considering the plants at each location and their integration with the brewery and district. Figure 3.29 schematically shows the location of each refinery/cement plant couple and the heat flows between them, the DHC network and the brewery. Figure 3.30 displays the integrated

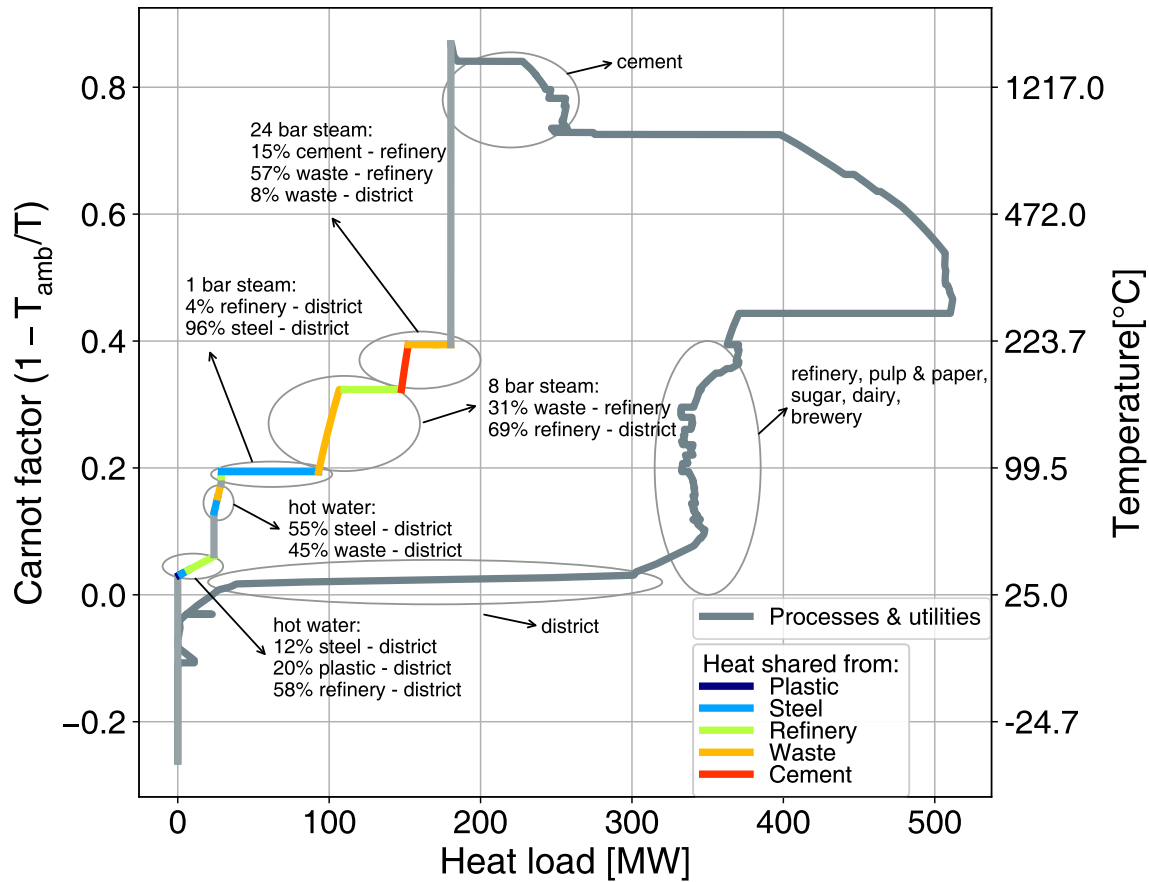


Figure 3.28 – Carnot composite curve highlighting heat transfer vs. processes and other utilities for solution A. Note: colors are used to highlight the share of heat transfer from different sources, not the exact temperature level at which the transfer takes place.

composite curves of each process for the different cases. The amount of heat transferred is also shown in more detail in Figure C.1 in Appendix C.2. For the first two locations (closest to the city), heat is transferred from the refinery and cement plant to the district, while for the last two locations (furthest from the city), heat integration is principally observed between the refinery and cement plant due to heat losses over longer distances. Since the industrial price of natural gas is lower, heat is not transferred to the brewery and the priority is given to the district to achieve the largest reduction in operating cost.

The impact of heat integration on the operating cost and environmental impact of the district is shown in Figure 3.31. 1 bar steam generation from waste heat is activated on the Shell and Esso refinery sites to share heat with the district. The integration with the Shell refinery leads to operating cost and CO<sub>2</sub> emission reductions of 6% and 13%, respectively; integration with the Esso refinery leads to operating cost and CO<sub>2</sub> emission reductions of 4% and 8%, respectively; the last

### 3.4. Results and discussion

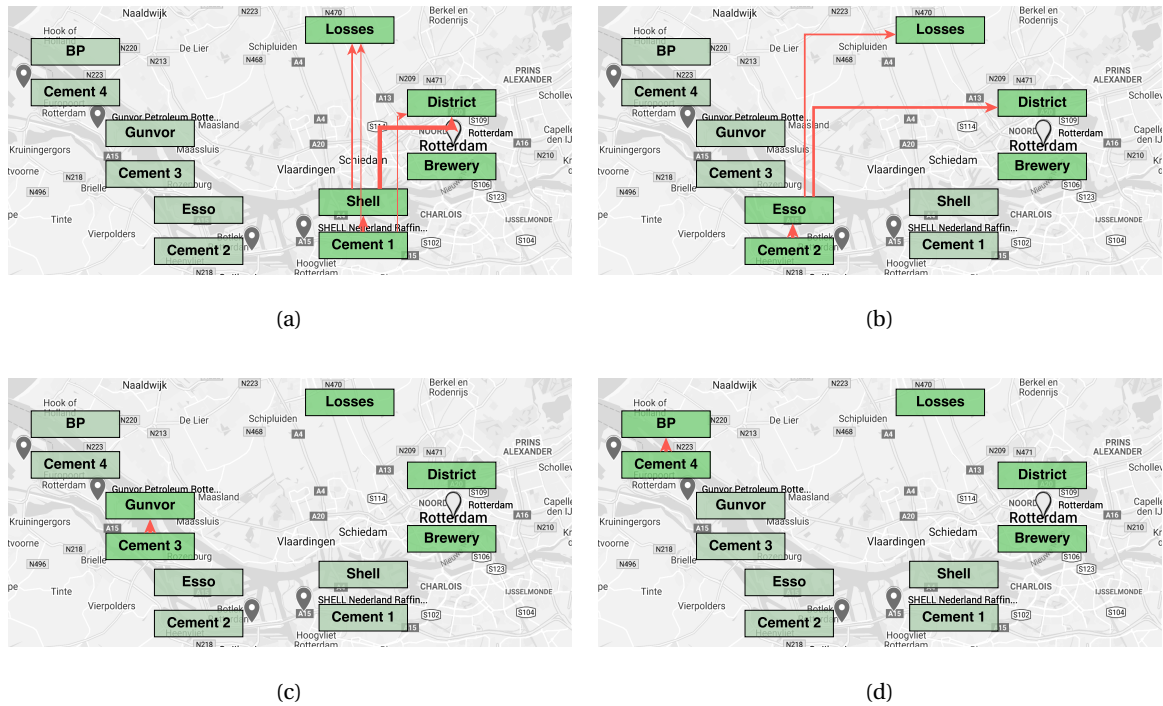


Figure 3.29 – Heat transfer and losses, refinery/cement plant couples considered individually.

two locations have almost no heat integration with the district and thus yield no improvement.

To assess the impact of expanding the system boundary, the refineries and cement plants were added sequentially, starting with the closest and ending with all four plants included in the optimization problem. Similarly to the case of refinery/cement plant couples considered individually, both the heat flows (Figure 3.32) and the resulting integrated composite curves (Figure 3.33) are displayed, and the detailed heat flows are given in Appendix C.2 (Figure C.2). As observed in the previous case, the cement plant and refinery couples located closest to the district transfer more heat to the district and to the brewery, while those located further away mostly exchange heat within the location.

The impact of the industrial heat integration on the operating cost and environmental impact of the district are shown in Figure 3.34. In this case, integrating the first two refineries leads to savings of 9% in operating cost and 20% in CO<sub>2</sub> emissions, while the last two refineries have negligible impact on the results. This was an expected result due to high heat losses associated with the transfer over larger distances.

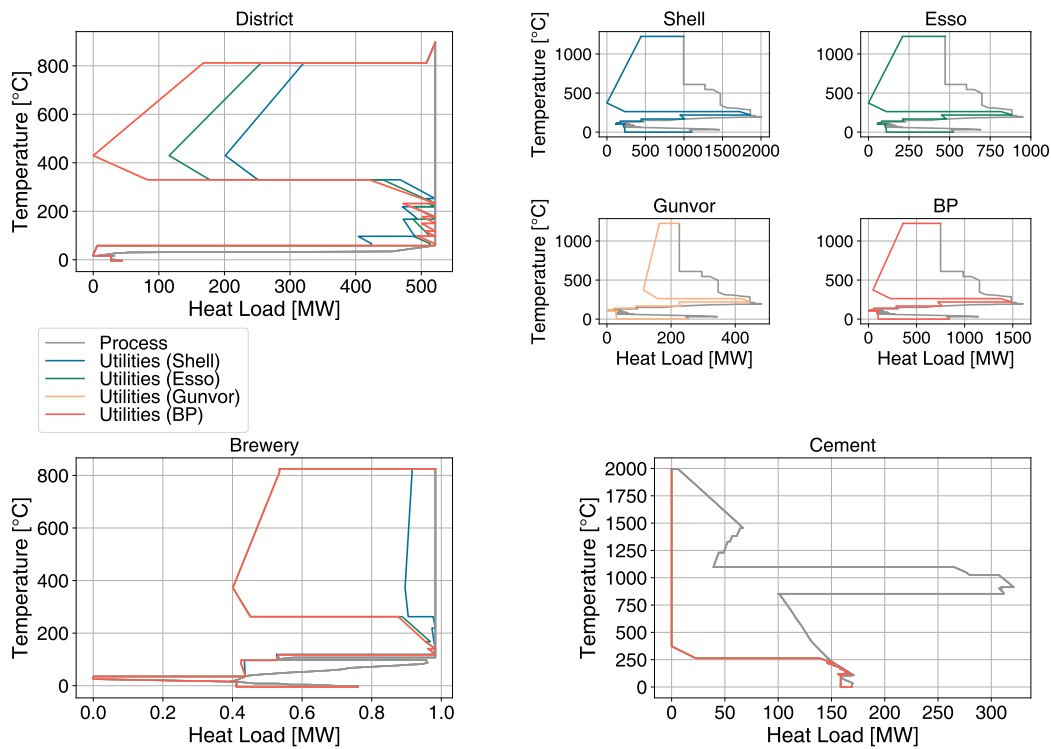


Figure 3.30 – Integrated composite curve of the processes considered, refinery/cement plant couples considered individually.

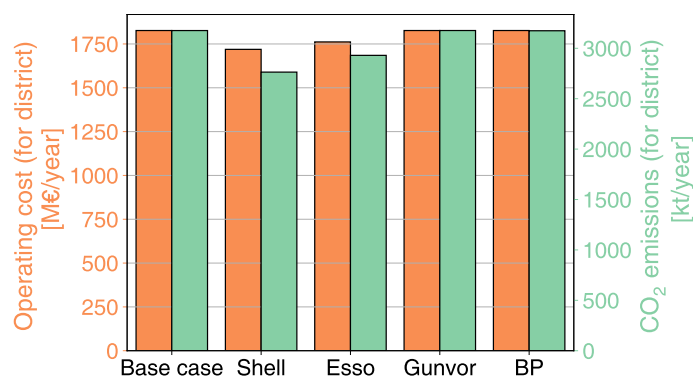


Figure 3.31 – Operating cost and CO<sub>2</sub> emissions, refinery/cement plant couples considered individually.

### 3.4. Results and discussion

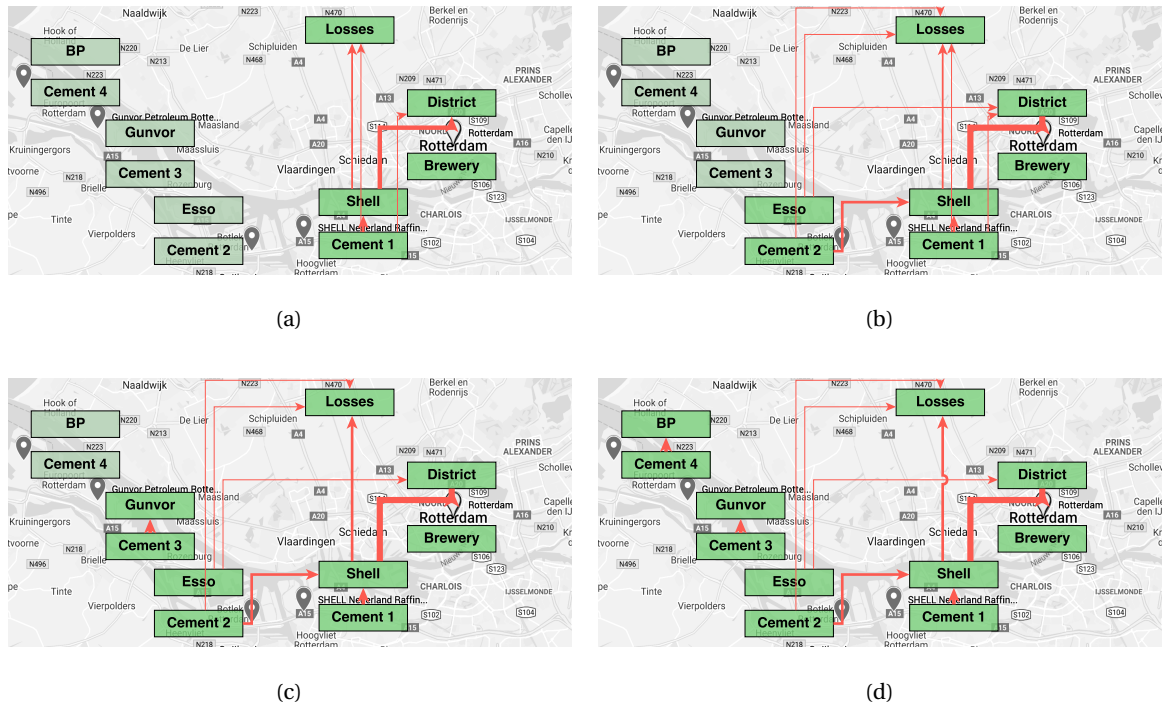


Figure 3.32 – Heat transfer and losses, refinery/cement plant couples considered individually.

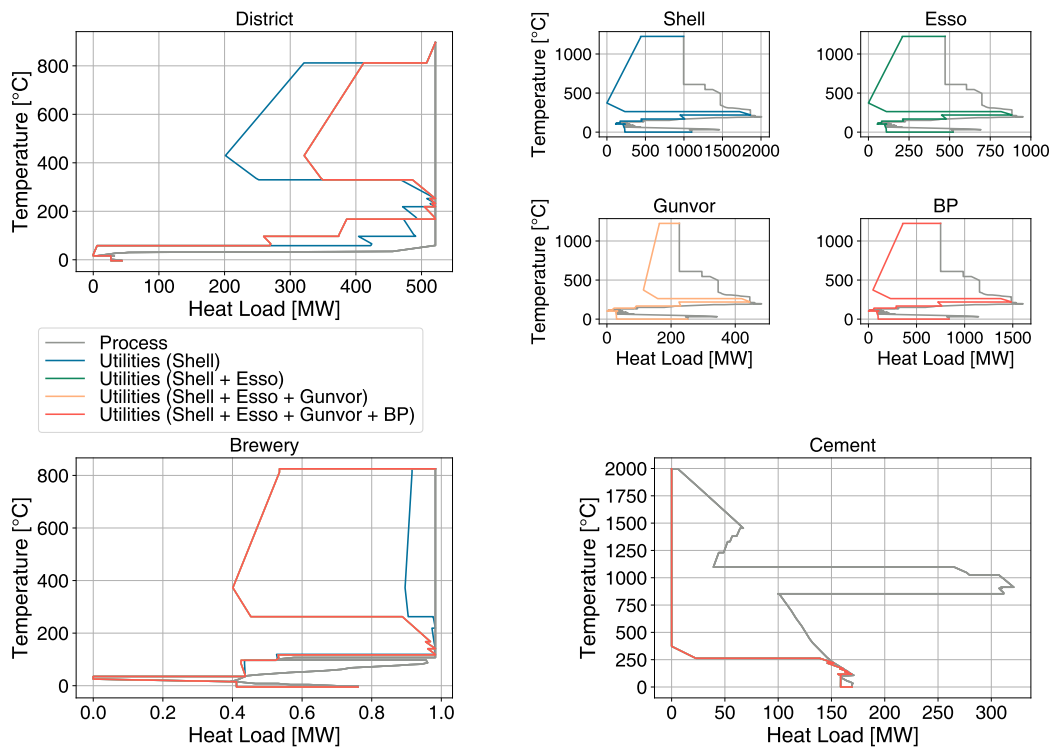


Figure 3.33 – Integrated composite curve of the processes considered, refinery/cement plant couples added sequentially.

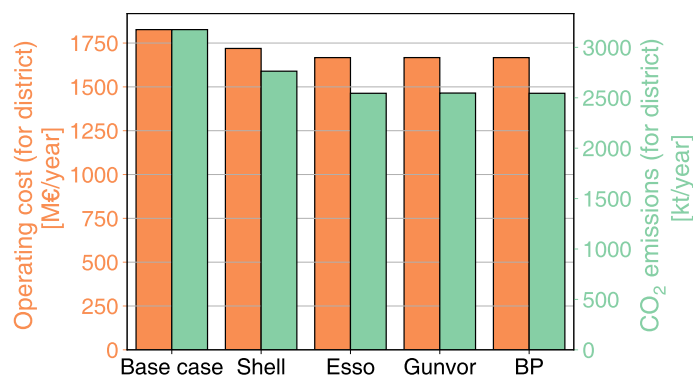


Figure 3.34 – Operating cost and CO<sub>2</sub> emissions, refinery/cement plant couples added sequentially.



### 3.5 Conclusion

This chapter aims at enriching the residential sector profile presented in chapter 1 by adding production data for ten main industries: cement, oil refining, steel, aluminum, waste incineration, plastic, pulp and paper, brewing, sugar and dairy. In this chapter, the residential sector profile was used to assess integration opportunities between urban centers and typical industries in the surroundings. Two categories of case studies are used, namely average European cities (small-, medium- and large-scale) including all ten industries and a real European case study in Rotterdam, NL. A brewery and four refinery/cement plant couples in the area are integrated in the latter case.

The results on the average European cities show that higher heat transfer takes place in a small-scale city, compared to medium or large ones, since the increase in distance between the district and the industries is larger than the increase in population (i.e. industry sizes). Consequently, the energy import savings vary between 20 - 26% for small scale cities, 10 - 16% for medium scale and 4 - 14% for large scale ones. Detailed results on the heat transfers show, for example, that solutions with very similar energy import savings can vary by up to 30% in the amount of heat transferred, due to the relative distances between the heat sharing parties, e.g. when the oil refinery plant is located between the waste incineration plant and the district, heat is first transferred to the refinery. The refinery uses the high temperature heat before delivering it to the district, at a lower temperature.

Furthermore, results on the real city highlight the fact that industries located at 5 km and 9 km transfer heat to the district energy network reducing its operating cost by as much as 9% and environmental impact by up to 20%, while industrial plants located further afield only integrate with each other, as heat losses are too large over long distances for profitable exchanges. These results are different from the average European city results, since they reflect the current situation of industrial systems, i.e. large facilities producing enough resources for several cities, and not just satisfying the needs of the nearest one.

Overall, excess industrial heat recovery for district heating is advantageous, especially when the industrial plants are located close to the city. However, an analysis which includes piping cost and pumping electricity is needed in order to have a full picture of the maximum distance between industry and district which makes heat integration profitable. Moreover, building similar sector profiles for all energy-intensive sectors would provide a complete set of tools for future modelling of energy efficient cities/countries.



# Systematic integration of energy-optimal buildings with district networks

## Overview

- The "typical European" urban demand is estimated in chapter 1;
- The natural and renewable resource valorization is explored in chapter 2;
- The industrial waste heat valorization is explored in chapter 3;
- This chapter looks into bridging the gap between building - and city - scale energy optimization.

*This chapter is partially a summary of [141, 142]*

The residential sector accounts for a large share of worldwide energy consumption, yet is difficult to characterize, since consumption profiles depend on several factors from geographical location to individual building occupant behavior. Given this difficulty, the fact that energy used in this sector is primarily derived from fossil fuels and the latest energy policies around the world (e.g., Europe 20-20-20), a method able to systematically integrate multi-energy networks and low carbon resources in urban systems is clearly required. This work proposes such a method, which uses process integration techniques and mixed integer linear programming to optimize energy systems at both the individual building and district levels. Parametric optimization is applied as a systematic way to generate interesting solutions for all budgets (i.e., investment cost limits) and two approaches to temporal data treatment are evaluated: monthly average and hourly typical day resolution. The city center of Geneva is used as a first case study to compare the time resolutions and results highlight that implicit peak shaving occurs when data are reduced to monthly averages. Consequently, solutions reveal lower operating costs and higher self-sufficiency scenarios compared to using a finer resolution but with similar relative cost contributions. Therefore, monthly resolution is used for the second case study, the whole canton of Geneva, in the interest of reducing the data processing and computation time as a primary objective of the study is to discover the main cost contributors. The canton is used as a case study to analyze the penetration of low temperature, 5G district energy networks with population density. The results reveal that only areas with a piping cost lower than 21.5 k€/100 m<sup>2</sup><sub>ERA</sub> connect to the low-temperature network in the intermediate scenarios, while all areas must

connect to achieve the minimum operating cost result. Parallel coordinates are employed to better visualize the key performance indicators at canton and commune level together with the breakdown of energy (electricity and natural gas) imports/exports and investment cost to highlight the main contributors.

## 4.1 Introduction

Increasing population, urbanization and rapid industrialization corresponds to parallel and continuous increases in world energy demand, where up to 65% of the energy consumption comes from urban areas [143]. While the consumption of major sectors, such as commercial, industrial, transportation and agriculture are relatively well-understood due to their centralized ownership, self-interest in reducing the energy consumption and high level of regulation, the residential sector is an energy sink which is difficult to characterize, since it encloses a large variety of geometries, structure sizes and envelope materials. At the same time, privacy concerns restrict energy consumption data collection and distribution and detailed metering of households bears high costs. Nevertheless, Pachauri et al. reports that there is a great potential to achieve significant reductions in energy consumption, mainly in the building sector, at a relatively modest cost [144], which highlights the requirement to better understand the defining characteristics of energy consumption in this sector.

### 4

Major end-use energy consumption groups in the residential sector are: space heating and cooling, energy required to overcome thermal flows through the building envelope, by conduction, radiation and through air infiltration/ventilation; domestic hot water-energy consumed to heat water to the comfort temperature; appliances and lighting-energy needed to operate appliances (e.g., refrigerator, electronics) and for supplying appropriate lighting. Fossil fuels are currently the main energy sources to supply these demands [145]; however, they have a high environmental impact and limited reserves which also correspond to fluctuating prices, which affects national economies and results in a prominent interest in using renewable energy sources. Renewable energy comes from a variety of sources, such as biomass, geothermal heat, ocean waves, sun, tides, water and wind. Hybrid (i.e., multi-source) renewable energy systems are favored over single sources since they are more reliable, more efficient, require less energy storage capacity and have lower levelized life cycle electricity generation cost under optimum design [146]. Multi-source generation makes hybrid system solutions complex, thus a techno-economic analysis of these systems is essential to ensure the optimal use of renewable sources. This, in turn, requires models and software which can be employed for design, optimization and techno-economic planning.

Another dilemma that arises with integration of renewable energies is the mismatch between renewable energy supply and demand profiles in the residential sector, which is often pronounced and requires extensive storage solutions [147]. Heat storage solutions already exist at small scale in individual buildings and via district heating networks in large bore-hole storage systems. Alternative

solutions exist for multi-energy systems, such as power-to-gas, fuel cells, electric/hydrogen mobility and large scale batteries [148, 149].

Balancing energy demand and supply both spatially and temporally can be modeled using computational methods, such as mathematical programming, among which linear programming techniques have been used to optimize multi-energy systems for more than thirty years [150]. Generally, there is a separation of topics in residential energy system analysis based on the scale, namely: individual building scale and urban scale. The former focuses principally or solely on the building itself and omits any relationship with the urban environment. It treats a building as an independent object, isolated from the built environment; however, real buildings are connected to their surroundings through physical means (infrastructure) and users (residents, workers). The latter scale focuses on the entire system, often without details at the building scale. Therefore, there are improvements to be made by coupling building-level models with those at the urban level while also using detailed equipment models (e.g., energy conversion technologies, heat pumps). Linking buildings with district systems requires tools for design, sizing, operation and control of energy system components, buildings and district networks. An even larger challenge, though, is to provide simple tools, which can aid decision-makers at an early stage in the design process at both the building and urban levels.

This chapter proposes a double-optimization approach with meta-models [151, 152] for the design and optimization of urban systems at building and urban levels, with interaction between the two scales, including renewable energy integration and long-term energy storage solutions. The connection between the building and the urban level is realized through a low-temperature 5G district energy network and meta-models are used to integrate building solutions into the district optimization. Therefore, this chapter contributes a novel approach for optimal design of urban energy systems, coupling optimal solutions for individual buildings with the larger energy system to provide guidance for holistic urban energy system design. Additionally, this work provides unique insights into various objectives of such systems and the inherent balance between them, providing a set of optimal solutions to be ultimately selected by decision-makers. Section 4.2 reviews the main tools and approaches currently employed for this purpose and their limitations, Section 4.3 presents the mathematical formulation and the case studies considered, Section 4.4 shows the results and conclusions are drawn in Section 4.5.

## 4.2 State of the art

Energy use in the residential sector has been studied extensively, across a variety of fields, such as civil engineering, architecture, economy, environmental assessment, sociology, transport, city and regional planning. Energy consumed in this sector is generally classified as either embodied or operational. Embodied energy is the energy required to produce and transport materials to the construction site and for the construction process itself, while operational energy is consumed for

the daily use of the building to provide electricity, water, hot water, ventilation, heating and cooling.

A clear distinction in the scale of the analysis arises when trying to summarize the research in the area, namely at the individual building and urban scales [143]. Research at the individual building scale usually covers topics such as building materials used, architectural design, structural and operational system and construction. Developments in the area include improving the accuracy of the models and reducing the computation time of the assessment [153], analyzing the results with different objectives [154] techniques to reduce energy and CO<sub>2</sub> emissions. Kofoworola et al. showed a combination of energy savings measures to reduce the electricity consumption in a typical office building in Thailand by 40–50% [155]. Ochoa et al. stated that the usage phase of buildings accounts for the largest share of the energy use and environmental impact, followed by the construction phase, while the disposal phase is negligible from both perspectives [156]. Junilla et al. presented the elements in the life-cycle assessment of office buildings which cause the highest emissions and should therefore be targeted for improvement [157] and in a similar study concluded that lighting, HVAC systems and outlets, manufacturing and maintenance of steel, manufacturing of concrete and paint and water use have the largest environmental impacts in office buildings [158].

The second scale of analysis for energy use in the residential sector is the urban scale. Research at this scale typically covers topics such as urban form, density, transportation, infrastructure and consumption. Studies in the field focus mainly on quantification of energy use, transportation infrastructure, water infrastructure, construction, and modeling of energy use in urban systems. Glaeser and Kahn studied the energy use and environmental impact due to driving, public transit, providing heating and electricity in households and found a strong negative correlation between emissions and land use regulations, leading them to conclude that cities have significantly lower emissions compared to suburban areas [159]. Kennedy et al. performed a study on ten global cities, showing correlations between public transit quality and personal income, and between heating and industrial fuel use [160]. Troy et al. quantified the embodied energy in urban areas and found it to be more significant than previously supposed and suggested that knowing the embodied energy consumed can be used for control tool development [161].

Jones et al. assessed energy consumption and environmental impact in urban areas due to transportation, energy, water, waste, food, goods and services, and suggested that results were highly dependent on the basic demographic characteristics of the area studied [162]. Regarding energy use modeling, Howard et al. developed a model to estimate end-use energy intensity in New York, as a tool for cost-efficient policies regarding renewable energy efficient solutions [163]. Gurney et al. used simulation tools, traffic data, power production reporting and local air pollution reporting to build a model which quantified CO<sub>2</sub> emissions across the city of Indianapolis [164]. Keirstead et al. reviewed approximately 220 papers on urban energy system modeling and concluded that the four most common challenges are data quality and uncertainty, model integration, model complexity and policy relevance [165]. They also concluded that urban energy system models have a significant

potential of moving toward a more integrated perspective, which could capture their intricacies.

While these references offer a first insight into multi-scale integration analysis, additional methodological developments are required to directly address the interaction between scales. In view of that, this chapter proposes a method which combines the work of Stadler et al. [21] on optimization at building level with the work of Suciu et al. [52] on optimization at district level, to perform a detailed multi-level energy integration optimization. The link between the building and the urban level is realized through a low-temperature 5G district heating and cooling network and meta-models are employed to embed the building solutions into the district level optimization.

### Low Temperature DHC Networks

Low temperature district energy networks provide a low temperature source, which can be used for heating via decentralized heat pumps, directly for cooling, indirectly as a low temperature source for chillers and can recover waste heat from processes and other buildings in the proximity; they are also often linked to large seasonal storage in the form of borehole fields [166].

Low-temperature networks have been discussed in the literature, for example, De Carli et al. performed an energo-economic analysis of a small-scale, low-temperature district heating and cooling network in Italy [167], Bestenlehner compared a low-temperature and a conventional district heating network in a quarter of Stuttgart [168], Ruesch modeled the time evolution of large borehole fields connected to low temperature district heating networks [166], Kräuchi et al. modelled a low-temperature district heating and cooling network using the IDA indoor climate energy (IDA ICE) simulation software [169] and Molyneaux et al. performed an enviro-economic optimization for low-temperature heat networks with heat pumps [170].

This work analyzes both conventional networks and low temperature refrigerant (CO<sub>2</sub>)-based networks. Weber and Favrat introduced the idea of distributing CO<sub>2</sub> in the district energy networks at a temperature below the critical pressure of 74 bar. 5G networks (Figure 4.1) use a double-pipe system to deliver both heating and cooling services. A pressure of 50 bar is suggested for use in the network to remain within the saturation temperature range of 12–18 °C, which allows network operations to leverage the latent heat and small pressure difference between liquid and gas phases to provide cooling services by gas expansion. Unlike water-based networks currently in place in several cities, 5G networks use phase change to realize the heat transfer and allow cooling services to provide heating, which is not possible with conventional systems. The approach is based on a CO<sub>2</sub> “closed-loop” concept, i.e., except for leaking (considered negligible) no CO<sub>2</sub> enters/leaves the network.

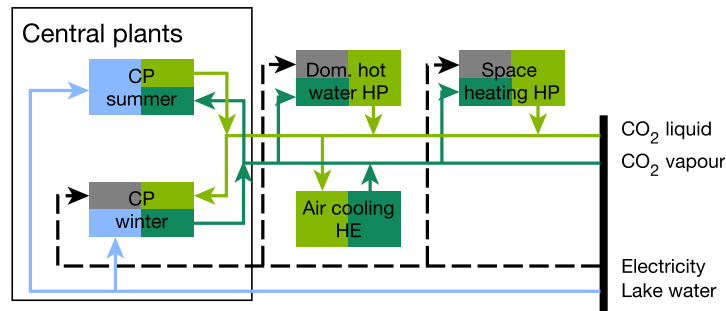


Figure 4.1 – 5G network schematic representation.

5G networks have also been integrated with advanced technologies for energy storage and heat integration, such as power-to-gas [52]. Power-to-gas systems use electricity in periods of high production (summer) to produce hydrogen and oxygen by water electrolysis and then methane in a Sabatier reaction, which is stored to provide electricity and heat during cold periods or periods of low electricity production (Figure 4.2). The waste heat of the co-generation system is first used in a steam network to produce electricity with the remaining low temperature heat used to vaporize  $\text{CO}_2$ , which is used to provide heating services.

4

This work proposes a method which links analysis and optimization in individual buildings with urban-level systems through low temperature 5G networks and long term power-to-gas storage systems. The method proposed uses a double optimization approach with surrogate models, using two different time scales: monthly averages and typical days.

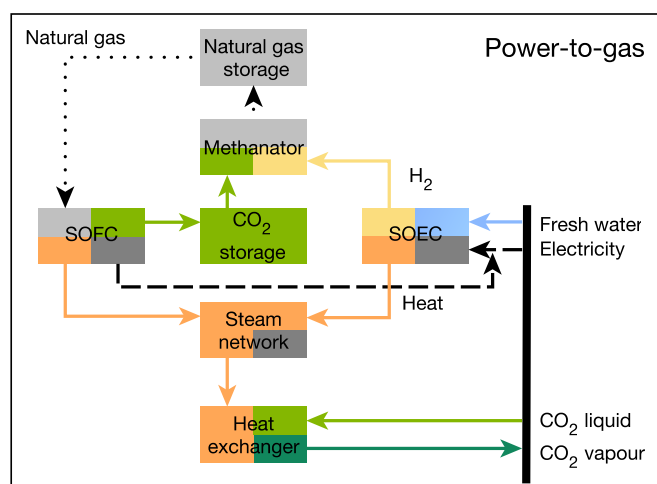


Figure 4.2 – P2G schematic representation.



### 4.3 Materials and methods

The proposed method models energy systems using a double optimization approach with meta-models (Figure 4.5). The first optimization is performed at the building level, where different utilities can be chosen, such as photo-voltaic panels with short-term electricity storage (batteries), CO<sub>2</sub> and air-water heat pumps, co-generation units, heat storage tanks, domestic hot water tanks, heat exchangers for cooling and electrical heaters as back up systems. The PV panels and co-generation units are described in detail in Appendix D.2, while the other units are described in Appendix D.1. Further details on the formulation can be found in [21]. This optimization is performed to ensure that each building is operated optimally, e.g., all the controllable loads are shifted to decrease the operating cost.

The buildings considered are residential (single- and multi-family houses), mixed (residential and administrative), administrative, commercial, education and hospitals. The buildings are also grouped according to the renovation stage, as existing (built before 2005), new (built after 2005) and renovated (built before 2005 but improved to meet modern standards) [49]. The pool of building meta-models is enriched by including two energy conversion technology configurations, one with and one without 5G network utilities. Within each scenario, parametric optimization is implemented on the investment cost (minimum operating cost, minimum investment cost and five intermediary scenarios, see Figure 4.3) to obtain a systematic approach for generating interesting solutions in cities and explore options for optimal utilities and connections to optimal buildings.

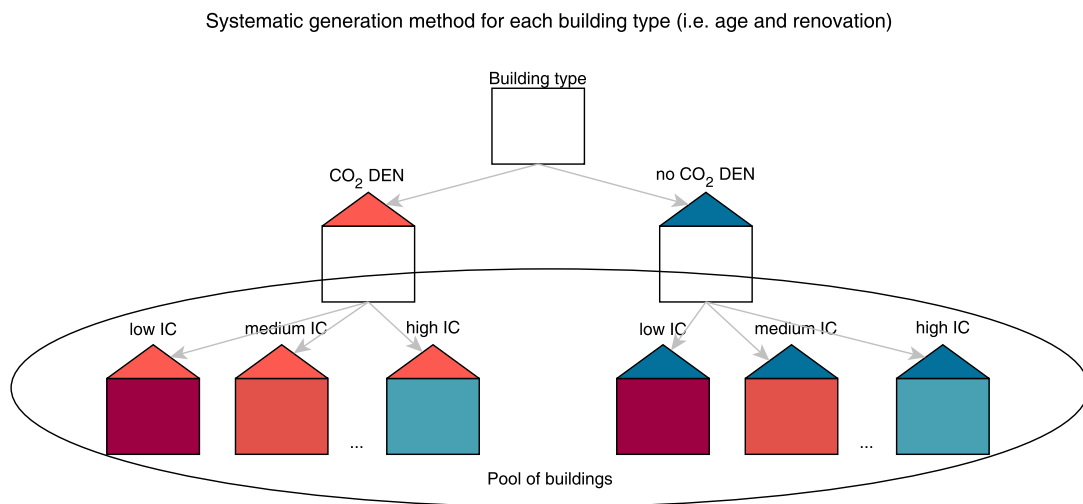


Figure 4.3 – Systematic generation method for each building type (i.e., age and renovation).

Figure 4.4 illustrates sample results of the building-level optimization. More specifically, it depicts the operating-investment cost Pareto frontier and self-sufficiency of residential single-family house (SFH)s of different renovation stages, with and without 5G network utilities. The concept of self-

sufficiency is further defined in Section 4.3.4 and is used to evaluate the autonomy of the energy systems studied, but is defined in simple terms as the percentage of electricity consumption supplied by self-production. For all solutions with an increase in investment cost, the operating cost decreases and renewable energy sources penetrate, leading to higher values of self-sufficiency. New and renovated buildings have reduced overall demands, and therefore lower operating cost. While the solutions connected to the CO<sub>2</sub> network yield no difference for low investment cost limits, they result in lower operating costs whenever the capital expenditure (capex) limit is high enough for these technologies. However, the piping cost of the CO<sub>2</sub> network is not considered at this stage, being included only at the canton/commune level (Switzerland has 26 cantons, each of them being divided in several communes. Cities can be comprised of several communes, e.g., Geneva has 48 communes).

The building-level solutions are then integrated in the main optimization, where each building is represented by its resource (CO<sub>2</sub> liquid and vapor, natural gas, electricity) import and export. Decision variables and constraints are used to permit selection of any number of buildings from any type, age and utility configuration as long as the overall mix is consistent with that of the case study considered. At the city level the optimizer chooses not only the best configuration of buildings, but also additional utilities to create an optimal city. The additional utilities at the upper level include PV panels, central plants which provide CO<sub>2</sub> liquid and vapor, and a power-to-gas storage system (Figure 4.5). The PV panel and CO<sub>2</sub> and CH<sub>4</sub> storage unit models are described in detail in [52], the co-generation solid oxide fuel cell-gas turbine unit is modeled according to [87] and the co-generation solid oxide electrolysis cell unit according to [88]. A detailed description of the unit models can be found in Appendix D.2 and in [52].

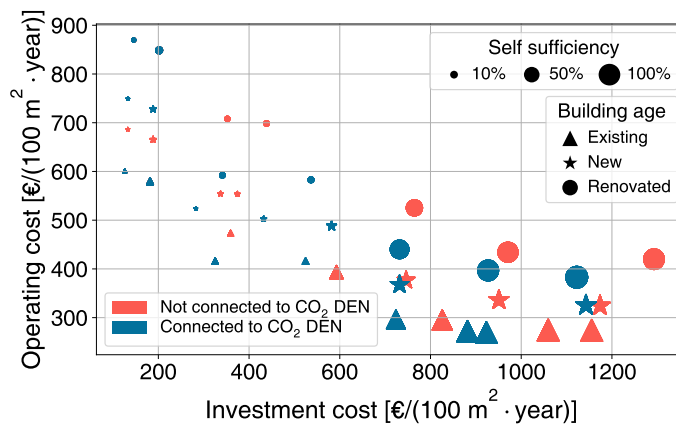


Figure 4.4 – Pareto frontier of residential SFH with different utility configurations and renovation stages.

A mixed-integer linear programming framework is used to find the optimal utility configurations and to integrate different technologies which satisfy the urban demand.

### 4.3. Materials and methods

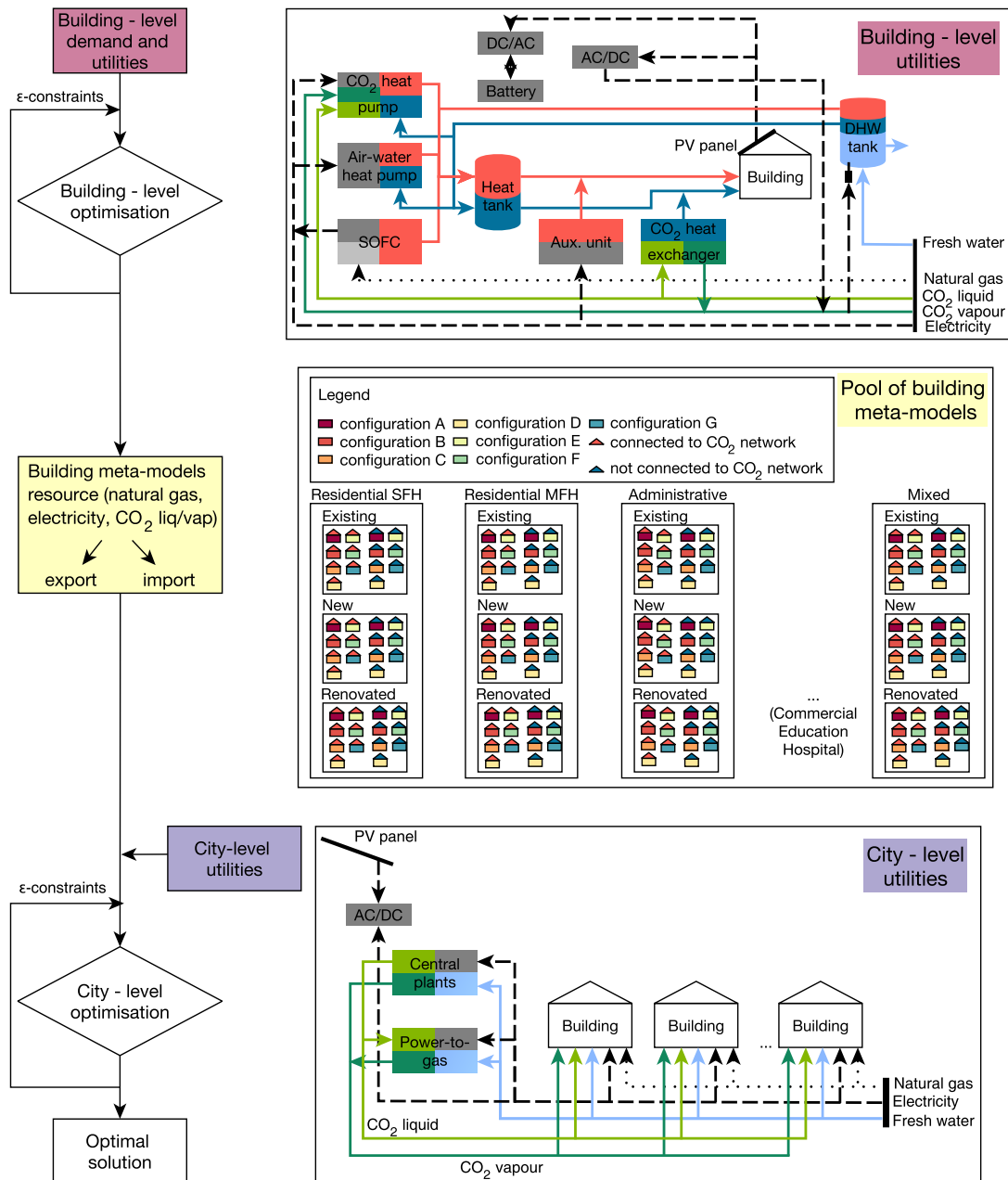


Figure 4.5 – Methodology overview.

#### 4.3.1 Mathematical Formulation

The building and city-level optimizations are formulated using mixed integer linear programming [28, 171–173]. This framework was chosen to represent building energy systems, since it can model both the discrete and the continuous behavior of the units. An additional benefit is

that this formulation always results in a global optimum and does not require extensive effort for problem initialization.

#### 4.3.1.1 Definition of Sets

Given that energy demand is time-dependent, the problem is defined using discrete time intervals (e.g.,  $p \in \mathbf{P} = \{1\}$  (1 year),  $t \in \mathbf{TOP}_p = \{1, 2, \dots, 14\}$  (12 months and two extreme days)). The system to be optimized is represented through several units, belonging to the set  $\mathbf{U}$ . The units are grouped in two subsets: the set of utility units ( $\mathbf{UU} = \{\text{PV panels, batteries, heat pumps, CHPs, storage tanks, heat exchangers}\}$ ) and the set of process units ( $\mathbf{PU} = \{\text{building demands: space heating, domestic hot water, air cooling, utilities}\}$ ). The process units represent the demand and hence have a fixed size, while the utility units represent the energy technologies used to satisfy the demand, with variable sizes, which are to be optimized. Units supply, demand, or convert resources ( $r \in \mathbf{R}$ ) (electricity and material) and heat (at different temperature intervals  $k \in \mathbf{K}$ ).

#### 4.3.1.2 Objective Function and Constraints

The objective function of the problem is the minimization of the operating cost (Equation (4.1)), with  $\epsilon$ -constraints on the investment cost (Equation (4.2)) [174]. The objective function accounts for both the fixed ( $C_u^{\text{op},1}$ ) and variable ( $C_u^{\text{op},2}$ ) operating costs. The additional terms in the objective function are the binary variables ( $y_{u,p,t}, y_u$ ) which decide whether a unit is used or not, the continuous variables ( $f_{u,p,t}, f_u$ ) which determine the size of a unit, the operating time parameter ( $t_t^{\text{op}}$ ) and the period occurrence ( $p_p^{\text{occ}}$ ).  $\epsilon$ -constraints consider the fixed ( $C_u^{\text{inv},1}$ ) and variable ( $C_u^{\text{inv},2}$ ) investment costs.

$$\min_{y_u, f_u} \sum_{u \in \mathbf{U}} \left( \sum_{p \in \mathbf{P}} \left( \sum_{t \in \mathbf{TOP}_p} \left( C_u^{\text{op},1} \cdot y'_{u,p,t} + C_u^{\text{op},2} \cdot f'_{u,p,t} \right) \cdot t_t^{\text{op}} \right) \cdot p_p^{\text{occ}} \right) \quad (4.1)$$

$$\sum_{u \in \mathbf{U}} (C_u^{\text{inv},1} \cdot y_u + C_u^{\text{inv},2} \cdot f_u) \leq \epsilon \quad \epsilon \in [C_{\min}^{\text{inv},2}, C_{\max}^{\text{inv},2}] \quad (4.2)$$

The main constraints of the problem include the energy conversion technology sizing and selection. Equations (4.3)–(4.6) bound the size of the unit in each time step  $t$  and period  $p$  to be smaller than the purchase size of the equipment, Equation (4.7) ensures that the purchase size of the equipment is between the minimum and maximum boundaries set ( $f_u^{\min}, f_u^{\max}$ ), and Equations (4.8) and (4.9)

fix the size of the process units.

$$y''_{u,p} \leq y_u \quad \forall u \in \mathbf{U}, \forall p \in \mathbf{P} \quad (4.3)$$

$$y'_{u,p,t} \leq y''_{u,p} \quad \forall u \in \mathbf{U}, \forall p \in \mathbf{P}, \forall t \in \mathbf{TOP}_p \quad (4.4)$$

$$f''_{u,p} \leq f_u \quad \forall u \in \mathbf{U}, \forall p \in \mathbf{P} \quad (4.5)$$

$$f'_{u,p,t} \leq f''_{u,p} \quad \forall u \in \mathbf{U}, \forall p \in \mathbf{P}, \forall t \in \mathbf{TOP}_p \quad (4.6)$$

$$f_u^{\min} \cdot y'_{u,p,t} \leq f'_{u,p,t} \leq f_u^{\min} \cdot y'_{u,p,t} \quad \forall u \in \mathbf{U}, \forall p \in \mathbf{P}, \forall t \in \mathbf{TOP}_p \quad (4.7)$$

$$y'_{u,p,t} = 1 \quad \forall u \in \mathbf{PU}, \forall p \in \mathbf{P}, \forall t \in \mathbf{TOP}_p \quad (4.8)$$

$$f_u^{\min} = f_u^{\min} = 1 \quad \forall u \in \mathbf{PU} \quad (4.9)$$

The heat cascade equations ensure that heat is transferred from higher temperature intervals to lower temperature intervals and close the energy balance in each temperature interval  $k$  (Equation (4.10a)). This is achieved using the residual heat  $\dot{R}_{p,t,k}$ , which cascades excess heat from higher temperature intervals ( $k$ ) to lower temperature intervals ( $k - 1$ ). The minimum residual heat is zero, when heat cannot be transferred from the corresponding temperature interval to lower ones (Equation (4.10b)). Similarly, residual heat in the first interval ( $\dot{R}_{t,1}$ ) is zero, as lower temperature intervals do not exist to accept a transfer of heat. Logically, heat cannot be cascaded to the  $k^{\text{th}}$  interval as it is the highest, so  $\dot{R}_{t,k+1}$  is also zero (Equation (4.10c)).  $\dot{Q}_{u,p,t,k}$  represents the reference heat load of a unit  $u$  in period  $p$ , time step  $t$  and temperature interval  $k$ .

$$\sum_{u \in \mathbf{U}} f_{u,p,t} \cdot \dot{Q}_{u,p,t,k} + \dot{R}_{p,t,k+1} - \dot{R}_{p,t,k} = 0 \quad \forall p \in \mathbf{P}, \forall t \in \mathbf{TOP}_p, \forall k \in \mathbf{K} \quad (4.10a)$$

$$\dot{R}_{p,t,k} \geq 0 \quad \forall p \in \mathbf{P}, \forall t \in \mathbf{TOP}_p, k \in \mathbf{K} \quad (4.10b)$$

$$\dot{R}_{p,t,1} = 0 \quad \dot{R}_{p,t,k+1} = 0 \quad \forall p \in \mathbf{P}, \forall t \in \mathbf{TOP}_p \quad (4.10c)$$

For each unit  $u$ , the supply  $\dot{M}_{r,u,p,t}^-$  and demand  $\dot{M}_{r,u,p,t}^+$  of a specific resource  $r \in \mathbf{R}$  are computed (Equations (4.11a) and (4.11b)) and the balance of each resource is closed for each period  $p$  and time step  $t$  (Equation (4.11c)).  $\dot{m}_{r,u,p,t}^-$  and  $\dot{m}_{r,u,p,t}^+$  are the reference supply and demand flows of a unit.

$$\dot{M}_{r,u,p,t}^- = \dot{m}_{r,u,p,t}^- \cdot f'_{u,p,t} \quad \forall r \in \mathbf{R}, \forall u \in \mathbf{U}, \forall p \in \mathbf{P}, \forall t \in \mathbf{TOP}_p \quad (4.11a)$$

$$\dot{M}_{r,u,p,t}^+ = \dot{m}_{r,u,p,t}^+ \cdot f'_{u,p,t} \quad \forall r \in \mathbf{R}, \forall u \in \mathbf{U}, \forall p \in \mathbf{P}, \forall t \in \mathbf{TOP}_p \quad (4.11b)$$

$$\sum_{u \in \mathbf{U}} \dot{M}_{r,u,p,t}^- = \sum_{u \in \mathbf{U}} \dot{M}_{r,u,p,t}^+ \quad \forall r \in \mathbf{R}, \forall p \in \mathbf{P}, \forall t \in \mathbf{TOP}_p \quad (4.11c)$$

## 4

#### 4.3.1.3 Constraint Linking Individual Building and Urban Scale

Specific constraints at the building scale are presented in detail in [21]. Additional variables and sets are introduced at the urban scale, which aid the formulation of the constraints, such as building types ( $bt \in \mathbf{BT} = \{\text{residentialSFH, residentialMFH, administrative, education, commercial, hospital, mixed}\}$ ), building units of type  $bt$  ( $bu \in \mathbf{BUT}_{bt}$ ), renovation stages ( $rs \in \mathbf{RS} = \{\text{existing, new, renovated}\}$ ), building units of renovation stage  $rs$  ( $bu \in \mathbf{BUR}_{rs}$ ), building units connected to the CO<sub>2</sub> network ( $bu \in \mathbf{BUC}$ ) and the set of cities/communes ( $c \in \mathbf{C}$ ). The extra constraints include fixing the number of buildings of a given type to the one of the case studies considered ( $N_{bt}$ ):

$$\sum_{p \in \mathbf{P}} \sum_{t \in \mathbf{TOP}} \sum_{bu \in \mathbf{BUT}_{bt}} f'_{bu,p,t} = N_{bt} \quad \forall bt \in \mathbf{BT} \quad (4.12)$$

And making the number of buildings at each renovation stage equal to that of the urban system studied ( $N_{rs}$ ):

$$\sum_{p \in \mathbf{P}} \sum_{t \in \mathbf{TOP}} \sum_{bu \in \mathbf{BUR}_{rs}} f'_{bu,p,t} = N_{rs} \quad \forall rs \in \mathbf{RS} \quad (4.13)$$

The investment cost for the CO<sub>2</sub> network in each city/commune is computed according to [49] (for details see Appendix D.3). The commune has the choice of investing in the CO<sub>2</sub> network or not ( $y_{u_{CO_2,c}}$ ), which translates in optimization terms as a big  $M$  constraint:

$$y_{u_{CO_2,c}} \geq f'_{bu,p,t} / M \quad \forall bu \in \mathbf{BUC}_c, \forall c \in \mathbf{C}, \forall p \in \mathbf{P}, \forall t \in \mathbf{TOP}_p \quad (4.14)$$

i.e., if the commune activates a building with CO<sub>2</sub> network utilities, it must invest in piping. The size/length of the network piping is fixed for all periods and times.

#### 4.3.1.4 Long-Term Energy Storage Model with Typical Day Resolution

To model the long-term storage units with typical day resolution, a series of new sets must be introduced (or re-defined). The equations here are based on using eight periods or typical days:

- **P**: periods, or typical days of the year, e.g., {1, 2, 3, 4, 5, 6, 7, 8};
- **TOP<sub>p</sub>**,  $\forall p \in \mathbf{P}$ : time steps in each period  $p$ , e.g.,  $\underbrace{\{1, 2, \dots, 24\}, \{25, 26, \dots, 48\}, \dots, \{169, 170, \dots, 192\}}_{8 \text{ typ. days}}$ ;
- **RD**: real days of the year, e.g., {1, 2, ..., 365};
- **PORD<sub>rd</sub>**,  $\forall rd \in \mathbf{RD}$ : typical day corresponding to each real day of the year, e.g.,  $\underbrace{\{2, 2, 4, \dots, 6\}}_{365 \text{ days}}$ ;
- **TORD<sub>rd</sub>** =  $t$ ,  $\forall t \in \mathbf{TOP}_{pr}$ ,  $\forall pr \in \mathbf{PORD}_{rd}$ ,  $\forall rd \in \mathbf{RD}$ : time steps in each real day of the year, e.g.,  $\underbrace{\underbrace{\{25, 26, \dots, 48\}}_{\text{time steps in typ. day 2}}, \underbrace{\{25, 26, \dots, 48\}}_{\text{time steps in typ. day 2}}, \underbrace{\{73, 74, \dots, 96\}}_{\text{time steps in typ. day 4}}, \dots, \underbrace{\{121, 122, \dots, 144\}}_{\text{time steps in typ. day 6}}}_{365 \text{ days}}$ ;
- **TOPNC<sub>p</sub>** = {1, 2, ..., card(**TOP<sub>p</sub>**)},  $\forall p \in \mathbf{P}$ : non cumulative time steps in each typical day  $p$ , e.g.,  $\underbrace{\{1, 2, \dots, 24\}, \{1, 2, \dots, 24\}, \dots, \{1, 2, \dots, 24\}}_{8 \text{ typ. days}}$ ;
- **RTORD<sub>rd,pr,t</sub>** =  $\sum_{i=1}^{rd-1} \text{card}(\mathbf{TORD}_i) + t - \sum_{j=1}^{pr-1} \text{card}(\mathbf{TOPNC}_j)$   $\forall t \in \mathbf{TOP}_{pr}$ ,  $\forall pr \in \mathbf{PORD}_{rd}$ ,  $\forall rd \in \mathbf{RD}$ : real time of each real day of the year, e.g.,  $\underbrace{\underbrace{\{1, 2, \dots, 24\}}_{\text{time steps in real day 1}}, \underbrace{\{25, 26, \dots, 48\}}_{\text{time steps in real day 2}}, \underbrace{\{49, 50, \dots, 72\}}_{\text{time steps in real day 3}}, \dots, \underbrace{\{8737, 8738, \dots, 8760\}}_{\text{time steps in real day 365}}}_{365 \text{ days}}$ ;
- **RT** = 1, ...,  $\sum_{rd \in \mathbf{RD}} \text{card}(\mathbf{TORD}_{rd})$ , (ordered set): real times of the year, e.g., {1, 2, ..., 8760}.

Given these sets above, the long-term storage units ( $u \in \mathbf{SU}$ ) are represented by the constraint:

$$SL_{rt} = \begin{cases} \text{if } rt = \text{first}(\mathbf{RT}) : & \sigma \cdot SL_{\text{last}(\mathbf{RT})} + \eta_{ch} \cdot M_{r,u,pr,t}^+ - \frac{1}{\eta_{dch}} \cdot M_{r,u,pr,t}^- \\ \text{else :} & \sigma \cdot SL_{rt-1} + \eta_{ch} \cdot M_{r,u,pr,t}^+ - \frac{1}{\eta_{dch}} \cdot M_{r,u,pr,t}^- \end{cases}$$

$$\forall r \in \mathbf{R}, \forall u \in \mathbf{SU}, \forall rd \in \mathbf{RD}, \forall pr \in \mathbf{PORD}_{pr}, \forall t \in \mathbf{TOP}_{pr}, \forall rt \in \mathbf{RTORD}_{rd,pr,top} \quad (4.15)$$

with  $SL_{rt}$  as the storage level of the unit at each real time step of the year  $rt \in \mathbf{RT}$ ,  $\sigma = 0.9992$  [175] the self-discharge rate of the unit, and  $\eta_{ch} = \eta_{dch} = 0.9$  [175] as the charging and discharging efficiencies of the unit. A summary of all the sets used in the problem formulation is given in Table 4.1.

Table 4.1 – Sets used in the mathematical formulation.

Set symbol	Name	Index	Increment	Cyclicity
<b>P</b>	periods	-	day	no
<b>TOP</b>	times of period	$p$	hour	no
<b>U</b>	units	-	-	no
<b>UU</b>	utility units	-	-	no
<b>PU</b>	process units	-	-	no
<b>SU</b>	storage units	-	-	no
<b>R</b>	resources	-	-	no
<b>K</b>	temperature intervals	-	-	no
<b>BT</b>	building types	-	-	no
<b>BUT</b>	building units of type	$bt$	-	no
<b>RS</b>	renovation stages	-	-	no
<b>BUR</b>	building units of renovation	$rs$	-	no
<b>C</b>	communes	-	-	no
<b>BUC</b>	building units connected to CO <sub>2</sub> DEN	$c$	-	no
<b>RD</b>	real days	-	day	no
<b>PORD</b>	periods of real day	$rd$	day	no
<b>TORD</b>	times of real day	$rd$	hour	no
<b>TOPNC</b>	times of period non cummulative	$pr$	hour	no
<b>RTORD</b>	real times of real day	$rd, pr, t$	hour	no
<b>RT</b>	real times	-	hour	yes

#### 4.3.2 Case Study

The case studies considered are Geneva city center (four communes: Genève-Cité, Genève-Plainpalais, Genève-Eaux-Vives and Genève-Petit-Saconnex) and the canton of Geneva (all 48 communes, Figure 4.6).

The building types are distinguished according to the RegBL database [176], as listed in Table 4.2. The corresponding parameter names in the RegBL report are listed in Table D.18 in the Appendix.



### 4.3. Materials and methods

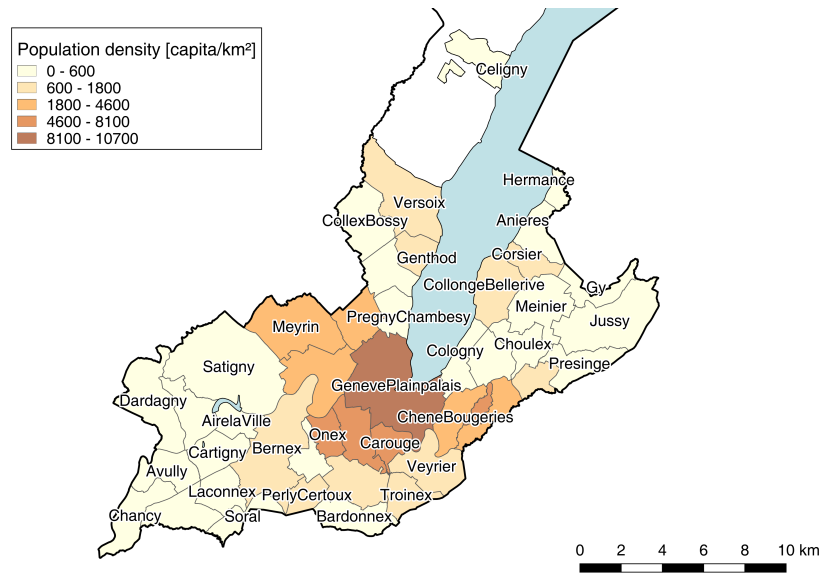


Figure 4.6 – Population density of communes in the canton of Geneva.

Table 4.2 – Building types present in the model of the canton of Geneva.

Building type	Building category	Building class
Residential SFH	1021, 1025, 1230	1110
Residential MFH	1025	1121
	1040	1130
Administrative	1040, 1060	1220
Commercial	1040, 1060	1230
Education	1040, 1060	1263
Hospital	1040, 1060	1264
Mixed	1030	1121, 1122

The energy reference area of the buildings ( $A_b^{\text{ERA}}$ ) is computed according to the same database, using the footprint area of the building ( $A_b$ ), the number of floors ( $N_b^{\text{floors}}$ ) and a factor of 0.9, an assumption used to account for the inner walls (Equation (4.16)).

$$A_b^{\text{ERA}} [\text{m}^2] = A_b [\text{m}^2] \cdot N_b^{\text{floors}} \cdot 0.9 \quad (4.16)$$

The photo-voltaic rooftop potential is calculated using the rooftop area of the building ( $A_b^{\text{roof}}$ ), the average solar irradiation on each roof ( $I_b$ ), a nominal global horizontal irradiation of  $1244.334 \text{ W}/(\text{m}^2 \cdot \text{K})$  and a factor of 0.75 to account for the part of the roof which cannot be covered with PV panels

(e.g., close to the periphery) (Equation (4.17) [177]).

$$A_{PV,b} [\text{m}^2] = A_b^{\text{roof}} [\text{m}^2] \cdot \frac{I_b [\text{W}/(\text{m}^2 \cdot \text{K})]}{1244.334 [\text{W}/(\text{m}^2 \cdot \text{K})]} \cdot 0.75 \quad (4.17)$$

The number of buildings of each category and renovation stage are considered according to [49] and Figure 4.7 displays a sample distribution, that of Geneva city center.

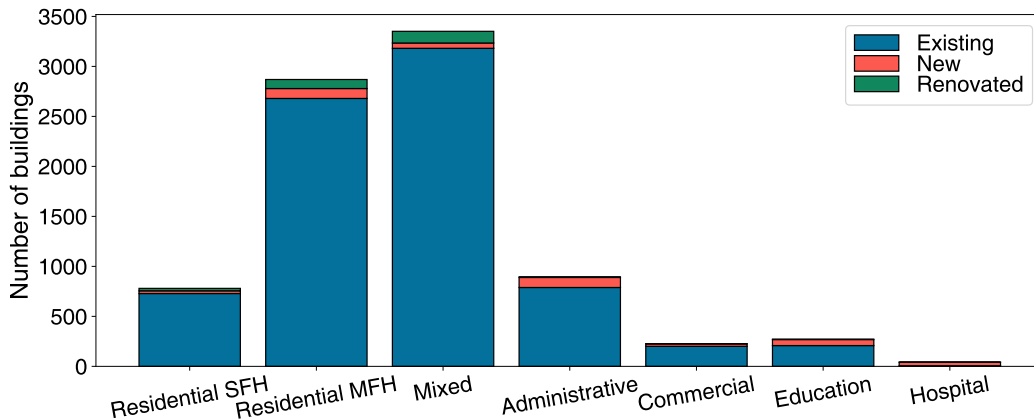


Figure 4.7 – Refurbishment level building distribution in Geneva city center.

4

The demands evaluated are space heating, domestic hot water, air cooling and electricity. The hourly demand profiles are built based on standards and existing heat signature models. The electricity and domestic hot water demand profiles are considered according to the standards of the Swiss society of engineers and architects SIA [56] with a typical day profile repeated throughout the year, while the heating and cooling demands are modeled based on a heating signature profile [49]. These profiles have been calibrated based on statistical data from the energy department of the canton of Geneva [49]. Figure 4.8 and Table 4.3 display the hourly demand profile of administrative buildings (existing, new and renovated) and their specific yearly demand. The domestic hot water and electricity demand is constant; therefore it is excluded from the hourly variation plots. The corresponding plot/table for all other building categories can be found in Appendix D.5.

Table 4.3 – Yearly specific energy service demand of administrative buildings.

Building renovation stage	Space heating [kWh/m <sup>2</sup> ]	Air cooling [kWh/m <sup>2</sup> ]	Dom. hot water [kWh/m <sup>2</sup> ]	Electricity [kWh/m <sup>2</sup> ]
Existing	84.2	8.9	2.9	43.2
New	36.4	3.8	2.9	43.2
Renovated	51.7	5.5	2.9	43.2

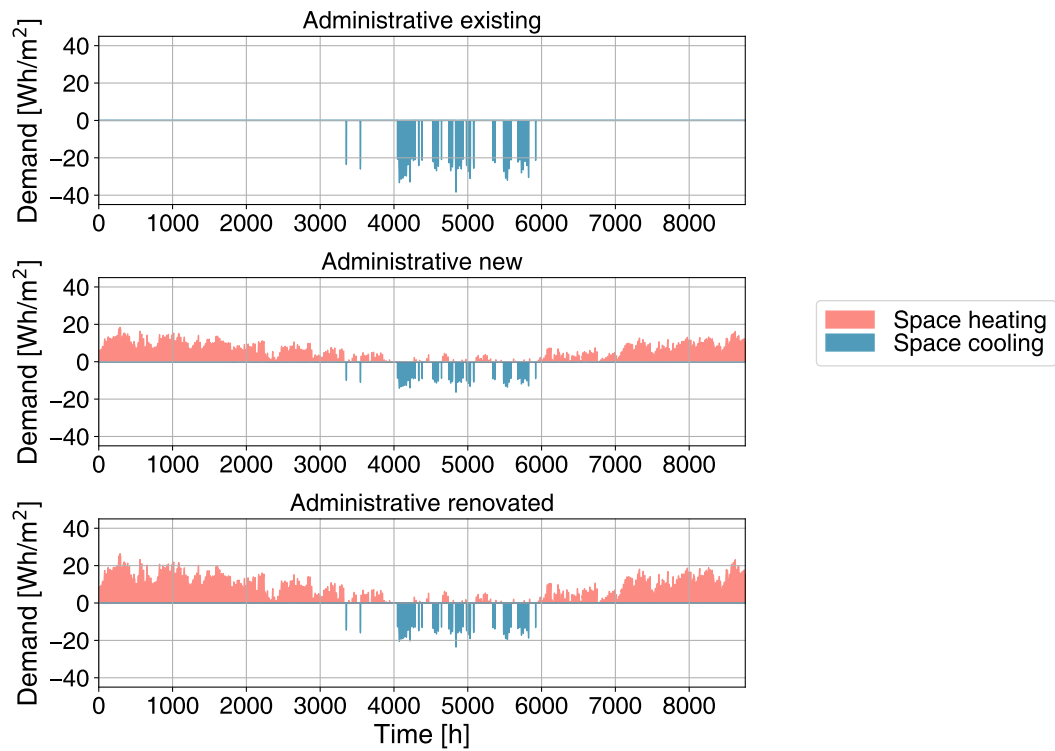


Figure 4.8 – Hourly specific energy service demand of administrative buildings.

### 4.3.3 Time Resolutions: Typical Days Algorithm

Two time resolutions are used to solve the optimization problem, namely the state-of-the-art monthly averages with two extreme periods, and hourly resolution. Since the computational time for solving the problem increases drastically with the problem size (Figure 4.9), a k-medoids-based data clustering algorithm is used to reduce the complexity of the problem studied (Figure 4.10) for hourly resolution. This approach selects the cluster centers based on the smallest sum of distances within each cluster, while the cluster size is selected based on a series of performance indicators [178, 179].

Two input parameters are considered for the clustering process, namely the ambient temperature ( $T_{\text{ext}}$ ) and the global horizontal irradiation (GI), since all resources and demands can either be computed using these two parameters, or are assumed constant. Other data such as consumption profiles and their corresponding temperatures of demand are defined based on the computed cluster centers. The k-medoids algorithm is applied between 2 and 25 typical days. A maximum of 6% error load duration curve (ELDC) is set and consequently the number of typical days should be greater than seven (Figure 4.9). To select the optimal number of typical days, the Davies-Bouldin (DB) index is used. The DB index is a measure of clustering scheme performance [180]. It accounts for the separation between the clusters—which should be as large as possible—and the within-cluster

scatter, which should be as low as possible. The index is defined as the ratio between the cluster separation and the within-cluster distance, where lower values express better cluster separation and the ‘tightness’ inside the clusters. As observed in Figure 4.9, the DB index has the lowest value for 8 typical days for the data set studied here. Therefore, this value is used for further analysis.

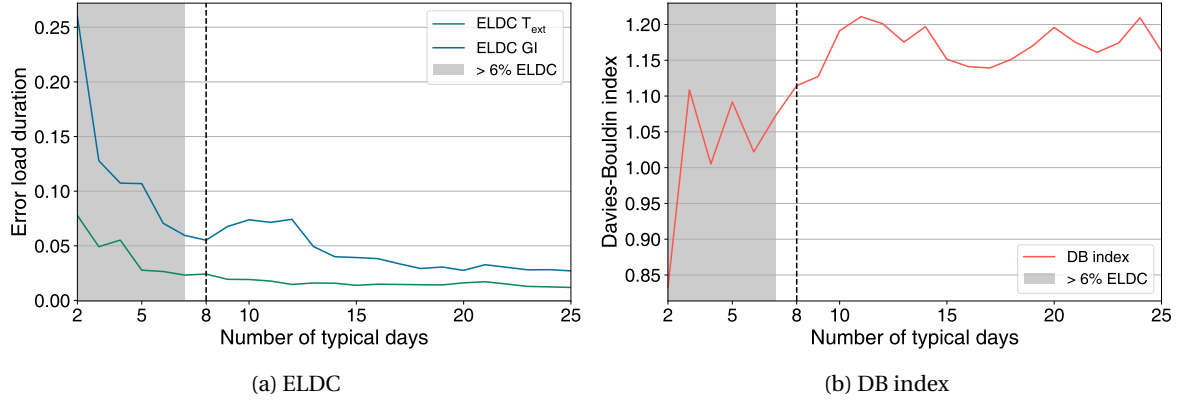


Figure 4.9 – Performance indicator evolution using the k-medoids algorithm for selecting the number of typical days.

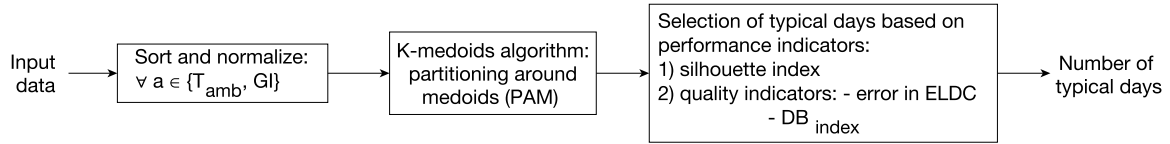


Figure 4.10 – Typical days algorithm.

Figure 4.11 depicts the real profile of the two attributes chosen to cluster the data in grey and the computed load duration curve in black. One can see that the load duration curve of both attributes is followed well with the number of typical days chosen.

To clarify contributions of the different time resolutions in the problem formulation, the objective function (Equation (2.1)) can be assessed in greater detail. For monthly resolution,  $p = 1$  (1 year),  $t = \{1, 2, \dots, 14\}$  represents 12 months and 2 extreme periods,  $p_p^{occ} = 1$  represent the occurrence of the year, and  $t_t^{op} = \{744, 672, 744, \dots, 744, 0, 0\}$  are the number of operating hours in each time step  $t$ . With hourly resolution,  $p = \{1, 2, \dots, 10\}$  are the eight typical days and the two extreme hours,  $t = \{24, 24, \dots, 24, 1, 1\}$  are the number of hours in each time step  $t$ ,  $p_p^{occ} = \{54, 46, 17, 49, 52, 68, 49, 30, 1, 1\}$  represents the number of times each operating period appears during the year, and  $t_t^{op} = \{1, 1, \dots, 1, 0, 0\}$  is the operating time of each time step. For both time resolutions, the operating time of the extreme periods is zero, since they are used only for unit sizing.

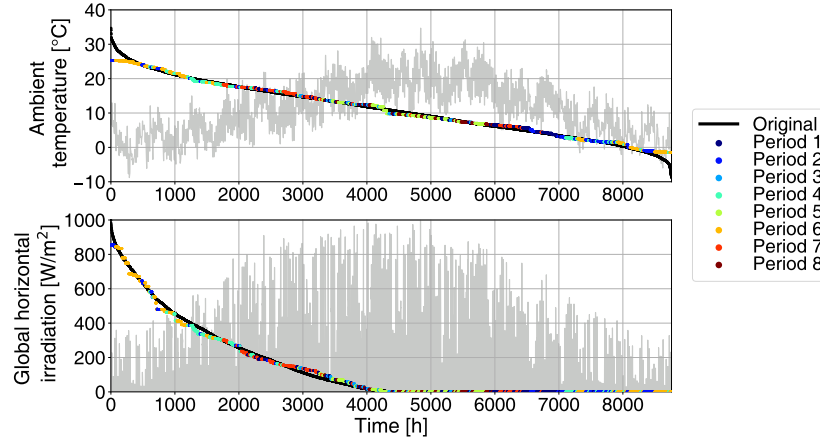


Figure 4.11 – Error load duration curve of typical day attributes.

#### 4.3.4 Measure of Energy Autonomy

In this work, a urban community is considered energy autonomous when the electricity import from the grid ( $E_i$ ) is zero, or likewise, when the self-sufficiency (SF) factor (Equation (4.18) [181]) is equal to unity. A solution is considered to be net zero-energy when the power grid export ( $E_e$ ) and import ( $E_i$ ) are equal, which is equivalent to when the self-sufficiency factor (Equation (refeq:SF)) equals the self-consumption (SC) factor (Equation (4.21), Figure 4.12), where  $E_g$  represents the electricity generation (e.g., by PV panels, co-generation units).

$$SF = \frac{E_g - E_e}{E_g - E_e + E_i} \quad (4.18)$$

where the numerator represents the demand:

$$E_g - E_e + E_i = \sum_{p \in \mathbf{P}} \sum_{t \in \mathbf{TOP}} \left( \dot{M}_{el, El\ heater, p, t}^+ + \dot{M}_{el, Battery, p, t}^+ + \dot{M}_{el, HPs+Ref, p, t}^+ + \dot{M}_{el, House, p, t}^+ + \dot{M}_{el, CPwinter, p, t}^+ + \dot{M}_{el, SOEC, p, t}^+ \right) \quad (4.19)$$

and the electricity generation is given by:

$$E_g = \sum_{p \in \mathbf{P}} \sum_{t \in \mathbf{TOP}} \left( \dot{M}_{el, PV, p, t}^- + \dot{M}_{el, SOFC, p, t}^- + \dot{M}_{el, Battery, p, t}^- \right) \quad (4.20)$$

$$SC = \frac{E_g - E_e}{E_g} \quad (4.21)$$

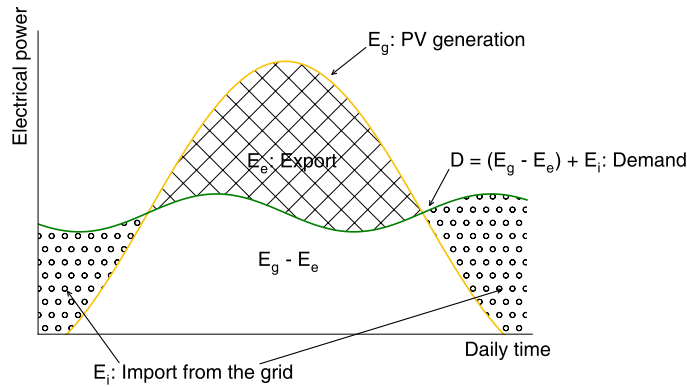


Figure 4.12 – Self-sufficiency and self-consumption visual depiction.

## 4.4 Results and discussion

### 4.4.1 Monthly vs. Typical Day Time Resolution

First, the two time resolutions considered (average monthly and typical day hourly) are analyzed for the case study of Geneva city center. Figure 4.13 depicts the operating-investment cost Pareto front for the two time resolutions, the size of the dots represents the self-sufficiency of the system and the solutions connected to the 5G network are highlighted in gray. By comparing the two time resolutions, it is observed that for the same investment cost limits, solutions using monthly resolution yield up to 31% lower operating cost, and 18% higher self-sufficiency (for the 8th investment cost limit). This occurs due to the fact that peak shaving is an implicit outcome of data aggregation for the monthly resolution, while peaks must be accounted for explicitly with the hourly resolution and adjustments must be made to buy electricity even when previous electricity sales may have occurred. This results in higher operating cost and lower self-sufficiency by considering scenarios with hourly profiles. This also stresses the importance of considering analysis with enough temporal detail to understand the real system requirements, since grid balancing must be completed on short time scales and thus analysis using average data may lead to problematic scenarios.

The cost breakdown of the two time resolutions is shown in Figure 4.14. The first figures on the left show the breakdown of total cost, the biggest contribution being the capex since the system optimal solutions require increasing investment to reduce the operating cost and increase the self-sufficiency. A high level of investment is required to supply the peak demand; however, investing approximately 60% of the maximum value yields solutions with self-sufficiency in excess of 60%. The second and third set of figures, the breakdown of investment cost at the building and city levels, show that both time resolutions highlight the same main contributors: heat pumps, SOFC s and PV panels at the building level and PV panels, power-to-gas and the 5G network pipes at the city level.

As shown in these results, both time resolutions show the same trends and main cost contributors.

#### 4.4. Results and discussion

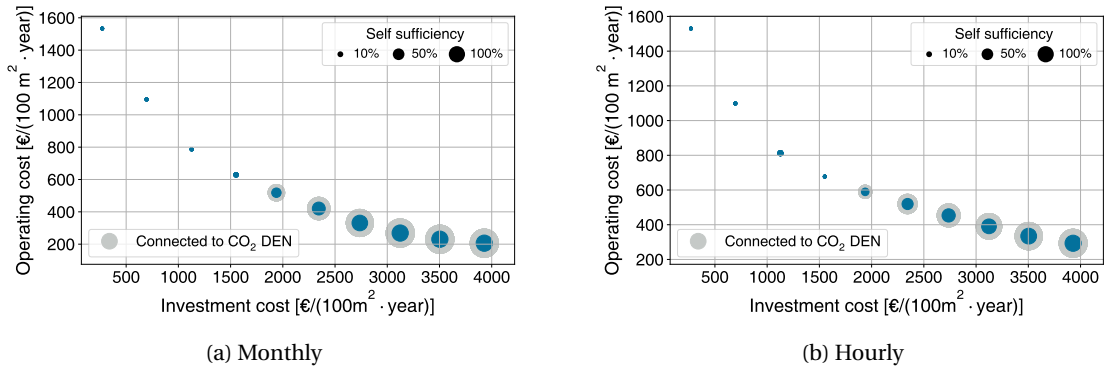


Figure 4.13 – Pareto Geneva city center different time resolutions.

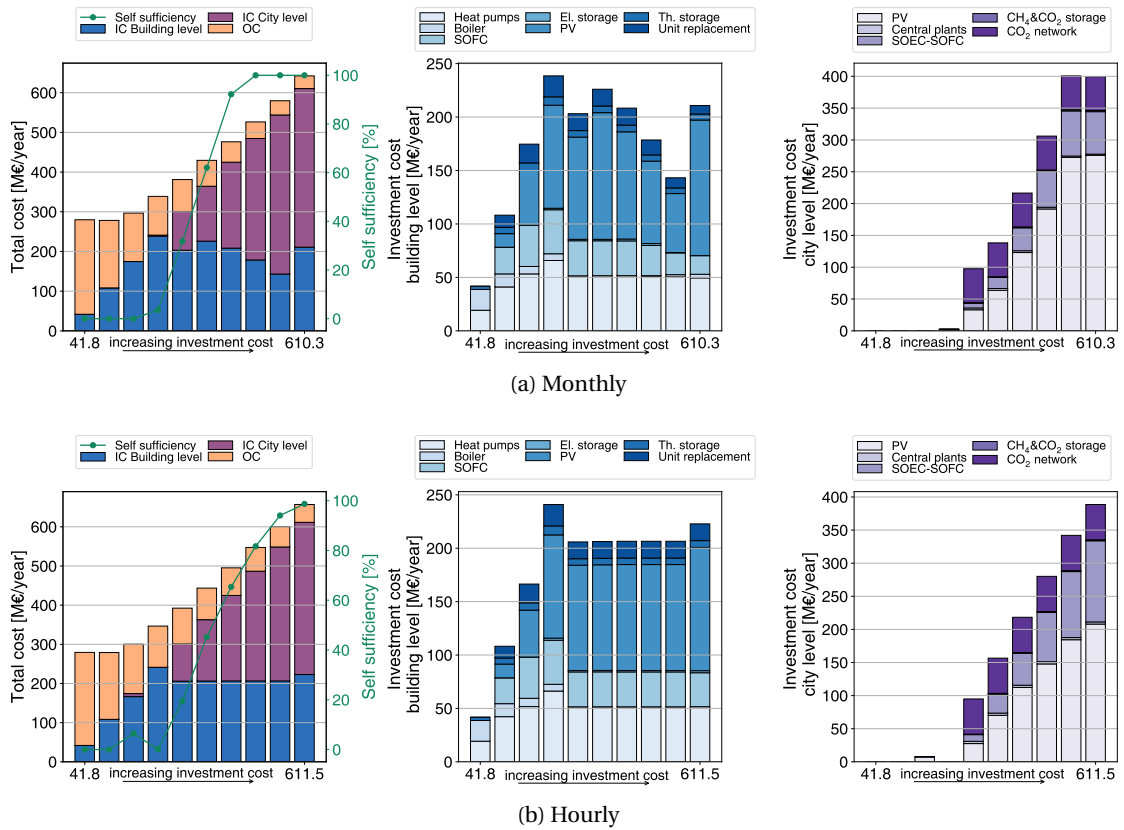


Figure 4.14 – Geneva city center cost breakdown for different time resolutions.

Therefore, despite the increased accuracy provided by hourly resolution and in the interest of reducing data processing and computation time, the remaining results, at canton level (48 communes), are obtained using a monthly resolution.

#### 4.4.2 5G DEN Penetration with Population Density

An  $\epsilon$ -constraint investment cost optimization for all 48 communes in the canton of Geneva is performed to study the 5G DEN penetration depending on the population density. The investment cost of the 5G network was considered to be explained in Equation (4.14). Figure 4.15 depicts the lowest investment cost, 40% of maximum IC, 90% of maximum IC and lowest operating cost scenarios. This figure shows that the scenario with the lowest investment cost does not prompt any of the communes to invest in the 5G network. With increasing investment cost limits, the communes which are most densely populated, with an investment cost per energy reference area lower than  $21.5 \text{ k€}/100 \text{ m}^2_{\text{ERA}}$ , start connecting to the 5G DEN. Finally, for the minimum operating cost scenario, all communes connect to the low temperature DEN.

The results are also represented using parallel coordinates. Figure 4.16 shows that higher investment cost limits logically correlate with reduced operating cost and CO<sub>2</sub> emissions in the canton. Moreover, higher overall investment cost solutions lead to the largest number of communes connected to the 5G DEN and the highest self-sufficiency of the canton. Regarding the investment cost at the building level, a mix of high and low investment cost buildings are selected for optimal operating cost, with a moderate investment in PV panels and heat pumps. The solution with the lowest operating cost is selected to explore detailed results, as highlighted in Figure 4.16. Compared with the current situation (i.e., lowest investment cost solution: mostly boilers supplying heating, no PV market penetration), the best scenario (from an economic standpoint) leads to approximately 90% savings in CO<sub>2</sub> emissions and operating cost, with a payback time of 17.5 years.

#### 4.4.3 Detailed Results of Solution with Lowest Operating Cost and Emissions

Figure 4.17 depicts the details of the solution highlighted above, for each of the 48 communes, sorted by population density. Most of the communes have low population and building densities, and correspondingly low energy flows (i.e., electricity and natural gas import/export). Generally, high population densities are associated with lower district network cost per energy reference area and with high CO<sub>2</sub> emissions. However, the environmental impact has a higher correlation with the overall population, i.e., with the total electricity and natural gas import.

Figure 4.18 is used to detail the energy flows in the communes, by displaying the detailed contributors of electricity and natural gas import/export at the building level for each commune and at the canton level. The results show that:

- the main electricity consumers at the building level are heat pump and refrigeration units ( $\approx 35\%$ ) and electrical appliances ( $\approx 65\%$ );
- the main electricity producers are PV panels, accounting for 91% of the production and SOFC co-generation units supplying the balancing 9%;



#### 4.4. Results and discussion

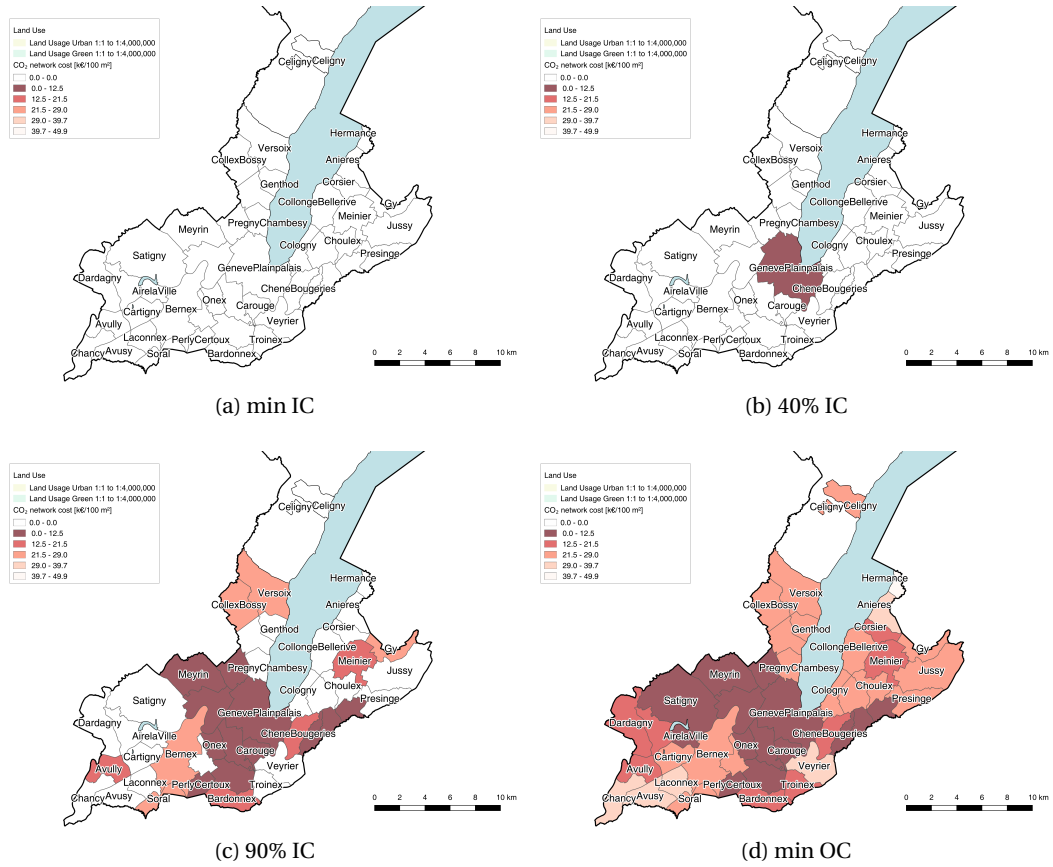


Figure 4.15 – 5G network cost.

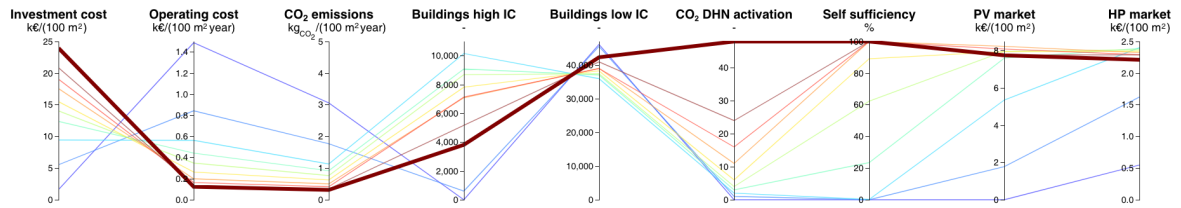


Figure 4.16 – Parallel coordinate representation of the canton solutions.

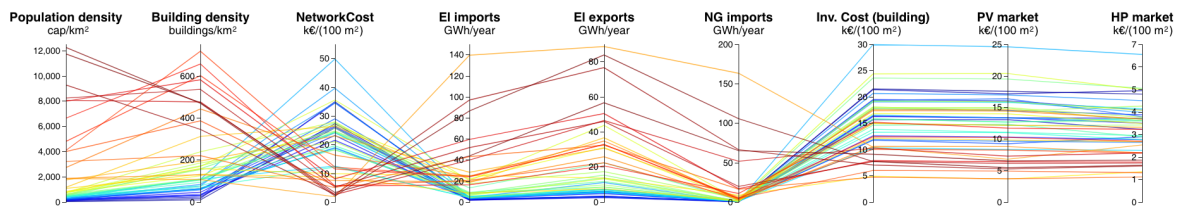


Figure 4.17 – Parallel coordinate representation of the communes for the lowest operating cost solution.

- the main natural gas consumers are boilers (47%) and SOFC co-generation units (53%).

At the cantonal level:

- electricity is consumed by the SOEC unit (35%), by the central plants to produce CO<sub>2</sub> (9%) vapor , and by net electricity importing buildings (56%);
- electricity is produced by PV panels (77%) and the SOFC co-generation unit (23%);
- natural gas is required for the SOFC unit (18%) and for net natural gas importing buildings (82%);
- natural gas is produced by the methanation unit in the power-to-gas system (18%) and purchased from the grid (82%).

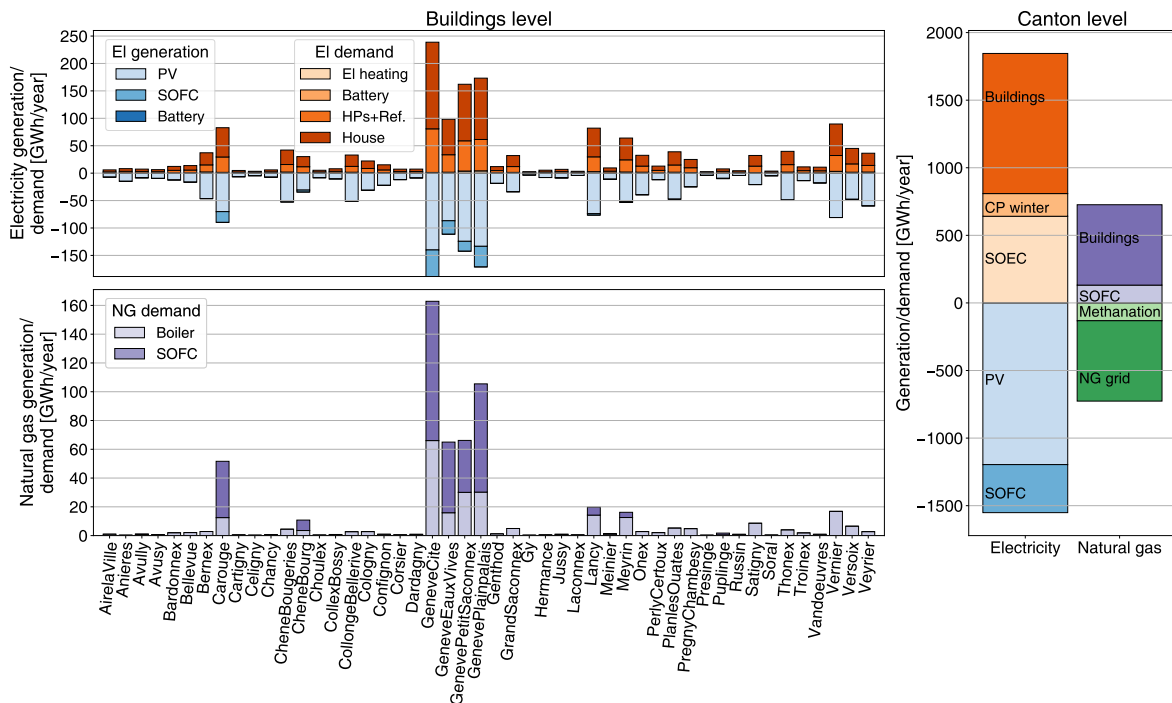


Figure 4.18 – Breakdown of electricity/natural gas import/export by commune and at building/canton level.

Figure 4.19 shows the cost breakdown at the building level, for each commune and at the canton level. Similar to the results shown for Geneva city center, building investments are principally concentrated in heat pumps and refrigeration units ( $\approx 20\%$ ), SOFC s ( $\approx 3\%$ ) and PV panels ( $\approx 71\%$ ), while the investment cost at the canton level is dominated by the 5G DEN piping (28%) followed by PV panels (19%) and the the power-to-gas system (9%).

Also in this case one of the solutions, the one of the commune Génève Cité (highlighted solution in Figures 4.17 and 4.19), is selected for additional exploration.

#### 4.4. Results and discussion

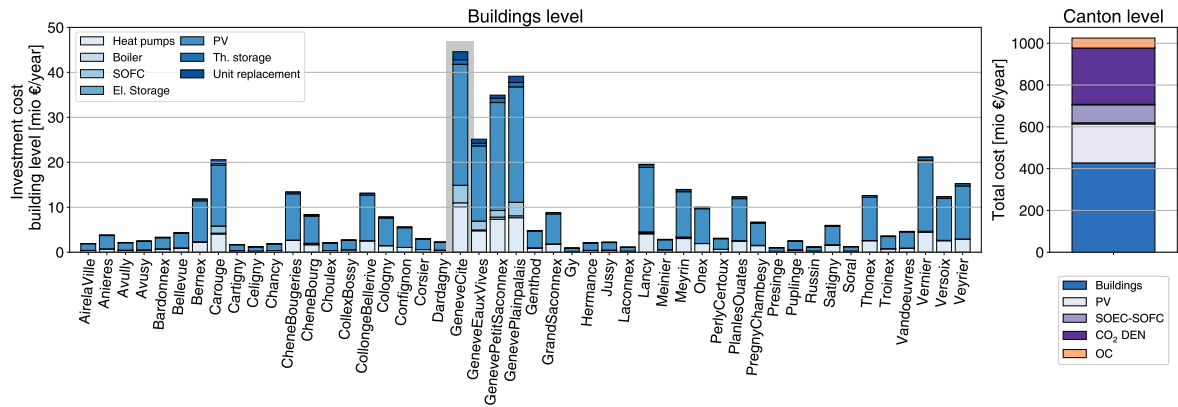


Figure 4.19 – Breakdown of investment and total cost at buildings/canton level.

The monthly energy import/export profiles of Génève Cité are shown in Figure 4.20. As observed in this figure, the electricity consumption of heat pumps is high in winter, when heating is required, and lower in summer, while the electricity demand for electrical appliances is assumed constant over the year. Electricity production from PV panels is higher in summer, corresponding to higher global horizontal irradiation, and the electricity production of SOFC co-generation units is higher in winter, since they provide the electricity requirement of heat pumps and co-generate heat for space heating and domestic hot water demand. Consequently, the natural gas consumption of the SOFC and boiler units are higher in winter, both related to supply of heating services.

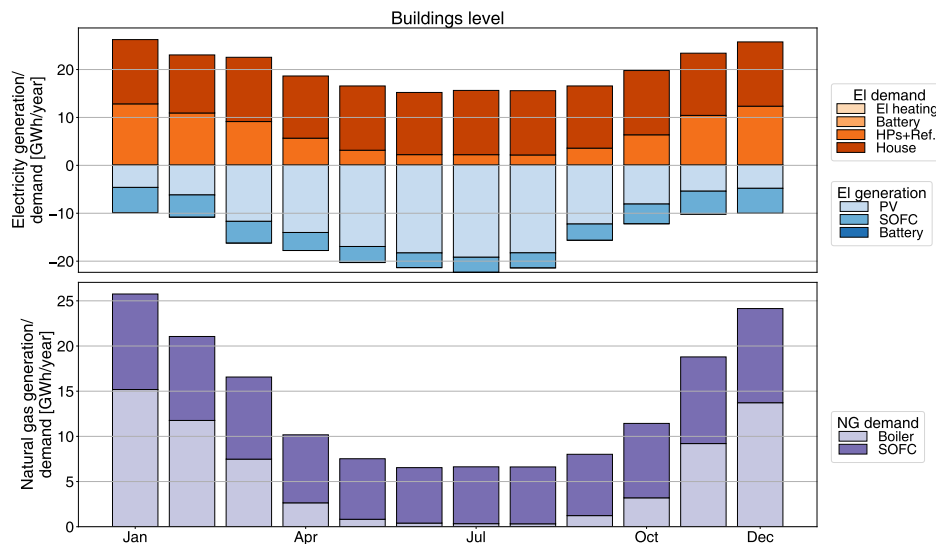


Figure 4.20 – Breakdown of electricity/natural gas import/export by month, for Génève Cité.

## 4.5 Conclusion

This chapter aims at providing a method to systematically integrate multi-energy networks and low carbon resources in cities. The method proposes a double optimization approach with meta-models to link analysis and optimization at both building and urban scales. The first optimization creates a pool of optimal building solutions of different types (residential single- and multi-family houses (SFH , MFH ), administrative, commercial, education, hospital and mixed), renovation stages (existing, new and renovated), energy system configurations (existing H<sub>2</sub>O-based networks or potential low-temperature CO<sub>2</sub>-based networks) and for different investment cost limits (i.e., budgets). The pool of optimal building meta-models is fed to the optimizer on top, which selects the best mix to optimize energy systems at city/canton level.

Geneva city center is used as a case study to analyze the impact of different temporal resolutions, namely monthly averages and hourly typical days. The results show that implicit peak shaving occurs in the monthly resolution by averaging demands, resulting in lower operating cost and higher self-sufficiency solutions, compared to the hourly resolution. However, the investment cost breakdown proves that the main contributors do not change, irrespective of the time resolution. Therefore, and in view of decreasing data processing and computation time, a monthly resolution is used for the results at canton level.

### 4

The second case study, the whole canton of Geneva (48 communes), is analyzed to assess 5G DEN penetration with population density. The results highlight that scenarios with moderate investment limits, only communes with high population density, i.e., a network cost below 21.5 k€/100 m<sup>2</sup><sub>ERA</sub> connect to the refrigerant-based network, while for the minimum operating cost scenario, all communes are connected to the 5G DEN. Parallel coordinates are employed to better visualize key performance indicators for the scenarios at the cantonal and communal levels. The energy and cost breakdown results for each commune show that electricity is mostly consumed in heat pumps, refrigeration units and for electrical appliances while being produced by PV panels and SOFC co-generation units, while natural gas is consumed for boilers and SOFCs. Consequently, at the building level, the investment cost is dominated by heat pumps (≈20%), SOFCs (≈3%) and PV panels (≈71%). At the canton level, the electricity importers are the buildings, SOEC unit and central plant, and the electricity exporters are PV panels and the SOFC unit, while the natural gas importers are the building and SOFC unit and the exporters are the methanator and natural gas grid. Consequently, the investment cost at the cantonal level is dominated by PV panels (19%), the power-to-gas system (9%) and 5G DEN piping (28%).

This work successfully develops an integrated framework, which embeds optimally operating buildings in districts. The framework was validated using the canton of Geneva; however, it is not case specific and can therefore be applied to different urban systems/conditions. This work allows engineers to assess the cost of reaching the Paris agreement targets and reduce the operating cost

#### 4.5. Conclusion

---

by approximately 90% in the residential sector, while using low-temperature 5G district energy networks. The model can also be used to study the integration of other types of large energy systems, e.g., by municipal bodies for future planning of urban energy supply with long planning horizons. Future work includes improving the pool of building meta-models, to cover a wider range of building types and a finer resolution on the building renovation stage and on budget scenarios. A typical day/full hourly resolution is suggested for future work to obtain more precise results and avoid inaccuracies stemming from implicit peak shaving. Further applications of the method in other geographical contexts would create a broader understanding of 5G DEN penetration and could potentially be extended to a European or global scale to assess feasibility as a multi-energy, fully renewable solution, coupled to long-term energy storage.



# Conclusions

## Overview

- Main results and contributions
- Future perspectives

## Main results and contributions

The main results and contributions of the thesis are presented, following the four research questions proffered in the introduction.

### Chapter 1: Estimating urban energy demand

*"How do we estimate urban energy demand?"*

This chapter provides a **parameterized residential energy and service profile** for any city in Europe, which gives an estimation of demands for heating, cooling, electricity for utilities, mobility and waste treatment. The profile is validated using a typical European city, the city of Rotterdam. Differences between the real demand and the proposed profile vary between 3-8% for the different services, showing the distinction between the Dutch consumption profile and the typical Western European one.

The functionality of the profile is demonstrated by comparing four different scenarios, based on different district energy systems and advancement in technologies. Distinct objective functions yield different solutions, however consistent results show good performance with a fully electrical system both for heating and mobility, potentially reaching zero CO<sub>2</sub> emissions, given a renewable electricity mix.

The sector profile can be used by forecasters, research institutes, governments, planners, energy consultants, energy start-ups, city planners, or utility companies to estimate current and future energy demand in urban areas around Europe.

### Chapter 2: Valorizing natural resources and human waste

*"How do valorize urban renewable resources?"*

This chapter assesses the **potential of future energy systems to valorize the energy wealth of European urban centers, while fulfilling their comfort requirements**. The challenge is to select and use technologies with a dual objective: to minimize the thermal use of electricity by distributing the heat at the appropriate temperature level and to maximize the capture and exploitation of local renewable resources. To fulfill the first requirement, a novel energy system is proposed, which combines a compact district heating and cooling network using CO<sub>2</sub> as a heat transfer fluid with a power-to-gas long term renewable energy storage system, (driven by a SOFC-GT coupled to a SOEC).

The system proposed is applied to four typical cities, built based on the parameterized residential energy and service profile introduced in chapter 1. For the second requirement, four different scenarios are analyzed. They show that using geothermal heat instead of fresh water source heat pumps saves approximately half of the electricity required in the first stage, which accounts for 30% of the total demand of the network. Moreover, performing heat recovery from waste treatment incineration reduces the load of the central plant and heating HPs and decreases the operating cost by an additional 10%. Finally, the last scenario assesses the potential for autonomy in different climate zones and proves that full autonomy can be reached for the South zone, while 50% of the electricity must be supplied from the grid for zones CEast and CWest and around 70% for the North zone.

With an estimated payback time of less than 17 years and the current cost of technologies an economically viable and technically feasible solution exists for fully autonomous cities, namely 5G DENs with advanced technologies.

### Chapter 3: Valorizing industrial waste heat

*"How do we valorize industrial waste heat?"*

The third chapter first adds 10 typical industries to the residential sector profile introduced in chapter 1, namely: oil refining, cement, brewing, aluminum processing, steel, waste incineration, pulp and paper, sugar, dairy production and plastics. It uses previously-developed industrial blueprints [127, 132] and European consumption data on each industry to construct typical European cities with specially-sized industries to provide the requirements of the urban population.

The enlarged typical city profile is tested for three city scales: small (using Zurich, CH as a model), medium (using Munich, DE) and large (using London, UK), while the locations of the large industries are permuted to study the impact of industry location on the heat transfer, heat loss, overall operating



cost, energy import and environmental impact. Analyzing a scenario in which industrial on-site heat recovery has been fully realized (therefore reducing the availability of industrial waste heat compared to the current situation) yielded energy savings of 16 - 26% for small cities, 10 - 16% for medium scale and 4 - 14% for large cities. However, solutions with similar energy savings may have large differences in the amount of heat transferred, depending on the relative distances between the different industries.

This chapter also uses the residential sector profile introduced in chapter 1 to assess the **integration opportunities between urban district heating and cooling networks and typical industries in the surroundings**, for a real case study using the city of Rotterdam, NL. A brewery and four refinery/cement plant couples are integrated for this purpose, and the results show that industries located at 5 km and 9 km transfer heat to the district energy network, reducing its operating cost by up to 9% and its CO<sub>2</sub> emissions by up to 20%, while industrial plants located further away only integrate with each other, as heat losses are too large over long distances.

### Chapter 4: Systematic integration of energy- optimal buildings with district networks

*"How do we bridge the gap between building scale and district scale analysis?"*

This chapter provides **a method to systematically integrate multi-energy networks and low carbon resources in cities**. Compared to the previous chapters, both the temporal and spatial resolutions are refined. The temporal scale is tackled by comparing monthly averages with the typical day, hourly resolution. The results highlight the peak shaving which occurs in the monthly resolution by averaging demands, resulting in lower operating cost and higher self-sufficiency solutions, compared to the hourly resolution. However, the investment cost breakdown proves that the main contributors do not change, irrespective of the time resolution.

Then, the spatial scale is addressed by using a double optimization approach with meta-models to interlink building - and urban - scale analysis. The first optimization aims at creating a pool of optimal building solutions of different types, renovation stages, energy system configurations and for different investment cost limits. The solutions for optimal buildings are passed to the second step of optimization, which determines networks, building configurations and mixes, and connections for optimized performance of regional energy systems.

The results show that except for the maximum investment cost scenario, only communes with high population density, i.e. a network cost below  $21.5 \text{ k€}/100\text{m}^2_{\text{ERA}}$  connect to the refrigerant-based network. *Parallel coordinates are employed in this chapter to better visualize key performance indicators both at commune and canton level.*

Further applications of the method in other geographical contexts would create a broader under-

standing of 5G DEN penetration and could potentially be extended to a European or global scale to assess feasibility as a multi-energy, fully renewable solution, coupled to long-term energy storage.

### Future perspectives

The **parameterized residential energy and service profile** presented in this thesis was built based on data from a typical European city; further improvements could include:

- using the building distribution and heat signature parameters of the city analyzed and not relying on data from a typical urban center;
- refining the European climatic zones (e.g. by using data clustering);
- extending the profile to other climatic areas (e.g. tropical cities). The heat signature model relies mostly on meteorological and reference demand data, making it flexible and adaptable to other climatic zones around the world.

The study on **potential of future energy systems to valorize the energy wealth of European urban centers, while fulfilling their comfort requirements** could be further improved by:

- including other water sources to supply heat from the environment (e.g. rivers, which have a constant temperature and therefore require lower temperature lifts in the central plant HPs);
- valorizing the organic part of the municipal solid waste. The organic part could be used for bio-methane production and consequently CO<sub>2</sub> capture, on the way towards negative CO<sub>2</sub> emitting cities;
- integrating waste heat recovery from industries in the vicinity (addressed in chapter 3).

The analysis on **integration opportunities between urban district energy networks and industrial plants in the surroundings** presented in chapter 3 was built considering ten major industries. Further investigations could include:

- accounting for pumping electricity and piping cost;
- building similar sector profiles for all energy-intensive sectors (other industries, but also transport, agriculture, etc.) to provide a complete set of tools for future modeling of energy efficient cities/communities;
- extending the industrial profiles to other continents around the world (i.e. collecting data on industry consumption, and adjusting the profiles based on the common industrial processes in the respective areas).

The **method to systematically integrate multi-energy networks and low carbon resources in cities** developed in chapter 4 could be refined by:

- improving the pool of building meta-models, to cover a wider range of building types and a finer resolution on the building renovation stage and on the budget scenarios;

- using a typical day/full hourly resolution to produce more precise results and avoid implicit peak shaving;
- including the potential for renovating buildings as another investment option for improving the energy efficiency instead of selecting building models to fit the current mix of building typology
- extending the 5G district energy network penetration analysis at European scale, as a multi-energy, fully renewable solution coupled to long term energy storage systems



# Appendix



# (Chapter 1)

## A.1 Unit models

### A.1.1 Scenario 1

**Natural gas and oil boiler** The natural gas and oil boilers are modelled according to [28]. The main streams are listed in Table A.1.

Table A.1 – Boiler streams.

Name	$T^{\text{in}}$ [°C]	$T^{\text{out}}$ [°C]	$\dot{Q}^-$ [kW]	$\dot{Q}^+$ [kW]	$\dot{m}^-$	$\dot{m}^+$
Radiation	826.85	826.85	61.0	-	-	-
Convection	826.85	120	35.7	-	-	-
Nat. gas	-	-	-	-	-	41.5 kW
Oil	-	-	-	-	-	58.5 kW

The thermal efficiency is computed as:

$$\eta^{\text{th}} = \frac{\dot{Q}_{\text{Radiation}}^- + \dot{Q}_{\text{Convection}}^-}{\dot{m}_{\text{Nat. gas}}^+ + \dot{m}_{\text{Oil}}^+} = 96.7\% \quad (\text{A.1})$$

**Central heating** Central heating is represented as a hot stream, with the properties given in Table A.2.

Table A.2 – Central heating streams.

Name	$T^{\text{in}}$ [°C]	$T^{\text{out}}$ [°C]	$\dot{Q}^-$ [kW]	$\dot{Q}^+$ [kW]	$\dot{m}^-$	$\dot{m}^+$
Hot water	90	60	100	-	-	-

**Electrical heating** The electric heater is modelled as a unit with 100% electricity to heat efficiency (Table A.3).

Table A.3 – Electrical heating streams.

Name	T <sup>in</sup> [°C]	T <sup>out</sup> [°C]	Q <sup>-</sup> [kW]	Q <sup>+</sup> [kW]	m <sup>-</sup>	m <sup>+</sup>
Hot water	90	60	100	-	-	-
Electricity	-	-	-	-	-	100 kW

**Refrigeration cycle** The refrigeration cycle considered uses as source ambient air (at 25 °C). The streams of the refrigeration cycle are listed in Table A.4.

Table A.4 – Refrigeration cycle streams.

Name	T <sup>in</sup> [°C]	T <sup>out</sup> [°C]	Q <sup>-</sup> [kW]	Q <sup>+</sup> [kW]	m <sup>-</sup>	m <sup>+</sup>
Evaporation	-5	-5	-	100	-	-
Electricity	-	-	-	-	-	22.1 kW

Where the coefficient of performance of the cycle is computed as:

$$COP_{REF} = \frac{T^{evap}}{T^{cond} - T^{evap}} \cdot \eta^{carnot} \quad (A.2)$$

with  $T^{evap} = -5^{\circ}\text{C}$ ,  $T^{cond} = T^{amb} + \Delta T^{min, water-air} = 25^{\circ}\text{C} + 5.5^{\circ}\text{C} = 30.5^{\circ}\text{C}$ , and  $\eta^{carnot} = 0.6$ .

**Waste boiler** The inorganic part of the waste (71% of the municipal solid waste [182]) is incinerated. The resulting heat and electricity streams corresponding to a mass flow rate of 1 kg/s of municipal solid waste are listed in Table A.5. A lower heating value of 16710.78 kJ/kg is assumed [183].

Table A.5 – Municipal waste plant streams.

Name	T <sup>in</sup> [°C]	T <sup>out</sup> [°C]	Q <sup>-</sup> [kW]	Q <sup>+</sup> [kW]	m <sup>-</sup>	m <sup>+</sup>
Heat	900	340	6406.9	-	-	-
Heat	180	60	1423.8	-	-	-
Heat	60	25	400.4	-	-	-
Electricity	-	-	-	-	-	249.2 kW

The heat from the steam network can be used either for direct heating or for CO<sub>2</sub> vaporization . The



## A.1. Unit models

reference streams used to model these HEs are given in Tables A.6 and A.7. A minimum temperature difference  $\Delta T^{\min, \text{water-refrigerant}} = 5.5^\circ\text{C}$  is assumed.

Table A.6 – CO<sub>2</sub> vaporization HE streams.

Name	$T^{\text{in}}$ [°C]	$T^{\text{out}}$ [°C]	$\dot{Q}^-$ [kW]	$\dot{Q}^+$ [kW]	$\dot{m}^-$	$\dot{m}^+$
Heat	20.5	25	-	186.4	-	-
CO <sub>2</sub> vap	-	-	-	-	1 kg/s	-
CO <sub>2</sub> liq	-	-	-	-	-	1 kg/s

Table A.7 – Direct heating supply HE streams.

Name	$T^{\text{in}}$ [°C]	$T^{\text{out}}$ [°C]	$\dot{Q}^-$ [kW]	$\dot{Q}^+$ [kW]	$\dot{m}^-$	$\dot{m}^+$
Heat	65	60.5	186.4	-	-	-

In the steam network, steam is produced at very high pressure and distributed at multiple lower pressure levels. The pressure levels are selected to fit the production profiles of the municipal waste plant. The parameters used to model the steam network are summarized in Table A.8.

Table A.8 – Steam network parameters.

Type	Header pressure [bar]	$T^{\text{superheat}}$ [°C]	Turbine
Production	120	100	yes
Distribution	30	2	yes
Distribution	10	2	yes
Distribution	5	2	yes
Distribution	2	2	no
Distribution	1	2	no
Distribution	0.2	2	no

### A.1.2 Scenario 2 (additional utilities)

**Combined heat and power plant** The combined heat and power plant is modelled according to [184]. The main streams are listed in Table A.9 and the cost parameters of all the additional utilities are given in Table A.10.

Table A.9 – Combined heat and power plant streams.

Name	$T^{\text{in}}$ [°C]	$T^{\text{out}}$ [°C]	$\dot{Q}^-$ [kW]	$\dot{Q}^+$ [kW]	$\dot{m}^-$	$\dot{m}^+$
Heat (Hot gases)	470	120	537	-	-	-
Heat (Cooling circuit)	87	80	653	-	-	-
Electricity	-	-	-	-	1063 kW	-
Nat. gas	-	-	-	-	-	2605 kW

The thermal and electrical efficiencies are computed as:

$$\eta^{\text{el}} = \frac{\dot{m}_{\text{Electricity}}^-}{\dot{m}_{\text{Nat. gas}}^+} = 40.8\% \quad (\text{A.3})$$

$$\eta^{\text{th}} = \frac{\dot{Q}_{\text{Hot gases}}^- + \dot{Q}_{\text{Cooling circuit}}^-}{\dot{m}_{\text{Nat. gas}}^+} = 45.7\% \quad (\text{A.4})$$

Table A.10 – Investment cost parameters.

Unit	$C_u^{\text{inv},1}$ [€]	$C_u^{\text{inv},2}$ [€/kW / €/m <sup>2</sup> ]	Attribute
CHP	11910	119096	$\dot{m}_{\text{Electricity}}^-$ [kW]
ST panels	-	196	$A_{\text{ST}}$ [m <sup>2</sup> ]
PV panels	-	247	$A_{\text{PV}}$ [m <sup>2</sup> ]
Heat pump	5680	1240	$\dot{m}_{\text{Electricity}}^+$ [kW]
Electrolyzer	-	4760	$\dot{m}_{\text{Electricity}}^+$ [kW]

**Solar thermal panel** The solar thermal panels are modelled using a quadratic performance curve, depending on the solar thermal panel temperature  $T^{\text{ST}}$ , the external temperature  $T^{\text{amb}}(t)$ , the incoming irradiation  $I(t)$  [W/m<sup>2</sup>], a maximum efficiency  $\eta^{\text{ST},0}$  and two experimental parameters  $a_1$ ,  $a_2$  [185]:

$$\eta^{\text{ST}} = \eta^{\text{ST},0} - a_1 \cdot \frac{T^{\text{ST}} - T^{\text{amb}}(t)}{I(t)} - a_2 \cdot \left( \frac{T^{\text{ST}} - T^{\text{amb}}(t)}{I(t)} \right)^2 \cdot I(t) \quad (\text{A.5})$$

The heat transmission coefficient  $a_1$  describes the the thermal losses. The higher this value, the more losses the collector has. The coefficient  $a_2$  is used to calculate the coefficient of heat transmission

dependent on temperature. The investment cost parameters are given in Table A.10 [186].

Table A.11 – Solar thermal panels parameters.

Parameter	Value	Unit
$T^{ST}$	67	°C
$\eta^{ST,0}$	0.735	–
$a_1$	3.60	W/(K · m <sup>2</sup> )
$a_2$	0.0087	W/(K <sup>2</sup> · m <sup>2</sup> )

**Photo-voltaic panel** The PV panels are modelled as described in [187], with  $A^{PV}(t)$  the PV area,  $\eta^{PV}(t)$  the PV efficiency,  $I(t)$  the incoming irradiation,  $T^{PV}(t)$  the PV temperature,  $U^{glass}$  the thermal transmission coefficient,  $T^{amb}(t)$  the ambient temperature, and  $f^{glass}$  the factor denoting the portion of the solar irradiation passing through the PV glass:

$$\dot{m}_{PV,electricity}^-(t) = A^{PV}(t) \cdot \eta^{PV}(t) \cdot I(t) \quad (A.6a)$$

$$\eta^{PV}(t) = \eta^{PV,0} - \eta^{PV,var} \cdot (T^{PV}(t) - T^{PV,0}) \quad (A.6b)$$

$$T^{PV}(t) = \frac{U^{glass} \cdot T^{amb}(t)}{U^{glass} - \eta^{PV,0} \cdot I(t)} + \frac{I(t) \cdot (f^{glass} - \eta^{PV,0} - \eta^{PV,var} \cdot T^{PV,0})}{U^{glass} - \eta^{PV,var} \cdot I(t)} \quad (A.6c)$$

The different parameters assumed are given in Table A.12 [187], the reference stream for  $A^{PV} = 100$  m<sup>2</sup> and  $I = 100$  W/m<sup>2</sup> is given in table A.13 and the investment cost parameters in table A.10 [89].

Table A.12 – PV panel parameters.

Parameter	Value	Unit
$T^{PV,ref}$	298	K
$U^{glass}$	29.1	W/(m <sup>2</sup> ·K)
$f^{glass}$	0.9	–
$\eta^{PV,0}$	0.14	–
$\eta^{PV,var}$	0.001	1/K

Table A.13 – PV panel streams.

Name	$T^{\text{in}}$ [°C]	$T^{\text{out}}$ [°C]	$\dot{Q}^-$ [kW]	$\dot{Q}^+$ [kW]	$\dot{m}^-$	$\dot{m}^+$
Electricity	-	-	-	-	1.66 kW	-

**Heat pump** The heat pump considered uses as source ambient air (at 25 °C). The streams of the heat pump are listed in Table A.14 and the investment cost parameters in Table A.10 [18]

Table A.14 – Heat pump streams.

Name	$T^{\text{in}}$ [°C]	$T^{\text{out}}$ [°C]	$\dot{Q}^-$ [kW]	$\dot{Q}^+$ [kW]	$\dot{m}^-$	$\dot{m}^+$
Heat	60.5	60.5	100	-	-	-
Electricity	-	-	-	-	-	20.5 kW

Where the COP of the cycle is computed as:

$$COP_{HP} = \frac{T^{\text{cond}}}{T^{\text{cond}} - T^{\text{evap}}} \cdot \eta^{\text{carnot}} \quad (\text{A.7})$$

with  $T^{\text{evap}} = T^{\text{amb}} - \Delta T^{\text{min, water-air}} = 25^\circ\text{C} - 5.5^\circ\text{C} = 19.5^\circ\text{C}$ ,  $T^{\text{cond}} = 60.5^\circ\text{C}$ , and  $\eta^{\text{carnot}} = 0.6$ .

**Electrolyzer** The electrolyzer was modelled according to [88] and the cost parameters were taken from [90]. The reference flows are given for an incoming flow of electricity of 100 kW. The electricity to hydrogen efficiency is computed using the higher heating value (HHV) of  $\text{H}_2$  of 141746 kJ/kg [188]:

$$\eta = \frac{\dot{m}_{\text{H}_2}^- \cdot \text{HHV}_{\text{H}_2}}{\dot{m}_{\text{electricity}}^+} = 94.2\% \quad (\text{A.8})$$

## A.1. Unit models

Table A.15 – Electrolyzer streams.

Name	$T^{\text{in}}$ [°C]	$T^{\text{out}}$ [°C]	$\dot{Q}^-$ [kW]	$\dot{Q}^+$ [kW]	$\dot{m}^-$	$\dot{m}^+$
Heat	91	58	3.05	-	-	-
Heat	58	27	1.66	-	-	-
Electricity	-	-	-	-	-	100 kW
H <sub>2</sub> O	-	-	-	-	-	5.98 g/s
H <sub>2</sub>	-	-	-	-	0.67 g/s (94.21 kW)	-

A fuel consumption of 38.4 L/km was assumed for hydrogen mobility [189] and a hydrogen density of 23.32 t/L at 350 bar and atmospheric temperature [190].



## (Chapter 2)

### B.1 Unit models: Decentralized energy conversion technologies

The main assumptions made in order to model the heating HPs and the REF cycle are given in table B.1.

Table B.1 – Parameters for decentralized energy conversion technologies.

Unit	HP space heating	HP hot water	REF cycle
Refrigerant [-]	R1234yf	CO <sub>2</sub>	CO <sub>2</sub>
$T^{\text{subcool}}$ [°C]	1	1	1
$T^{\text{superheat}}$ [°C]	2	2	2
$\eta^{\text{comp}}$ [-]	0.8	0.8	0.8
$dT^{\text{min, evap}}$ [°C]	1	1	5.5
$dT^{\text{min, cond}}$ [°C]	5.5	5.5	1

The reference flows of the HPs are the heat in the evaporator,  $\dot{Q}^{\text{evap}} = \dot{m}^{\text{CO}_2} \cdot L^{\text{v, CO}_2} = 186.4$  kW (for a reference flow of 1 kg/s of CO<sub>2</sub> [190]) and the reference flow in the REF cycle is the heat in the condenser  $\dot{Q}^{\text{cond}} = \dot{m}^{\text{CO}_2} \cdot L^{\text{v, CO}_2}$ . The electricity consumed by the compressor and the corresponding heat delivered/extracted are computed by solving the thermodynamic cycles, based on the parameters given above. Coolprop [190] is used to calculate the thermodynamic properties. The reference streams of the units are given in tables B.2, B.3, and B.4 for a reference flow of CO<sub>2</sub> of 1 kg/s.

Table B.2 – Streams for space heating HP.

Name	$T^{\text{in}}$ [°C]	$T^{\text{out}}$ [°C]	$\dot{Q}^-$ [kW]	$\dot{Q}^+$ [kW]	$\dot{m}^-$	$\dot{m}^+$
Heat evaporator	12	14	-	186.4 kW	-	-
Heat condenser	$T^{\text{demand}} + 5.5$	$T^{\text{demand}} + 4.5$	$186.4 \cdot \frac{COP}{COP-1}$ kW	-	-	-
Electricity	-	-	-	-	-	$186.4 \cdot \frac{1}{COP-1}$ kW
CO <sub>2</sub> <sup>vap</sup>	-	-	-	-	-	1 kg/s
CO <sub>2</sub> <sup>liq</sup>	-	-	-	-	1 kg/s	-

Table B.3 – Streams for domestic hot water HP.

Name	$T^{\text{in}}$ [°C]	$T^{\text{out}}$ [°C]	$\dot{Q}^-$ [kW]	$\dot{Q}^+$ [kW]	$\dot{m}^-$	$\dot{m}^+$
Heat evaporator	2	4	-	186.4 kW	-	-
Heat condenser	60.5	15.5	$186.4 \cdot \frac{COP}{COP-1}$ kW	-	-	-
Electricity	-	-	-	-	-	$186.4 \cdot \frac{1}{COP-1}$ kW
CO <sub>2</sub> <sup>vap</sup>	-	-	-	-	-	1 kg/s
CO <sub>2</sub> <sup>liq</sup>	-	-	-	-	1 kg/s	-

Table B.4 – Streams for refrigeration cycle.

Name	$T^{\text{in}}$ [°C]	$T^{\text{out}}$ [°C]	$\dot{Q}^-$ [kW]	$\dot{Q}^+$ [kW]	$\dot{m}^-$	$\dot{m}^+$
Heat evaporator	-4.5	-2.5	-	$186.4 \cdot \frac{COP}{COP+1}$ kW	-	-
Heat condenser	15	13	186.4 kW	-	-	-
Electricity	-	-	-	-	-	$186.4 \cdot \frac{1}{COP+1}$ kW
CO <sub>2</sub> <sup>vap</sup>	-	-	-	-	1 kg/s	-
CO <sub>2</sub> <sup>liq</sup>	-	-	-	-	-	1 kg/s

One should note that the space heating HPs have a variable temperature in the condenser, which depends on the temperature of the demand. This temperature varies both across the different building types and different operating times. Consequently, the heat delivered in the condenser and the work needed by the compressor vary as a function of the demand temperature. Moreover, the domestic hot water HP is modelled as a super-critical HP, which delivers sensible heat in the condenser, and not heat resulting from phase change. The coefficients of performance of the HPs



## B.2. Unit models: centralized energy conversion technologies

and of the REF cycle:

$$\text{COP}^{\text{HP}} = \left( \eta^{\text{carnot}} \cdot \frac{T^{\text{cond}}}{T^{\text{cond}} - T^{\text{evap}}} \right) = \frac{\dot{Q}^{\text{cond}}}{\dot{m}_{\text{electricity}}^+}, \quad \text{COP}^{\text{REF}} = \left( \eta^{\text{carnot}} \cdot \frac{T^{\text{evap}}}{T^{\text{cond}} - T^{\text{evap}}} \right) = \frac{\dot{Q}^{\text{evap}}}{\dot{m}_{\text{electricity}}^+} \quad (\text{B.1})$$

are given in figure B.1 together with the schematic flowsheet according to which the units are modelled [18]

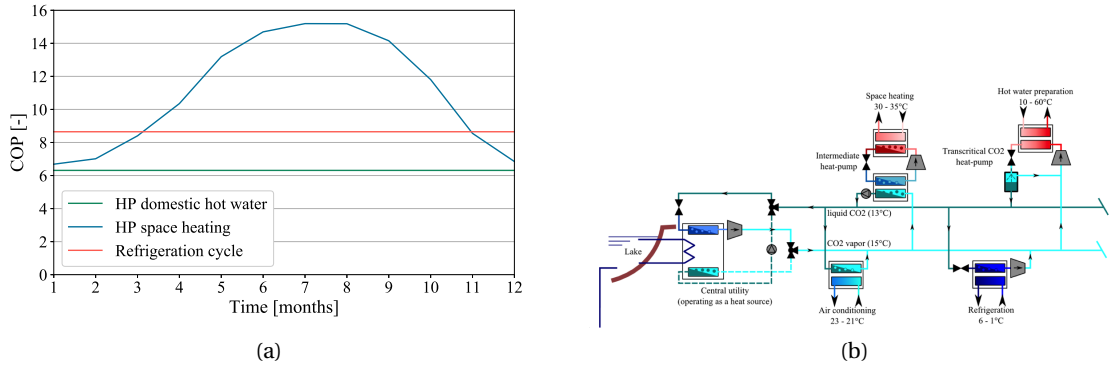


Figure B.1 – COP for heating HPs and REF cycle by month, zone CWest / Schematic flowsheet of a CO<sub>2</sub> DEN.

The parameters used for the air cooling HE are the reference flow  $\dot{Q} = \dot{m}^{\text{CO}_2} \cdot L^v$ , CO<sub>2</sub> and the minimum temperature difference in the HE ( $dT^{\text{min}} = 5.5^\circ\text{C}$ ). The reference streams of the unit are given in table B.5 for a mass flow of CO<sub>2</sub> of 1 kg/s.

Table B.5 – Streams for air cooling heat exchanger.

Name	T <sup>in</sup> [°C]	T <sup>out</sup> [°C]	$\dot{Q}^-$ [kW]	$\dot{Q}^+$ [kW]	$\dot{m}^-$	$\dot{m}^+$
Heat	15	13	-	186.4 kW	-	-
CO <sub>2</sub> <sup>vap</sup>	-	-	-	-	1 kg/s	-
CO <sub>2</sub> <sup>liq</sup>	-	-	-	-	-	1 kg/s

## B.2 Unit models: centralized energy conversion technologies

### B.2.1 PV panels

The PV panels are modelled as described in [187], with  $A^{\text{PV}}$  the PV area,  $\eta^{\text{PV}}$  the PV efficiency,  $I$  the irradiation of the sun,  $T^{\text{PV}}$  the PV temperature,  $U^{\text{glass}}$  the thermal transmission coefficient,  $T^{\text{amb}}$

the ambient temperature, and  $f^{\text{glass}}$  the factor denoting the portion of the solar irradiation passing through the PV glass:

$$\dot{m}_{\text{PV,electricity}} = A^{\text{PV}} \cdot \eta^{\text{PV}} \cdot I \quad (\text{B.2a})$$

$$\eta^{\text{PV}} = \eta^{\text{PV,ref}} - \eta^{\text{PV,var}} \cdot (T^{\text{PV}} - T^{\text{PV,ref}}) \quad (\text{B.2b})$$

$$T^{\text{PV}} = \frac{U^{\text{glass}} \cdot T^{\text{amb}}}{U^{\text{glass}} - \eta^{\text{PV,var}} \cdot I} + \frac{I \cdot (f^{\text{glass}} - \eta^{\text{PV,ref}} - \eta^{\text{PV,var}} \cdot T^{\text{PV,ref}})}{U^{\text{glass}} - \eta^{\text{PV,var}} \cdot I} \quad (\text{B.2c})$$

The different parameters assumed are given in Table B.6 [187] and the reference stream for  $A^{\text{PV}} = 100 \text{ m}^2$  and  $I = 100 \text{ W/m}^2$  is given in table B.7.

Table B.6 – Parameters for PV panels.

Parameter	Value	Unit
$T^{\text{amb}}$	288	K
$T^{\text{PV,ref}}$	298	K
$U^{\text{glass}}$	29.1	$\text{W}/(\text{m}^2 \cdot \text{K})$
$f^{\text{glass}}$	0.9	–
$\eta^{\text{PV,ref}}$	0.14	–
$\eta^{\text{PV,var}}$	0.001	$1/\text{K}$

Table B.7 – Streams for PV panel.

Name	$T^{\text{in}} [^{\circ}\text{C}]$	$T^{\text{out}} [^{\circ}\text{C}]$	$\dot{Q}^- [\text{kW}]$	$\dot{Q}^+ [\text{kW}]$	$\dot{m}^-$	$\dot{m}^+$
Electricity	-	-	-	-	1.66 kW	-

### B.2.2 SOEC-SOFC co-generation and methanation

The co-generation SOFC-GT unit is modelled according to [87] and the co-generation SOEC unit according to [191]. A list of the reference streams in the different units are given in tables B.8, B.9, and B.10.

## B.2. Unit models: centralized energy conversion technologies

Table B.8 – Streams for SOEC unit.

Name	T <sup>in</sup> [°C]	T <sup>out</sup> [°C]	$\dot{Q}^-$ [kW]	$\dot{Q}^+$ [kW]	$\dot{m}^-$	$\dot{m}^+$
Heat	91	58	3.05 kW	-	-	-
Heat	58	27	1.66 kW	-	-	-
Electricity	-	-	-	-	-	100 kW
H <sub>2</sub> O	-	-	-	-	-	5.98 g/s
H <sub>2</sub>	-	-	-	-	0.67 g/s (94.21 kW)	-

The reference flows for the SOEC unit are given for an incoming flow of electricity of 100 kW. The electricity to hydrogen efficiency is computed using the HHV of H<sub>2</sub> of 141746 kJ/kg [188]:

$$\eta = \frac{\dot{m}_{\text{H}_2}^- \cdot \text{HHV}^{\text{H}_2}}{\dot{m}_{\text{electricity}}^+} = 94.2\% \quad (\text{B.3})$$

Table B.9 – Streams for SOFC-GT unit.

Name	T <sup>in</sup> [°C]	T <sup>out</sup> [°C]	$\dot{Q}^-$ [kW]	$\dot{Q}^+$ [kW]	$\dot{m}^-$	$\dot{m}^+$
Heat	648.8	260.0	16.28 kW	-	-	-
Heat	109.8	35.2	9.44 kW	-	-	-
Heat	35.2	30.2	1.44 kW	-	-	-
Electricity	-	-	-	-	100 kW	-
CH <sub>4</sub>	-	-	-	-	-	-2.41 g/s (133.48 kW)
CO <sub>2</sub>	-	-	-	-	6.60 g/s	-

The reference flows for the SOFC-GT unit are given for an outgoing flow of electricity of 100 kW. The electrical and thermal efficiencies are calculated using the HHV of CH<sub>4</sub> of 55484 kJ/kg [188]:

$$\eta^{\text{el}} = \frac{\dot{m}_{\text{electricity}}^-}{\dot{m}_{\text{CH}_4}^+ \cdot \text{HHV}^{\text{CH}_4}} = 74.9\% \quad (\text{B.4a})$$

$$\eta^{\text{th}} = \frac{\sum_{k \in \mathbf{K}} \dot{Q}_{\text{SOFC}}^k}{\dot{m}_{\text{CH}_4}^+ \cdot \text{HHV}^{\text{CH}_4}} = 20.3\% \quad (\text{B.4b})$$

Table B.10 – Streams for methanation unit.

Name	T <sup>in</sup> [°C]	T <sup>out</sup> [°C]	$\dot{Q}^-$ [kW]	$\dot{Q}^+$ [kW]	$\dot{m}^-$	$\dot{m}^+$
Heat	625.4	507.3	138.4 kW	-	-	-
Heat	507.3	507.1	0.3 kW	-	-	-
Heat	507.1	233.0	585.3 kW	-	-	-
Heat	233.0	228.0	9.3 kW	-	-	-
Heat	228.0	227.0	0.7 kW	-	-	-
Heat	227.0	215.0	12.7 kW	-	-	-
Heat	215.0	203.0	27.1 kW	-	-	-
Heat	203.0	186.7	25.3 kW	-	-	-
Heat	186.7	28.0	358.0 kW	-	-	-
Electricity	-	-	-	-	-	100 kW
H <sub>2</sub>	-	-	-	-	-	0.2 kg/s (28349.2 kW)
CO <sub>2</sub>	-	-	-	-	-	1.1 kg/s
CH <sub>4</sub>	-	-	-	-	0.4 kg/s (22193.6 kW)	-

The reference flows for the methanation unit are given for an incoming flow of electricity of 100 kW.

### B.2.3 CO<sub>2</sub> and CH<sub>4</sub> storage

The storage tanks are modelled using the following equations:

$$SL_{tank,t+1} = SL_{tank,t} + \eta^{ch} \cdot \dot{M}_{fuel,t}^+ - \frac{1}{\eta^{dch}} \cdot \dot{M}_{fuel,t}^- \quad (B.5a)$$

$$SL_{tank,t} = f_{tank,t} \quad \forall t \in T \quad (B.5b)$$

where  $SL_{tank,t}$  represents the storage level of the tank at time step  $t$ ,  $\dot{M}_{fuel,t}^+$  and  $\dot{M}_{fuel,t}^-$  the flow rates in and out of the unit at time step  $t$ , and  $\eta^{ch}, \eta^{dch}$  the charging and discharging efficiencies. CO<sub>2</sub> is stored in liquid form at atmospheric pressure and temperature (i.e. 1 bar, 25°C). Methane is also stored as a liquid, at the operating pressure of 1 bar and the corresponding temperature required for the liquid state, of -162°C.

### B.2.4 Municipal waste plant and steam network

The inorganic part of the waste (71% of the municipal solid waste [182]) is incinerated. The resulting heat and electricity streams corresponding to a mass flow rate of 1 kg/s of municipal solid waste are shown in table B.11. A lower heating value of 16710.78 kJ/kg is assumed [183].

Table B.11 – Streams for municipal waste plant.

Name	$T^{\text{in}}$ [°C]	$T^{\text{out}}$ [°C]	$\dot{Q}^-$ [kW]	$\dot{Q}^+$ [kW]	$\dot{m}^-$	$\dot{m}^+$
Heat	900	340	6406.9	-	-	-
Heat	180	60	1423.8	-	-	-
Heat	60	25	400.4	-	-	-
Electricity	-	-	-	-	249.2	-

The heat from the steam network can be used either for direct heating or for CO<sub>2</sub> vaporization. The reference streams used to model these HEs are given in table B.12 and B.13. A minimum temperature difference  $dT_{\text{min}} = 5.5^\circ\text{C}$  is assumed.

Table B.12 – Streams for CO<sub>2</sub> vaporization HE.

Name	$T^{\text{in}}$ [°C]	$T^{\text{out}}$ [°C]	$\dot{Q}^-$ [kW]	$\dot{Q}^+$ [kW]	$\dot{m}^-$	$\dot{m}^+$
Heat	25	20.5	-	186.4 kW	-	-
CO <sub>2</sub> <sup>vap</sup>	-	-	-	-	1 kg/s	-
CO <sub>2</sub> <sup>liq</sup>	-	-	-	-	-	1 kg/s

Table B.13 – Streams for direct heating supply HE.

Name	$T^{\text{in}}$ [°C]	$T^{\text{out}}$ [°C]	$\dot{Q}^-$ [kW]	$\dot{Q}^+$ [kW]	$\dot{m}^-$	$\dot{m}^+$
Heat	65	60.5	-	186.4 kW	-	-
CO <sub>2</sub> <sup>vap</sup>	-	-	-	-	1 kg/s	-
CO <sub>2</sub> <sup>liq</sup>	-	-	-	-	-	1 kg/s

In the steam network, steam is produced at very high pressure and distributed at multiple lower pressure levels. The pressure levels are selected to fit the production profiles of the municipal waste plant and P2G units. The parameters used to model the steam network are summarized in table B.14.

Table B.14 – Parameters for steam network.

Type	Header pressure [bar]	$T^{\text{superheat}}$ [°C]	Turbine
Production	120	100	yes
Distribution	30	2	yes
Distribution	10	2	yes
Distribution	5	2	yes
Distribution	2	2	no
Distribution	1	2	no
Distribution	0.2	2	no

### B.2.5 Central plant HP and geothermal wells

The central plant in winter is modelled either as a HP using a lake (at a constant temperature of 7.5°C) as the heat source and CO<sub>2</sub> as the refrigerant, or as geothermal wells. A summary of the parameters used for the central plant HP can be observed in table B.15 and a schematic flowsheet according to which it was modelled in figure B.1.

Table B.15 – Parameters for central plant HP.

Unit	HP central plant
$T^{\text{subcool}}$ [°C]	1
$T^{\text{superheat}}$ [°C]	2
$\eta^{\text{comp}}$ [–]	0.8
$dT^{\text{min, evap}}$ [°C]	5.5
$dT^{\text{min, cond}}$ [°C]	1

Similarly to the decentralized HPs, the reference flow of the central plant HP is  $\dot{Q}^{\text{cond}} = \dot{m}_{\text{CO}_2} \cdot L_{\text{CO}_2}^{\text{v}}$  and the electricity consumption of the compressor and the heat extracted at the evaporator are calculated solving the thermodynamic cycle. The reference streams of the unit are given in table B.16 for a mass flow of CO<sub>2</sub> of 1 kg/s. The COP of the central plant HP is constant throughout the year, at 15.1.

## B.2. Unit models: centralized energy conversion technologies

Table B.16 – Streams for central plant HP (winter).

Name	T <sup>in</sup> [°C]	T <sup>out</sup> [°C]	$\dot{Q}^-$ [kW]	$\dot{Q}^+$ [kW]	$\dot{m}^-$	$\dot{m}^+$
Heat evaporator	2	4	-	$186.4 \cdot \frac{COP-1}{COP}$ kW	-	-
Heat condenser	15	13	186.4 kW	-	-	-
Electricity	-	-	-	-	$186.4 \cdot \frac{1}{COP}$ kW	-
CO <sub>2</sub> <sup>vap</sup>	-	-	-	-	1 kg/s	-
CO <sub>2</sub> <sup>liq</sup>	-	-	-	-	-	1 kg/s

In order to compute the pumping energy required when geothermal wells are considered, first the pressure drop ( $\Delta P$ ) is calculated using the friction factor (ff), the fluid density ( $\rho$ ), the fluid velocity (v), the geothermal well height (h), and its hydrolic diameter ( $D^h$ ):

$$\Delta P = \frac{ff \cdot \rho \cdot v^2 \cdot h}{2 \cdot D^h} \quad (B.6)$$

The values of the different parameters can be found in table B.17 and details on the way they are found in [192]. The pumping energy is then calculated using the pressure drop, the mass flow of the fluid ( $\dot{m}$ ), its density, and an average geothermal pump efficiency ( $\eta^{\text{geoth}} = 0.8$  [193]):

$$\dot{m}_{\text{electricity}}^+ = \eta^{\text{geoth}} \frac{\Delta P \cdot \dot{m}_{\text{CO}_2}}{\rho} \quad (B.7)$$

Table B.17 – Parameters for geothermal wells.

Unit	Geothermal wells
ff [-]	0.018 (vapor )/ 0.019 (liquid)
$\rho^{\text{CO}_2}$ [kg/m <sup>3</sup> ]	154.122 (vapor )/ 840.842 (liquid)
v [m/s]	8.068 (vapor )/ 1.479 (liquid)
h [m]	333.333
$D^h$ [m]	0.032
$\eta^{\text{geoth}}$ [-]	0.8
$\Delta P$ [bar]	9.570 (vapor )/ 1.809 (liquid)

The reference streams of the unit are given in table B.18 for a mass flow of CO<sub>2</sub> of 1 kg/s.

Table B.18 – Streams for geothermal wells.

Name	$T^{\text{in}}$ [°C]	$T^{\text{out}}$ [°C]	$\dot{Q}^-$ [kW]	$\dot{Q}^+$ [kW]	$\dot{m}^-$	$\dot{m}^+$
Heat condenser	15	13	186.4 kW	-	-	-
Electricity	-	-	-	-	-	6.4 kW
CO <sub>2</sub> <sup>vap</sup>	-	-	-	-	1 kg/s	-
CO <sub>2</sub> <sup>liq</sup>	-	-	-	-	-	1 kg/s

The central plant in summer is modelled as a HE with the reference flow  $\dot{Q} = \dot{m}_{\text{CO}_2} \cdot L_{\text{CO}_2}^{\text{v}}$  and a minimum temperature difference  $dT_{\text{min}} = 5.5^\circ\text{C}$ . The reference streams of the unit are given in table B.19 for a mass flow of CO<sub>2</sub> of 1 kg/s.

Table B.19 – Streams for central plant HE (summer).

Name	$T^{\text{in}}$ [°C]	$T^{\text{out}}$ [°C]	$\dot{Q}^-$ [kW]	$\dot{Q}^+$ [kW]	$\dot{m}^-$	$\dot{m}^+$
Heat	7.5	9.5	-	186.4 kW	-	-
CO <sub>2</sub> <sup>vap</sup>	-	-	-	-	-	1 kg/s
CO <sub>2</sub> <sup>liq</sup>	-	-	-	-	1 kg/s	-

### B.3 Investment cost of energy conversion technologies

The fixed and variable IC parameters, as well as the reference flows for the different units can be found in table B.20.

Table B.20 – Parameters for IC.

Unit	$C^{\text{inv},1}$ [€]	$C^{\text{inv},2}$ [€/kW / €/m <sup>2</sup> ]	Attribute
HP space heating	5680	1240	$\dot{m}_{\text{electricity}}^+$ [kW]
HP hot water	5680	1240	$\dot{m}_{\text{electricity}}^+$ [kW]
REF cycle	5680	1240	$\dot{m}_{\text{electricity}}^+$ [kW]
HE air cooling	184	197	$A^{\text{HE}}$ [m <sup>2</sup> ]
PV panels	-	247	$A^{\text{PV}}$ [m <sup>2</sup> ]
SOEC-SOFC	-	4760	$\max(\dot{m}_{\text{electricity, SOEC}}^+, \dot{m}_{\text{electricity, SOFC}}^+) \text{ [kW]}$
HP CP (winter)	5680	1240	$\dot{m}_{\text{electricity}}^+$ [kW]
HE CP (summer)	184	197	$A^{\text{HE}}$ [m <sup>2</sup> ]
Geothermal wells	95468	-	-



### B.3. Investment cost of energy conversion technologies

---

The cost of the air cooling and (summer) central plant HEs is computed using a linearized version of the costs derived in [18].



## (Chapter 3)

### C.1 Heat transfer results

Tables show detailed selected results used to build figures 3.15, 3.18 and 3.21 (i.e. no heat sharing, no heat losses and every tenth solution from the industry permutations):

Table C.1 – Heat transfer solutions, Zurich.

Heat transfer SN [GWh]	Heat loss SN [GWh]	Heat transfer HW [GWh]	Heat loss HW [GWh]	Operating cost savings [%]	Env. impact savings [%]	Energy import savings [%]
0	0	0	0	-	-	-
844.7	357.9	402	152.4	11.6	17.2	20.9
832.7	338.1	401	139.1	12.1	18.2	21.6
1213.2	364.1	376.8	99.9	12.2	18.4	21.8
888	252.6	402.8	158.3	13	19.7	23
959	238.1	399.4	133.7	13.5	20.4	23.9
1266.9	278.1	372.1	84.9	13.6	20.6	24
937	194.1	400	157.7	13.8	20.9	24.3
1347.6	230.9	374.2	119	13.8	21.1	24.3
972	161.5	397.4	166.7	14.1	21.4	24.8
964.8	173	397.4	150.4	14.1	21.4	24.9
1359.4	205.9	376.8	117.7	14.2	21.7	24.8
992.4	110.7	396.8	153.9	14.9	22.9	26.2
1052.4	0	1002.8	0	18.4	28.4	32

## Appendix C. (Chapter 3)

Table C.2 – Heat transfer solutions, Munich.

Heat transfer SN [GWh]	Heat loss SN [GWh]	Heat transfer HW [GWh]	Heat loss HW [GWh]	Operating cost savings [%]	Env. impact savings [%]	Energy import savings [%]
0	0	0	0	-	-	-
164.7	62.2	3545.8	1992.8	7	8.7	10.1
713.4	81.1	2976.3	1781.6	7.8	9.7	11.2
710.7	79.3	2973.7	1731.5	8	10	11.5
552.3	20.5	3173.4	1790.5	8.1	10	11.5
546.5	17.2	3180.2	1782.2	8.1	10.1	11.6
410.8	68.5	3439.3	1676	8.3	10.4	11.9
1372.8	518.6	2061.7	1057.3	8.8	10.7	12.9
1918.8	535.8	1491.8	861	9.5	11.7	13.9
2702.5	528.9	1956.9	786.9	9.9	12.3	14.4
1807.5	107.7	1838.6	1016.2	10.8	13.6	15.5
1656.7	55	2031.9	1038.2	11	13.8	15.7
1643.3	46.2	2038.6	992.4	11.2	14.1	16
3902.2	0	1412.4	0	15.5	19.6	22.3

Table C.3 – Heat transfer solutions, London.

Heat transfer SN [GWh]	Heat loss SN [GWh]	Heat transfer HW [GWh]	Heat loss HW [GWh]	Operating cost savings [%]	Env. impact savings [%]	Energy import savings [%]
0	0	0	0	-	-	-
1632.2	1719.4	17105.6	13038.2	3.7	4.1	4.9
603.3	89	15937.6	11786.4	3.8	4.3	5
604	124.5	15894.8	11684.9	3.9	4.3	5.1
54.7	97.9	16453.7	11450.1	4.1	4.6	5.3
603.2	84.6	18850.2	14070.1	4.3	4.9	5.7
603.3	89	15928.4	10264.3	5	5.6	6.6
54.7	97.9	16577.3	9611.8	5.6	6.4	7.4
430.6	81.8	18836.2	11722.6	6	6.9	8
430.6	86.2	18994.5	10372.3	7.1	8.3	9.5
5767.2	361.2	10635.7	3746.8	9.8	11.4	13.2
6745	1274.6	12386.5	4960.4	10	11.7	13.6
5767.2	361.2	13240.6	5434.5	10.5	12.3	14.2
6626.3	0	15493	0	15.1	17.8	20.4

### C.1.1 Steam network

In the steam network, steam is produced at high pressure and distributed at multiple lower pressure levels. The pressure levels are selected to fit the production profiles of the industrial plants. The parameters used to model the steam network are summarized in table C.4.

Table C.4 – Parameters for steam network.

Type	Header pressure [bar]	T <sup>superheat</sup> [°C]	Turbine
Production	45	110	yes
Distribution	24	5	yes
Distribution	8	5	yes
Distribution	4	5	no
Distribution	2	5	no
Distribution	1	5	no

### C.1.2 Hot water loop

Two hot water loops are considered, one at 35°- 45°C for space heating and one at 70°- 90°C for hot water. The corresponding heat losses were computed assuming the following parameters [190]:

Table C.5 – Parameters for hot water loop.

Parameter	Symbol	Value 35° / 45°C & 70° / 90°C	Unit
specific heat	c <sub>p</sub>	4.1806	kJ/(kg · K)
insulation thickness	D <sup>i</sup>	0.1	m
density	ρ	994 / 990 & 977 / 965	kg/m <sup>3</sup>
velocity	v	2.5	m/s

The diameter of the pipes (D<sup>p</sup>) is computed according to:

$$\frac{\dot{m} \cdot \rho}{v} = \frac{\dot{V}}{v} = \frac{\pi \cdot D^p}{4} \quad (C.1)$$

with  $\dot{m}$  and  $\dot{V}$  the mass/volumetric flows of the hot water in the respective pipe:

$$\dot{m} = \frac{\dot{Q}}{c_p \cdot \Delta T} \quad (C.2)$$

## C.2 Industrial symbiosis heat flows

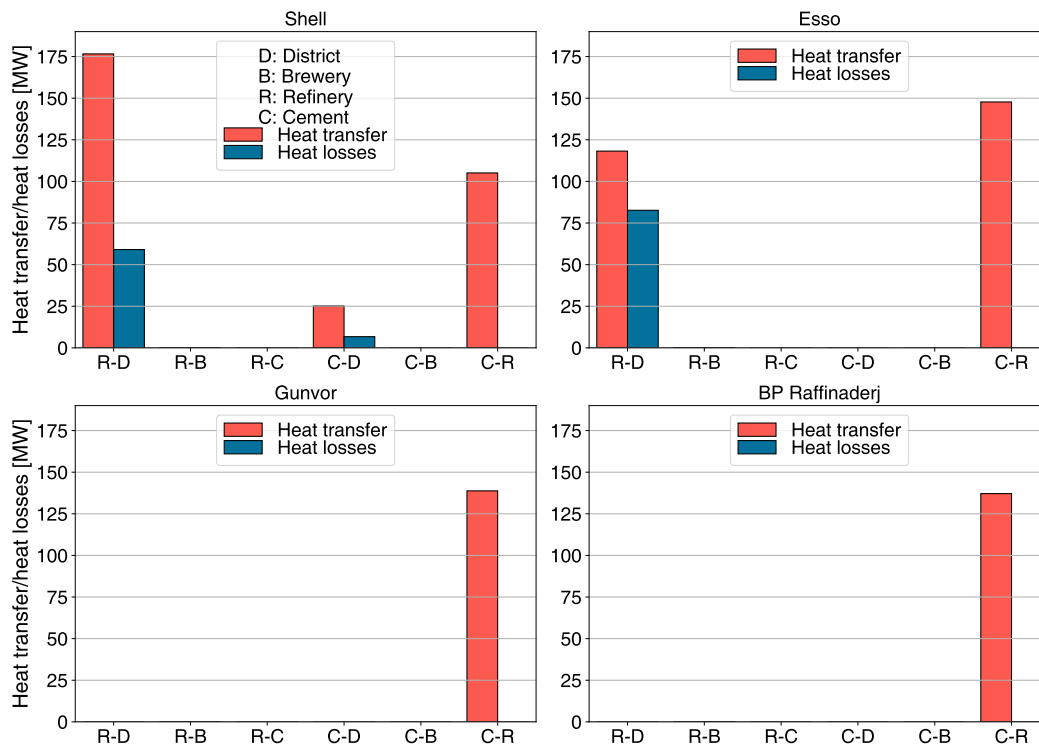


Figure C.1 – Heat transfer/losses integration of refineries considered individually.

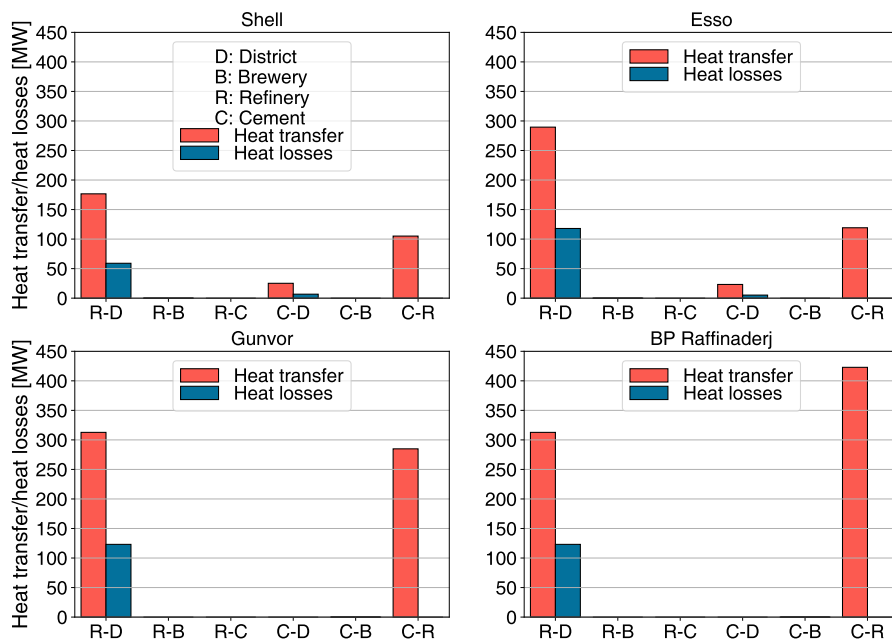


Figure C.2 – Heat transfer/losses integration of refineries added sequentially.

## (Chapter 4)

### D.1 Unit Models at Building Level

#### D.1.1 Building

The thermal behavior of the building is described using a first order dynamic 1R1C model, as illustrated in Figure D.1. The entire construction is aggregated into a single capacity  $C_b$  while considering a single temperature node  $T_b$  [187, 194]. Equation (D.1) highlights the corresponding energy balance, where  $T_b$  denotes the internal temperature,  $T^{\text{ext}}$  the external temperature,  $U_b^{\text{ext}} = 1/R_b^{\text{ext}}$  the combined thermal transfer coefficient,  $\Phi_b^{\text{sun+o}}$  the stochastic gains from solar and occupancy sources and  $\dot{Q}_b^+$  the heat supplied by the energy system. In the case of partially non-residential dwellings with cooling requirements, a second zone is added to the model and connected through the internal insulation resistance  $R_b^{\text{int}}$ .  $T^{\text{min/max}}$  in Equation (D.2) define the comfort tolerance on the internal temperature.

$$C_b \cdot (T_{b,p,t+1} - T_{b,p,t}) = U_b^{\text{ext}} \cdot (T_{p,t}^{\text{ext}} - T_{b,p,t}) + \Phi_{b,p,t}^{\text{sun+o}} + \dot{Q}_{b,p,t}^+ \quad \forall p \in \mathbf{P}, t \in \mathbf{TOP} \quad (\text{D.1})$$

$$T_{b,p,t}^{\text{min}} \leq T_{b,p,t} \leq T_{b,p,t}^{\text{max}} \quad \forall p \in \mathbf{P}, t \in \mathbf{TOP} \quad (\text{D.2})$$

#### D.1.2 Boiler

The natural gas Boiler is described using a static system model formulation (Equations (7a)–(7c)) and is implemented as an auxiliary heating utility, the sizing dimension being the thermal power output. The main parameter required to model this unit, the thermal efficiency ( $\eta_{\text{BOI}}$ ), is listed in Table D.1.

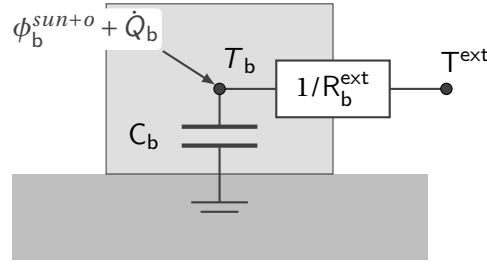


Figure D.1 – 1R1C building model.

Table D.1 – Parameter data.

Parameter	Value	Unit	Ref.
$\eta_{BOI}$	0.98	[-]	[179]

### D.1.3 Electrical heater

As with the Boiler unit, the electrical heater is also described using a static system model formulation (Equations (7a)–(7c)) and implemented as an auxiliary heating utility, the sizing dimension being the thermal power output. The main parameter required to model this unit, the thermal efficiency ( $\eta_{ELH}$ ), is listed in Table D.2.

Table D.2 – Parameter data (ELH).

Parameter	Value	Unit	Ref.
$\eta_{ELH}$	0.98	[-]	estimate

### D.1.4 Heat Pumps

The air-source heat pump unit (AHP) is described using a static system formulation (Equations (7a)–(7c)), the sizing dimension being the electrical power input. The conversion efficiency (Equations (D.3) and (D.4)) is determined using the ideal coefficient of performance and the second law efficiency  $\eta$ , which accounts for the irreversibilities in the different cycle components (e.g., compressor). In order to avoid non-linearities coming from the variable supply temperature, the generated heat load is discretized into  $n_s = |\mathbf{S}_{AHP}|$  streams  $s$ . When considering different heat sources (e.g., water-source heat pumps) in the problem formulation, a similar model definition can be applied, the solely modification being the source temperature (e.g.,  $T_{p,t}^{\text{water}}$ ) and the respective second-law efficiency  $\eta$ . The values of the parameters considered for the air-water heat pump are given in Table



## D.1. Unit Models at Building Level

D.3 and for the corresponding refrigeration cycle (VAC) in Table D.4.

$$\text{COP}_{\text{AHP},s,p,t} = \frac{T_{\text{AHP},s}^{\text{sink}}}{T_{\text{AHP},s}^{\text{sink}} - T_{p,t}^{\text{source}}} \quad \forall s \in \mathbf{S}_{\text{AHP}}, p \in \mathbf{P}, t \in \mathbf{TOP} \quad (\text{D.3})$$

$$\dot{q}_{\text{AHP},s,p,t}^- = \eta_{\text{AHP},s,p,t} \cdot \text{COP}_{\text{AHP},s,p,t} \quad \forall s \in \mathbf{S}_{\text{AHP}}, p \in \mathbf{P}, t \in \mathbf{TOP} \quad (\text{D.4})$$

Table D.3 – Default parameters values for the AHP second-law efficiency and part-load limit, evaluated from [2].

	Par.	$T^{\text{sink}}$ [°C]	$T^{\text{source}}$ [°C]									
			−20	−15	−10	−7	−2	2	7	10	15	20
AHP	$\eta$	35	0	0.464	0.458	0.458	0.469	0.462	0.435	0.416	0.37	0.307
		45	0	0.445	0.463	0.464	0.46	0.446	0.439	0.436	0.43	0.396
		55	0	0	0	0.421	0.423	0.416	0.439	0.436	0.412	0.395
	$\dot{m}_{\text{electricity}}^{+, \text{max}}$	35	0	0.62	0.65	0.65	0.65	0.65	0.68	0.68	0.68	0.68
		45	0	0.74	0.74	0.74	0.76	0.79	0.82	0.82	0.79	0.79
		55	0	0	0	0.91	0.94	0.97	0.97	0.97	1	1

Table D.4 – Default parameters values for the VAC second-law efficiency and part-load limit, evaluated from [2].

	Par.	$T^{\text{sink}}$	$T^{\text{source}} \text{ [}^{\circ}\text{C]}$					
			20	25	30	35	40	45
VAC	$\eta$	13	0.103	0.159	0.198	0.219	0.249	0.224
		15	0.076	0.14	0.181	0.243	0.243	0.224
		18	0.033	0.101	0.146	0.209	0.209	0.218
		22	0	0.005	0.106	0.184	0.184	0.215
	$\dot{m}_{\text{electricity}}^{+, \text{max}}$	13	0.71	0.78	0.86	0.95	0.91	1
		15	0.73	0.78	0.87	0.95	0.91	0.96
		18	0.73	0.8	0.89	0.96	0.93	0.89
		22	0.75	0.82	0.91	1	0.95	0.8

### D.1.5 Storage Units

#### D.1.5.1 Battery stack (BAT)

Stationary batteries are described using a single state dynamic model, the sizing dimension being the electrical energy stored. The model accounts for the system self-discharging rate ( $\sigma$ ) as well

as the charging and discharging losses ( $\eta$ ). To limit any premature degradation of the stack, the minimum ( $SL_{BAT}^{\min}$ ) and maximum ( $SL_{BAT}^{\max}$ ) battery storage levels are fixed (Equations (D.5) and (D.6)). The parameters used to model this unit are listed in Table D.5.

$$f_{BAT,p,t} \geq SL_{BAT}^{\min} \cdot f_{BAT} \quad \forall p \in \mathbf{P}, t \in \mathbf{TOP} \quad (D.5)$$

$$f_{BAT,p,t} \leq SL_{BAT}^{\max} \cdot f_{BAT} \quad \forall p \in \mathbf{P}, t \in \mathbf{TOP} \quad (D.6)$$

Table D.5 – Parameter data (BAT).

Parameter	Value	Unit	Ref.
$\eta^{\text{ch}}$	0.9	[-]	[175]
$\eta^{\text{dch}}$	0.9	[-]	[175]
$\sigma$	0	[-]	[175]
$SL_{BAT}^{\max}$	0.8	[-]	[195]
$SL_{BAT}^{\min}$	0.2	[-]	[195]

#### D.1.5.2 Heat storage tank (HST)

The thermal energy storage tanks are described through a single state, first order dynamic model formulation, the sizing dimension being the unit volume. The minimum storage level  $SL^{\min}$  is set as the current building return temperature  $T_{b,p,t}^{\text{h,r}}$  during space heating periods, while the maximum operating temperature  $T_{HST}^{\max}$  is defined as the lowest value between the heat pump operating limit and the nominal supply temperature of the heating system ( $T_b^{\text{h,s}}$ ). The required parameters include the tank diameter  $D_{HST}$ , the specific heat loss rate  $U_{HST}$  as well as the charging and discharging efficiencies  $\eta$ . The unit is consequently added into the heat cascade formulation through the single charging (cold) and discharging (hot) streams as defined in Equations (D.7)–(D.10). The parameter values are given in Table D.6.

$$\sigma_{HST} = \frac{4 \cdot U_{HST}}{D_{HST}} \cdot (T_{HST}^{\max} - T_{b,p,t}^{\text{h,r}}) \quad \forall p \in \mathbf{P}, t \in \mathbf{TOP} \quad (D.7)$$

$$\kappa_{HST} = \frac{4 \cdot U_{HST}}{D_{HST}} \cdot (T_{b,p,t}^{\text{h,r}} - T^{\text{amb}}) \quad \forall p \in \mathbf{P}, t \in \mathbf{TOP} \quad (D.8)$$

## D.2. Unit Models at City Level

$$\dot{q}_{\text{HST},s,p,t}^+ = c_p \cdot \rho \cdot (T_{\text{HST}}^{\max} - T_{b,p,t}^{\text{h},r}) \quad \forall p \in \mathbf{P}, t \in \mathbf{TOP} \quad (\text{D.9})$$

$$\dot{q}_{\text{HST},s,p,t}^- = c_p \cdot \rho \cdot (T_{\text{HST}}^{\max} - T_{b,p,t}^{\text{h},r}) \quad \forall p \in \mathbf{P}, t \in \mathbf{TOP} \quad (\text{D.10})$$

Table D.6 – Parameter data (HST).

Parameter	Value	Unit	Ref.
$c_p$	4.186	[kJ/(kg · K)]	estimate
$\rho$	1000	[kg/m <sup>3</sup> ]	estimate
$\eta^{\text{ch}}$	0.99	[-]	estimate
$\eta^{\text{dch}}$	0.99	[-]	estimate
$D_{\text{HST}}$	0.98	[m]	estimate
$U_{\text{HST}}$	0.0013	[kW/m <sup>2</sup> ]	[179]

## D.2 Unit Models at City Level

### D.2.1 PV Panels

The PV panels are modeled as described in [187], with  $A^{\text{PV}}$  the PV area,  $\eta^{\text{PV}}$  the PV efficiency,  $I$  the irradiation of the sun,  $T^{\text{PV}}$  the PV temperature,  $U^{\text{glass}}$  the thermal transmission coefficient,  $T^{\text{amb}}$  the ambient temperature, and  $f^{\text{glass}}$  the factor denoting the portion of the solar irradiation passing through the PV glass:

$$\dot{m}_{\text{PV,electricity}}^- = A^{\text{PV}} \cdot \eta^{\text{PV}} \cdot I \quad (\text{D.11a})$$

$$\eta^{\text{PV}} = \eta^{\text{PV,ref}} - \eta^{\text{PV,var}} \cdot (T^{\text{PV}} - T^{\text{PV,ref}}) \quad (\text{D.11b})$$

$$T^{\text{PV}} = \frac{U^{\text{glass}} \cdot T^{\text{amb}}}{U^{\text{glass}} - \eta^{\text{PV,var}} \cdot I} + \frac{I \cdot (f^{\text{glass}} - \eta^{\text{PV,ref}} - \eta^{\text{PV,var}} \cdot T^{\text{PV,ref}})}{U^{\text{glass}} - \eta^{\text{PV,var}} \cdot I} \quad (\text{D.11c})$$

The different parameters assumed are given in Table D.7 [187] and the reference stream for  $A^{\text{PV}} = 100 \text{ m}^2$  and  $I = 100 \text{ W/m}^2$  is given in Table D.8.

Table D.7 – Parameters for PV panels.

Parameter	Value	Unit
$T^{\text{amb}}$	288	K
$T^{\text{PV, ref}}$	298	K
$U^{\text{glass}}$	29.1	W/(m <sup>2</sup> ·K)
$f^{\text{glass}}$	0.9	–
$\eta^{\text{PV, ref}}$	0.14	–
$\eta^{\text{PV, var}}$	0.001	1/K

Table D.8 – Streams for PV panel.

Type	$T^{\text{in}}$ [°C]	$T^{\text{out}}$ [°C]	$\dot{Q}$	$\dot{m}^-$	$\dot{m}^+$
Electricity	-	-	-	1.66 kW	-

### D.2.2 SOEC-SOFC Co-Generation and Methanation

The co-generation SOFC-GT unit is modeled according to [87] and the co-generation SOEC unit according to [88]. A list of the reference streams in the different units are given in Tables D.9–D.11.

Table D.9 – Streams for SOEC unit.

Type	$T^{\text{in}}$ [°C]	$T^{\text{out}}$ [°C]	$\dot{Q}$	$\dot{m}^-$	$\dot{m}^+$
Heat	91	58	3.05 kW	-	-
Heat	58	27	1.66 kW	-	-
Electricity	-	-	-	-	100 kW
H <sub>2</sub> O	-	-	-	-	5.98 g/s
H <sub>2</sub>	-	-	-	0.67 g/s (94.21 kW)	-

Table D.10 – Streams for SOFC-GT unit.

Type	$T^{\text{in}}$ [°C]	$T^{\text{out}}$ [°C]	$\dot{Q}$	$\dot{m}^-$	$\dot{m}^+$
Heat	648.8	260.0	16.28 kW	-	-
Heat	109.8	35.2	9.44 kW	-	-
Heat	35.2	30.2	1.44 kW	-	-
Electricity	-	-	-	100 kW	-
CH <sub>4</sub>	-	-	-	-	-2.41 g/s (133.48 kW)
CO <sub>2</sub>	-	-	-	6.60 g/s	-

The reference flows for the SOEC unit are given for an incoming flow of electricity of 100 kW.

## D.2. Unit Models at City Level

Table D.11 – Streams for methanation unit.

Type	T <sup>in</sup> [°C]	T <sup>out</sup> [°C]	$\dot{Q}$	$\dot{m}^-$	$\dot{m}^+$
Heat	625.4	507.3	138.4 kW	-	-
Heat	507.3	507.1	0.3 kW	-	-
Heat	507.1	233.0	585.3 kW	-	-
Heat	233.0	228.0	9.3 kW	-	-
Heat	228.0	227.0	0.7 kW	-	-
Heat	227.0	215.0	12.7 kW	-	-
Heat	215.0	203.0	27.1 kW	-	-
Heat	203.0	186.7	25.3 kW	-	-
Heat	186.7	28.0	358.0 kW	-	-
Electricity	-	-	-	100 kW	-
H <sub>2</sub>	-	-	-	-	0.2 kg/s (28349.2 kW)
CO <sub>2</sub>	-	-	-	-	1.1 kg/s
CH <sub>4</sub>	-	-	-	0.4 kg/s (22193.6 kW)	-

The electricity to hydrogen efficiency is computed using the HHV of H<sub>2</sub> of 141,746 kJ/kg [188]:

$$\eta = \frac{\dot{m}_{\text{H}_2}^- \cdot \text{HHV}^{\text{H}_2}}{\dot{m}_{\text{electricity}}^+} = 94.2\% \quad (\text{D.12})$$

The reference flows for the SOFC-GT unit are given for an outgoing flow of electricity of 100 kW. The electrical and thermal efficiencies are calculated using the HHV of CH<sub>4</sub> of 55,484 kJ/kg [188]:

$$\eta^{\text{el}} = \frac{\dot{m}_{\text{electricity}}^-}{\dot{m}_{\text{CH}_4}^+ \cdot \text{HHV}^{\text{CH}_4}} = 74.9\% \quad (\text{D.13a})$$

$$\eta^{\text{th}} = \frac{\sum_{k \in \mathbf{K}} \dot{Q}_{\text{SOFC}}}{\dot{m}_{\text{CH}_4}^+ \cdot \text{HHV}^{\text{CH}_4}} = 20.3\% \quad (\text{D.13b})$$

The reference flows for the methanation unit are given for an incoming flow of electricity of 100 kW.

### D.2.3 Steam Network

In the steam network, steam is produced at very high pressure and distributed at multiple lower pressure levels. The pressure levels are selected to fit the production profiles of the P2G units. The parameters used to model the steam network are summarized in Table D.12.

Table D.12 – Parameters for steam network.

Type	Header pressure [bar]	T <sup>superheat</sup> [°C]	Turbine
Production	120	100	yes
Distribution	30	2	yes
Distribution	10	2	yes
Distribution	5	2	yes
Distribution	2	2	no
Distribution	1	2	no
Distribution	0.2	2	no

#### D.2.4 CO<sub>2</sub> and CH<sub>4</sub> Storage

The storage tanks are modeled using the following equations:

$$SL_{tank,t+1} = SL_{tank,t} + \eta^{ch} \cdot \dot{M}_{fuel,t}^+ - \frac{1}{\eta^{dch}} \cdot \dot{M}_{fuel,t}^- \quad (D.14a)$$

$$SL_{tank,t} = f_{tank,t} \quad \forall t \in \mathbf{T} \quad (D.14b)$$

where  $SL_{tank,t}$  represents the storage level of the tank at time step  $t$ ,  $\dot{M}_{fuel,t}^+$  and  $\dot{M}_{fuel,t}^-$  the flow rates in and out of the unit at time step  $t$ , and  $\eta^{ch}, \eta^{dch}$  the charging and discharging efficiencies. CO<sub>2</sub> is stored in liquid form at atmospheric pressure and temperature (i.e., 1 bar, 25 °C). Methane is also stored as a liquid, at the operating pressure of 1 bar and the corresponding temperature required for the liquid state, of −162 °C.

#### D.2.5 Central Plants

The central plant in winter is modeled as a HP using a lake (at a constant temperature of 7.5 °C) as the heat source and CO<sub>2</sub> as the refrigerant. A summary of the parameters used for the central plant HP can be observed in table D.13.

Table D.13 – Parameters for central plant HP.

Unit	HP Central Plant
T <sup>subcool</sup> [°C]	1
T <sup>superheat</sup> [°C]	2
$\eta^{comp}$ [–]	0.8
dT <sup>min, evap</sup> [°C]	5.5
dT <sup>min, cond</sup> [°C]	1

### D.3. Heat Distribution Cost

The reference flow of the central plant HP is  $\dot{Q}^{\text{cond}} = \dot{m}_{\text{CO}_2} \cdot L_{\text{CO}_2}^{\text{v}}$  and the electricity consumption of the compressor and the heat extracted at the evaporator are calculated solving the thermodynamic cycle. The reference streams of the unit are given in Table D.14 for a mass flow of CO<sub>2</sub> of 1 kg/s. The COP of the central plant HP is constant throughout the year, at 15.1.

Table D.14 – Streams for central plant HP (winter).

Type	T <sup>in</sup> [°C]	T <sup>out</sup> [°C]	$\dot{Q}$	$\dot{m}^-$	$\dot{m}^+$
Heat evaporator	2	4	$186.4 \cdot \frac{\text{COP}-1}{\text{COP}}$ kW	-	-
Heat condenser	15	13	186.4 kW	-	-
Electricity	-	-	-	-	$186.4 \cdot \frac{1}{\text{COP}}$ kW
CO <sub>2</sub> <sup>vap</sup>	-	-	-	1 kg/s	-
CO <sub>2</sub> <sup>liq</sup>	-	-	-	-	1 kg/s

The central plant in summer is modeled as a HE with the reference flow  $\dot{Q} = \dot{m}_{\text{CO}_2} \cdot L_{\text{CO}_2}^{\text{v}}$  and a minimum temperature difference  $dT_{\text{min}} = 5.5^\circ\text{C}$ . The reference streams of the unit are given in Table D.15 for a mass flow of CO<sub>2</sub> of 1 kg/s.

Table D.15 – Streams for central plant HE (summer).

Type	T <sup>in</sup> [°C]	T <sup>out</sup> [°C]	$\dot{Q}$	$\dot{m}^-$	$\dot{m}^+$
Heat	7.5	9.5	186.4 kW	-	-
CO <sub>2</sub> <sup>vap</sup>	-	-	-	-	1 kg/s
CO <sub>2</sub> <sup>liq</sup>	-	-	-	1 kg/s	-

#### D.2.6 Investment Cost of Energy Conversion Technologies

The fixed and variable IC parameters, as well as the reference flows for the different units can be found in Table D.16.

### D.3 Heat Distribution Cost

The heat distribution cost of the networks is calculated using the formulation of [49]. First, the length of the network ( $L^{\text{DHN}}$ ) is calculated based on the number of buildings ( $N_b$ ), the land surface area ( $A^{\text{land}}$ ) and a correlation coefficient ( $K$ ) [49]:

$$L^{\text{DHN}} = 2 \cdot (N_b - 1) \cdot K \cdot \sqrt{\frac{A^{\text{land}}}{N_b}} \quad (\text{D.15})$$

Table D.16 – Parameters for IC.

Unit	$C^{\text{inv},1}$ [€]	$C^{\text{inv},2}$ [€/kW/€/m <sup>2</sup> ]	Attribute
Boiler	3990	110	$\dot{Q}^-$ [kW]
Electrical heater	968	13	$\dot{Q}^-$ [kW]
Heat pumps/Ref cycle	10224	2232	$\dot{m}_{\text{electricity}}^+$ [kW]
Battery stack	825	1290	$\max(f_{\text{BAT},p,t})$ [kW]
Heat storage tank	1421	1945	V [kW]
Domestic hot water tank	496	10248	V [kW]
PV panels	-	247	$A^{\text{PV}}$ [m <sup>2</sup> ]
SOEC-SOFC	-	4760	$\max(\dot{m}_{\text{electricity}}^+, \text{SOEC}, \dot{m}_{\text{electricity}}^+, \text{SOFC})$ [kW]
HP CP (winter)	5680	1240	$\dot{m}_{\text{electricity}}^+$ [kW]
HE CP (summer)	184	197	$A^{\text{HE}}$ [m <sup>2</sup> ]

And for each segment (between each two buildings):

$$L_k^{\text{DHN}} = \frac{L^{\text{DHN}}}{N_b} \quad (\text{D.16})$$

Next, the mass flow in the pipes is computed using the maximum heat flow in the pipe  $\dot{Q}^{\text{DHN}}$  and the specific heat flows  $q_{\text{water}} = c_{p, \text{water}}(T_s - T_r)$ ,  $q_{\text{CO}_2} = L^V$ :

$$\dot{m}^{\text{DHN}, \max} = \frac{\dot{Q}^{\text{DHN}}}{q^{\text{DHN}}} \quad (\text{D.17})$$

And for each segment ( $k$ ):

$$\dot{m}_k^{\text{DHN}} = \frac{\dot{Q}^{\text{DHN}} \cdot (N_b - k + 1)}{N_b \cdot q^{\text{DHN}}} \quad (\text{D.18})$$

Then, the diameter of the pipes ( $D^{\text{DHN}}$ ) is calculated using the mass flow  $\dot{m}^{\text{DHN}}$ , the sizing velocity of the fluids ( $v$ ) [18] and the density of the fluids ( $\rho$ ):

$$D_k^{\text{DHN}} = \sqrt{\frac{4 \cdot \dot{m}_k^{\text{DHN}}}{\pi \cdot v \cdot \rho}} \quad (\text{D.19})$$

Finally, the investment cost ( $C^{\text{inv}}$ ) of the networks is computed by summing up the different seg-



#### D.4. RegBL Database Parameter Names

ments, using the cost coefficients  $c_1$  and  $c_2$  [18], an interest rate  $i = 5\%$  and a lifetime  $l_t = 60$  years [49]:

$$f^{\text{an, DHN}} = \frac{(i + 1)^{l_t} - 1}{i \cdot (i + 1)^{l_t}} \quad (\text{D.20})$$

$$C^{\text{inv}} = \sum_{k=1}^{N_b-1} \frac{L_k^{\text{DHN}} (c_1 \cdot D_k^{\text{DHN}} + c_2)}{f^{\text{an, DHN}}} \quad (\text{D.21})$$

The values of the parameters present in the equations above can be found in Table D.17.

Table D.17 – Network cost parameters.

Parameter	Unit	Value (CO <sub>2</sub> network)	Value (H <sub>2</sub> O network)
$N_b$	[-]	11903	11903
$K$	[-]	0.23	0.23
$A^{\text{land}}$	[m <sup>2</sup> ]	15785286	15785286
$L^{\text{DHN}}$	[km]	3630.3	3630.3
$q^{\text{DHN}}$	[kJ/kg]	186.4	18.8
$\dot{Q}^{\text{DHN}}$	[MW]	2938.1	2942.7
$\dot{m}^{\text{DHN, max}}$	[t/s]	15.8	156.5
$v$	[m <sup>2</sup> /s]	3 (liquid), 6 (vapor )	3
$\rho$	[kg/m <sup>3</sup> ]	837.7 (liquid), 160.9 (vapor )	1000
$D^{\text{DHN, max}}$	[m]	4 (liquid), 10.4 (vapor )	33.2
$c_1$	[€/m <sup>2</sup> ]	5670	5670
$c_2$	[€]	613	613
$i$	[-]	0.06	0.06
$l_t$	[-]	60	60
$C^{\text{inv}}$	[M€/y]	153.5	330.6

#### D.4 RegBL Database Parameter Names

Table D.18 – RegBL database corresponding parameter notations.

Parameter Description	Notation (This Paper)	Notation (RegBL)
Building category	-	GKAT
Building class	-	GKLAS
Building footprint area	$A_b$	GAREA
Building number of floors	$N^{\text{floors}}$	GASTW
Building rooftop area	$A_b^{\text{roof}}$	FLAECHE
Building average solar irradiation	$I_b$	MSTRAHLUNG

## D.5 Energy Service Demand of Different Building Categories



Figure D.2 – Hourly specific energy service demand of residential SFH buildings.

Table D.19 – Yearly specific energy service demand of residential SFH buildings.

Building renovation stage	Space heating [kWh/m²]	Air cooling [kWh/m²]	Dom. hot water [kWh/m²]	Electricity [kWh/m²]
Existing	80.3	0.0	13.6	18.2
New	44.0	0.0	13.6	18.2
Renovated	55.9	0.0	13.6	18.2

## D.5. Energy Service Demand of Different Building Categories

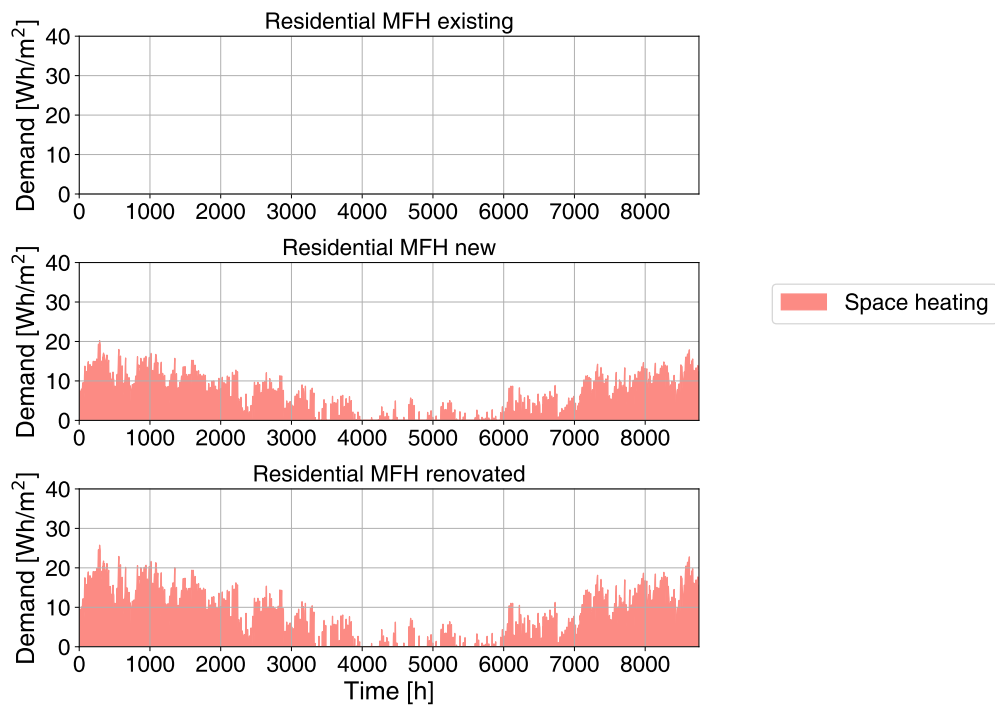


Figure D.3 – Hourly specific energy service demand of residential MFH buildings.

Table D.20 – Yearly specific energy service demand of residential MFH buildings.

Building renovation stage	Space heating [kWh/m <sup>2</sup> ]	Air cooling [kWh/m <sup>2</sup> ]	Dom. hot water [kWh/m <sup>2</sup> ]	Electricity [kWh/m <sup>2</sup> ]
Existing	80.3	0.0	17.8	18.4
New	44.0	0.0	17.8	18.4
Renovated	55.9	0.0	17.8	18.4

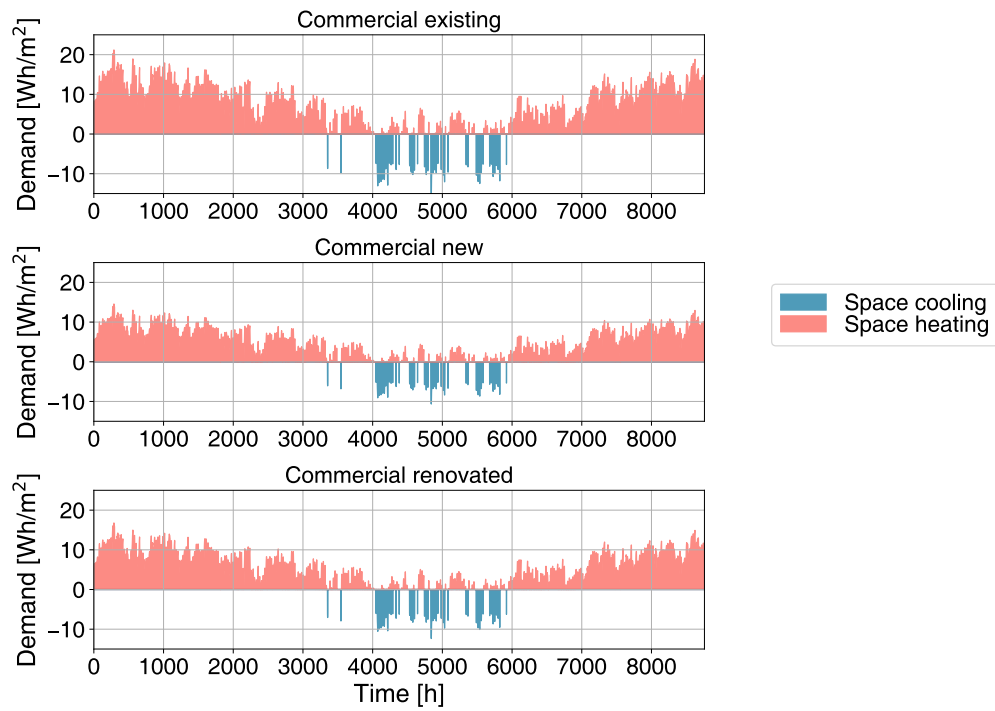


Figure D.4 – Hourly specific energy service demand of commercial buildings.

Table D.21 – Yearly specific energy service demand of commercial buildings.

Building renovation stage	Space heating [kWh/m <sup>2</sup> ]	Air cooling [kWh/m <sup>2</sup> ]	Dom. hot water [kWh/m <sup>2</sup> ]	Electricity [kWh/m <sup>2</sup> ]
Existing	49.2	3.3	1.8	114.4
New	33.5	2.3	1.8	114.4
Renovated	38.4	2.7	1.8	114.4

## D.5. Energy Service Demand of Different Building Categories

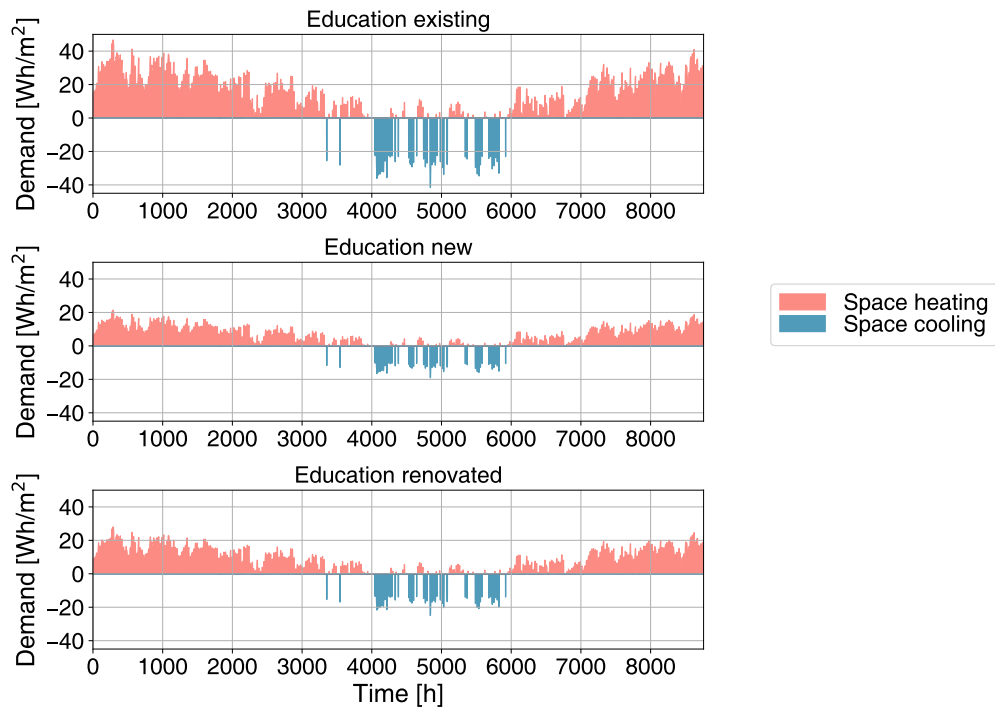


Figure D.5 – Hourly specific energy service demand of education buildings.

Table D.22 – Yearly specific energy service demand of education buildings.

Building renovation stage	Space heating [kWh/m <sup>2</sup> ]	Air cooling [kWh/m <sup>2</sup> ]	Dom. hot water [kWh/m <sup>2</sup> ]	Electricity [kWh/m <sup>2</sup> ]
Existing	91.8	9.7	4.5	23.8
New	41.9	4.4	4.5	23.8
Renovated	55.1	5.8	4.5	23.8

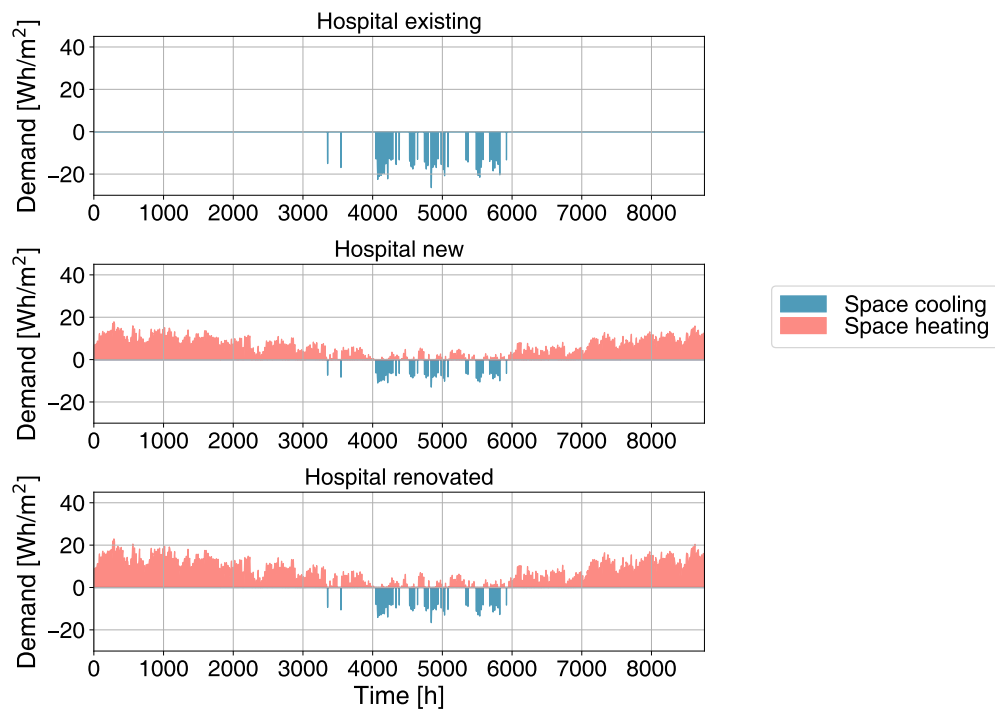


Figure D.6 – Hourly specific energy service demand of hospital buildings.

Table D.23 – Yearly specific energy service demand of hospital buildings.

Building renovation stage	Space heating [kWh/m <sup>2</sup> ]	Air cooling [kWh/m <sup>2</sup> ]	Dom. hot water [kWh/m <sup>2</sup> ]	Electricity [kWh/m <sup>2</sup> ]
Existing	83.5	5.8	34.1	34.0
New	41.2	2.8	34.1	34.0
Renovated	53.3	3.6	34.1	34.0

## D.5. Energy Service Demand of Different Building Categories

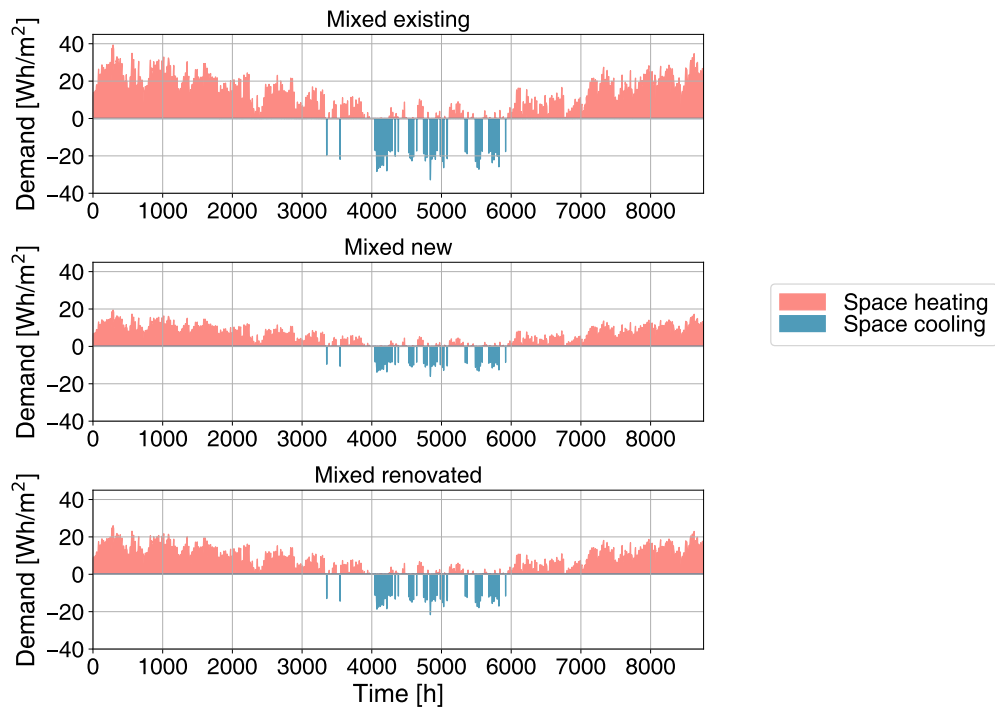


Figure D.7 – Hourly specific energy service demand of mixed buildings.

Table D.24 – Yearly specific energy service demand of mixed buildings.

Building renovation stage	Space heating [kWh/m <sup>2</sup> ]	Air cooling [kWh/m <sup>2</sup> ]	Dom. hot water [kWh/m <sup>2</sup> ]	Electricity [kWh/m <sup>2</sup> ]
Existing	81.6	7.5	11.9	28.4
New	40.9	3.7	11.9	28.4
Renovated	54.1	4.9	11.9	28.4

Table D.25 – Heat signature coefficients for all building types and ages.

Building Type	Building Age	k1 [kW/(m <sup>2</sup> ·°C)]	k2 [kW/m <sup>2</sup> ]	T <sub>base, h</sub> [°C]	T <sub>base, c</sub> [°C]
Residential SFH	existing	–1.52	23.59	15.52	-
	new	–0.83	12.91	15.55	-
	renovated	–1.06	16.43	15.5	-
Residential MFH	existing	–1.52	23.59	15.52	-
	new	–0.83	12.91	15.55	-
	renovated	–1.06	16.43	15.5	-
Administrative	existing	–1.87	26.51	14.18	25
	new	–0.8	11.41	14.26	25
	renovated	–1.15	16.29	14.17	25
Commercial	existing	–0.84	13.81	16.44	25
	new	–0.58	9.47	16.33	25
	renovated	–0.67	10.89	16.25	25
Education	existing	–2.03	28.84	14.21	25
	new	–0.93	13.19	14.18	25
	renovated	–1.22	17.32	14.2	25
Hospital	existing	–1.44	23.54	16.34	25
	new	–0.71	11.62	16.37	25
	renovated	–0.91	14.96	16.44	25
Mixed	existing	–1.86	27.83	14.98	25
	new	–0.82	12.31	15.05	25
	renovated	–1.1	16.37	14.94	25

## D.6 Results from Parallel Coordinates

This section presents the detailed results presented schematically in Figures 4.16 and 4.17.



Table D.26 – Detailed results for Figure 4.16.

Inv. cost M€/y	Op. cost M€/y	CO <sub>2</sub> emissions kt <sub>CO<sub>2</sub></sub> /y)	Buildings high IC -	Buildings low IC -	CO <sub>2</sub> activation -	Self sufficiency %	PV market M€/y	HP market M€/y
1.61	1.49	3.06	0	46121	0	0	0.00	0.55
5.53	0.84	1.77	604	45517	1	0	1.78	1.62
9.44	0.56	1.13	10164	35957	2	0	5.36	2.40
12.38	0.44	0.92	9088	37033	3	24	7.61	2.39
14.03	0.35	0.76	8696	37425	4	62	7.97	2.37
15.50	0.26	0.62	7828	38293	6	89	7.96	2.35
17.56	0.20	0.50	7091	39030	11	100	8.24	2.32
19.05	0.16	0.41	7143	38978	16	100	8.09	2.29
20.86	0.13	0.34	5173	40948	24	100	7.78	2.29
23.96	0.12	0.31	3816	42305	48	100	7.76	2.21

Table D.27 – Detailed results for Figure 4.17.

Pop. density cap/km <sup>2</sup>	Building density buildings/km <sup>2</sup>	Network cost k€/ (100 m <sup>2</sup> )	El imp. GWh/y	El exp. GWh/y	NG imp. GWh/y	Investment cost €/ (100 m <sup>2</sup> y)	PV market €/ (100 m <sup>2</sup> y)	HP market €/ (100 m <sup>2</sup> y)
40.11	10.15	27.33	2.39	3.40	0.45	21.50	17.55	4.79
58.50	17.00	35.00	2.31	3.09	0.56	21.38	17.14	4.94
113.57	24.25	25.83	1.76	2.96	0.33	15.65	13.06	3.23
116.61	31.49	23.22	1.71	2.48	0.33	16.40	13.35	3.72
160.73	46.59	26.20	2.12	3.40	0.33	16.25	13.34	3.50
180.15	36.63	21.53	4.70	6.01	0.89	12.60	10.29	2.77
187.03	31.44	34.56	3.72	5.14	0.67	19.49	16.04	4.09
196.87	62.05	26.64	3.11	4.74	0.56	17.69	14.50	3.87
199.46	63.62	18.84	3.17	2.97	0.89	11.77	9.24	2.89
214.65	57.61	29.01	3.15	6.20	0.45	19.35	16.36	3.79
260.72	63.40	24.15	4.29	5.89	1.03	11.89	9.63	2.65
276.87	84.11	34.66	3.96	7.11	0.67	20.66	16.96	4.50
291.60	76.49	39.68	4.48	11.13	0.33	19.03	15.89	3.98
309.17	108.03	49.88	3.31	5.86	0.56	29.96	24.60	6.55
386.72	60.20	19.02	4.56	5.63	1.19	16.54	13.34	3.62
396.37	108.66	12.55	4.02	5.36	1.00	10.33	8.34	2.30
426.46	108.21	24.20	4.96	7.47	0.78	19.21	15.79	4.14
449.19	77.06	18.32	5.62	7.31	1.33	13.30	11.00	2.77
451.83	69.68	12.20	4.36	6.58	1.74	13.84	11.05	2.95
453.07	93.66	19.60	8.45	8.57	2.00	15.85	12.65	3.71
516.24	104.00	24.50	13.50	22.37	2.80	14.61	12.32	2.90
522.15	108.09	24.30	9.19	11.76	2.11	15.77	12.72	3.60

Pop. density cap/km <sup>2</sup>	Building density buildings/km <sup>2</sup>	Network cost k€/ (100 m <sup>2</sup> )	El emp. GWh/y	El exp. GWh/y	NG imp. GWh/y	Inv. cost €/ (100 m <sup>2</sup> y)	PV market €/ (100 m <sup>2</sup> y)	HP market €/ (100 m <sup>2</sup> y)
523.17	158.29	27.67	7.18	13.80	1.25	23.60	19.49	5.04
610.19	109.39	25.75	8.43	15.36	0.94	17.77	14.90	3.61
612.01	153.92	18.14	7.70	9.80	1.92	15.01	12.11	3.42
620.96	172.37	24.72	17.53	17.35	4.86	18.10	14.39	4.26
732.32	185.79	21.03	4.15	8.62	0.58	17.98	14.97	3.76
741.13	239.07	27.94	6.35	13.27	0.92	19.20	15.92	4.07
745.72	168.91	35.57	20.60	43.73	2.77	24.37	20.37	4.99
779.53	124.44	26.99	21.98	31.12	2.86	16.82	13.98	3.49
840.58	158.87	9.90	25.22	13.69	8.65	4.92	3.65	1.34
1082.86	132.25	8.72	8.59	7.55	2.08	12.12	9.83	2.68
1167.01	312.19	26.38	18.57	36.68	2.74	17.61	14.70	3.67
1748.21	195.00	23.07	28.29	30.75	6.57	14.94	12.19	3.32
1861.24	107.12	1.85	139.65	88.72	163.25	10.41	6.79	2.53
1881.48	129.81	7.55	19.11	25.83	2.82	10.56	8.80	2.19
2733.63	442.72	16.36	24.62	34.80	4.48	17.39	14.43	3.69
3221.26	220.61	5.01	43.20	32.43	16.25	4.74	3.69	1.11
4003.78	386.20	5.65	20.67	22.41	4.96	6.01	4.90	1.30
4089.72	717.10	12.13	24.46	32.82	5.27	10.04	8.23	2.18
4806.17	601.28	11.55	23.87	32.92	4.02	12.41	10.23	2.70
6645.17	656.63	5.62	16.44	20.66	10.81	15.17	11.73	3.23
7986.28	581.02	8.09	59.56	50.51	16.93	7.89	6.37	1.77
8062.12	475.77	2.61	39.95	46.55	51.74	10.26	7.28	2.18
8236.85	535.86	5.24	51.80	45.99	19.83	7.70	6.11	1.73
9276.93	345.32	2.63	96.98	76.68	66.33	7.05	5.23	1.60

Pop. density cap/km <sup>2</sup>	Building density buildings/km <sup>2</sup>	Network cost k€/ (100 m <sup>2</sup> )	El emp. GWh/y	El exp. GWh/y	NG imp. GWh/y	Inv. cost €/ (100 m <sup>2</sup> y)	PV market €/ (100 m <sup>2</sup> y)	HP market €/ (100 m <sup>2</sup> y)
11739.54	472.16	3.32	43.93	56.65	65.12	9.11	6.53	1.86
12249.21	469.20	2.10	86.68	83.92	105.68	7.71	5.45	1.63

# Bibliography

- [1] M. Kavgic, A. Mavrogianni, D. Mumovic, A. Summerfield, Z. Stevanovic, and M. Djurovic-Petrovic. A review of bottom-up building stock models for energy consumption in the residential sector. *Building and Environment*, 45(7):1683–1697, July 2010. ISSN 03601323. doi: 10.1016/j.buildenv.2010.01.021. URL <http://linkinghub.elsevier.com/retrieve/pii/S0360132310000338>.
- [2] Hoval. Hoval Wärmepumpen Dimensionierungshilfen. Technical report, Feldmeilen, Switzerland, 2014. URL [https://www.hoval.ch/de\\_CH/Effiziente-Wärmepumpen/waermepumpe.html](https://www.hoval.ch/de_CH/Effiziente-Wärmepumpen/waermepumpe.html).
- [3] The World Bank. Website of the world bank group, data on urban development. Technical report, Washington, D.C., U.S. URL <https://data.worldbank.org/topic/urban-development>.
- [4] J. Owen Lewis, Ní, and Antonio Sadhbhd and Borghi. Building energy efficiency in European cities. Cities of Tomorrow – Action Today. URBACT II Capitalisation. Projetc report, Uppsala, Sweden, October 2013. URL <http://eprints.sparaochbevara.se/739/>.
- [5] Matteo Morandin, Roman Hackl, and Simon Harvey. Economic feasibility of district heating delivery from industrial excess heat: A case study of a Swedish petrochemical cluster. *Energy*, 65:209–220, February 2014. ISSN 03605442. doi: 10.1016/j.energy.2013.11.064. URL <https://linkinghub.elsevier.com/retrieve/pii/S0360544213010347>.
- [6] Ilyes Ben Hassine and Ursula Eicker. Impact of load structure variation and solar thermal energy integration on an existing district heating network. *Applied Thermal Engineering*, 50(2):1437–1446, February 2013. ISSN 13594311. doi: 10.1016/j.applthermaleng.2011.12.037. URL <https://linkinghub.elsevier.com/retrieve/pii/S1359431111007344>.
- [7] D. K. Baker and S. A. Sherif. HEAT TRANSFER OPTIMIZATION OF A DISTRICT HEATING SYSTEM USING SEARCH METHODS. *International Journal of Energy Research*, 21(3):233–252, March 1997. ISSN 0363-907X, 1099-114X. doi: 10.1002/(SICI)1099-114X(199703)21:3<233::AID-ER250>3.0.CO;2-H. URL <http://doi.wiley.com/10.1002/%28SICI%291099-114X%28199703%2921%3A3%3C233%3A%3AAID-ER250%3E3.0.CO%3B2-H>.

- [8] Henrik Lund, Sven Werner, Robin Wiltshire, Svend Svendsen, Jan Eric Thorsen, Frede Hvelplund, and Brian Vad Mathiesen. 4th Generation District Heating (4gdh): Integrating smart thermal grids into future sustainable energy systems. *Energy*, 68(Supplement C):1–11, April 2014. ISSN 0360-5442. doi: 10.1016/j.energy.2014.02.089. URL <http://www.sciencedirect.com/science/article/pii/S0360544214002369>.
- [9] Svend Frederiksen and Sven Werner. *District heating and cooling*. Studentlitteratur, Lund, 2013. ISBN 978-91-44-08530-2. OCLC: 915569849.
- [10] Atli Benonysson, Benny Bøhm, and Hans F. Ravn. Operational optimization in a district heating system. *Energy Conversion and Management*, 36(5):297–314, May 1995. ISSN 01968904. doi: 10.1016/0196-8904(95)98895-T. URL <http://linkinghub.elsevier.com/retrieve/pii/019689049598895T>.
- [11] L. Adamo, G. Cammarata, A. Fichera, and L. Marletta. Improvement of a district heating network through thermoeconomic approach. *Renewable Energy*, 10(2-3):213–216, February 1997. ISSN 09601481. doi: 10.1016/0960-1481(96)00066-3. URL <http://linkinghub.elsevier.com/retrieve/pii/0960148196000663>.
- [12] Mariya Marinova, Catherine Beaudry, Abdelaziz Taoussi, Martin Trépanier, and Jean Paris. Economic Assessment of Rural District Heating by Bio-Steam Supplied by a Paper Mill in Canada. *Bulletin of Science, Technology & Society*, 28(2):159–173, April 2008. ISSN 0270-4676, 1552-4183. doi: 10.1177/0270467607313953. URL <http://journals.sagepub.com/doi/10.1177/0270467607313953>.
- [13] Per J. Agrell and Peter Bogetoft. Economic and environmental efficiency of district heating plants. *Energy Policy*, 33(10):1351–1362, July 2005. ISSN 03014215. doi: 10.1016/j.enpol.2003.12.011. URL <https://linkinghub.elsevier.com/retrieve/pii/S0301421503003793>.
- [14] Services Industriels de Genève. Geothermal energy. Technical report, Geneva, Switzerland, 2014. URL <https://ww2.sig-ge.ch>.
- [15] ETH Zürich. Anergy grid. Technical report, Zurich, Switzerland, 2012. URL <https://www.ethz.ch/en/the-eth-zurich/sustainability/campus/environment/energy/anergy-grid.html>.
- [16] Université de Genève. Genève-Lac-Nation (GLN) project: application of a European project. Technical report, Geneva, Switzerland, 2015. URL <https://www.unige.ch/energy/>.
- [17] Celine Weber and Daniel Favrat. Conventional and advanced CO<sub>2</sub> based district energy systems. *Energy*, 35(12):5070–5081, 2010. URL <http://www.sciencedirect.com/science/article/pii/S0360544210004354>.
- [18] Samuel Henchoz, Céline Weber, François Maréchal, and Daniel Favrat. Performance and profitability perspectives of a CO<sub>2</sub> based district energy network in Geneva’s City Centre.

- Energy*, 85:221–235, June 2015. ISSN 03605442. doi: 10.1016/j.energy.2015.03.079. URL <http://linkinghub.elsevier.com/retrieve/pii/S0360544215003886>.
- [19] Samuel Henchoz. On a Multi-service, CO<sub>2</sub> Based, District Energy System for a Better Energy Efficiency of Urban Areas. 2011. URL <https://infoscience.epfl.ch/record/169243>.
- [20] Samuel Henchoz, Daniel Favrat, François Maréchal, and Luc Girardin. Novel district heating and cooling energy network using CO<sub>2</sub> as a heat and mass transfer fluid. *Proceedings of 12th IEA Heat Pump Conference*, 2017. URL <https://infoscience.epfl.ch/record/231699>.
- [21] Paul Stadler, Luc Girardin, Araz Ashouri, and François Maréchal. Contribution of Model Predictive Control in the Integration of Renewable Energy Sources within the Built Environment. *Frontiers in Energy Research*, 6, May 2018. ISSN 2296-598X. doi: 10.3389/fenrg.2018.00022. URL <http://journal.frontiersin.org/article/10.3389/fenrg.2018.00022/full>.
- [22] T. Gundersen, IEA., and Trondheim SINTEF Energy Research. *A Process Integration PRIMER*. SINTEF Energy Research, 2000. URL <https://books.google.ch/books?id=KgqfXwAACAAJ>.
- [23] Ian C. Kemp. *Pinch analysis and process integration: a user guide on process integration for the efficient use of energy*. Butterworth-Heinemann, Amsterdam ; Boston, 2nd ed edition, 2007. ISBN 978-0-7506-8260-2. OCLC: ocm74969693.
- [24] Bodo Linnhoff and Vimal Sahdev. Pinch Technology. In Wiley-VCH Verlag GmbH & Co. KGaA, editor, *Ullmann's Encyclopedia of Industrial Chemistry*. Wiley-VCH Verlag GmbH & Co. KGaA, Weinheim, Germany, June 2000. ISBN 978-3-527-30673-2. doi: 10.1002/14356007.b03\_13. URL [http://doi.wiley.com/10.1002/14356007.b03\\_13](http://doi.wiley.com/10.1002/14356007.b03_13).
- [25] Ignacio E. Grossmann. Mixed-integer programming approach for the synthesis of integrated process flowsheets. *Computers & Chemical Engineering*, 9(5):463–482, 1985. ISSN 00981354. doi: 10.1016/0098-1354(85)80023-5. URL <http://linkinghub.elsevier.com/retrieve/pii/0098135485800235>.
- [26] Ferenc Friedler. Process integration, modelling and optimisation for energy saving and pollution reduction. *Applied Thermal Engineering*, 30(16):2270–2280, November 2010. ISSN 13594311. doi: 10.1016/j.applthermaleng.2010.04.030. URL <https://linkinghub.elsevier.com/retrieve/pii/S1359431110001936>.
- [27] Jiří Jaromír Klemeš, editor. *Handbook of process integration (PI): minimisation of energy and water use, waste and emissions*. Number number 61 in Woodhead publishing series in energy. Woodhead Publishing, Oxford ; Philadelphia, 2013. ISBN 978-0-85709-593-0.
- [28] François Marechal and Boris Kalitventzeff. Targeting the integration of multi-period utility systems for site scale process integration. *Applied Thermal Engineering*, 23(14):1763–1784,

- October 2003. ISSN 13594311. doi: 10.1016/S1359-4311(03)00142-X. URL <http://linkinghub.elsevier.com/retrieve/pii/S135943110300142X>.
- [29] YV Haimes. On a Bicriterion Formulation of the Problems of Integrated System Identification and System Optimization. *IEEE Transactions on Systems, Man, and Cybernetics*, SMC-1(3): 296–297, July 1971. ISSN 0018-9472, 2168-2909. doi: 10.1109/TSMC.1971.4308298. URL <http://ieeexplore.ieee.org/document/4308298/>.
- [30] Raluca Suciu, Ivan Kantor, Hur Butun, Luc Girardin, and Francois Marechal. Geographically parameterized residential sector energy and service profile. *Chemical Engineering Transactions*, pages 709–714, 2018. doi: 10.3303/CET1870119. URL <http://www.aidic.it/cet/18/70/119.pdf>.
- [31] Raluca Suciu, Ivan Kantor, Hr Btn, and Franois Marchal. Geographically Parameterized Residential Sector Energy and Service Profile. *Frontiers in Energy Research*, 7, July 2019. ISSN 2296-598X. doi: 10.3389/fenrg.2019.00069. URL <https://www.frontiersin.org/article/10.3389/fenrg.2019.00069/full>.
- [32] R. Saidur, H.H. Masjuki, and M.Y. Jamaluddin. An application of energy and exergy analysis in residential sector of Malaysia. *Energy Policy*, 35(2):1050–1063, February 2007. ISSN 03014215. doi: 10.1016/j.enpol.2006.02.006. URL <http://linkinghub.elsevier.com/retrieve/pii/S0301421506000930>.
- [33] Maria da Graa Carvalho. EU energy and climate change strategy. *Energy*, 40(1):19–22, April 2012. ISSN 03605442. doi: 10.1016/j.energy.2012.01.012. URL <http://linkinghub.elsevier.com/retrieve/pii/S0360544212000175>.
- [34] Hai-xiang Zhao and Frdric Magouls. A review on the prediction of building energy consumption. *Renewable and Sustainable Energy Reviews*, 16(6):3586–3592, August 2012. ISSN 13640321. doi: 10.1016/j.rser.2012.02.049. URL <http://linkinghub.elsevier.com/retrieve/pii/S1364032112001438>.
- [35] Luis Prez-Lombard, Jos Ortiz, and Christine Pout. A review on buildings energy consumption information. *Energy and Buildings*, 40(3):394–398, January 2008. ISSN 03787788. doi: 10.1016/j.enbuild.2007.03.007. URL <http://linkinghub.elsevier.com/retrieve/pii/S0378778807001016>.
- [36] U.S. Energy Information Administration. Annual Energy Review 2011 DOE/EIA-0384(2011). Technical report, 2011.
- [37] Department for Communities and Local Government. *English house condition survey 2007: technical report*. Department for Communities and Local Government, London, 2010. ISBN 978-1-4098-2459-6. OCLC: 912938925.



- [38] Reinhard Haas and Lee Schipper. Residential energy demand in OECD-countries and the role of irreversible efficiency improvements. *Energy Economics*, 20(4):421–442, September 1998. ISSN 01409883. doi: 10.1016/S0140-9883(98)00003-6. URL <http://linkinghub.elsevier.com/retrieve/pii/S0140988398000036>.
- [39] Eric J Miller, John Douglas Hunt, John E Abraham, and Paul A Salvini. Microsimulating urban systems. *Computers, Environment and Urban Systems*, 28(1-2):9–44, January 2004. ISSN 01989715. doi: 10.1016/S0198-9715(02)00044-3. URL <http://linkinghub.elsevier.com/retrieve/pii/S0198971502000443>.
- [40] Ld Shorrock and Je Dunster. The physically-based model BREHOMES and its use in deriving scenarios for the energy use and carbon dioxide emissions of the UK housing stock. *Energy Policy*, 25(12):1027–1037, October 1997. ISSN 03014215. doi: 10.1016/S0301-4215(97)00130-4. URL <http://linkinghub.elsevier.com/retrieve/pii/S0301421597001304>.
- [41] A. J. Summerfield, R. J. Lowe, and T. Oreszczyn. Two models for benchmarking UK domestic delivered energy. *Building Research & Information*, 38(1):12–24, February 2010. ISSN 0961-3218, 1466-4321. doi: 10.1080/09613210903399025. URL <http://www.tandfonline.com/doi/abs/10.1080/09613210903399025>.
- [42] Qingyuan Zhang. Residential energy consumption in China and its comparison with Japan, Canada, and USA. *Energy and Buildings*, 36(12):1217–1225, December 2004. ISSN 03787788. doi: 10.1016/j.enbuild.2003.08.002. URL <http://linkinghub.elsevier.com/retrieve/pii/S0378778804000532>.
- [43] Nicholas Rivers and Mark Jaccard. Combining Top-Down and Bottom-Up Approaches to Energy-Economy Modeling Using Discrete Choice Methods. *The Energy Journal*, 26(1):83–106, January 2015. doi: 10.2307/41323052. URL [https://www.researchgate.net/publication/46523413\\_Combining\\_Top-Down\\_and\\_Bottom-Up\\_Approaches\\_to\\_Energy-Economy\\_Modeling\\_Using\\_Discrete\\_Choice\\_Methods](https://www.researchgate.net/publication/46523413_Combining_Top-Down_and_Bottom-Up_Approaches_to_Energy-Economy_Modeling_Using_Discrete_Choice_Methods).
- [44] Lukas G. Swan and V. Ismet Ugursal. Modeling of end-use energy consumption in the residential sector: A review of modeling techniques. *Renewable and Sustainable Energy Reviews*, 13(8):1819–1835, October 2009. ISSN 13640321. doi: 10.1016/j.rser.2008.09.033. URL <http://linkinghub.elsevier.com/retrieve/pii/S1364032108001949>.
- [45] Alan Shek-Lun Fung. *Modeling of national and regional residential energy consumption and associated greenhouse gas emissions*. PhD Thesis, Dalhousie University, Halifax, Nova Scotia, February 2003.
- [46] Margaret Fels. PRISM: An introduction. *Energy and Buildings*, 9(1-2):5–18, February 1986. doi: 10.1016/0378-7788(86)90003-4. URL [http://marean.mycpanel.princeton.edu/images/prism\\_intro.pdf](http://marean.mycpanel.princeton.edu/images/prism_intro.pdf).

- [47] Rébha Ghedamsi, Noureddine Settou, Abderrahmane Gouareh, Adem Khamouli, Nadia Saifi, Bakhta Recioui, and Boubekker Dokkar. Modeling and forecasting energy consumption for residential buildings in Algeria using bottom-up approach. *Energy and Buildings*, 121:309–317, June 2016. ISSN 03787788. doi: 10.1016/j.enbuild.2015.12.030. URL <http://linkinghub.elsevier.com/retrieve/pii/S037877881530462X>.
- [48] David Fischer, Tobias Wolf, Johannes Scherer, and Bernhard Wille-Haussmann. A stochastic bottom-up model for space heating and domestic hot water load profiles for German households. *Energy and Buildings*, 124:120–128, July 2016. ISSN 03787788. doi: 10.1016/j.enbuild.2016.04.069. URL <http://linkinghub.elsevier.com/retrieve/pii/S0378778816303358>.
- [49] Luc Girardin, François Marechal, Matthias Dubuis, Nicole Calame-Darbellay, and Daniel Favrat. EnerGis: A geographical information based system for the evaluation of integrated energy conversion systems in urban areas. *Energy*, 35(2):830–840, February 2010. ISSN 03605442. doi: 10.1016/j.energy.2009.08.018. URL <http://linkinghub.elsevier.com/retrieve/pii/S0360544209003582>.
- [50] BEAR-ID Nobatek. European climate zones and bio-climatic design requirements. Project report, Paris, France, September 2016.
- [51] Euroheat & Power. ECOHEATCOOL, Work package 1, The European Cold Market, Final Report. Technical report, European Commission, Brussels, Belgium, 2015. URL [https://ec.europa.eu/energy/intelligent/projects/sites/iee-projects/files/projects/documents/ecoheatcool\\_the\\_european\\_cold\\_market\\_final\\_report.pdf](https://ec.europa.eu/energy/intelligent/projects/sites/iee-projects/files/projects/documents/ecoheatcool_the_european_cold_market_final_report.pdf).
- [52] Raluca Suci, Luc Girardin, and François Maréchal. Energy integration of CO<sub>2</sub> networks and power to gas for emerging energy autonomous cities in Europe. *Energy*, 157:830–842, August 2018. ISSN 03605442. doi: 10.1016/j.energy.2018.05.083. URL <https://linkinghub.elsevier.com/retrieve/pii/S0360544218309034>.
- [53] SITG. SITG- indice de dépense de chaleur admissible. Technical report, Geneva, Switzerland, 2018. URL <https://www.etat.ge.ch/geoportail/pro/?method=showextractpanel>.
- [54] ODYSEE-MURE Database. ODYSEE-MURE Database - Key indicators. Technical report, Grenoble, France, 2017. URL <http://www.indicators.odyssee-mure.eu/energy-efficiency-database.html>.
- [55] Swiss Federal Office of Energy. SmartGrid – Polysun: Design Tool for Local Load Management. Final report. Technical report, Switzerland, September 2015. URL <https://www.aramis.admin.ch/Default.aspx?DocumentID=14324&Load=true>.
- [56] Société suisse des ingénieurs et des architectes (SIA). SIA 2024 (2015): Données d’utilisation des locaux pour l’énergie et les installations du bâtiment. Technical report. Technical report,

- Zürich, Switzerland, October 2015. URL <http://www.webnorm.ch/collection%20des%20normes/architecte/sia%202024/f/2015/F/Product>.
- [57] SITG. SITG-CAD Bâtiment. Technical report, Geneva, Switzerland, 2018. URL <https://www.etat.ge.ch/geoportail/pro/?method=showextractpanel>.
- [58] Daniel Hoornweg and Perinaz Bhada-Tata. What a waste: a global review of solid waste management. *Urban development series knowledge papers*, 15:1–98, 2012. URL <http://scholar.google.com/scholar?cluster=7098011471289121717&hl=en&oi=scholar>.
- [59] Ministry of infrastructure and water monitor. Climate monitor Databank Netherlands. Technical report, 2018. URL <https://klimaatmonitor.databank.nl/dashboard/>.
- [60] Centraal Bureau voor de Statistiek. *Trends in the Netherlands 2016*. 2016. ISBN 978-90-357-2026-8. OCLC: 965814917.
- [61] François Maréchal and Boris Kalitventzeff. Process integration: Selection of the optimal utility system. *Computers & Chemical Engineering*, 22:S149–S156, March 1998. ISSN 00981354. doi: 10.1016/S0098-1354(98)00049-0. URL <http://linkinghub.elsevier.com/retrieve/pii/S0098135498000490>.
- [62] Swiss Federal Office of Statistics. Indice des prix à la consommation, carburants - Prix moyens par litre en francs. Technical report, Zurich, Switzerland, 2015. URL <https://www.bfs.admin.ch/bfs/fr/home/statistiques/catalogues-banques-donnees/publications.assetdetail.349969.html>.
- [63] Samuel Henchoz. Potential of refrigerant based district heating and cooling networks. 2016. doi: 10.5075/epfl-thesis-6935,urn:nbn:ch:bel-epfl-thesis6935-2. URL <https://infoscience.epfl.ch/record/217013>.
- [64] Swiss Federal Office of Statistics. Indice des prix à la production et à l'importation. Technical report. Technical report, 2015.
- [65] IPCC. Safeguarding the Ozone Layer and the Global Climate System: Issues Related to Hydrofluorocarbons and Perfluorocarbons, IPCC/TEAP Special Report. Technical report, 2005. URL [https://www.ipcc.ch/pdf/special-reports/sroc/sroc\\_full.pdf](https://www.ipcc.ch/pdf/special-reports/sroc/sroc_full.pdf).
- [66] Harald Hagemann. Internal Rate of Return. In Palgrave Macmillan, editor, *The New Palgrave Dictionary of Economics*, pages 1–4. Palgrave Macmillan UK, London, 2008. ISBN 978-1-349-95121-5. doi: 10.1057/978-1-349-95121-5\_798-2. URL [http://link.springer.com/10.1057/978-1-349-95121-5\\_798-2](http://link.springer.com/10.1057/978-1-349-95121-5_798-2).
- [67] Stephen A. Ross. Uses, Abuses, and Alternatives to the Net-Present-Value Rule. *Financial Management*, 24(3):96, 1995. ISSN 00463892. doi: 10.2307/3665561. URL <http://doi.wiley.com/10.2307/3665561>.

## Bibliography

---

- [68] Araz Ashouri François Maréchal Raluca Suciu, Paul Stadler. Towards energy-autonomous cities using CO<sub>2</sub> networks and Power to Gas storage, 2016.
- [69] Raluca-Ancuta Suci, Luc Girardin, and François Maréchal. Energy integration of CO<sub>2</sub> networks and Power to Gas for emerging energy autonomous cities in Europe. *Proceedings of ECOS 2017*, 2017. URL <https://infoscience.epfl.ch/record/232012>.
- [70] Eurostat Statistics Explained. Archive: Consumption of energy. Technical report, Luxembourg, June 2017. URL [https://ec.europa.eu/eurostat/statistics-explained/index.php?title=Archive:Consumption\\_of\\_energy](https://ec.europa.eu/eurostat/statistics-explained/index.php?title=Archive:Consumption_of_energy).
- [71] Sustainable Energy Authority of Ireland. Energy in the Residential Sector. Technical report, Dublin, Ireland, September 2013. URL <https://www.seai.ie/resources/publications/Energy-in-the-Residential-Sector-2013.pdf>.
- [72] European Environment Agency. *Annual European Union greenhouse gas inventory 1990-2014 and inventory report 2016: submission to the UNFCCC Secretariat*. 2016. ISBN 978-92-9213-746-5. URL <http://bookshop.europa.eu/uri?target=EUB:NOTICE:THAL16014:EN:HTML>. OCLC: 1001821958.
- [73] EEA. Urban environment, 2017. URL <https://www.eea.europa.eu/themes/urban>.
- [74] Igor Sartori, Assunta Napolitano, and Karsten Voss. Net zero energy buildings: A consistent definition framework. *Energy and Buildings*, 48(Supplement C):220–232, May 2012. ISSN 0378-7788. doi: 10.1016/j.enbuild.2012.01.032. URL <http://www.sciencedirect.com/science/article/pii/S0378778812000497>.
- [75] Paul A. Torcellini and Drury B. Crawley. Understanding Zero-Energy Buildings. *ASHRAE Journal; New York*, 48(9):62–64,66–69, September 2006. ISSN 00012491. URL <https://search.proquest.com/docview/220461230/abstract/162FA304867D4AB8PQ/1>.
- [76] Raluca Suci, Paul Stadler, Araz Ashouri, and François Maréchal. Towards energy-autonomous cities using CO<sub>2</sub> networks and Power to Gas storage. *Proceedings of ECOS 2016*, 2016. URL <https://infoscience.epfl.ch/record/226186>.
- [77] Alberto Cavallini. Properties of CO<sub>2</sub> as a refrigerant. In *European Seminar-CO<sub>2</sub> as a refrigerant: theoretical and design aspects*, 2004. URL <http://www.centrogalileo.it/NUOVAPA/Articoli%20tecnici/INGLESE%20CONVEGNO/CO2/Cavallini%20-%20Milano04CO2.pdf>.
- [78] Gustav Lorentzen. Revival of carbon dioxide as a refrigerant. *International Journal of Refrigeration*, 17(5):292–301, 1994. URL <http://www.sciencedirect.com/science/article/pii/0140700794900590>.
- [79] Friedli S. Felix J. Personal communication. Services Industriels de Genève, 2006.

- 
- [80] J. Söderman, G. Ohman, A. Aittomäki, A. Mäkinen, K. Sipilä, and M. Rämä. Design and operation of integrated cooling and heating systems in regions and buildings. Technical report, Technical Report 2006-3, Faculty of Technology, Heat Engineering Laboratory, Abo Akademi University, Finland, 2006. URL <http://scholar.google.com/scholar?cluster=4909109074471230242&hl=en&oi=scholar>.
- [81] Michael Sterner. *Bioenergy and renewable power methane in integrated 100% renewable energy systems: Limiting global warming by transforming energy systems*, volume 14. kassel university press GmbH, 2009. URL [http://books.google.com/books?hl=en&lr=&id=5Rzza2R8j\\_UC&oi=fnd&pg=PP1&dq=info:Mx8SbswuSooJ:scholar.google.com&ots=FsRAtdLagq&sig=zw5MzU4Pa5qzeKikqESzBDj7Qzc](http://books.google.com/books?hl=en&lr=&id=5Rzza2R8j_UC&oi=fnd&pg=PP1&dq=info:Mx8SbswuSooJ:scholar.google.com&ots=FsRAtdLagq&sig=zw5MzU4Pa5qzeKikqESzBDj7Qzc).
- [82] M. Specht, J. Brellochs, V. Frick, B. Stürmer, U. Zuberbühler, M. Sterner, and G. Waldstein. Storage of renewable energy in the natural gas grid. *Erdoel, Erdgas, Kohle*, 126:342–345, 2010. URL <http://scholar.google.com/scholar?cluster=4819084727408747544&hl=en&oi=scholar>.
- [83] Volker Quaschnig. *Regenerative Energiesysteme: Technologie, Berechnung, Simulation. 8., aktual. ed.* München: Hanser Verlag, 2013. URL <http://scholar.google.com/scholar?cluster=14338036460286604694&hl=en&oi=scholar>.
- [84] Søren Højgaard Jensen, C. Graves, M. Mogensen, C. Wendel, R. Braun, G. Hughes, Z. Gao, and S. A. Barnett. Large-scale electricity storage utilizing reversible solid oxide cells combined with underground storage of CO<sub>2</sub> and CH<sub>4</sub>. *Energy & Environmental Science*, 8(8):2471–2479, 2015. URL <http://pubs.rsc.org/is/content/articlehtml/2015/ee/c5ee01485a>.
- [85] Easa I. Al-Musleh, Dharik S. Mallapragada, and Rakesh Agrawal. Continuous power supply from a baseload renewable power plant. *Applied Energy*, 122:83–93, 2014. URL <http://www.sciencedirect.com/science/article/pii/S030626191400141X>.
- [86] Luc Girardin, Raffaele Bolliger, and Francois Marechal. On the use of process integration techniques to generate optimal steam cycle configurations for the power plant industry. *Chemical Engineering Transactions*, pages 171–176, May 2009. doi: 10.3303/CET0918026. URL <http://www.aidic.it/cet/09/18/026.pdf>.
- [87] Emanuele Facchinetti, Daniel Favrat, and François Maréchal. Innovative Hybrid Cycle Solid Oxide Fuel Cell-Inverted Gas Turbine with CO<sub>2</sub> Separation. *Fuel Cells*, 11(4):565–572, 2011. URL <http://onlinelibrary.wiley.com/doi/10.1002/fuce.201000130/full>.
- [88] Ligang Wang, Mar Pérez-Fortes, Hossein Madi, Stefan Diethelm, Jan Van herle, and François Maréchal. Optimal design of solid-oxide electrolyzer based power-to-methane systems: A comprehensive comparison between steam electrolysis and co-electrolysis. *Applied Energy*, 211:1060–1079, February 2018. ISSN 03062619. doi: 10.1016/j.apenergy.2017.11.050. URL <http://linkinghub.elsevier.com/retrieve/pii/S0306261917316367>.

## Bibliography

---

- [89] Solaranlagen Portal. Solaranlagen Portal <http://www.solaranlagen-portal.com/solar/solaranlage/preise/modulpreise> [accessed: 02.11.2016], 2016. URL <http://www.solaranlagen-portal.com/solar/solaranlage/preise/modulpreise>.
- [90] Carlos Rubio-Maya, Javier Uche-Marcuello, Amaya Martínez-Gracia, and Angel A. Bayod-Rújula. Design optimization of a polygeneration plant fuelled by natural gas and renewable energy sources. *Applied Energy*, 88(2):449–457, 2011. URL <http://www.sciencedirect.com/science/article/pii/S030626191000262X>.
- [91] Gael D. Ulrich. *A guide to chemical engineering process design and economics*. Wiley New York, 1984. URL <http://www.sidalc.net/cgi-bin/wxis.exe/?IsisScript=LIBRO.xis&method=post&formato=2&cantidad=1&expresion=mfn=005040>.
- [92] Richard Turton, Richard C. Bailie, Wallace B. Whiting, and Joseph A. Shaeiwitz. *Analysis, synthesis and design of chemical processes*. Pearson Education, 2008. URL <http://books.google.com/books?hl=en&lr=&id=kWXyhVXztZ8C&oi=fnd&pg=PT3&dq=info:XL-inU04110J:scholar.google.com&ots=pYpVsGrQsA&sig=WXxa2Lrgx2nwGu-w4pstWZh6UMg>.
- [93] Frédéric Louis-Pierre Raphaël Marie Amblard. Geothermal energy integration in urban systems. The case study of the city of Lausanne. Technical report, 2015. URL <http://infoscience.epfl.ch/record/208829>.
- [94] Swiss Federal Office for Statistics, Bern, Switzerland. spreadsheet showing the heating oil average annual prices in CHF per 100 1978-2013, 2013. URL <http://www.bfs.admin.ch/bfs/portal/fr/index/themen/05/02/blank/key/durchschnittspreise.html>[accessed04.07.14].
- [95] Jérôme Faessler, Anthony Haroutunian, Pierre Hollmuller, and Bernard Marie Lachal. Etude d'opportunité pour le projet GLU/GLA : pertes thermiques du réseau Lac, connexion aux bâtiments et potentiel de froid : évaluations et recommandations. 2011. URL <https://archive-ouverte.unige.ch/unige:23583>.
- [96] Jérôme Faessler. *Valorisation intensive des énergies renouvelables dans l'agglomération franco-valdo-genevoise (VIRAGE) dans une perspective de société à 2000W*. PhD thesis, University of Geneva, 2011. URL <https://archive-ouverte.unige.ch/unige:17272?gathStatIcon=true>.
- [97] European Environment Agency. Final energy consumption by sector and fuel. Technical report, Copenhagen, Denmark, . URL <https://www.eea.europa.eu/data-and-maps/indicators/final-energy-consumption-by-sector-9/assessment-4>.
- [98] Eurostat Statistics Explained. Consumption of energy. Technical report, Luxembourg. URL [https://ec.europa.eu/eurostat/statistics-explained/index.php?title=Archive:Consumption\\_of\\_energy](https://ec.europa.eu/eurostat/statistics-explained/index.php?title=Archive:Consumption_of_energy).



## Bibliography

---

- [99] International Energy Agency. Total final consumption. Technical report, Paris, France, . URL <https://www.iea.org/statistics/kwes/consumption/>.
- [100] Union européenne and Direction générale de la recherche. *Energy-Efficient Buildings multi-annual roadmap for the contractual PPP under Horizon 2020*. Publications Office of the European Union, Luxembourg, 2013. ISBN 978-92-79-31239-7. OCLC: 877078774.
- [101] Agence internationale de l'énergie and Organisation de coopération et de développement économiques. *Energy technology perspectives: scenarios & strategies to 2050 : in support of the G8 Plan of action*. OECD, IEA, Paris, 2006. ISBN 978-92-64-10982-7 978-92-64-04142-4 978-92-64-08597-8 978-92-64-17488-7. OCLC: 878599919.
- [102] U.S. Department of Energy. Waste heat recovery: technology and opportunities in U.S. industry. Technical report, United States. URL [https://www1.eere.energy.gov/manufacturing/intensiveprocesses/pdfs/waste\\_heat\\_recovery.pdf](https://www1.eere.energy.gov/manufacturing/intensiveprocesses/pdfs/waste_heat_recovery.pdf).
- [103] American Society of Mechanical Engineers, editor. *Proceedings of the ASME Heat Transfer Division–2006: presented at 2006 ASME International Mechanical Engineering Congress and Exposition: November 5-10, 2006, Chicago, Illinois*. Number vol. 377 in HTD. American Society of Mechanical Engineers, New York, N.Y, 2007. ISBN 978-0-7918-4784-8 978-0-7918-4785-5 978-0-7918-4786-2. OCLC: ocn132692658.
- [104] Sarah Brueckner, Laia Miró, Luisa F. Cabeza, Martin Pehnt, and Eberhard Laevemann. Methods to estimate the industrial waste heat potential of regions – A categorization and literature review. *Renewable and Sustainable Energy Reviews*, 38:164–171, October 2014. ISSN 13640321. doi: 10.1016/j.rser.2014.04.078. URL <https://linkinghub.elsevier.com/retrieve/pii/S1364032114003165>.
- [105] Stephane Bungener, Roman Hackl, Greet Van Eetvelde, Simon Harvey, and Francois Marechal. Multi-period analysis of heat integration measures in industrial clusters. *Energy*, 93:220–234, December 2015. ISSN 03605442. doi: 10.1016/j.energy.2015.09.023. URL <https://linkinghub.elsevier.com/retrieve/pii/S0360544215012177>.
- [106] Matthias Bendig, François Maréchal, and Daniel Favrat. Defining “Waste Heat” for industrial processes. *Applied Thermal Engineering*, 61(1):134–142, October 2013. ISSN 13594311. doi: 10.1016/j.applthermaleng.2013.03.020. URL <https://linkinghub.elsevier.com/retrieve/pii/S1359431113001907>.
- [107] Helen Becker and François Maréchal. Energy integration of industrial sites with heat exchange restrictions. *Computers & Chemical Engineering*, 37:104–118, February 2012. ISSN 00981354. doi: 10.1016/j.compchemeng.2011.09.014. URL <https://linkinghub.elsevier.com/retrieve/pii/S0098135411002857>.

- [108] Vladan Karamarković, Miljan Marašević, Rade Karamarković, and Miodrag Karamarković. Recuperator for waste heat recovery from rotary kilns. *Applied Thermal Engineering*, 54 (2):470–480, May 2013. ISSN 13594311. doi: 10.1016/j.applthermaleng.2013.02.027. URL <https://linkinghub.elsevier.com/retrieve/pii/S1359431113001324>.
- [109] Ramón González-Bravo, José María Ponce-Ortega, and Mahmoud M. El-Halwagi. Optimal Design of Water Desalination Systems Involving Waste Heat Recovery. *Industrial & Engineering Chemistry Research*, 56(7):1834–1847, February 2017. ISSN 0888-5885, 1520-5045. doi: 10.1021/acs.iecr.6b04725. URL <http://pubs.acs.org/doi/10.1021/acs.iecr.6b04725>.
- [110] Paul Cunningham. Waste Heat/Cogen Opportunities in the Cement Industry. *Cogeneration & Distributed Generation Journal*, 17(3):31–51, July 2002. ISSN 1545-3669. doi: 10.1080/10668680209508978. URL <http://www.tandfonline.com/doi/abs/10.1080/10668680209508978>.
- [111] L. Zhang and T. Akiyama. How to recuperate industrial waste heat beyond time and space. *International Journal of Exergy*, 6(2):214, 2009. ISSN 1742-8297, 1742-8300. doi: 10.1504/IJEX.2009.023999. URL <http://www.inderscience.com/link.php?id=23999>.
- [112] Laia Miró, Sarah Brückner, and Luisa F. Cabeza. Mapping and discussing Industrial Waste Heat (IWH) potentials for different countries. *Renewable and Sustainable Energy Reviews*, 51:847–855, November 2015. ISSN 13640321. doi: 10.1016/j.rser.2015.06.035. URL <https://linkinghub.elsevier.com/retrieve/pii/S1364032115006073>.
- [113] I Johnson, B Choate, and S Dillich. Waste heat recovery: opportunities and challenges. *EDP Congress*, pages 47–52, 2008. URL [https://www.researchgate.net/publication/283159005\\_Waste\\_heat\\_recovery\\_Opportunities\\_and\\_challenges](https://www.researchgate.net/publication/283159005_Waste_heat_recovery_Opportunities_and_challenges).
- [114] Ziya Söğüt, Zuhul Oktay, and Hikmet Karakoç. Mathematical modeling of heat recovery from a rotary kiln. *Applied Thermal Engineering*, 30(8-9):817–825, June 2010. ISSN 13594311. doi: 10.1016/j.applthermaleng.2009.12.009. URL <https://linkinghub.elsevier.com/retrieve/pii/S1359431109003561>.
- [115] R.C. McKenna and J.B. Norman. Spatial modelling of industrial heat loads and recovery potentials in the UK. *Energy Policy*, 38(10):5878–5891, October 2010. ISSN 03014215. doi: 10.1016/j.enpol.2010.05.042. URL <https://linkinghub.elsevier.com/retrieve/pii/S0301421510004131>.
- [116] Hong-kui Lian, Yan Li, Guang-yangzi Su, and Chun-wei GU. An overview of domestic technologies for waste heat utilization. *Energy Conservation Technology*, 2, 2011.
- [117] Kristina Holmgren. Role of a district-heating network as a user of waste-heat supply from various sources – the case of Göteborg. *Applied Energy*, 83(12):1351–1367, December 2006.



- ISSN 03062619. doi: 10.1016/j.apenergy.2006.02.001. URL <https://linkinghub.elsevier.com/retrieve/pii/S030626190600016X>.
- [118] K Konigs, G Eisenbauer, and H Eisemburger. The use of industrial surplus heat in the district heat supply at Duisburg – Rheinhausen. *FernwaermeInternational*, 11(2):60–64, 1982.
- [119] C Belaz. From concept to implementation of a district heating system using waste heat from an industrial plant. *Bull de l'Association Suisse des Electr (Organe Commun de l'Association Suissedes Electr (ASE) de l'Union des Centrales Suisses d'Electricite (UCS)*, 77(10):587–590, 1986.
- [120] J de Jong. Favourable results with the application of electrically driven heat pumps. II. PNEM heat pump in district heating with industrial waste heat as source of heat. *Elektrotechnik*, 68(1):30–35, 1990.
- [121] Augustine N. Ajah, Anish C. Patil, Paulien M. Herder, and Johan Grievink. Integrated conceptual design of a robust and reliable waste-heat district heating system. *Applied Thermal Engineering*, 27(7):1158–1164, May 2007. ISSN 13594311. doi: 10.1016/j.applthermaleng.2006.02.039. URL <https://linkinghub.elsevier.com/retrieve/pii/S1359431106001074>.
- [122] A Ajah, A Mesbah, J Grievink, P Herder, P Falcao, and S Wennekes. On the robustness, effectiveness and reliability of chemical and mechanical heat pumps for low-temperature heat source district heating: A comparative simulation-based analysis and evaluation. *Energy*, 33(6):908–929, June 2008. ISSN 03605442. doi: 10.1016/j.energy.2007.12.003. URL <https://linkinghub.elsevier.com/retrieve/pii/S0360544207002204>.
- [123] Qun Chen, Karen Finney, Hanning Li, Xiaohui Zhang, Jue Zhou, Vida Sharifi, and Jim Swithenbank. Condensing boiler applications in the process industry. *Applied Energy*, 89(1):30–36, January 2012. ISSN 03062619. doi: 10.1016/j.apenergy.2010.11.020. URL <https://linkinghub.elsevier.com/retrieve/pii/S0306261910004836>.
- [124] Inger-Lise Svensson, Johanna Jönsson, Thore Berntsson, and Bahram Moshfegh. Excess heat from kraft pulp mills: Trade-offs between internal and external use in the case of Sweden—Part 1: Methodology. *Energy Policy*, 36(11):4178–4185, November 2008. ISSN 03014215. doi: 10.1016/j.enpol.2008.07.017. URL <https://linkinghub.elsevier.com/retrieve/pii/S0301421508003637>.
- [125] Hao Fang, Jianjun Xia, Kan Zhu, Yingbo Su, and Yi Jiang. Industrial waste heat utilization for low temperature district heating. *Energy Policy*, 62:236–246, November 2013. ISSN 03014215. doi: 10.1016/j.enpol.2013.06.104. URL <https://linkinghub.elsevier.com/retrieve/pii/S0301421513006113>.
- [126] Ankur Kapil, Igor Bulatov, Robin Smith, and Jin-Kuk Kim. Process integration of low grade heat in process industry with district heating networks. *Energy*, 44(1):11–19, August 2012. ISSN

03605442. doi: 10.1016/j.energy.2011.12.015. URL <https://linkinghub.elsevier.com/retrieve/pii/S0360544211008097>.
- [127] Ivan Kantor, Anna S. Wallerand, Maziar Kermani, Hür Bütün, Alessio Santecchia, Raphaël Norbert, Hélène Cervo, Sebastian Arias, Franz Wolf, Greet Van Eetvelde, and François Maréchal. Thermal profile construction for energy-intensive industrial sectors. In *Proceedings of ECOS 2018 – The 31st International Conference on Efficiency, Cost, Optimization, Simulation and Environmental Impact of Energy Systems*, 2018. URL <http://hdl.handle.net/1854/LU-8563219>.
- [128] Frauke Schorcht, Ioanna Kourti, Bianca Maria Scalet, Serge Roudier, Luis Delgado Sancho, and Institute for Prospective Technological Studies. *Best available techniques (BAT) reference document for the production of cement, lime and magnesium oxide: Industrial Emissions Directive 2010/75/EU (integrated pollution prevention and control)*. Publications Office, Luxembourg, 2013. ISBN 978-92-79-32944-9. URL <http://dx.publications.europa.eu/10.2788/12850>. OCLC: 870616548.
- [129] Barthe Pascal, Michel Chaugny, Luis Delgado Sancho, Serge Roudier, and Institute for Prospective Technological Studies. *Best available techniques (BAT) reference document for the refining of mineral oil and gas industrial emissions: Industrial Emissions Directive 2010/75/EU (integrated pollution prevention and control)*. Publications Office, Luxembourg, 2015. ISBN 978-92-79-46198-9. URL <http://dx.publications.europa.eu/10.2791/010758>. OCLC: 908060686.
- [130] European IPCC Bureau. *Best available techniques (BAT) reference document for Food, Drink and Milk Industries: Industrial Emissions Directive 2010/75/EU (integrated pollution prevention and control)*. Publications Office, Luxembourg, 2018. URL [http://eippcb.jrc.ec.europa.eu/reference/BREF/FDM/FDM\\_02-10-2018BW.pdf](http://eippcb.jrc.ec.europa.eu/reference/BREF/FDM/FDM_02-10-2018BW.pdf).
- [131] Michael Suhr, Gabriele Klein, Ioanna Kourti, Miguel Rodrigo Gonzalo, Germán Giner Santonja, Serge Roudier, Luis Delgado Sancho, and Institute for Prospective Technological Studies. *Best Available Techniques (BAT) reference document for the production of pulp, paper and board*. Publications Office, Luxembourg, 2015. ISBN 978-92-79-48167-3. URL <http://dx.publications.europa.eu/10.2791/370629>. OCLC: 930993772.
- [132] Industrial Process and Energy Systems Engineering (IPESE) at and École Polytechnique Fédérale de Lausanne (EPFL). Potential Impact of SCCER-EIP Work Package 4 Toward Switzerland's ES2050. Technical report, Sion, Switzerland, April 2017.
- [133] Gianluca Cusano, Miguel Rodrigo Gonzalo, Frank Farrell, Rainer Remus, Serge Roudier, and Luis Delgado Sancho. *Best Available Techniques (BAT) Reference Document for the Non-Ferrous Metals Industries: Industrial Emissions Directive 2010/75/EU (integrated pollution prevention and control)*. Publications Office, Luxembourg, 2017. URL [http://eippcb.jrc.ec.europa.eu/reference/BREF/NFM/JRC107041\\_NFM\\_Bref\\_2017.pdf](http://eippcb.jrc.ec.europa.eu/reference/BREF/NFM/JRC107041_NFM_Bref_2017.pdf).

## Bibliography

---

- [134] Serge Roudier, Luis Delgado Sancho, Miguel A Aguado-Monsonet, Rainer Remus, and Institute for Prospective Technological Studies. *Best available techniques (BAT) reference document for iron and steel production industrial emissions Directive 2010/75/EU: integrated pollution prevention and control*. Publications Office, Luxembourg, 2013. OCLC: 1044331489.
- [135] European IPCC Bureau. *Best Available Techniques (BAT) Reference Document on Polymers*. Publications Office, Luxembourg, 2007. URL [http://eippcb.jrc.ec.europa.eu/reference/BREF/pol\\_bref\\_0807.pdf](http://eippcb.jrc.ec.europa.eu/reference/BREF/pol_bref_0807.pdf).
- [136] Port of Rotterdam Authority. Over 120 industrial companies. One powerful cluster. Make it happen. Technical report, Rotterdam, The Netherlands, February 2016. URL <https://www.portofrotterdam.com/sites/default/files/facts-figures-energy-port-and-petrochemical-cluster.pdf>.
- [137] The brewers of Europe. Beer statistics 2017 edition. Technical report, 2017. URL <https://brewersofeurope.org/uploads/mycms-files/documents/publications/2017/Statistics-201712-001.pdf>[accessed:22.12.2018].
- [138] Hür Bütün, Ivan Kantor, and François Maréchal. A heat integration method with location-dependent heat distribution losses. In *Computer Aided Chemical Engineering*, volume 44, pages 1195–1200. Elsevier, 2018. ISBN 978-0-444-64241-7. doi: 10.1016/B978-0-444-64241-7.50194-4. URL <https://linkinghub.elsevier.com/retrieve/pii/B9780444642417501944>.
- [139] Benny Bøhm. On transient heat losses from buried district heating pipes. *International Journal of Energy Research*, 24(15):1311–1334, December 2000. ISSN 0363-907X, 1099-114X. doi: 10.1002/1099-114X(200012)24:15<1311::AID-ER648>3.0.CO;2-Q. URL <http://doi.wiley.com/10.1002/1099-114X%28200012%2924%3A15%3C1311%3A%3AAID-ER648%3E3.0.CO%3B2-Q>.
- [140] D. Marcotte and P. Pasquier. On the estimation of thermal resistance in borehole thermal conductivity test. *Renewable Energy*, 33(11):2407–2415, November 2008. ISSN 09601481. doi: 10.1016/j.renene.2008.01.021. URL <https://linkinghub.elsevier.com/retrieve/pii/S0960148108000372>.
- [141] Raluca Suci, Paul Stadler, Luc Girardin, and François Maréchal. Multi-period multi-time optimisation of CO<sub>2</sub> based district energy systems. In *Computer Aided Chemical Engineering*, volume 43, pages 1057–1062. Elsevier, 2018. ISBN 978-0-444-64235-6. doi: 10.1016/B978-0-444-64235-6.50185-6. URL <https://linkinghub.elsevier.com/retrieve/pii/B9780444642356501856>.
- [142] Raluca Suci, Paul Stadler, Ivan Kantor, Luc Girardin, and François Maréchal. Systematic Integration of Energy-Optimal Buildings With District Networks. *Energies*, 12(15):2945, July 2019. ISSN 1996-1073. doi: 10.3390/en12152945. URL <https://www.mdpi.com/1996-1073/12/15/2945>.

## Bibliography

---

- [143] John E. Anderson, Gebhard Wulforth, and Werner Lang. Energy analysis of the built environment—A review and outlook. *Renewable and Sustainable Energy Reviews*, 44:149–158, April 2015. ISSN 13640321. doi: 10.1016/j.rser.2014.12.027. URL <https://linkinghub.elsevier.com/retrieve/pii/S136403211401079X>.
- [144] R. K. Pachauri, Leo Mayer, and Intergovernmental Panel on Climate Change, editors. *Climate change 2014: synthesis report*. Intergovernmental Panel on Climate Change, Geneva, Switzerland, 2015. ISBN 978-92-9169-143-2. OCLC: 914851124.
- [145] INTERNATIONAL ENERGY AGENCY. *WORLD ENERGY BALANCES 2018*. ORGANIZATION FOR ECONOMIC, S.I., 2018. ISBN 978-92-64-30155-9. OCLC: 1054217453.
- [146] Sunanda Sinha and S.S. Chandel. Review of software tools for hybrid renewable energy systems. *Renewable and Sustainable Energy Reviews*, 32:192–205, April 2014. ISSN 13640321. doi: 10.1016/j.rser.2014.01.035. URL <https://linkinghub.elsevier.com/retrieve/pii/S136403211400046X>.
- [147] Peter D. Lund, Jani Mikkola, and J. Ypyä. Smart energy system design for large clean power schemes in urban areas. *Journal of Cleaner Production*, 103:437–445, September 2015. ISSN 09596526. doi: 10.1016/j.jclepro.2014.06.005. URL <https://linkinghub.elsevier.com/retrieve/pii/S0959652614005915>.
- [148] Pierluigi Mancarella. MES (multi-energy systems): An overview of concepts and evaluation models. *Energy*, 65:1–17, February 2014. ISSN 03605442. doi: 10.1016/j.energy.2013.10.041. URL <https://linkinghub.elsevier.com/retrieve/pii/S0360544213008931>.
- [149] R. Niemi, J. Mikkola, and P.D. Lund. Urban energy systems with smart multi-carrier energy networks and renewable energy generation. *Renewable Energy*, 48:524–536, December 2012. ISSN 09601481. doi: 10.1016/j.renene.2012.05.017. URL <https://linkinghub.elsevier.com/retrieve/pii/S0960148112003424>.
- [150] Leslie G. Fishbone and Harold Abilock. Markal, a linear-programming model for energy systems analysis: Technical description of the bnl version. *International Journal of Energy Research*, 5(4):353–375, 1981. ISSN 0363907X, 1099114X. doi: 10.1002/er.4440050406. URL <http://doi.wiley.com/10.1002/er.4440050406>.
- [151] Yew S. Ong, Prasanth B. Nair, and Andrew J. Keane. Evolutionary Optimization of Computationally Expensive Problems via Surrogate Modeling. *AIAA Journal*, 41(4):687–696, April 2003. ISSN 0001-1452, 1533-385X. doi: 10.2514/2.1999. URL <http://arc.aiaa.org/doi/10.2514/2.1999>.
- [152] Bryan Eisenhower, Zheng O’Neill, Satish Narayanan, Vladimir A. Fonoberov, and Igor Mezić. A methodology for meta-model based optimization in building energy models. *Energy and*

- Buildings*, 47:292–301, April 2012. ISSN 03787788. doi: 10.1016/j.enbuild.2011.12.001. URL <https://linkinghub.elsevier.com/retrieve/pii/S0378778811005962>.
- [153] R. Ries and A. Mahdavi. Integrated Computational Life-Cycle Assessment of Buildings. *Journal of Computing in Civil Engineering*, 15(1):59–66, January 2001. ISSN 0887-3801, 1943-5487. doi: 10.1061/(ASCE)0887-3801(2001)15:1(59). URL <http://ascelibrary.org/doi/10.1061/%28ASCE%290887-3801%282001%2915%3A1%2859%29>.
- [154] Minna Sunikka-Blank and Ray Galvin. Introducing the prebound effect: the gap between performance and actual energy consumption. *Building Research & Information*, 40(3):260–273, June 2012. ISSN 0961-3218, 1466-4321. doi: 10.1080/09613218.2012.690952. URL <http://www.tandfonline.com/doi/abs/10.1080/09613218.2012.690952>.
- [155] Oyeshola F. Kofoworola and Shabbir H. Gheewala. Life cycle energy assessment of a typical office building in Thailand. *Energy and Buildings*, 41(10):1076–1083, October 2009. ISSN 03787788. doi: 10.1016/j.enbuild.2009.06.002. URL <https://linkinghub.elsevier.com/retrieve/pii/S0378778809001121>.
- [156] Luis Ochoa, Chris Hendrickson, and H. Scott Matthews. Economic Input-output Life-cycle Assessment of U.S. Residential Buildings. *Journal of Infrastructure Systems*, 8(4):132–138, December 2002. ISSN 1076-0342, 1943-555X. doi: 10.1061/(ASCE)1076-0342(2002)8:4(132). URL <http://ascelibrary.org/doi/10.1061/%28ASCE%291076-0342%282002%298%3A4%28132%29>.
- [157] Seppo Junnila, Arpad Horvath, and Angela Acree Guggemos. Life-Cycle Assessment of Office Buildings in Europe and the United States. *Journal of Infrastructure Systems*, 12(1): 10–17, March 2006. ISSN 1076-0342, 1943-555X. doi: 10.1061/(ASCE)1076-0342(2006)12: 1(10). URL <http://ascelibrary.org/doi/10.1061/%28ASCE%291076-0342%282006%2912%3A1%2810%29>.
- [158] Seppo Junnila and Arpad Horvath. Life-Cycle Environmental Effects of an Office Building. *Journal of Infrastructure Systems*, 9(4):157–166, December 2003. ISSN 1076-0342, 1943-555X. doi: 10.1061/(ASCE)1076-0342(2003)9:4(157). URL <http://ascelibrary.org/doi/10.1061/%28ASCE%291076-0342%282003%299%3A4%28157%29>.
- [159] Edward L. Glaeser and Matthew E. Kahn. The greenness of cities: Carbon dioxide emissions and urban development. *Journal of Urban Economics*, 67(3):404–418, May 2010. ISSN 00941190. doi: 10.1016/j.jue.2009.11.006. URL <https://linkinghub.elsevier.com/retrieve/pii/S0094119009001028>.
- [160] Christopher Kennedy, Julia Steinberger, Barrie Gasson, Yvonne Hansen, Timothy Hillman, Miroslav Havránek, Diane Pataki, Aumnad Phdungsilp, Anu Ramaswami, and Gara Villalba Mendez. Greenhouse Gas Emissions from Global Cities. *Environmental Science & Technology*,

## Bibliography

---

- 43(19):7297–7302, October 2009. ISSN 0013-936X, 1520-5851. doi: 10.1021/es900213p. URL <https://pubs.acs.org/doi/10.1021/es900213p>.
- [161] Patrick Troy, Darren Holloway, Stephen Pullen, and Raymond Bunker. Embodied and Operational Energy Consumption in the City. *Urban Policy and Research*, 21(1):9–44, March 2003. ISSN 0811-1146, 1476-7244. doi: 10.1080/0811114032000062128. URL <http://www.tandfonline.com/doi/abs/10.1080/0811114032000062128>.
- [162] Christopher M. Jones and Daniel M. Kammen. Quantifying Carbon Footprint Reduction Opportunities for U.S. Households and Communities. *Environmental Science & Technology*, 45(9):4088–4095, May 2011. ISSN 0013-936X, 1520-5851. doi: 10.1021/es102221h. URL <https://pubs.acs.org/doi/10.1021/es102221h>.
- [163] B. Howard, L. Parshall, J. Thompson, S. Hammer, J. Dickinson, and V. Modi. Spatial distribution of urban building energy consumption by end use. *Energy and Buildings*, 45:141–151, February 2012. ISSN 03787788. doi: 10.1016/j.enbuild.2011.10.061. URL <https://linkinghub.elsevier.com/retrieve/pii/S037877881100524X>.
- [164] Kevin R. Gurney, Igor Razlivanov, Yang Song, Yuyu Zhou, Bedrich Benes, and Michel Abdul-Massih. Quantification of Fossil Fuel CO<sub>2</sub> Emissions on the Building/Street Scale for a Large U.S. City. *Environmental Science & Technology*, 46(21):12194–12202, November 2012. ISSN 0013-936X, 1520-5851. doi: 10.1021/es3011282. URL <http://pubs.acs.org/doi/10.1021/es3011282>.
- [165] James Keirstead, Mark Jennings, and Aruna Sivakumar. A review of urban energy system models: Approaches, challenges and opportunities. *Renewable and Sustainable Energy Reviews*, 16(6):3847–3866, August 2012. ISSN 13640321. doi: 10.1016/j.rser.2012.02.047. URL <https://linkinghub.elsevier.com/retrieve/pii/S1364032112001414>.
- [166] Jonas Allegrini, Kristina Orehounig, Georgios Mavromatidis, Florian Ruesch, Viktor Dorer, and Ralph Evins. A review of modelling approaches and tools for the simulation of district-scale energy systems. *Renewable and Sustainable Energy Reviews*, 52:1391–1404, December 2015. ISSN 13640321. doi: 10.1016/j.rser.2015.07.123. URL <https://linkinghub.elsevier.com/retrieve/pii/S1364032115007704>.
- [167] Michele De Carli, Antonio Galgaro, Michele Pasqualetto, and Angelo Zarrella. Energetic and economic aspects of a heating and cooling district in a mild climate based on closed loop ground source heat pump. *Applied Thermal Engineering*, 71(2):895–904, October 2014. ISSN 13594311. doi: 10.1016/j.applthermaleng.2014.01.064. URL <https://linkinghub.elsevier.com/retrieve/pii/S1359431114000702>.
- [168] Dominik Bestenlehner, Harald Drück, and Andrea Stübler. Energetisches Einsparpotential eines kalten Nahwärmenetzes zur Wärmeversorgung eines Stadtquartiers im Vergle-



- ich zu einem konventionellen Nahwärmenetz. Bad Staffelstein, Germany, 2014. URL [https://www.researchgate.net/publication/309761891\\_Energetisches\\_Einsparpotential\\_eines\\_kalten\\_Nahwarmeretzes\\_zur\\_Warmeversorgung\\_eines\\_Stadtquartiers\\_im\\_Vergleich\\_zu\\_einem\\_konventionellen\\_Nahwarmeretz/related](https://www.researchgate.net/publication/309761891_Energetisches_Einsparpotential_eines_kalten_Nahwarmeretzes_zur_Warmeversorgung_eines_Stadtquartiers_im_Vergleich_zu_einem_konventionellen_Nahwarmeretz/related).
- [169] Ph Kräuchi, M Kolb, Th Gautschi, U-P Menti, and M Sulzer. MODELLBILDUNG FÜR THERMISCHE AREALVERNETZUNG MIT IDA-ICE. RWTH Aachen University, Aachen, Germany, 2014.
- [170] A. Molyneaux, G. Leyland, and D. Favrat. Environomic multi-objective optimisation of a district heating network considering centralized and decentralized heat pumps. *Energy*, 35(2):751–758, February 2010. ISSN 03605442. doi: 10.1016/j.energy.2009.09.028. URL <https://linkinghub.elsevier.com/retrieve/pii/S0360544209004216>.
- [171] Thomas Schütz, Lutz Schiffer, Hassan Harb, Marcus Fuchs, and Dirk Müller. Optimal design of energy conversion units and envelopes for residential building retrofits using a comprehensive MILP model. *Applied Energy*, 185:1–15, January 2017. ISSN 03062619. doi: 10.1016/j.apenergy.2016.10.049. URL <https://linkinghub.elsevier.com/retrieve/pii/S0306261916314933>.
- [172] Céline Weber, François Maréchal, Daniel Favrat, and Steven Kraines. Optimization of an SOFC-based decentralized polygeneration system for providing energy services in an office-building in Tōkyō. *Applied Thermal Engineering*, 26(13):1409–1419, September 2006. ISSN 13594311. doi: 10.1016/j.applthermaleng.2005.05.031. URL <https://linkinghub.elsevier.com/retrieve/pii/S1359431105002152>.
- [173] Araz Ashouri, Samuel S. Fux, Michael J. Benz, and Lino Guzzella. Optimal design and operation of building services using mixed-integer linear programming techniques. *Energy*, 59:365–376, September 2013. ISSN 03605442. doi: 10.1016/j.energy.2013.06.053. URL <https://linkinghub.elsevier.com/retrieve/pii/S0360544213005525>.
- [174] Samira Fazlollahi, Pierre Mandel, Gwenaelle Becker, and Francois Maréchal. Methods for multi-objective investment and operating optimization of complex energy systems. *Energy*, 45(1):12–22, September 2012. ISSN 03605442. doi: 10.1016/j.energy.2012.02.046. URL <https://linkinghub.elsevier.com/retrieve/pii/S0360544212001600>.
- [175] Frauke Oldewurtel, Andreas Ulbig, Manfred Morari, and Goran Andersson. Building control and storage management with dynamic tariffs for shaping demand response. In *2011 2nd IEEE PES International Conference and Exhibition on Innovative Smart Grid Technologies*, pages 1–8, Manchester, United Kingdom, December 2011. IEEE. ISBN 978-1-4577-1421-4 978-1-4577-1422-1 978-1-4577-1420-7. doi: 10.1109/ISGTEurope.2011.6162694. URL <http://ieeexplore.ieee.org/document/6162694/>.

- [176] Swiss Federal Office of Statistics. Catalogue des caractères. Registre fédéral des bâtiments et des logements. Version 4. Technical report, Neuchâtel, Switzerland, August 2017. URL <https://www.bfs.admin.ch/bfs/fr/home/statistiques/catalogues-banques-donnees/publications.assetdetail.2881743.html>.
- [177] Eidgenössisches Departement für Umwelt, Verkehr, Energie und Kommunikation UVEK. Solarpotentialanalyse für Sonnendach.ch Schlussbericht. Technical report, Zurich, Switzerland, February 2016. URL <https://www.bfe.admin.ch/bfe/de/home/versorgung/statistik-und-geodaten/geoinformation/geodaten/solar/solarenergie-eignung-hausdach.html>.
- [178] Paul Stadler, Araz Ashouri, and François Maréchal. Model-based optimization of distributed and renewable energy systems in buildings. *Energy and Buildings*, 120:103–113, May 2016. ISSN 03787788. doi: 10.1016/j.enbuild.2016.03.051. URL <http://linkinghub.elsevier.com/retrieve/pii/S0378778816302079>.
- [179] Jakob Moritz Fabian Rager. Urban Energy System Design from the Heat Perspective using mathematical Programming including thermal Storage. 2015. doi: 10.5075/epfl-thesis-6731, urn:nbn:ch:bel-epfl-thesis6731-3. URL <https://infoscience.epfl.ch/record/210788>.
- [180] David L. Davies and Donald W. Bouldin. A Cluster Separation Measure. *IEEE Transactions on Pattern Analysis and Machine Intelligence*, PAMI-1(2):224–227, April 1979. ISSN 0162-8828, 2160-9292. doi: 10.1109/TPAMI.1979.4766909. URL <http://ieeexplore.ieee.org/document/4766909/>.
- [181] Rasmus Luthander, Joakim Widén, Daniel Nilsson, and Jenny Palm. Photovoltaic self-consumption in buildings: A review. *Applied Energy*, 142:80–94, March 2015. ISSN 03062619. doi: 10.1016/j.apenergy.2014.12.028. URL <http://linkinghub.elsevier.com/retrieve/pii/S0306261914012859>.
- [182] D-WASTE Hellas. Waste Atlas 2013 Report. Technical report, 2013. URL [http://www.iswa.org/fileadmin/galleries/News/WASTE\\_ATLAS\\_2013\\_REPORT.pdf](http://www.iswa.org/fileadmin/galleries/News/WASTE_ATLAS_2013_REPORT.pdf).
- [183] Agence de l’environnement et de la maîtrise de l’énergie (France), Service public 2000 (France), Bureau de recherches géologiques et minières (France), and du génie rural Centre national du machinisme agricole, des eaux et des forêts (France). *La composition des ordures ménagères et assimilées en France [campagne nationale de caractérisation 2007]*. ADEME, Angers, 2010. ISBN 978-2-35838-093-5. OCLC: 708358934.
- [184] GE-Jenbacher. Jenbacher Gas Enging. Technical report, Jenbach, Austria, 2018. URL <https://www.ge.com/power/gas/reciprocating-engines/jenbacher/type-2>.



- [185] John A. Duffie and William A. Beckman. *Solar Engineering of Thermal Processes: Duffie/Solar Engineering 4e*. John Wiley & Sons, Inc., Hoboken, NJ, USA, April 2013. ISBN 978-1-118-67160-3 978-0-470-87366-3. doi: 10.1002/9781118671603. URL <http://doi.wiley.com/10.1002/9781118671603>.
- [186] Institut für Solartechnik. Solar Prüfung Forschung (SPF), Hochschule für Technik Rapperswil. Technical report, Rapperswil, Switzerland, 2016. URL [http://www.spf.ch/index.php?id=111&no\\_cache=1](http://www.spf.ch/index.php?id=111&no_cache=1).
- [187] Araz Ashouri. *Simultaneous Design and Control of Energy Systems*. PhD thesis, Diss., Eidgenössische Technische Hochschule ETH Zürich, Nr. 21908, 2014, 2014. URL <http://e-collection.library.ethz.ch/view/eth:9057>.
- [188] Vincent Shen. Standard Reference Simulation Website, NIST Standard Reference Database 173, 2006.
- [189] Bent Sørensen. Comparison between hydrogen fuel cell vehicles and bio-diesel vehicles. *16th world hydrogen energy conference, Lyon, France: paper S24-111, IHEA CDROM #111, Sevanova (2006)*, pages 1–11, 2006. URL <https://core.ac.uk/download/pdf/12517743.pdf>.
- [190] Ian H. Bell, Jorrit Wronski, Sylvain Quoilin, and Vincent Lemort. Pure and pseudo-pure fluid thermophysical property evaluation and the open-source thermophysical property library CoolProp. *Industrial & engineering chemistry research*, 53(6):2498–2508, 2014. URL <http://pubs.acs.org/doi/abs/10.1021/ie4033999>.
- [191] Ligang Wang, M Pérez-Fortes, H Madi, S Diethelm, J Van herle, and François Maréchal. Optimal design of solid-oxide electrolyzer based power-to-methane systems: A comprehensive comparison between steam electrolysis and co-electrolysis. *Applied Energy (accepted for publication)*, 2017.
- [192] Theodore L. Bergman and Frank P. Incropera. *Fundamentals of Heat and Mass Transfer*. John Wiley & Sons, April 2011. ISBN 978-0-470-50197-9. Google-Books-ID: vvyIoXEywMoC.
- [193] Stuart J. Self, Bale V. Reddy, and Marc A. Rosen. Geothermal heat pump systems: Status review and comparison with other heating options. *Applied Energy*, 101:341–348, 2013. URL <http://www.sciencedirect.com/science/article/pii/S0306261912000542>.
- [194] Samuel F. Fux, Araz Ashouri, Michael J. Benz, and Lino Guzzella. EKF based self-adaptive thermal model for a passive house. *Energy and Buildings*, 68:811–817, January 2014. ISSN 03787788. doi: 10.1016/j.enbuild.2012.06.016. URL <https://linkinghub.elsevier.com/retrieve/pii/S0378778812003039>.
- [195] Michael Koller, Theodor Borsche, Andreas Ulbig, and Goran Andersson. Defining a degradation cost function for optimal control of a battery energy storage system. In *2013 IEEE*

## Bibliography

---

*Grenoble Conference*, pages 1–6, Grenoble, France, June 2013. IEEE. ISBN 978-1-4673-5669-5.  
doi: 10.1109/PTC.2013.6652329. URL <http://ieeexplore.ieee.org/document/6652329/>.

---

# RALUCA ANCUTA SUCIU

RUE DE PRÉ-FLEURI 4, SION, VS 1950

+41 78 692 4146 | [raluca.suciu91@gmail.com](mailto:raluca.suciu91@gmail.com)

Skype: ralu.suciu

LinkedIn: [www.linkedin.com/in/raluca-suciu](http://www.linkedin.com/in/raluca-suciu)



---

## PROFESSIONAL SUMMARY

**Skilled in the field of optimisation, thermo-economic modelling of energy systems, district heating and cooling and renewable energy technologies, I seek an opportunity for contributing my international experience and proven language skills in a multicultural environment.**

---

## SKILLS

- Optimisation: Mixed-integer linear programming (MILP), Mathematical programming (AMPL)
- Programming: Python, Lua, Matlab, C, C++
- Analysis: Data analysis, Environmental impact analysis, Techno-economic analysis
- Personal: extremely organized, self-motivated
- Communication and writing: Interpersonal and written communication, Report writing
- Computer skills: Microsoft Office (Excel, Word, PowerPoint)

---

## CORE EXPERIENCE

### INDUSTRIAL PROCESS AND ENERGY SYSTEMS ENGINEERING, EPFL

*Researcher | Lausanne, VD | August 2015 - Present*

Swiss project funded by EOS Holding, a leader in the field of renewable energy penetration - focusing on modelling of urban energy demand, thermo-economic optimisation of systems comprising renewable energy sources such as hydro, geothermal and solar energy and refrigerant based district energy networks, potential of industrial waste heat recovery and cost-based penetration of low temperature district heating networks in Europe - combining programming (Lua, Python), mathematical programming (AMPL) and visual data analysis (GIS plots) knowledge.

### FRAUNHOFER INSTITUTE FOR WIND ENERGY

*Energy Consultant | Bremerhaven, Germany | June 2013 - August 2013*

Familiarising with the Dakota multi-objective optimisation environment and implementing it in the One Wind turbine simulation platform through high-level programming (Python).

### MAX PLANCK INSTITUTE FOR PLASMA PHYSICS

*Research Intern | Munich, Germany | June 2012 - August 2012*

Reviewing existing literature on the Kuramoto-Sivashinsky equation as a simple model for plasma turbulence. Developing and implementing a Matlab code which calculates the parameters of the fourth-order nonlinear partial differential equation based on previous simulations.

---

## **ADDITIONAL EXPERIENCE**

### **JACOBS UNIVERSITY BREMEN**

*Research Assistant / Bremen, Germany / September 2012 - June 2013*

Familiarizing with the theoretical basis of general relativity. Developing a Fortran code to study the behavior of the mass, charge and density of boson stars in relation to their radius.

### **INFORMATION RESOURCE CENTER, JACOBS UNIVERSITY BREMEN**

*Student supervisor / Bremen, Germany / September 2012 - June 2013*

Checking-in, checking-out, book shelving , shelf reading. Task assigning to co-workers.

---

## **EDUCATION**

### **ÉCOLE POLYTECHNIQUE FÉDÉRALE DE LAUSANNE**

#### **PH.D Energy Engineering**

*Lausanne, VD | 2019*

### **JACOBS UNIVERSITY BREMEN**

#### **MASTER OF SCIENCE Physical Sciences**

*Bremen, HB | 2015*

on President's list based on overall GPA: 1.24 (1.0 best, 4.33 worst passing grade)

### **JACOBS UNIVERSITY BREMEN**

#### **BACHELOR OF SCIENCE Physics**

*Bremen, HB | 2013*

on President's list based on overall GPA: 1.39 (1.0 best, 4.33 worst passing grade)

---

## **PUBLICATIONS**

### **JOURNALS**

#### **ENERGIES**

*12(15), 2945 / 2019*

R. Suciu, P. Stadler, I. Kantor, L. Girardin, F. Maréchal, Systematic Integration of Energy-Optimal Buildings With District Networks, doi: 10.3390/en12152945.

#### **FRONTIERS IN ENERGY RESEARCH**

*7 (69) / 2019*

R. Suciu, I. Kantor, H. Bütün, F. Maréchal, Geographically Parameterized Residential Sector Energy and Service Profile, doi: 10.3389/fenrg.2019.00069

#### **ENERGY**

*157, 830 - 842 / 2018*

R. Suciu, L. Girardin, F. Maréchal, Energy integration of CO<sub>2</sub> networks and Power to Gas for emerging energy autonomous cities in Europe, doi: [10.1016/j.energy.2018.05.083](https://doi.org/10.1016/j.energy.2018.05.083).

## **CONFERENCE PROCEEDINGS**

### **PSE ASIA, AIP CONFERENCE PROCEEDINGS**

*/ Bangkok 2019*

R. Suciu, I. Kantor, H. Bütün, F. Maréchal, Exergy-based method for determining heat pricing.

### **PRES, CHEMICAL ENGINEERING TRANSACTIONS**

*70, 709 - 714 / Prague 2018*

R. Suciu, I. Kantor, H. Bütün, F. Maréchal, Geographically parametrized residential sector energy and service profile, doi: [10.3303/CET1870119](https://doi.org/10.3303/CET1870119).

### **PSE, COMPUTER AIDED CHEMICAL ENGINEERING**

*44, 1849 - 1854 / San Diego 2018*

R. Suciu, P. Stadler, L. Girardin, F. Maréchal, Solar thermal and geothermal integration with low temperature CO<sub>2</sub> DENs, doi: [10.1016/B978-0-444-64241-7.50303-7](https://doi.org/10.1016/B978-0-444-64241-7.50303-7).

### **ESCAPE, COMPUTER AIDED CHEMICAL ENGINEERING**

*43, 1057 - 1062 / Graz 2018*

R. Suciu, P. Stadler, L. Girardin, F. Maréchal, Multi-period multi-time optimization of CO<sub>2</sub> based district energy systems, doi: [10.1016/B978-0-444-64235-6.50185-6](https://doi.org/10.1016/B978-0-444-64235-6.50185-6).

### **ECOS, PROCEEDINGS OF ECOS 2017**

*/ San Diego 2017*

R. Suciu, P. Stadler, L. Girardin, F. Maréchal, Energy integration of CO<sub>2</sub> networks and Power to Gas for emerging energy autonomous cities in Europe.

### **ECOS, PROCEEDINGS OF ECOS 2016**

*/ Portorož 2016*

R. Suciu, P. Stadler, A. Ashouri, F. Maréchal, Towards energy-autonomous cities using CO<sub>2</sub> networks and Power to gas storage.

---

## **LANGUAGES**

- English: fluent spoken and written (C1-C2)
- German: working level spoken and written (B2)
- French: working level spoken and written (B2)
- Spanish: intermediate level spoken (B1) and beginner level written (A2)
- Romanian: Native language

---

## **EXTRA-CURRICULAR ACTIVITIES**

Team running: Titze de Noel, Sion, Switzerland

Voluntary work for the Matterhorn Ultraks race, Zermatt, Switzerland

Voluntary work for the Open House event at Jacobs University

Voluntary work for the Orientation week event at Jacobs University

---

*PERSONAL INFORMATION*

Age: 27, Civil status: single, Citizenship: Romanian, Swiss permit: B